UNIVERSITY OF LONDON

IMPERIAL COLLEGE OF SCIENCE AND TECHNOLOGY

Department of Electrical Engineering

THE EFFECT OF REGULATION OF EXCITATION ON THE STABILITY OF SYNCHRONOUS MACHINES

Thesis submitted for the degree of
Doctor of Philosophy in Engineering

by

Linos Jacovou Jacovides, M.Sc.

August 1965

INDEX

ABSTRACT

The steady state stability of an alternator connected by a transmission line to an infinite bus and provided with a regulator is investigated by the method of small oscillations. Two alternative modes of analysis are developed based on the stability of closed loop systems having either voltage or torque as feedback and using the Nyquist criterion of stability. The transfer function of the alternator to small signals for different conditions of operation is presented, taking into account the effects of rotor damping and of the armature resistance.

It is found that typical regulators used in practice, can be divided into four types according to the position of the regulator frequency response locus on the complex plane. Thus we have, (a) "Simple" type with a constant transfer function, (b) "Delay" type with a phase-lag, (c) "Derivative" type with a phase-lead and (d) "Integrator" type involving one integration. It is established that a simple regulator effectively replaces X_d by X'_d and thus the region of stability is considerably increased. Both the delay and the integrator types improve stability to a lesser extent. The derivative regulator, however, improves the stability further, but an upper limit exists when X_d is replaced by the transmission line reactance.

Since such an improvement of steady state stability is not required in a practical system, other aspects of regulator performance, namely the speed of response to small changes and the accuracy of regulation are considered.

Experiments were performed using a model machine and a simulated regulator. The steady state stability limit as a function of gain for the different types of regulator and the frequency response locus of the alternator to small signals were determined. Also the transient response to small steps was recorded and the accuracy of regulation measured. All experiments are compared with computed results showing reasonable agreement.

ACKNOWLEDGEMENTS

The work presented in this thesis was carried out under the supervision of Dr. B. Adkins, D.Sc., M.A., M.I.E.E., Reader in Electrical Engineering, Imperial College of Science and Technology. I wish to thank Dr. Adkins for the help and constant encouragement that he has given to me.

I also acknowledge with thanks a grant from the Central Electricity Generating Board.

LIST OF SYMBOLS

A small case letter denoting voltage or current is the instantaneous value. The capital of the same letter denotes the R.M.S. value.

v_d , V_d - v_q , V_q	:	Direct and quadrature axis voltages.
i_d , I_d - i_q , I_q	:	Direct and quadrature axis currents.
v_{fe}, V_{fe}- i_f	:	Alternator field voltage and current.
v_t , V_t	:	Alternator terminal voltage.
V	:	Infinite bus voltage.
V_o	:	Induced voltage ($= X_{md}\, i_f$).
$X_d(p)$, $X_q(p)$	:	Direct and quadrature axis operational impedances.
$Y_d(p)$, $Y_q(p)$	:	Direct and quadrature axis operational admittances.
T'_{do} , T''_{do} - T'_d , T''_d	:	Direct axis open- and short-circuit time constants.
T''_{qo} - T''_q	:	Quadrature axis open- and short-circuit time constants.
X_d , X'_d , X''_d	:	Direct axis synchronous, transient and subtransient reactances.
X_q , X''_q	:	Quadrature axis synchronous and subtransient reactances.
X_{md}	:	Direct axis magnetizing reactance.
r_f	:	Field resistance.
r_a	:	Armature resistance.
X_c	:	Transmission line reactance.
Q	:	Reactive power at the infinite bus.
P	:	Power or number of poles with positive real part.
Z	:	Number of zeros with positive real part.
J	:	Moment of inertia of machine rotor.
T_m , T_e , T_i	:	Turbine, electrical and inertia torques.
S_o	:	Slope of the power-angle curve.
S'_o	:	Slope of the transient power-angle curve.
K_s , K_d	:	Synchronizing and damping torque coefficients.
$K(p)$	:	Regulator transfer function.
K	:	Regulator gain.
K_o	:	Constant ($= -r_f/X_{md}$).

K_{ss}	:	Gain for maximum stability limit.
K_{sr}	:	Gain for optimum speed of response.
K_{min} , K_{max}	:	Limiting values of K for steady state stability.
T_1 , T_2	:	Delays in K(p), see Eqn. (7.6).
T_α, T_β	:	Phase-lead terms in K(p), see Eqn. (7.6).
G	:	Stability ratio ($= K_{max}/K_{min}$).
H(p)	:	Alternator transfer function.
L(p)	:	System open loop transfer function.
T(p)	:	System closed loop transfer function.
δ	:	Generator load angle with respect to infinite bus.
δ_g	:	Minus the load angle ($= -\delta_o$).
δ_k	:	Stability limit with infinite gain, simple regulator.
δ_s	:	Peak of the power-angle curve.
δ'_s	:	Peak of the transient power-angle curve.
δ_l	:	Stability limit of the transmission line.
λ	:	Angular frequency of small oscillations.
λ_1	:	Angular frequency at the intersection of the $H(j\lambda)$ locus with the negative real axis.
μ	:	Angular frequency at the intersection of the $L(j\lambda)$ locus with the negative real axis.
ε	:	Integral square error for a small change.
ρ	:	Regulation of the system.
$\phi(p)$	:	Feedback transfer function in the torque method.
o	:	used as a suffix denotes the original steady state condition.
Δ	:	used as a prefix denotes the differential of the following quantity.
p	:	is the differential operator d/dt.

1. INTRODUCTION

The voltage regulators used with the alternators supplying a power system have the following functions to perform:

1) Maintenance of the voltage at various points in the system, usually at the machine terminals.
2) Control of the share of the reactive power taken by each generator.
3) Improvement of the system transient stability.
4) Increase in the steady state stability limits of the system.

The earlier, discontinuous types of regulator with mechanical contacts performed the first two functions adequately during slow changes, but had little effect on stability. Modern continuously-acting regulators not only give quicker response but bring about an improvement of both steady state and transient stability. An efficient regulator must give satisfactory results both as regards stability and regulation.

The investigation covered by the present thesis consisted of experimental work combined with a theoretical study. It relates to the steady state stability of a system comprising an alternator connected through a reactance to an infinite bus, as indicated by Fig. 1.1. The use of such a simplified system may be justified on the following grounds: a) Individual power stations are relatively small units compared with the whole of the power system. b) In many cases steady state stability is a problem concerning a hydroelectric station, connected by a transmission line to a large system. c) By keeping the external network as simple as possible attention is focused on the effect of the regulator. d) This arrangement is almost always used in the literature. The regulated quantity is the terminal voltage V_t of the alternator. A signal V_{fo}, related to V_t by the transfer function $K(p)$, is compared with a reference voltage V_{fi} and the difference is used to supply the alternator excitation.

A detailed analysis is given of the special condition, in which the regulator, including the exciter, is assumed to have no delays, i.e. its transfer function $K(p)$ is assumed to be constant. Such a

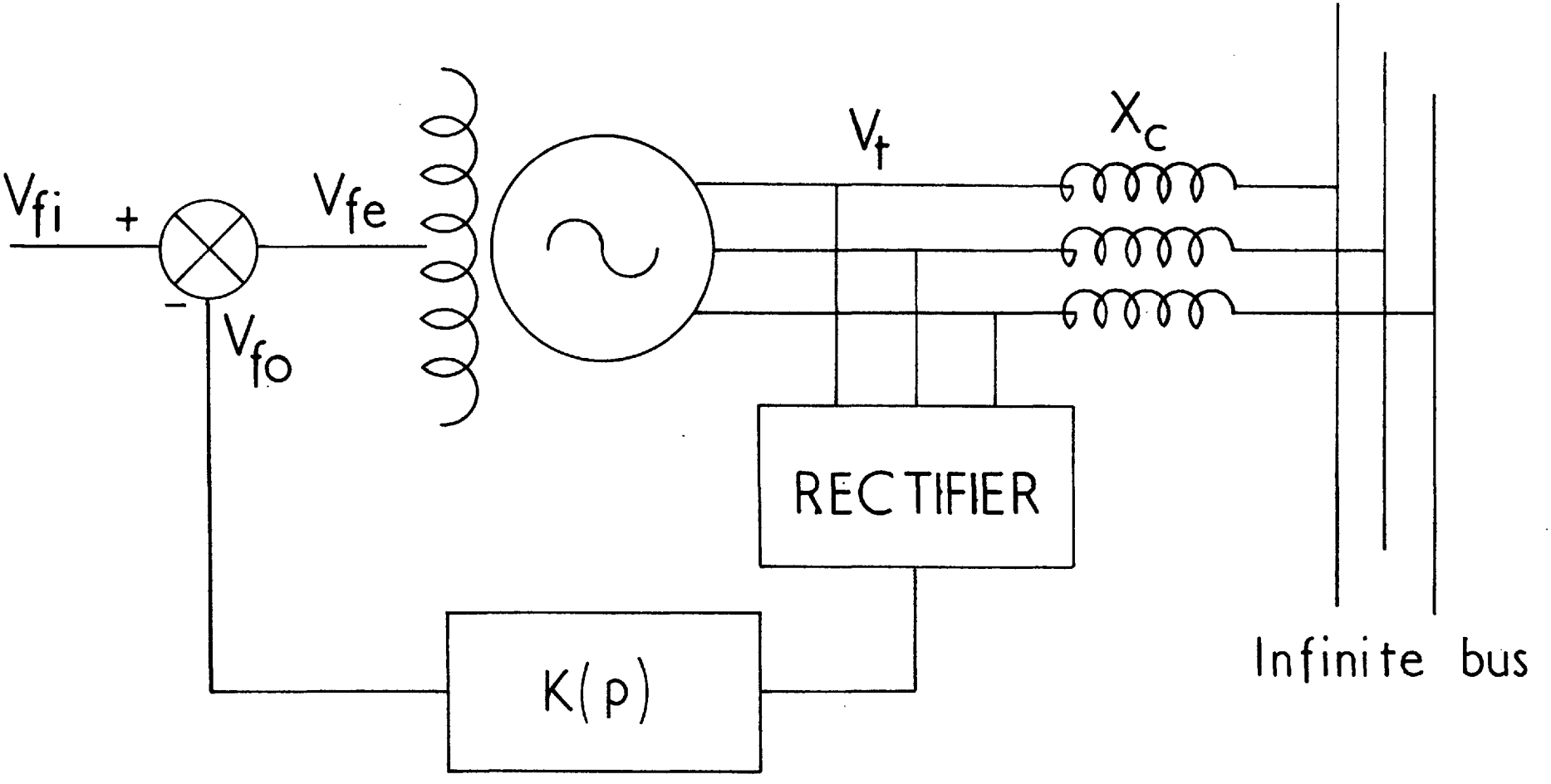

FIG. 1.1 THE SYSTEM

regulator is referred to as a "simple regulator". The behaviour of the system with any type of regulator can be determined by multiplying the system open loop frequency response loci for the simple regulator case by the appropriate regulator transfer function. Three typical forms of a practical regulator are investigated and the results show the main features of each of the three main families of regulator, i.e. a) delay, e.g. as produced by a separately-excited exciter. b) integrator or "buck-boost" regulator, and c) derivative, with combination of first and second derivative as well as proportional signals.

Consider first an alternator with constant excitation. The steady state stability limit is reached when the load angle δ_g of the generator, with respect to the bus, reaches a value δ_s at the maximum point of the steady power-angle curve. For a perfectly round rotor machine $(X_d = X_q)$ $\delta_s = 90^o$. Fig. 1.2 is a power chart, for which the coordinates P and Q are the values at the infinite bus. The machine used in the investigation has a small degree of saliency and curve a shows the steady state stability limit with constant excitation $(K = 0)$. The corresponding curve for a round rotor machine is shown by curve b.

When there is a simple regulator the stability limit is extended and as the gain is increased from zero the limit curve is moved to the left as shown by curves d , e and f , Fig. 1.2. The system is then said to be operating in the region of "artificial stability". Consider the alternator operating at 0.8 p.u. power, say, while the reference voltage V_{fi} is reduced very slowly, i.e. operation is limited to the constant power line, c . At a certain value of gain the angle at the stability limit becomes a maximum and for higher gains the curve moves back to the right. At high values of gain instability occurs to the right of curve a . Fig. 1.3 shows the relation between the angle δ_g at the stability limit and the regulator gain, with a given power output $(P = 0.8$ p.u.). This curve provides a means of assessing the effectiveness of a given regulator from the point of view of stability.

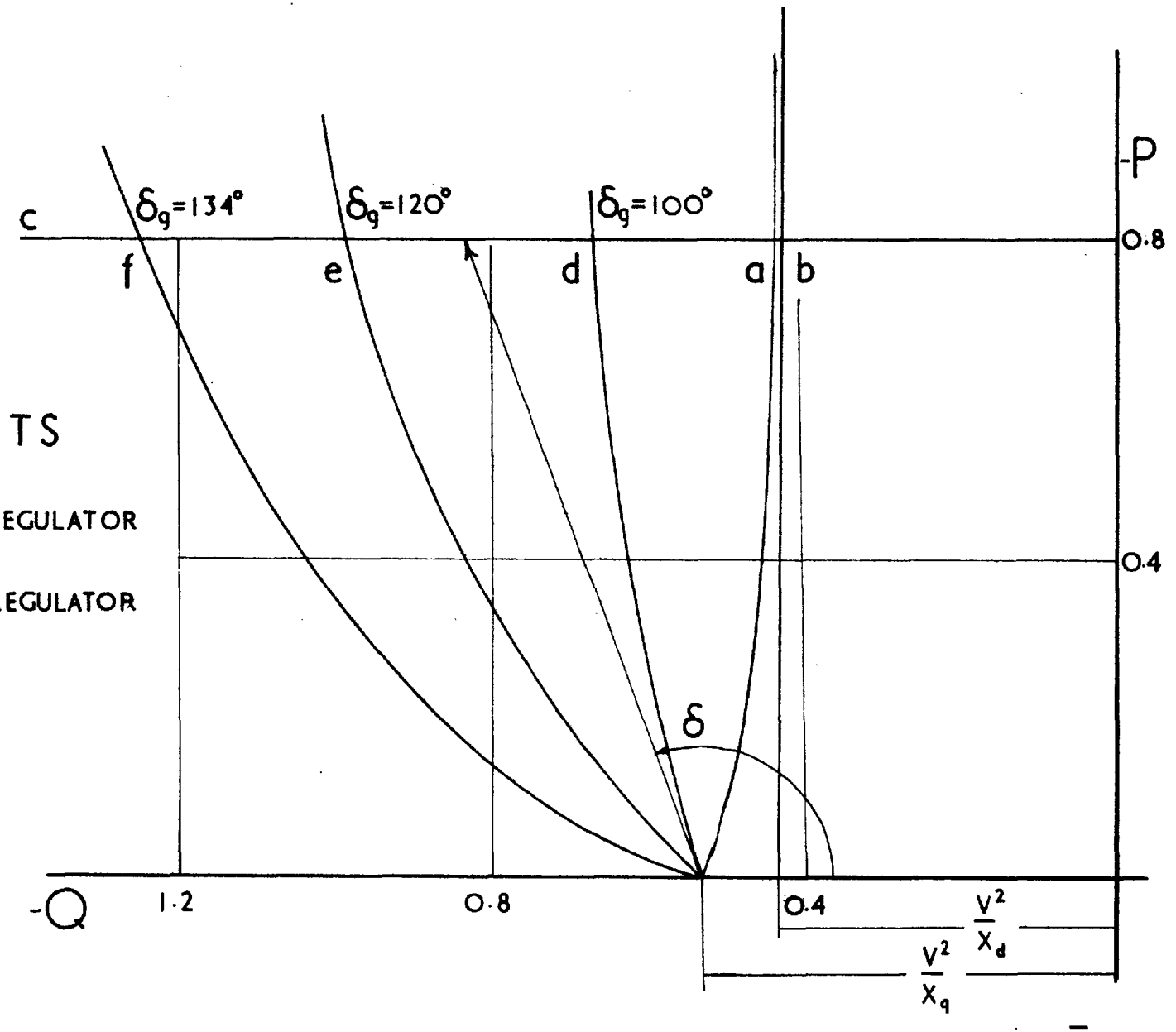

FIG. 1.2 POWER CHART

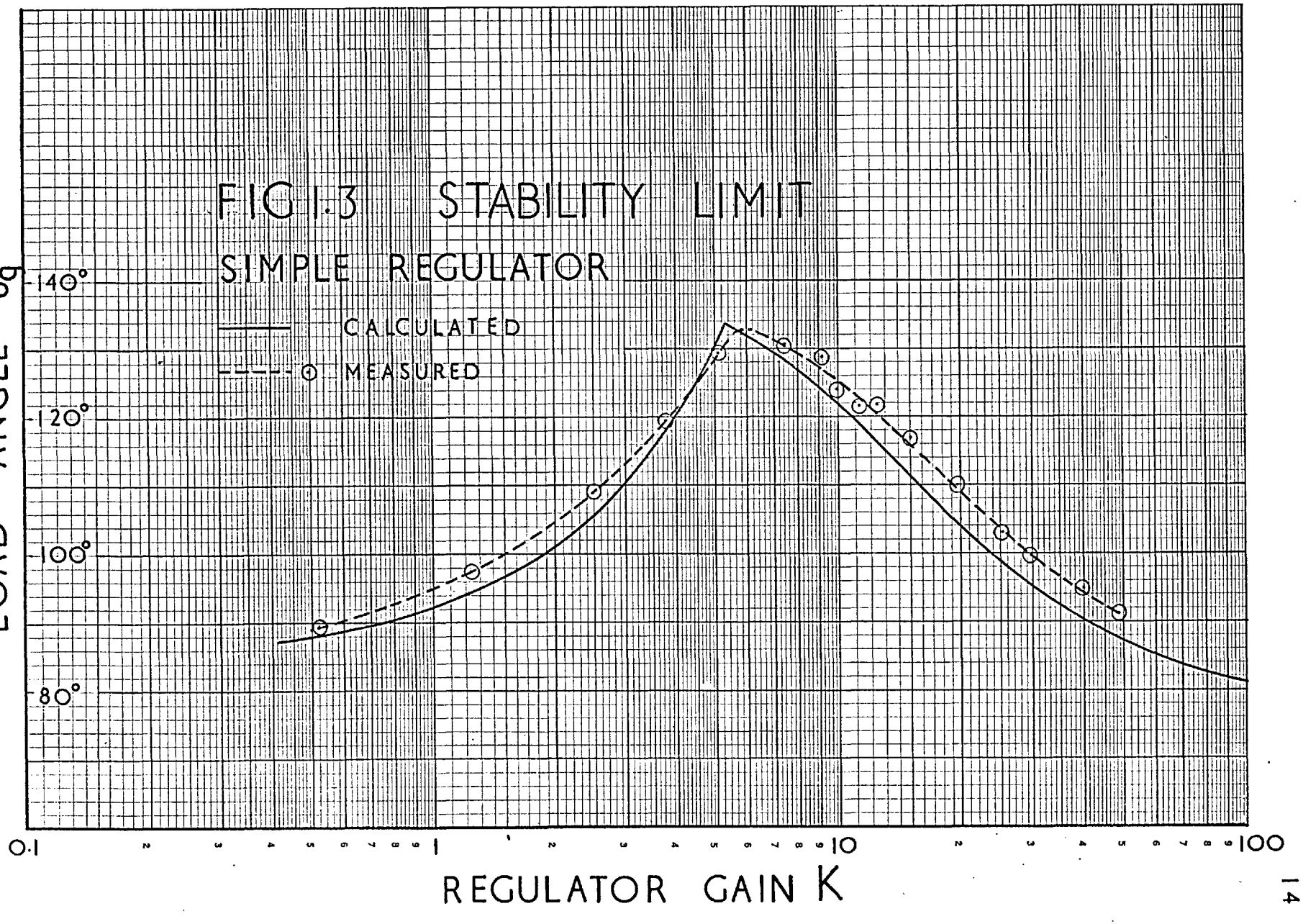
FIG 1.3 STABILITY LIMIT
SIMPLE REGULATOR
CALCULATED
MEASURED
LOAD ANGLE δ_g
140°
120°
100°
80°
0.1
1
10
100
REGULATOR GAIN K

Similar results are obtained with the other types of regulator. As the gain is increased the stability limit curve, on the power chart, moves to the left, reaches a maximum, and then moves back and eventually crosses over to the right of curve a . The maximum value of δ_g that can be achieved by varying the gain, depends on the type of regulator. δ_g can, however, never exceed the value for which the phase difference between V_t and V is 90°.

The fact that the machine is stable only for a certain region on the power chart indicates a non-linear system. This becomes apparent when the equations for the alternator, the line and the regulator are considered. There are products of two dependent variables as well as trigonometrical functions.

The stability of the system at a given steady condition may be determined as follows. It is assumed that a disturbance is introduced and that the resulting changes in the variables are calculated. If these remain finite with time then the system is stable at the original steady state condition. The magnitude of the disturbance is very important when the system is non-linear. The condition is referred to as "steady state stability" when the system is stable after a small disturbance and "transient stability" when a large disturbance is concerned.

If the disturbance is small, the equations relating the changes in the variables are linear and the standard methods for analyzing linear systems may be used to determine stability. It should be noted that the coefficients of the linearized equations are functions of the steady state conditions and hence the stability conditions are different for each point on the power chart. Sufficient information on the action of the regulator is obtained if the investigation is limited to points on a straight line of constant power on the power chart. For the numerical part of the investigation 0.8 p.u. power is considered corresponding to full load of the alternator rated at 0.8 p.f. Nevertheless it is demonstrated that the regulator does not

improve the stability at no load. The determination of stability by means of a small disturbance is known as the "method of small oscillations".

For large disturbances the equations cannot be linearised and other methods must be used. The transient behaviour of the system, however, lies outside the scope of this study.

The linearised equations can be arranged to correspond to either of two alternative feedback control systems, using voltage or torque feedback and represented respectively by the block diagrams of Figs. 1.4 and 1.5. In the "torque feedback method" the disturbance used for testing the stability is introduced at the turbine shaft and the output variable is the change in the load angle. The torque method is thus associated with mechanical quantities and the loss of synchronism is directly related to instability in δ_g. The "voltage feedback method" corresponds more closely to the actual system as shown in Fig. 1.1. The disturbance is introduced at the reference voltage and the output is the change in the terminal voltage of the alternator. Loss of synchronism is associated with the large changes in the terminal voltage during pole slipping.

In the literature both the voltage and the torque method have been used separately and by different authors. The equations for each, however, may be derived simultaneously, thus emphasizing the electromechanical nature of the system. The voltage method is more useful in studying the effects of the regulator whereas the torque method forms the link between the small oscillation theory and the conventional analysis of steady state stability. The Nyquist criterion is used to investigate the stability from the open loop transfer function of each system. A typical locus of the alternator transfer function, for the voltage case, is shown in Fig. 1.6.

Although the primary objective of the present investigation is the steady state stability performance of the regulated alternator, the other functions of the excitation regulator as given above should not be

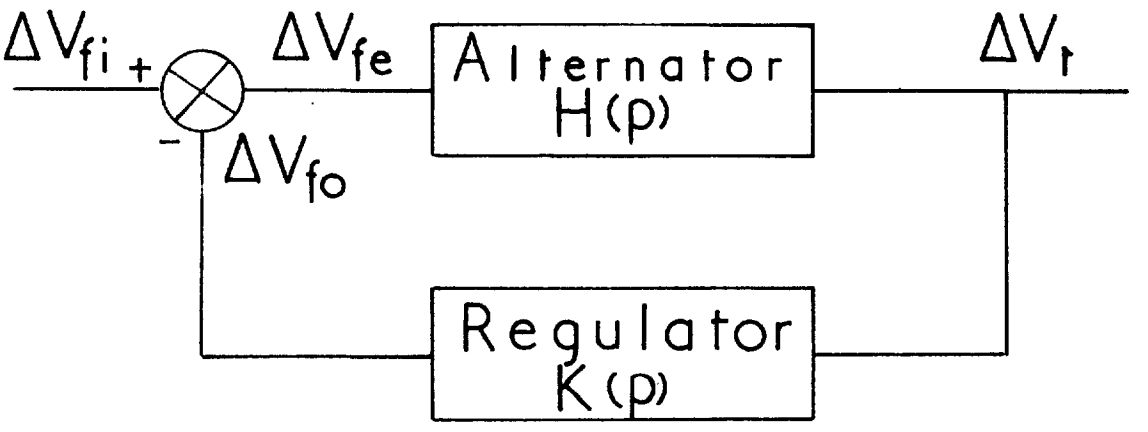

FIG 1.4 VOLTAGE DIAGRAM

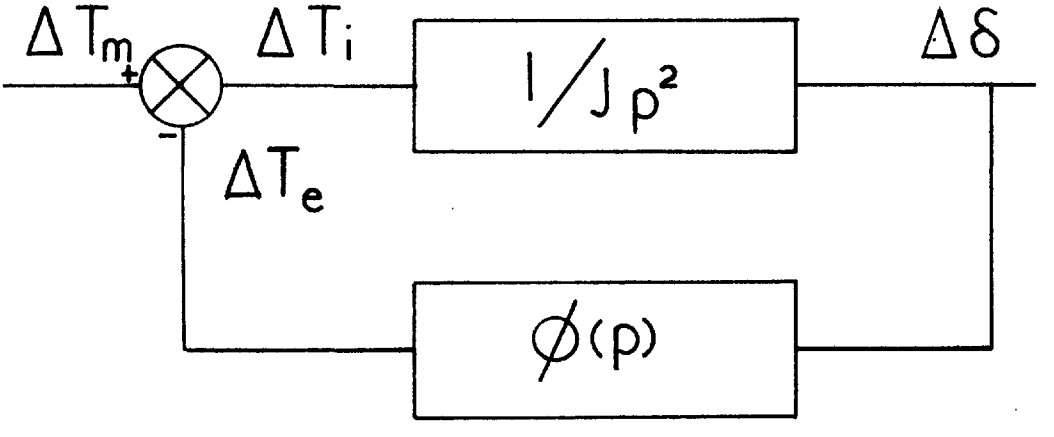

FIG. 1.5 TORQUE DIAGRAM

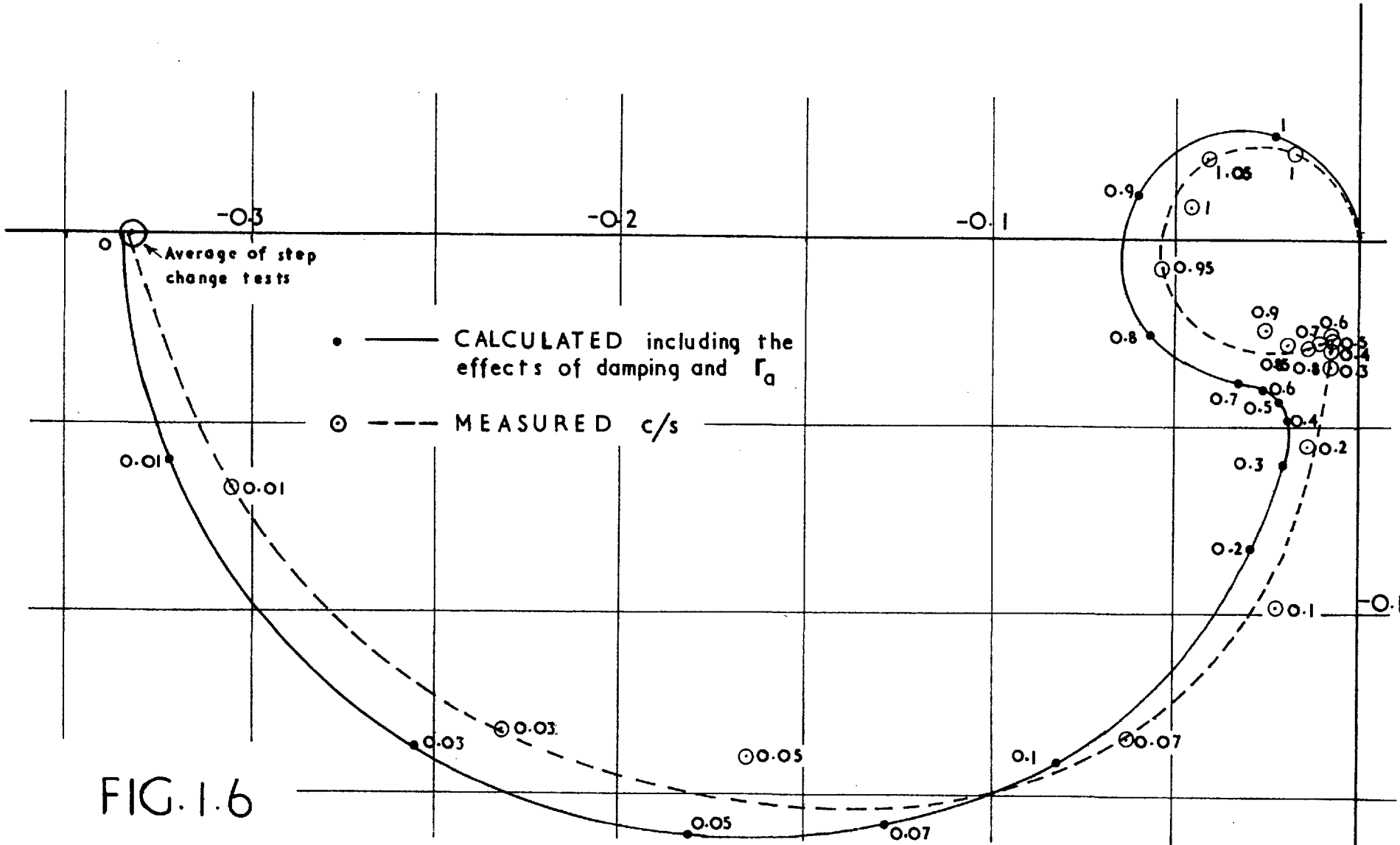

FIG. 1.6

ALTERNATOR TRANSFER FUNCTION $\delta_g = 110^\circ$

overlooked. As it happens the accuracy of regulation and the behaviour of the system under transient conditions may be linked with the frequency response loci used in determining the steady state stability.

The accuracy of regulation may be measured in two ways. a) By using the definition of steady state error of the linear control system theory on the small oscillation equations or b) By determining the change in V_t for a change in the steady operating point, e.g. between no load and full load.

There is no simple way of measuring the improvement of transient stability. The proximity, type and duration of fault in addition to the operating condition are independent parameters and for every combination of these the effect of the regulator is different. All transient disturbances, however, are in effect changes of the terminal voltage or current and one should expect no abrupt difference in the behaviour of the system as these changes become smaller and smaller. Thus the speed of response and the degree of damping for a small disturbance may be used as a measure of the effectiveness of the regulator in improving the transient stability. As the system is linear to small changes, the determination of the transient response is straightforward. It is convenient to use the Fourier Transform to evaluate the integral numerically instead of the formal solution by means of the Laplace Transform.

An important result of the present investigation is the possibility of optimizing the design of the regulator with respect to three performance indices, namely, the steady state stability, the accuracy of voltage regulation and the speed of response to small changes. The family of Nyquist loci shows clearly the form of the regulator frequency response to achieve extension of the steady state stability limit. The accuracy of regulation depends on the zero frequency point of the open loop transfer function. From the same loci the speed of response of the system to small changes may be computed. The speed of response may be improved by minimizing one of several quantities.

As an example the integral square error is chosen.

The experimental part of the investigation was carried out on one of the micromachines in the College laboratory. This is a small machine rated at 2kVA, but which has been designed to have the same parameters on a per unit basis, as a typical large machine. A small analogue computer was used to simulate the various regulators. Experiments were made to verify all the points discussed.

The most important new results of the investigation may be summarized as follows:

a) The derivation of the equations in a matrix form is such that the controlled variable as well as the regulator transfer function may be changed easily. The equations for both the Voltage and the Torque method may be derived from one system matrix.

b) The rotor damper circuits and the armature resistance are taken into account. In the literature damping is either assumed constant, see section 1.1.3, or it is neglected altogether. No reference could be found including the effect of r_a. A comparison is given between the results obtained when a) damping and r_a are neglected, b) r_a is neglected and c) both damping and r_a are taken into account.

c) A method is provided for determining the regulator parameters in order to achieve extension of the stability limit.

d) Following a review of literature it is suggested that regulators should be classified according to the position of their frequency response loci on the complex plane, for low frequencies approximately 0 to 2 c/s. Under this classification four main types exist, viz: a) a) simple, b) delay, c) integrator, and d) derivative.

e) It is shown that the ultimate stability limit occurs when the phase angle between the infinite bus and the alternator terminal voltage is 90°. The possibility of operating at load angles well beyond the peak of the transient power-angle curve is also demonstrated experimentally.

f) Comparison between theory and experiment is provided by measuring (i) the frequency response locus of the alternator and (ii) the stability limit as a function of gain for different regulators. Only a recent paper, Ref. 65-4, could be found giving a limited comparison with theory of measured stability limits.

g) Since the possible improvement in the steady state stability appears to be greater than required, other functions of the excitation regulator may be considered. The transient response of the system to a small step and the accuracy of regulation are considered theoretically and the results were verified by experiment. Little information on these performance indices appears to exist in the literature.

1.1. Survey of Literature.

1.1.1 The Controlled Variables.

One of the functions of the excitation regulator is to control a certain quantity in the system. This is achieved by comparing a signal proportional to the quantity with another signal proportional to the required value. The difference is then used to control the excitation. The types can be classified in terms of the controlled variable as follows:

1) Voltage at any point in the system, usually at the machine terminals. This is by far the commonest type and is used on all large systems. A full discussion with references is given in section 1.1.3, for the theoretical aspects, and in section 7.2, for the practical applications.

2) Load angle of the alternator with respect to any other point in the system. See Refs. 46-1, 46-2, 48-3, 56-1, 59-5, 62-3 and 64-1. Experiments in the artificial stability region have been performed involving quite elaborate regulators, but for various reasons angle regulators are not often used in practice. Sometimes an auxiliary control to limit the load angle is used, e.g. Ref. 60-10.

3) In phase component of the generator current.

4) The rate of change of active power.

5) The reactive power supplied by the generator.

The last three types have been suggested by Kron[54-1] but do not appear to have been used in practice. In addition combinations of these signals have been considered.

a) Voltage, and rate of change of load angle, e.g. Refs: 56-1, 65-1.

b) Voltage and alternator current, e.g. Ref. 62-9.

c) Voltage, 1st and (or) 2nd derivatives of current, e.g. Refs. 62-3 and 60-12.

d) Voltage and reactive power. The control of reactive power is one of the primary functions of a regulator and this combination of signals is invariably used with German, Swiss and Swedish schemes. Instead, the regulator may be arranged to operate on the voltage signal only, until the stability limit is reached and then a reactive power limiter takes over and prevents loss of synchronism, see, e.g. Refs. 48-1, 54-3, 56-4 and 59-3.

1.1.2. The Regulators.

The content of individual papers may be either.

a) Theoretical, dealing with operation in the artificial stability region, or

b) Practical, purely describing a particular installation including sometimes transient response or steady state stability tests.

The theoretical content of the papers is dealt with below, section 1.1.3, whereas discussion of the practical aspect is deferred until section 7.2. It is important to derive the transfer function of actual regulators so that typical examples may be investigated and this need arises in Chapter 7.

Unfortunately the division between theoretical and practical papers is not merely a matter of emphasis. The majority of the theoretical papers make use of the Routh criterion and consequently consider simplified regulator transfer functions and limit the investigation to the improvement of steady state stability. Any complex regulator transfer function raises the degree of the characteristic equation, and increases the number of conditions that must be satisfied for stability. In addition the evaluation of the transient response from the characteristic equation is laborious and no attempted investigation of this kind could be found in the literature.

The practical papers on the other hand describe extremely complex systems and often no attempt is made to indicate the really significant parts of the regulator. The record of complexity is Hedstrom[50-1], where the regulator has three inner loops with derivative feedbacks and where the outer loop gain depends on the operating point. Only one paper, Pavesi and Simonetti[60-2] gives an experimental frequency response of an actual regulator.

Practical papers are interested in "good" transient response but this may mean either a first cross-over in 0.3 to 2 sec. or even an overdamped response. The fact that a regulator adjusted to give optimum transient response on open circuit will give an overdamped response on load is stressed by Bloedt and Waldmann[62-4]. Nevertheless the speed of response is usually shown by a step change on open circuit.

5 The importance of high accuracy of regulation is emphasized in the practical papers and here a realistic test is often used by measuring the change in the alternator terminal voltage from full load to no load. Figures quoted vary down to $\frac{1}{2}\%$. With the exception of Venikov[64-1] theoretical papers do not mention the accuracy of regulation. No formulae giving either regulation or a quantitative measure of the speed of response could be found.

The fact that a regulator designed to give food voltage regulation

and fast response will normally give poor results in the artificial stability region seems to have been missed completely, Venikov[64-1] being the only exception. Cooper and Girling[60-4] discovered this experimentally, apparently to their surprise. Yet Doherty[28-1] states that "... the excitation systems which are satisfactory for the one (artificial stability region) may be altogether unsatisfactory for the other (transient stability)."

As stated earlier the present investigation is concerned with the following requirements imposed on the excitation regulator, a) extension of the steady state stability limit, b) fast transient response and c) good accuracy. With a certain controlled variable, the effect of the regulator on these three aspects of operation of the system can be determined by considering only the transfer function of the regulator rather than the practical details of the components used and their interconnection. It is appreciated, however, that, in many cases, reliability, ease of maintenance and alternative excitation in case of failure are more important than the three requirements listed above, see e.g. Ref. 63-4.

An important type of regulator for which it is impossible to obtain a transfer function giving the alternator terminal voltage in terms of the error is not covered by the present investigation. This occurs either when one of the stabilizing feedbacks is proportional to some function of the field current, as in Ref. 54-1, or when a series exciter is used, see Ref. 50-3. It is interesting to note that series exciters as means of extending the steady state stability limit were considered as early as in 1925. In general the field voltage is a function of both the field current and the d-axis current and hence the regulator and alternator transfer functions cannot be considered separately. It does not appear that such excitation systems are used in practice to a great extent.

All references to electromechanical regulatorshave been ignored since no operation in the artificial stability region is possible. There

will always be an oscillation. An exception to this is made for the Tirrill regulator which, given sufficiently high frequency of vibration may be thought of as continuously-acting.

Table I, p.221 contains results of operation in the artificial stability region reported in the literature. Experiments made with large machines or with specially designed models only are included. For comparison column 6 gives the maximum value of δ_g that can be achieved with a simple regulator in each case, see section 7.1.3. Only three of the five voltage regulators, however, give sufficient information about the system to allow calculation of this.

1.1.3. Theoretical Investigations.

The majority of the theoretical investigations into the steady state stability of a regulated machine are concerned with voltage as the controlled variable. This is to be expected since all practical schemes normally regulate the terminal voltage. Exceptions to this are the following papers using,

1) Load angle, Refs. 46-1, 48-3, 56-2, 62-3 and 64-1.

2) Generator current, Refs. 56-2 and 64-1.

3) Combination of voltage and the 2nd derivative of generator current, Ref. 62-3.

A number of different stability criteria have been used as follows:

a) The Nyquist, Refs. 55-1, 56-1, 59-3, 60-3, 60-10, 61-2, and 62-6. Of these Refs. 60-3 and 61-2 use the torque feedback method and the rest the voltage feedback method.

b) The Routh, Refs. 44-1, 46-1, 48-3, 50-2, 56-1, 56-2, 62-3, 64-1 and 65-4. A comparison between the results obtained using the Routh and the Nyquist criteria is given in Appendix IV.

c) The Root-locus method, Ref. 64-2.

d) The domain separation method (also called "method D" or "stability contour diagram"), Refs. 55-1, 56-2, 56-3, 58-2.

e) A method similar to Routh involving the roots of several equations derived from the characteristic equations, Ref. 65-3.

f) The analogue computer by observing instability, Refs. 52-1, 58-3, and 60-10.

g) Determination of the roots of the characteristic equation using a digital computer, Ref. 58-5.

The effect of the rotor damping circuits is taken into account by Aldred and Shackshaft[61-2] only. In this paper however, a machine without a voltage regulator is considered. The following include a constant term in the mechanical equation of the motion to "allow for rotor damper circuits and turbine damping" : 52-1, 55-1, 56-3, 58-2, 60-3, 64-2 and 65-4. The inadequacy of this assumption is illustrated in Cooper and Girling[60-4]. In different experiments they obtained values of 300 p.u. and 10-20 p.u. for the damping coefficient. The justification for using a value of 100 p.u. appears to be merely that it lies between 10 and 300 and gives a frequency of oscillation as observed in the field tests.

The effect of the armature resistance is always neglected. It is well known that r_a is important in investigating hunting[11-1, 30-1]. In fact the armature resistance has a small stabilizing effect, see section 7. Comments on individual papers may be summarized as follows:

Concordia[44-1], although one of the earliest papers, contain some remarkable results, namely, a) gain has an optimum value, b) damper windings have little effect on the maximum reactive power limit, c) a small regulator time constant increases the maximum gain that may be used and d) the stabilizing transformer does not affect the maximum load angle although it improves the accuracy of regulation. Regulators with one or two time lags only were considered. The results are presented as plots of the stability limit against the regulator gain.

Concordia[50-2] considers the "buck-boost" regulator which has an integrator transfer function. Although this type of regulator cannot by itself, extend the stability limit, it has a very good steady state regulation. It is shown in Ref. 50-2 that with proper stabilization it may be used to extend the stable region of operation considerably. The derivative feedback for stabilization is taken either from the exciter voltage or from the generator voltage. For both cases plots are shown of the stability limit against the regulator gain.

Heffron and Phillips[52-1] derive the small oscillation equation, which they then set up on an analogue computer. Stability is established by injecting a small disturbance at the reference voltage and observing the subsequent behaviour.

Messerle and Bruck[55-1] give a frequency response locus of the alternator transfer function for one operating condition. The regulator is the same as that used by Concordia[50-2]. Their results are given as plots of the regulator gain against the stabilizer gain for various conditions. These plots correspond to the domain separation method (see Ref. 64-1) with application limited to two parameters, viz: regulator and stabilizer gain. Since two parameters may be optimized at once the method is very useful in determining values in a particular problem. The overall picture, however seems to be lost. Similar plots are used in Messerle[56-3, 58-2] to investigate the effect of parameter variation. Synchronous reactance, transmission line reactance, regulator and exciter time constants are among the parameters considered.

Frey[56-1] in his thesis gives a comprehensive analysis including frequency response loci of the alternator transfer function. A regulator with an integrator transfer function as well as the simple regulator is considered. It is realised that the maximum stability limit with a simple regulator occurs at the peak of the transient power-angle curve. However, when further extension of the artificial stability region is considered, the argument used a necessary but not sufficient condition of the Routh criterion. Consequently an incorrect conclusion is reached

namely, that the first derivative of voltage, or of angle would extend the artificial stability region further, see section 7.3.3. A simplified analysis of the stability of a system with a series exciter is also given.

The coefficients of the characteristic equation in Venikov and Litkens[56-2] are in the form $(\alpha_n + \beta_n)$, where α_n is a function of the operating point and β_n a function of the regulator gain. A table of these coefficients for voltage, angle and current regulation is given. At first there is a discussion based on the fact that all the coefficients in the characteristic equation should be positive. This seems pointless since this condition is not sufficient. The effects of parameter variation is studied by means of the domain separation method. The pairs of parameters considered are the coeffients of the first and second derivatives for the three controlled variables, i.e. voltage, current and angle. It is stated that with first and second derivatives the stability limit for the transmission line may be achieved. Delays in the differentiators (even less than 0.01 sec) are said to reduce this ultimate stability limit in practice. See section 7.3.3., however, for the necessity of these delays.

Aldred and Shackshaft[58-3] represent the non-linear equations of the system on an analogue computer. The stability limit was reached by increasing the input power. In addition to the usual types of regulator a stabilizing signal proportional to the rate of change of the field current was used as first proposed in Ref. 54-1. It is claimed that considerable improvement in the steady state stability limits is achieved.

In their second paper the same authors, Ref. 60-3, present a comprehensive analysis of the torque feedback method. Again a feedback proportional to the rate of change of i_f is considered as well as more conventional regulators. It is found that in the former case the expressions for $X_d(p)$ and the damping torque coefficient must be modified but that otherwise the torque method may be used. Most of the results refer to load angles less than 90° and only one Nyquist locus for 100° is given. In a third paper the same authors, Ref. 61-2,

use the torque method to analyze the effect of rotor damper circuits. Although there is no voltage regulator the paper is useful because it gives a complete analysis of the effect of damping using the small oscillation theory.

Johansson[59-3] and Easton, Fitzpatrick and Parton[60-10] do not give any important theoretical results. They both quote an expression for the open loop transfer function, in general terms and give the alternator frequency response locus. In addition in Ref. 60-10 the small oscillation equations were solved on an analogue computer and the response to small step changes is quoted. The progressive reduction of damping as the load angle is increased is clearly shown.

Using a digital computer Glavitsch[62-3] was able to study fairly complicated regulators, but the formulae used are not given. The results are presented as stability limits on a power chart and operation at load angles greater than the peak of the transient power angle curve is shown as possible. The block diagram of the system is interesting. The alternator is represented as having three transfer functions for voltage, current and load angle. Signals proportional to each of these are added together with another set of signals formed by taking the first and second derivatives of the same output variables. The sum is compared with the reference and the error is passed through a regulator with constant gain or up to two delays. With one exception results are quoted for one controlled variable only.

Nielsen[62-6] is a mainly "experimental" paper. It quotes, however, calculated frequency response sof the open-loop transfer function with proportional and integral regulators.

Venikov[64-1] gives by far the most comprehensive treatment of the extension of the steady state stability region using a voltage regulator. The simple and the one delay regulators are fully analyzed. The expressions for the conditions of stability are given for either voltage or current or angle regulation. A very important contribution is the

treatment of a regulator involving first and second derivatives of the controlled variables. The expressions are simplified by introducing symbols for the slopes of the power-angle curves obtained with the synchronous, the transient and the line reactances. It may be noted that an unjustified approximation is made by neglecting the q-axis component of ΔV_t. In the second Russian edition, however, this has been corrected, see Ref. 64-3. A chapter is devoted to the domain separation method.

The only application of the Root-locus method is given by Stapleton[64-2]. This powerful technique is very useful when the poles and zeros of the open loop transfer function are known, which is often the case with linear control systems. For the regulated alternator, however, these vary with the operating point and a digital computer is used to calculate them. In such a case it appears that it may be more profitable to compute the closed loop poles and zeros for a range of regulator gains as in Ref. 58-5.

A particular voltage regulator is used by Battisson and Mullineux[65-3] as an example for applying an interesting stability criterion that they develop. From the characteristic equation a number of polynomials of lower degree is derived. The system is stable if the roots of these have no positive real parts. A check of the method is obtained by observing the response to a small step function when the small oscillation equations are set up on an analogue computer.

Gove[65-4] presents an interesting geometric construction of the stability limits on a power chart with constant excitation and with a simple regulator with optimum gain. An expression for the alternator transfer function assuming constant damping is given. Also there is an expression for the maximum stability limit of a delay regulator. Reference is made to the same tests as described by Mason Aylett and Birch[59-6].

Frey[46-1] and Concordia[48-3] investigate the stability of the system with an angle regulator. Their contribution is not considered here in detail since no angle regulators are considered in the present investigation.

2. DERIVATION OF THE ALTERNATOR TRANSFER FUNCTIONS.

The operation of an alternator is described by the well-known Park Equations. They are non-linear differential equations and, as indicated in the Introduction, the small oscillations method is used to determine the stability of the system. It is possible to prove that this method gives the necessary and sufficient conditions for the steady state stability, but since all references take this for granted it is unnecessary to consider this point here, see Refs. 59-2 and 64-1 for discussion.

In this section a system matrix is set up for an alternator, connected by a transmission line to an infinite bus and provided with an excitation regulator. This matrix equation may be applied to either of the two alternative closed loop systems using torque and voltage as feedback. The open loop transfer functions of the two systems are derived and are briefly discussed. The more detailed investigation of each system is deferred until sections 5, 6 and 7.

For the derivation of the system matrix the armature resistance is not neglected and a quadrature axis field winding is assumed. The armature resistance contributes to the stabilization of the system and the use of a quadrature axis field has been suggested as a possibility, Refs. 62-5 and 64-5. In the application of the equations the quadrature field is omitted. Also the armature resistance is neglected in the main theoretical development in order to show the general relations more clearly. However, the full equations, including r_a, are used in comparing experimental results with the theory and in sections 4 and 6 there is a detailed discussion of the effects of r_a.

2.1. The Machine Equations.

Consider a synchronous machine connected through a reactance to an infinite bus, as in Fig. 1.1. This arrangement is almost universally

used for assessing the effect of the excitation regulator, although some studies have been made where a two machine system is also considered, e.g. Refs. 44-1, 56-1 and 64-1. An extension of the theory to include shunt loads is given by Heffron[54-2]. The line reactance is considered as part of the leakage reactance of a "modified alternator". The reactances and time constants corresponding to this modified machine are calculated and the system is reduced to that of a generator connected to the infinite bus. The controlled variable, however, is still V_t, the terminal voltage of the actual machine.

Park's equations for the modified machine are as follows. (For an explanation of the sign convention see Ref. 57-6 and section 2.4.) The term $G_q(p)V_{fq}$ is included to allow for the possibility of a quadrature axis winding.

$$v_d = p\,\psi_d + \nu\,\psi_q + r_a i_d$$

$$v_q = -\nu\psi_d + p\,\psi_q + r_a i_q$$

$$T_e = \frac{\omega}{2}(\psi_d\, i_q - \psi_q\, i_d) \qquad (2.1)$$

where

$$\psi_d = \frac{X_d(p)}{\omega}\, i_d + \frac{G(p)}{\omega}\, v_{fe}$$

$$\psi_q = \frac{X_q(p)}{\omega}\, i_q + \frac{G_q(p)}{\omega}\, v_{fq}$$

These equations are considerably simplified if it is assumed that transient changes are slow in relation to the a.c. cycle. This implies that the frequency of the small oscillations superposed on the variables is much lower than the system frequency, 50 c/s. In fact, see sections 6 and 7, the highest frequency of interest is 2 c/s and so the assumption is justified. Compare however with section 9.1.4.

Neglecting the $p\psi$ terms and assuming the $\nu = \omega$ = constant, the first two equations become:

$$v_d = \omega \psi_q + r_a i_d \tag{2.2}$$

$$v_q = -\omega \psi_d + r_a i_q \tag{2.3}$$

Substituting ψ_d and ψ_q from Eqns. (2.2) and (2.3) in the Torque equation,

$$T_e = -\tfrac{1}{2}\left[(v_q - r_a i_q) i_q + (v_d - r_a i_d) i_d\right] \tag{2.4}$$

It is shown in Appendix I that, if V_m is the amplitude of the infinite bus phase voltage,

$$v_d = V_m \sin\delta$$

$$v_q = V_m \cos\delta \tag{2.5}$$

When the values of ψ_d, ψ_q, v_d and v_q from Eqns. (2.1) and (2.5) are substituted into Eqns. (2.2), (2.3) and (2.4) these become:

$$V_m \sin\delta = X_q(p)\, i_q + r_a i_d + G_q(p)\, v_{fq}$$

$$V_m \cos\delta = -X_d(p)\, i_d + r_a i_q - G(p)\, v_{fe} \tag{2.6}$$

$$T_e = -\tfrac{1}{2}\left[(V_m \cos\delta - r_a i_q) i_q + (V_m \sin\delta - r_a i_d) i_d\right]$$

The small oscillation equations are relations between the differentials of the variables in the last three equations. They are obtained from the well known result, viz:

If $f(x, y, z, \ldots) = C$ a constant then

$$\frac{\partial f}{\partial x}\ \Delta x\ +\ \frac{\partial f}{\partial y}\ \Delta y + \frac{\partial f}{\partial z}\ \Delta z\ + \ldots\ldots\ =\ 0$$

Hence Eqns. (2.6) become:

$$V_m \cos\delta\ \Delta\delta = X_q(p)\ \Delta I_q + r_a\ \Delta I_d + G_q(p)\ \Delta V_{fq}$$

$$-V_m \sin\delta_o \Delta\delta = -X_d(p)\ \Delta I_d + r_a\ \Delta I_q - G(p)\ \Delta V_{fe} \qquad (2.7)$$

$$\Delta T_e = \tfrac{1}{2}\Big[(-V_m \sin\delta_o + 2\, r_a i_{do})\ \Delta I_d + (V_m \sin\delta_o\, i_{qo} - V_m \cos\delta_o\, i_{do})\ \Delta\delta - (-V_m \cos\delta_o + 2\, r_a i_{qo})\ \Delta I_q\Big]$$

where the suffix o denotes initial conditions.

In addition to Eqns. (2.7) describing the electrical quantities in the alternator there is the mechanical equation of the motion of the rotor, i.e.

$$T_m - T_e = J\, p^2\theta = T_i$$

$$T_i = J\, p^2(\omega t - \delta)$$

and the corresponding small oscillation equation is,

$$\Delta T_i = -J\, p^2\, \Delta\delta \qquad (2.8)$$

Since $V_m \sin\delta_o = v_{do}$

$V_m \cos\delta_o = v_{qo}$

Eqns. (2.7) and (2.8) may be written in matrix form as follows:

$$\begin{bmatrix} G(p)\,\Delta V_{fe} \\ G_q(p)\Delta V_{fq} \\ \Delta T_e \\ \Delta T_i \end{bmatrix} = \begin{bmatrix} -X_d(p) & v_{do} & r_a \\ -r_a & v_{qo} & -X_q(p) \\ -\tfrac{1}{2} v_{do} + r_a i_{do} & -Q'_o & -\tfrac{1}{2} v_{qo} + r_a i_{qo} \\ & -J p^2 & \end{bmatrix} \begin{bmatrix} \Delta I_d \\ \Delta\delta \\ \Delta I_q \end{bmatrix} \qquad (2.9)$$

where $Q'_o = \frac{1}{2}(i_{do} v_{qo} - i_{qo} v_{do})$

If rows 3 and 4 are added together a 3 X 3 matrix results. Thus the alternator may be regarded as a link in a control system with three output variables I_d, I_q and δ and three input variables, V_{fe}, V_{fq} and T_m. Any combination of the output variables, including their derivatives, may be used to control any one or more of the input variables, thus forming a closed loop control system. Normally the turbine governor controls the T_m from a speed signal, i.e. proportional to $\frac{d\delta}{dt}$ and the voltage regulator controls the direct axis field voltage from a signal derived from the terminal voltage, which is a function of I_d, I_q and δ. Eqn. (2.9) can be used to study the steady state stability of any possible control arrangement. What is required is an additional equation giving the dependence of the controlled variables on the output variables, i.e. the equation of the controller. For the present investigation only a conventional voltage regulator is considered.

For the rest of this section r_a is neglected and from now on V_{fq} is set to zero as explained on p. 31.

2.2. The Regulator Equation.

The voltage supplied to the exciter is the difference between the reference voltage V_{fi} and the output of the rectifier V_{fo}, see

Fig. 2.1. In order to determine V_{fo}, V_t must be expressed in terms of the three output variables I_d, I_q and δ. The resistance of the transmission line is neglected. From the phasor diagram, Fig. 2.1

$$V_t = \left((V_{do} - X_c I_{qo})^2 + (V_{qo} + X_c I_{do})^2 \right)^{\frac{1}{2}}$$

and hence the instantaneous value is

$$\left| v_t \right| = \left((V_m \sin \delta_o - X_c i_{qo})^2 + (V_m \cos \delta_o + X_c i_{do})^2 \right)^{\frac{1}{2}} \qquad (2.10)$$

The output of the rectifier is proportional to the average peak voltage between lines. If balanced operation is assumed the constant of proportionality can be absorbed in the regulator transfer function. It is convenient to introduce a factor K_o so that

$$v_{fo} = K_o K(p) \left| v_t \right|$$

The corresponding small oscillation equation is:

$$\begin{aligned} \Delta V_{fo} &= K_o K(p) \left(\frac{\partial v_t}{\partial \delta} \Delta\delta + \frac{\partial v_t}{\partial i_q} \Delta I_q + \frac{\partial v_t}{\partial i_d} \Delta I_d \right) \\ &= K_o K(p) \left((v_{qo} + X_c i_{do}) \Delta I_d - (v_{qo} i_{qo} + v_{do} i_{do}) \Delta\delta - \right. \\ &\quad \left. - (v_{do} - X_c i_{qo}) \Delta I_q \right) \frac{X_c}{|v_{to}|} \\ &= K_o K(p) \left(A_1 \Delta I_d + A_2 \Delta\delta + A_3 \Delta I_q \right) \quad \text{say} \qquad (2.11) \end{aligned}$$

K_o affects only the units of the regulator transfer function and since, in any case, the per unit system is used, any convenient value may

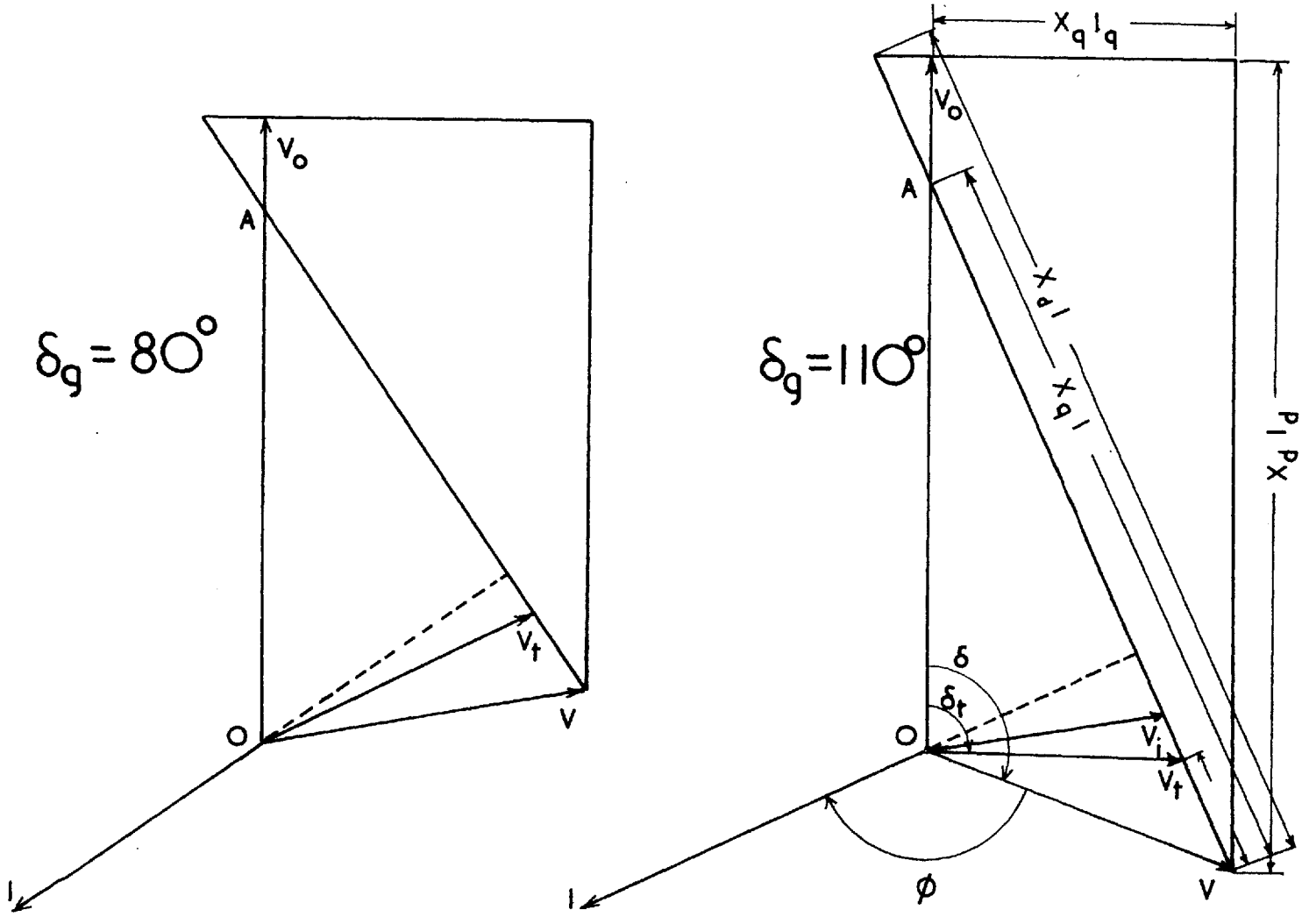

FIG 2.1a PHASOR DIAGRAM

SCALE 1 p.u. = 2 in.

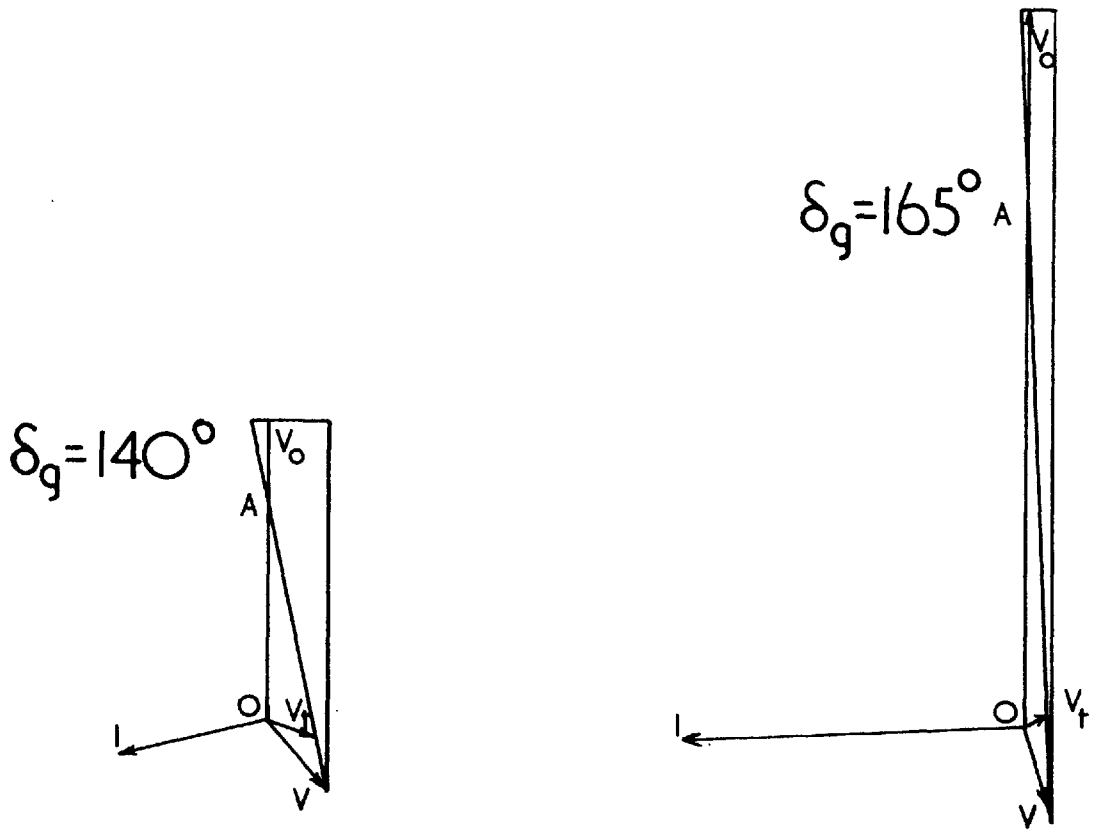

FIG. 2.1b PHASOR DIAGRAM

SCALE 1p.u.=0.5in.

be chosen. It is found that if

$$K_o = - \frac{r_f}{X_{md}} \qquad (2.12)$$

some equations are simplified and both the regulator and the alternator transfer functions have comparable values. The negative sign is introduced so that $K(0)$ is positive.

2.3. System Matrix and Block Diagram.

Eqns. (2.9) and (2.11) may be combined to form the system matrix as follows:

$$\begin{bmatrix} G(p)\,\Delta V_{fe} \\ G(p)\,\Delta V_{fo} \\ \Delta T_e \\ \Delta T_i \\ \\ \end{bmatrix} = \begin{bmatrix} -X_d(p) & v_{do} & \\ G(p)K_oK(p)\,A_1 & G(p)K_oK(p)\,A_2 & G(p)K_oK(p)\,A_3 \\ -\tfrac{1}{2}\,v_{do} & -Q_o & -\tfrac{1}{2}\,v_{qo} \\ & -J\,p^2 & \\ & v_{qo} & -X_q(p) \end{bmatrix} \begin{bmatrix} \Delta I_d \\ \Delta\delta \\ \Delta I_q \end{bmatrix} \qquad (2.13)$$

where Q_o' is replaced by Q_o since when r_a is neglected Q_o' is the steady state reactive power at the infinite bus.

Let B_{ijk} be a 3rd order determinant whose 1st, 2nd and 3rd rows are the rows i, j and k of the matrix in Eqn. (2.13). The expressions for these determinants, when the armature resistance is included are given in Appendix II. It is advantageous to define new functions A_{ijk} related to B_{ijk} as shown below:

$$A_{135} = \frac{B_{135}}{X_d(p)\,X_q(p)} = - \left(Q_o + V_{qo}^2\,Y_q(p) + V_{do}^2\,Y_d(p) \right) \qquad (2.14)$$

$$A_{235} = \frac{B_{235}}{X_d(p)X_q(p)K_oK(p)} = \frac{X_c(Q_o X_c + V^2)(I_{do} + V_{qo} Y_q(p))}{V_{to}} F(p) \quad (2.15)$$

$$A_{245} = \frac{B_{245}}{X_d(p)X_q(p)K_oK(p)(-J p^2)} = - \frac{X_c(V_{qo} + X_c I_{do})}{V_{to}} F(p) \quad (2.16)$$

$$A_{145} = \frac{B_{145}}{X_d(p)X_q(p)(-J p^2)} = 1 \quad (2.17)$$

where $$F(p) = G(p)\, Y_d(p)$$

It should be noted that Capitals denote the R.M.S. value.

In the analysis it is found convenient to separate the effects of the field and the rotor damper circuits and for this reason the functions $Y_d(p)$ and $Y_q(p)$ are used instead of $X_d(p)$ and $X_q(p)$. C.f. Eqns. (4.1) and (4.2).

In order to assess stability a small disturbance is introduced and the subsequent behaviour examined. Eqn. (2.13) is in such a form that the disturbance may be introduced at either of two points in the system, namely, at the turbine torque or at the regulator reference voltage. When a disturbance ΔT_m is used, ΔV_{fi} is zero, and vice versa. Assume first that the turbine torque remains constant,

$$\Delta T_e + \Delta T_i = \Delta T_m = 0$$

Rows 3 and 4 of Eqn. (2.13) may be added together to give a 4 X 3 matrix. From the four equations expressed by this matrix the ratio $\Delta V_{fe} / \Delta V_{fo}$ may be obtained.

$$\frac{\Delta V_{fo}}{\Delta V_{fe}} = \frac{B_{235} + B_{245}}{B_{135} + B_{145}} = \frac{K_oK(p)\,(A_{235} + A_{245}(-J p^2))}{A_{135} + (-J p^2)} \quad (2.18)$$

Eqn. (2.18) may be considered as giving the open loop transfer function of a feedback system as shown in Fig. 1.4.

If the reference voltage is now assumed constant,

$$\Delta V_{fo} + \Delta V_{fe} = \Delta V_{fi} = 0$$

and rows 1 and 2 of Eqn. (2.13) may be added together. The ratio $\Delta T_e/\Delta T_i$ is given by:

$$\frac{\Delta T_e}{\Delta T_i} = \frac{B_{135} + B_{235}}{B_{145} + B_{245}} = \frac{A_{135} + K_o K(p) A_{235}}{(-J p^2)(1 + K_o K(p) A_{245})} \qquad (2.19)$$

Thus another control system may be constructed with an input ΔT_m and an output $\Delta\delta$ as shown in Fig. 1.5. The open loop transfer function is given by Eqn. (2.19). Physically it is obvious that, if, due to some small change in T_m, the rotor angle change $\Delta\delta$ increases with time, the alternator will fall out of synchronism. Either ΔT_e or ΔT_i could be used as the feedback quantity. Since however, the application of the Nyquist Test is simpler when the open loop transfer function remains stationary at infinite frequency, ΔT_e is chosen as shown in Fig. 1.5, where

$$\phi(p) = (-J p^2) \frac{B_{135} + B_{235}}{B_{145} + B_{245}} \qquad (2.20)$$

Both systems, referred to as "Voltage feedback" and "Torque feedback", are linear and the alternator with the regulator is stable when these feedback control systems are stable on closed loop. The conditions for stability can be determined by the usual methods of control system analysis as described in Appendix III. The stability of the system is considered in detail in section 5, using the Torque feedback, and in sections 6 and 7, using the Voltage feedback.

It is worth noting here that when both $\Delta T_m = \Delta V_{fi} = 0$ and when the 2nd row of Eqn. (2.13) is added to the 1st and the 4th to the 3rd we have a 3 X 3 matrix. The determinant associated with this matrix is

$$\Delta = B_{135} + B_{145} + B_{235} + B_{245} \qquad (2.21)$$

Another method for determining the stability of the system is to examine the roots of the equation

$$\Delta = 0 \qquad (2.22)$$

using the Routh Test. If any roots have positive real parts then the system is unstable. Appendix IV shows the application of this method. In fact the characteristic equation of the system as obtained by either the Voltage feedback method or the Torque method is the same and is given by Eqn. (2.22).

2.4. Note on Sign Convention.

Before proceeding with the analysis a note on sign conventions is required.

In spite of the fact that we are dealing exclusively with a generator a sign convention based on motor operation is used. It is considered that having negative quantities in the numerical calculation was not as serious a disadvantage as the deviation from the conventions of the General Machine Theory applicable to all machines. For explanation purposes the symbol δ_g is defined as the steady state generator angle. Hence $\delta_g = -\delta_o$ so that δ_g is positive for generator operation.

The generator convention is that used by Park, and others, who used also a unit of time defined so as to make synchronous speed equal to unity. The following table indicates the main differences when the machine runs as a generator.

Motor Convention	Generator Convention
1) Load angle negative.	1) Load angle positive.
2) Electrical power output negative.	2) Electrical power output positive.
3) Turbine torque positive.	3) Turbine torque positive.
4) Time unit - 1 sec.	4) Time unit - 1/314 sec.

Eqns. (2.1) in the Generator convention are

$$v_d = p\psi_d - r_a i_d - \nu\psi_q$$

$$v_q = p\psi_q - r_a i_q + \nu\psi_d$$

with

$$\psi_d = G(p)\, v_{fe} - X_d(p) i_d$$

$$\psi_q = G_q(p)\, v_{fq} - X_q(p)\, i_q$$

also

$$T_e = \tfrac{3}{2}\, i_q \psi_d - i_d \psi_q$$

$$T_m = T_e + J\, p^2 \theta$$

From the steady state conditions the sign of $K_o K(p)$ must be changed and this implies that K_o is positive. Using these equations the resulting system matrix is identical with Eqn. (2.13) with a negative sign outside. The stability conditions therefore remain the same.

3. THE EXPERIMENTAL EQUIPMENT

The experiments were carried out on a three-phase "micro-alternator" in the College laboratory, used in conjunction with a fixed supply and an external series reactance as indicated in Fig. 3.1. The micro-alternator is designed to have parameters, on a per unit basis, similar to those of large synchronous machines. The parameters of the alternator were determined using a static impedance test as well as the standard sudden short-circuit test.

A rectifier and filter unit was constructed and a small analogue computer was used to simulate the excitation regulator. The comparison with the reference voltage was made inside the analogue computer box, see Fig. 3.1.

The frequency response tests, in this section as well as in section 9, were performed using a Transfer Function Analyzer. This is an electronic instrument consisting of a variable frequency oscillator, a phase-sensitive voltmeter and a phase-shifter. The oscillator is used to supply the test signal to the system under test and the voltmeter gives the in-phase and quadrature components of the output of the system with respect to the output of the oscillator. The phase-shifter is normally used to give the output of the system in polar coordinates, which was considered unnecessary for the experiments performed. The phase-shifter was, however, used in a different mode as described in section 9.2.1.

3.1. The Micromachine and its Parameters.

A number of the micro-alternator parameters can be varied so that a range of machines may be simulated. For the present investigation a typical large turbo-alternator was considered.

The unit voltage was chosen to be as low as possible so that saturation effects are minimized. In a saturated machine X_d and X_q vary with the operating point. Also if $X_d(p)$ and $X_q(p)$ are the

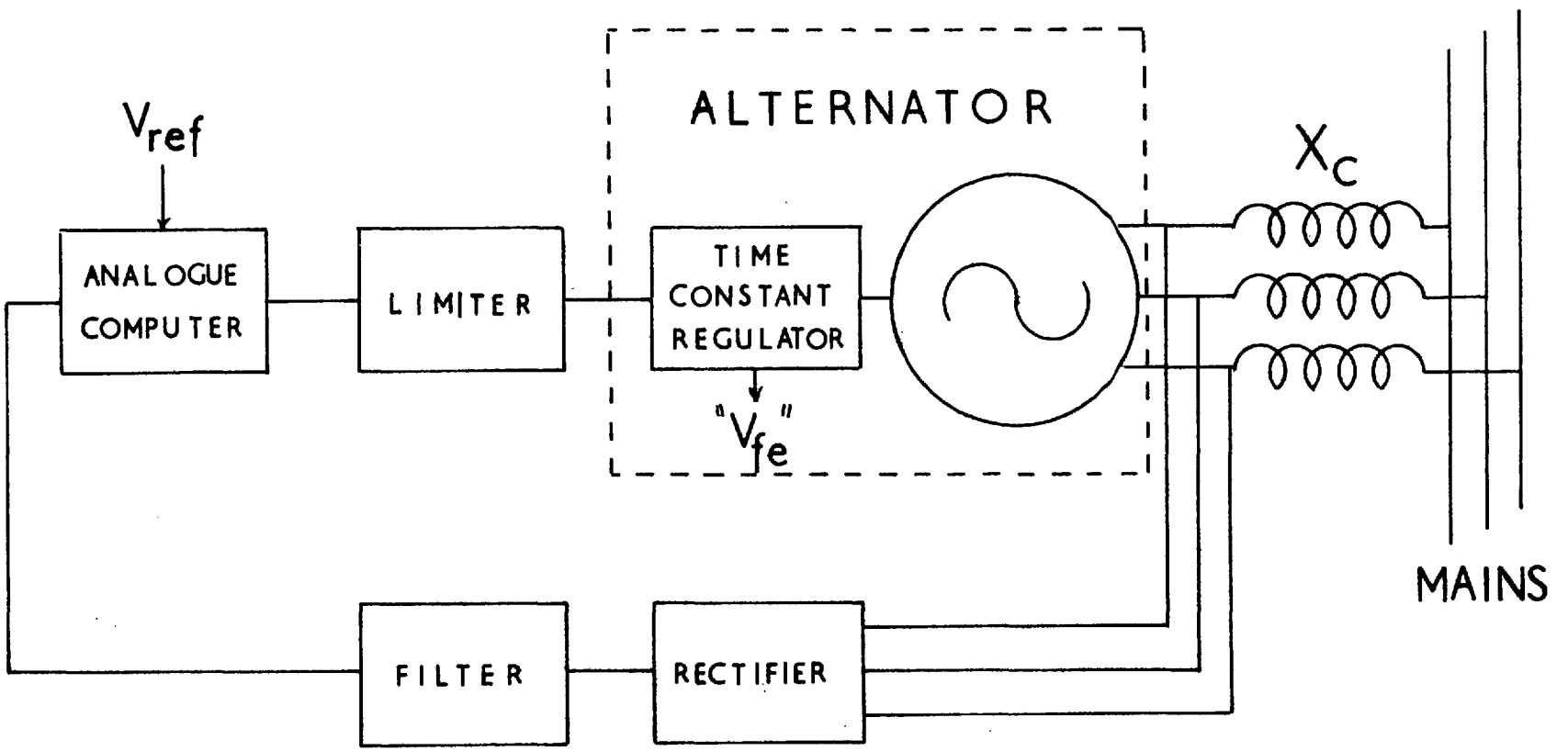

FIG. 3.1 THE EXPERIMENTAL SYSTEM

incremental values in the small oscillation equations and X_d and X_q the values obtained from the steady state conditions then for a saturated machine $X_d(0) \neq X_d$ and $X_q(0) \neq X_q$. The time constants are also affected by saturation. In section 2.1, where the generator equations are derived the concept of the "modified alternator" is introduced with the line reactance included in the leakage reactance. Thus X_d, X'_d, X''_d, X_q, X''_q, T'_d, T''_d and T''_q are modified. The unit voltamperes was chosen so that X_d for the unmodified machine is 2.0 p.u.

The simulation of a large machine is achieved by the design of the micromachine with the exception of r_f, which is considerably larger. An auxiliary "time constant regulator" is used to increase the effective field time constant, see Ref. 63-6. This device, which may be considered as an integral part of the machine was set to produce the required time constant. The excitation of the alternator is controlled by a low power input signal to the time constant regulator, which is supplied from the analogue computer, see Fig. 3.1.

Table II, p.222 gives the parameters of the modified alternator as used in the calculations. The transient time constants given are obtained with the time constant regulator in operation.

3.1.1. Variable frequency static impedance tests.

Two methods were used to determine the transient and subtransient reactances and time constants.

(i) The standard sudden short-circuit test, which gives the d-axis quantities only. See Ref. 45-1 for details.

(ii) A variable frequency static impedance test using a low frequency alternating current as follows. Two phases of the machine were connected in series opposition and supplied with low frequency current. The voltage across the two phases, V_1, as well as the voltage across a shunt, V_2, were measured with the Transfer Function Analyzer. Hence V_1 and V_2 are known in magnitude and phase. With the rotor in the

d- or the q-axis position the corresponding operational impedances are given by,

$$\frac{V_1}{2\,V_2} R = j \frac{\lambda}{\omega} X_d(j\lambda) + r_a \quad \text{for the d-axis position.}$$

$$= j \frac{\lambda}{\omega} X_q(j\lambda) + r_a \quad \text{for the q-axis position.}$$

where R is the resistance of the shunt and $\lambda/2\pi$ is the frequency of the supplied current. By varying λ the loci for the operational impedances are obtained (see Refs. 56-6 and 63-7).

In the q-axis position one set of measurements was taken. The time constant regulator was in operation and the field current was zero. It is assumed that the q-axis parameters are not affected by saturation. It was verified that the results were not affected when the field was open circuited. Fig. 3.2a shows the experimental curve, dotted line. The parameters for the computed curve were chosen to give good agreement with the measured points, especially at low frequencies.

In the d-axis position two sets of measurements were taken, both with the time constant regulator in operation.

a) The field current was adjusted to the value that would give 1.0 p.u. terminal voltage with the alternator on open-circuit and at normal speed. Thus the armature current produced a small oscillating flux which was superimposed on the field flux.

b) The field current was set to zero.

During the steady state stability tests the air-gap flux is less than 1.0 p.u. at some angle between the d- and the q-axes. The direct axis parameters therefore lie between the values obtained from tests a and b. Fig. 3.2b shows that the saturated values of $Y_d(j\lambda)$, test a are larger than the unsaturated ones, test b . The scatter of the results however, makes the determination of separate saturated and unsaturated parameters unreliable. Under these circumstances the five

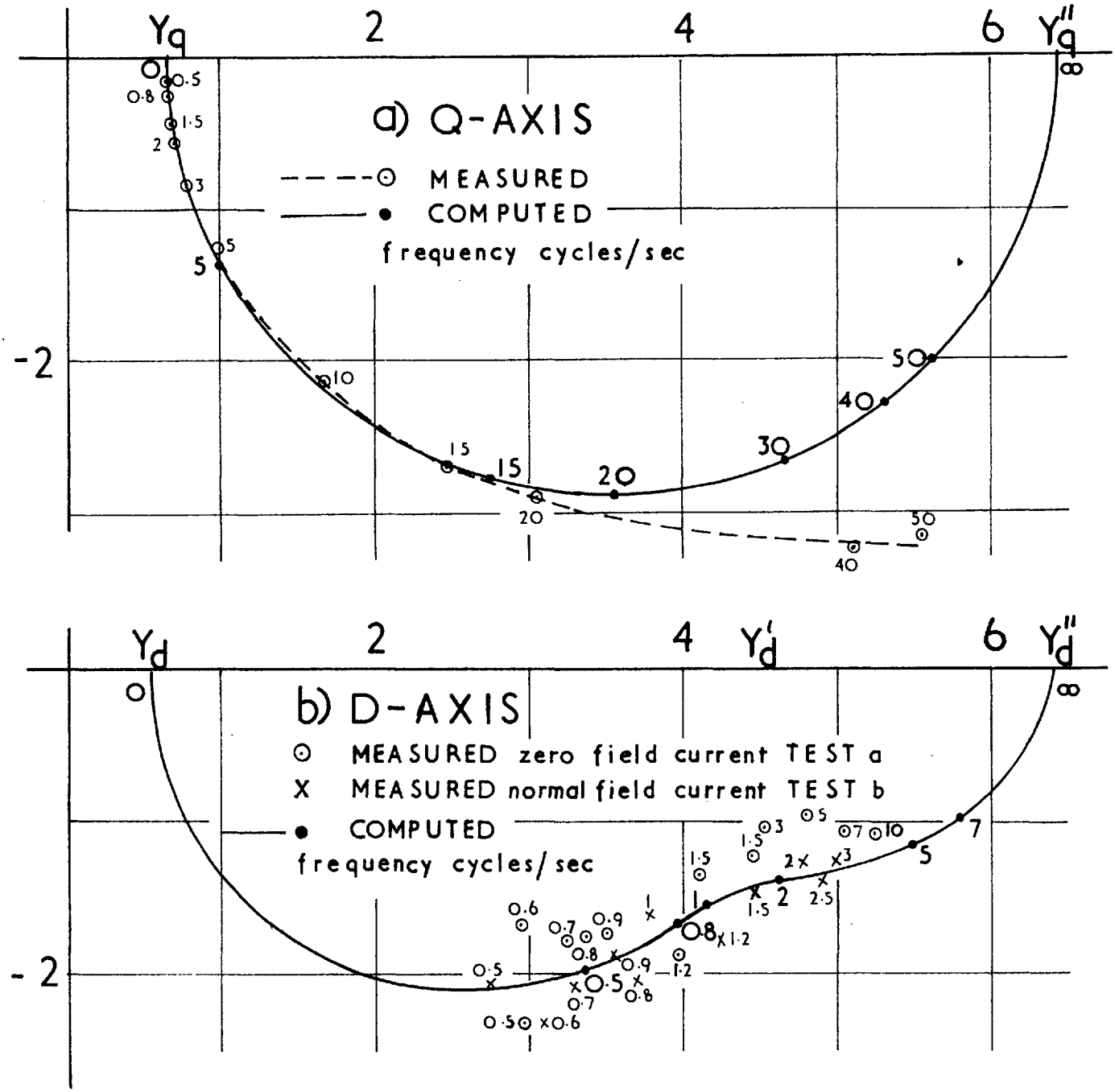

FIG. 3.2 OPERATIONAL ADMITTANCES

Modified Alternator

parameters required to specify $Y_d(j\lambda)$ cannot be uniquely determined and several alternative combinations were tried. Finally the values were chosen so that the computed $Y_d(j\lambda)$ locus, full line in Fig. 3.2b is an average curve through all experimental points.

Methods (i) and (ii) yield different values for the machine parameters. The discrepancy is partly due to the inadequacy of a single circuit to represent the rotor damping phenomena. When the alternator transfer function is determined the conditions of operation correspond to those of method (ii). The values obtained from this method were therefore used in the calculations. It is clear, however, from Fig. 3.2 that extrapolation to $\lambda = 0$ is not reliable and so X_d and X_q were determined from a steady state test as described below, section 3.1.2. In addition a small error in the measurement of either V_1 or V_2 produces a large error in the transient time constant. T'_{do} is therefore determined from a decay test when the input to the time constant regulator is suddenly removed with the alternator running at normal speed and on open circuit. This test is effectively the same as short-circuiting the exciter in a normal machine, see Ref. 45-1.

3.1.2. Determination of X_d and X_q.

The operating conditions of the alternator during the stability tests and calculations are restricted to a constant power output, 0.8 p.u. a constant infinite bus voltage and a range of values of δ_g from 80° to 165°. The values of X_d and X_q were determined from a steady state test under similar conditions, for a reduced range of δ_g.

With a steady load angle and 0.8 p.u. power V_t, I, I_f and Q were measured. Assuming the value of the alternator leakage reactance as given by the design data, the voltage behind leakage, V_i may be calculated, see Fig. 2.1. The induced voltage is then assumed to be

$$V_o = V_i \frac{I_f}{I_{fi}}$$

where I_f is the measured field current and

I_{fi} is the field current to give V_i on open circuit, (obtained from the open-circuit characteristic.)

The phasor diagram may then be completed and the values of X_d and X_q obtained. Measurements were taken for several values of δ_g from 70^o to 120^o and it was found that X_d and X_q do not show any significant variation with δ_g. The average values from this test are shown in Table II, p. 222.

The external series reactance, simulating the transmission line, was determined by measuring the voltage drop across its terminals on steady operation of the system.

3.2. The Regulator.

The regulator used in the experiments consists of two essential components:

a) a rectifier producing a direct voltage proportional to the alternating voltage at the machine terminals, and

b) a device for simulating various excitation system transfer functions. For this purpose a small analogue computer was used.

Two more components were added, see Fig. 3.1, for practical reasons:

c) a filter to reduce the harmonic content of the rectified voltage, and

d) a limiter to protect the time constant regulator from overvoltages.

These components were designed so that, with the analogue computer set to unity, a transfer function with minimum attenuation and phase-shift was obtained at low frequencies. This is, of course, necessary for measurements using the simple regulator. In addition it is very convenient if the regulator outside the analogue computer can be represented by a constant.

As stated earlier the time constant regulator may be considered

as an integral part of an alternator with reduced field resistance. However, the input to the time constant regulator does not correspond to the field terminals of the "fictitious" alternator. For reasons that need not be discussed here the time constant regulator has a transfer function of 0.5. This means that the output of the limiter is twice V_{fe} the "alternator field voltage". Nevertheless for measurement purposes the field terminals of this fictitious alternator are accessible (shown as "V_{fe}" in Fig. 3.1).

Fig. 3.3 gives the measured frequency response of the complete regulator excluding the rectifier. The loop was broken between the rectifier and the filter and a signal was injected from the Transfer Function Analyzer oscillator. Point "V_{fe}" was considered as the output. It should be noted that there is very little phase-shift below 5 c/s. Since the highest frequency appearing in the $H(j\lambda)$ plots, Fig. 6.1, is approximately 1.5 c/s the regulator transfer function outside the analogue computer may be represented by a constant.

3.2.1. The rectifier and the filter.

The rectifier consists of six silicon diodes connected in a bridge and supplied from three single-phase transformers connected delta/star. The primary of the transformers is connected to the alternator terminals. The output of the rectifier is therefore proportional to the average peak voltage of the alternator line voltages. With this arrangement the harmonics present in the output are 300 c/s, 600 c/s etc. Unbalance in the alternator line voltages was corrected by adjusting a variable resistance in series with the primary of the transformers but some 150 c/s component was present in the output. Also present is a 50 c/s signal due to pick-up. All these harmonics must be removed because they affect the operation of the amplifiers that follow and for this purpose a three section filter is used. Fig. 3.4 shows the circuit diagram of the filter together with its frequency response. The first section is a parallel T tuned to 300 c/s and the other two are low pass filters with cut-off at just over 30 c/s. The attenuation at 50 c/s

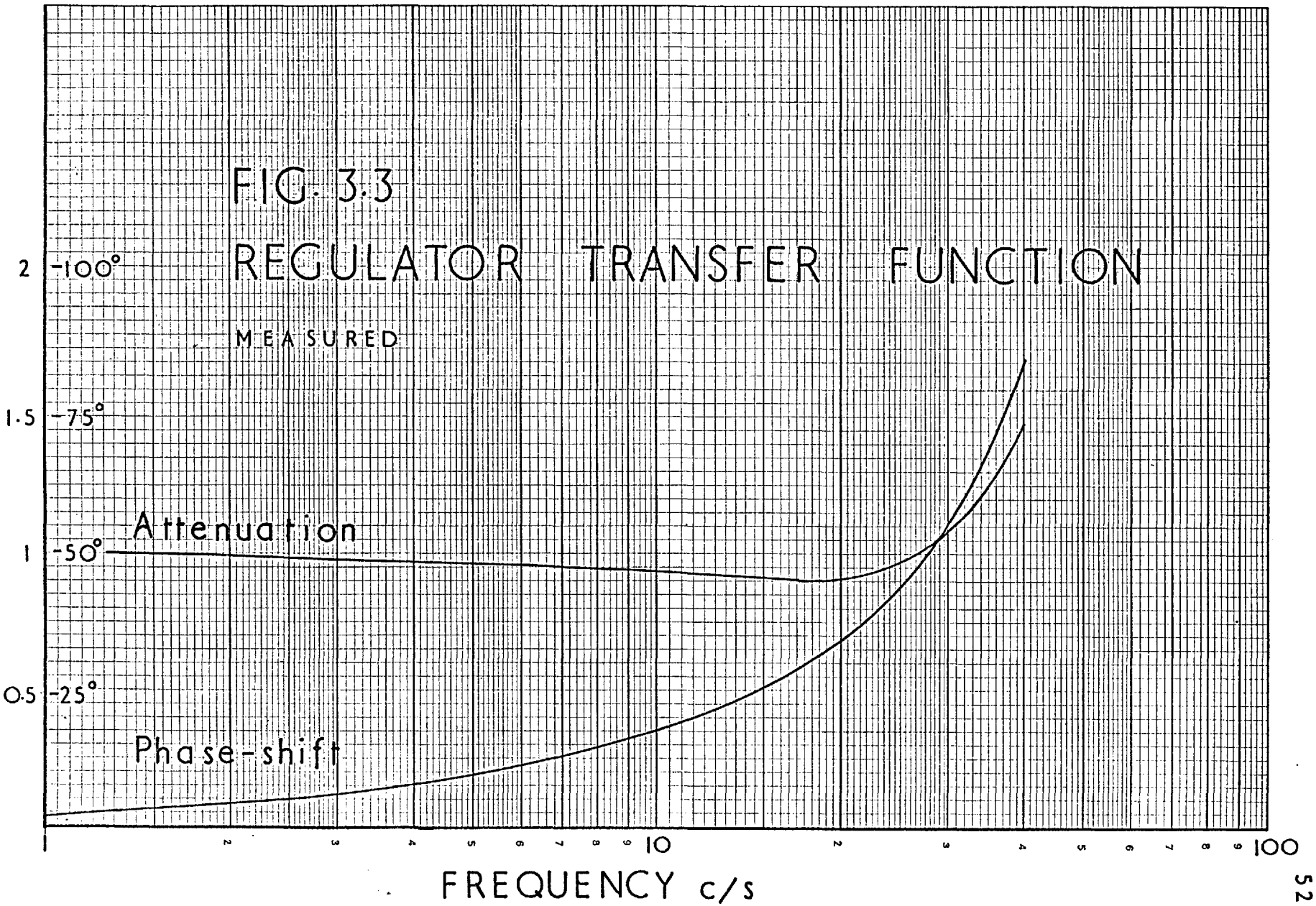
FIG. 3.3
REGULATOR TRANSFER FUNCTION
MEASURED
2
-100°
1·5
-75°
Attenuation
1
-50°
0·5
-25°
Phase-shift
10
100
FREQUENCY c/s

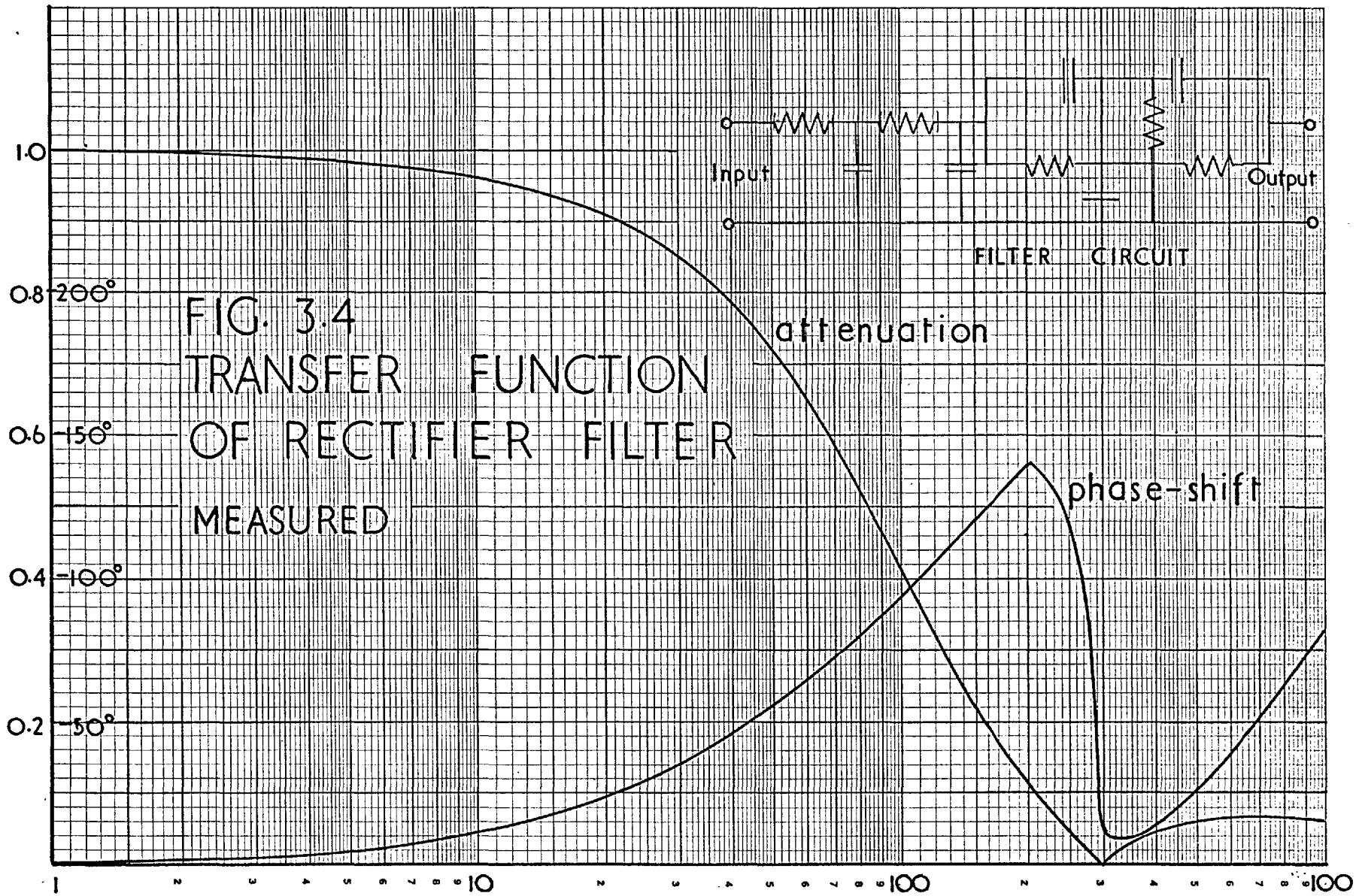

FIG. 3.4
TRANSFER FUNCTION
OF RECTIFIER FILTER
MEASURED

could not be increased without increasing the attenuation and phase-shift at low frequencies. Insufficient attenuation of 50 c/s pick-up caused some difficulties with the derivative regulator.

The transfer function of the rectifier itself could not be determined. It may safely be assumed, however, that the rectifier does not introduce any time lags. The relation between the A.C. input and the D.C. output is shown in Fig. 3.5. The terminal voltage of the alternator for operation in the region of a load angle is 110° is approximately 145V (line) and therefore the characteristic is sufficiently linear. Because of loading of the filter the transfer function of the unit cannot be taken from Fig. 3.5 and must be determined when the system is in operation. Its value is 0.193 (D.C. volts/ peak A.C. phase volts.)

3.2.2. The analogue computer and the limiter.

A small analogue computer, with the following facilities was used to simulate the various regulator transfer functions.

There are six operational amplifiers (high D.C. gain, low drift), four of which may be connected as integrators. There are eight coefficient potentiometers and facilities for their accurate setting. The input resistors are either 1 MΩ or 100 kΩ and the feedback ones 1 MΩ thus allowing a gain of up to 10 per amplifier. A very useful facility is a removable patch-board which enables one to change the type of regulator by plugging-in a different panel. The regulator gain is set on a precision decade potentiometer which precedes the last amplifier. The frequency response of one of the amplifiers connected as an adder shows negligible phase-shift up to 1 kc/s and therefore it is not necessary to quote it here.

The transfer function of a high gain amplifier with an input impedance Z_1 and a feedback impedance Z_2 is

$$\frac{V_o}{V_i} = (-) \frac{Z_2}{Z_1}$$

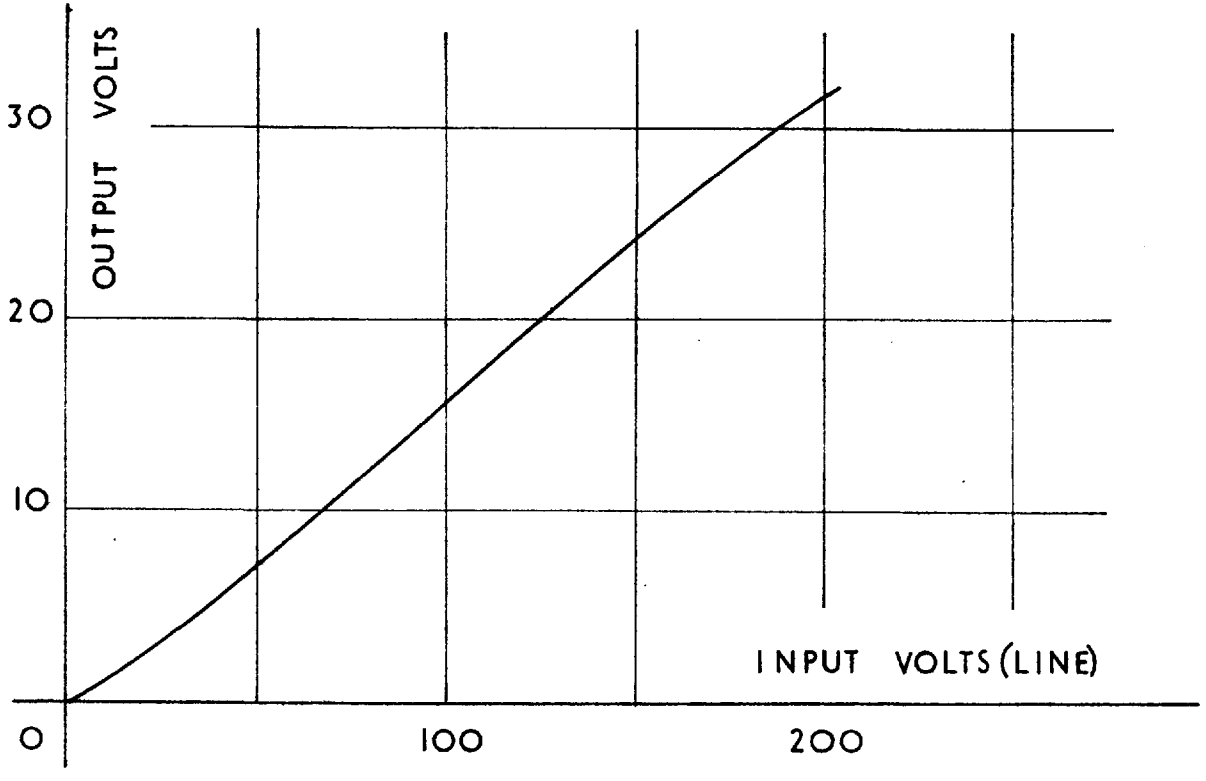

FIG. 3.5 RECTIFIER CHARACTERISTIC

Thus for

1)	Constant gain	$Z_1 = R_1$	$Z_2 = R_2$
2)	One time lag	$Z_1 = R_1$	$Z_2 = \frac{R_2}{p\,C_2R_2+1}$
3)	Integrator	$Z_1 = R_1$	$Z_2 = \frac{1}{p\,C_2}$
4)	Differentiator with one time lag	$Z_1 = \frac{1}{p\,C_1}$	$Z_2 = \frac{R_2}{p\,C_2R_2+1}$

By combining these a large variety of regulator transfer functions may be obtained.

The limiter consists of two pairs of Zener diodes connected back to back. When the output of the regulator exceeds the breakdown voltage of two Zeners, about 16 V in this case, these conduct and so the input to the time constant regulator is limited. Normally however, the Zeners are cut-off and the limiter may be considered as having a constant attenuation. Its transfer function is then 0.385.

3.2.3. The regulator gain.

The regulator gain is equal to the product of the component transfer functions (see Fig. 3.1) i.e.

$$K\,K_o = K_1 \times 0.193 \times 0.385 \times 0.5 = 0.0372\,K_1$$

where K_1 is the gain in the analogue computer. The units of $K\,K_o$ are volts/volt with V_t being equal to the peak phase value. $H(j\lambda)$ however, is expressed in per unit quantities and hence the regulator gain in p.u. is,

$$K\,K_o = 0.0372\,K_1\,\frac{186}{\sqrt{3}\ 965} = 0.00414\,K_1$$

where 186 is the base A.C. voltage and
965 is the base field voltage.

Now $$K_o = (-) \frac{r_f}{X_{md}}$$

Hence $$K = 0.00414 \times \frac{1.89}{0.001425} K_1$$

$$= 5.49 K_1$$

4. THE FUNCTIONS A_{ijk}.

The quantities A_{ijk} are defined in Eqns. (2.14) to (2.17) and are functions of the operating condition as well as of the machine parameters. It is apparent from Eqns. (2.18) and (2.19) that A_{ijk} are the "building blocks" for both the Voltage and the Torque Feedback Methods. Before proceeding to consider these two methods in detail it is advantageous to investigate in the present section their constituent parts.

When damping and the effect of the armature resistance are taken into account the expressions for A_{ijk} are complicated and it is difficult to draw useful conclusions. Therefore, at first, damping and the armature resistance are neglected and the simplified expressions are considered algebraically. Then computed loci are introduced for the experimental system at typical load angles for,

1) No damping.
2) Damping but r_a neglected.
3) Damping and r_a. The expressions for A_{ijk} in this case are given in Appendix II.

The last two are considered as modifications of the first. Power is constant throughout at 0.8 p.u. (see Fig. 1.2). For reasons that will become apparent in section 6, four A_{ijk} loci are considered in detail, namely those for δ_g at 80°, 110°, 140° and 165°. These loci are shown in Figs. 4.1, 4.2 and 4.3.

In order to avoid cluttering-up the complex plots with the values of frequency the following convention is adopted. The frequency for three points only is shown, i.e. for the minimum frequency (usually zero), the maximum (usually infinity) and for one intermediate value. The other computed points are shown and the frequency values can be determined by reference to Table III p.223 . This convention is used for all loci in sections 4, 6 and 7 which involve frequencies.

When dealing with these functions it is useful to have the expressions

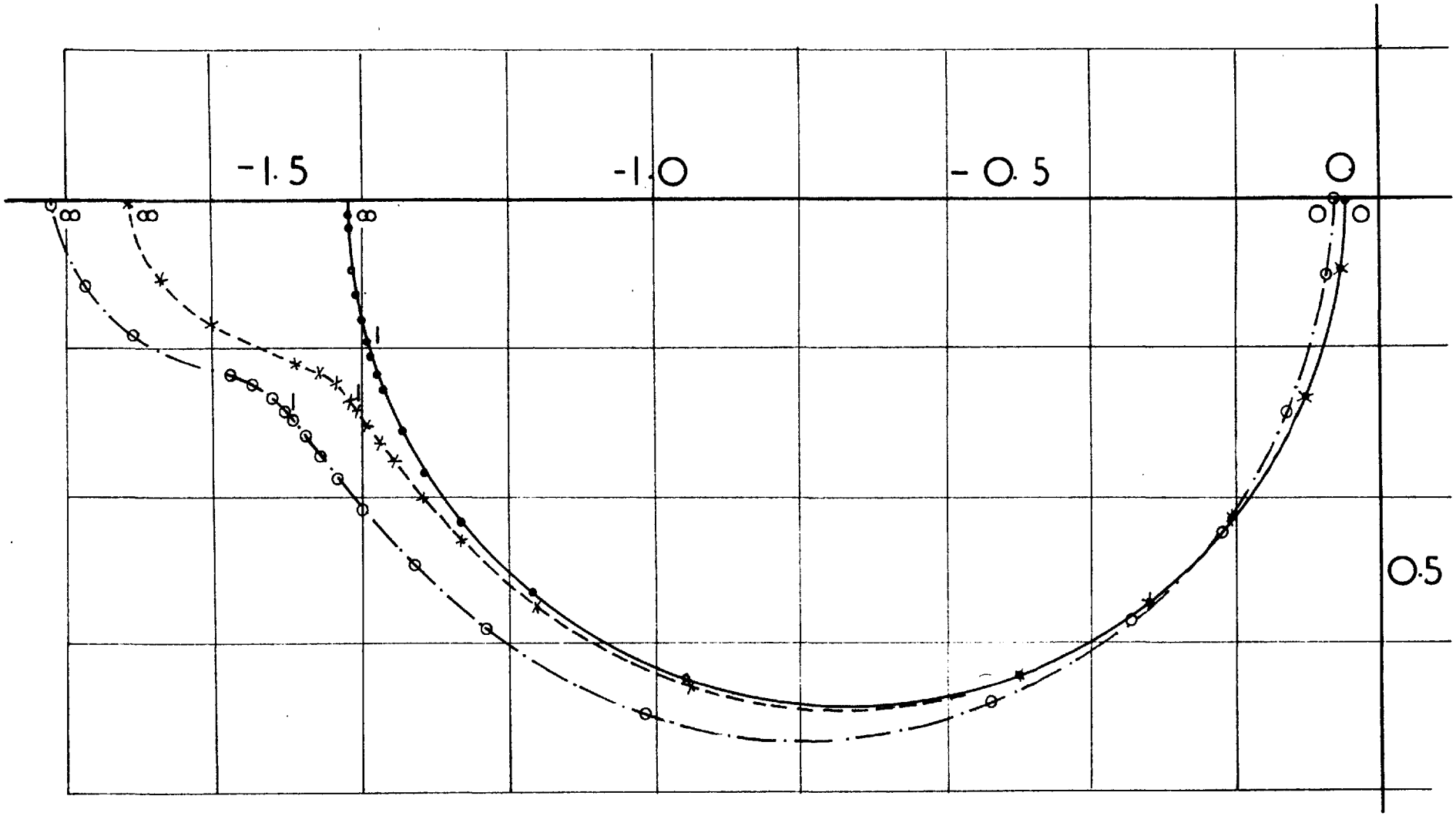

FIG. 4.1a PLOTS OF A_{135} $\delta_g = 80°$

• —— NO DAMPING

x - - - - - DAMPING $r_a = 0$

⊙ —·—·— DAMPING AND r_a

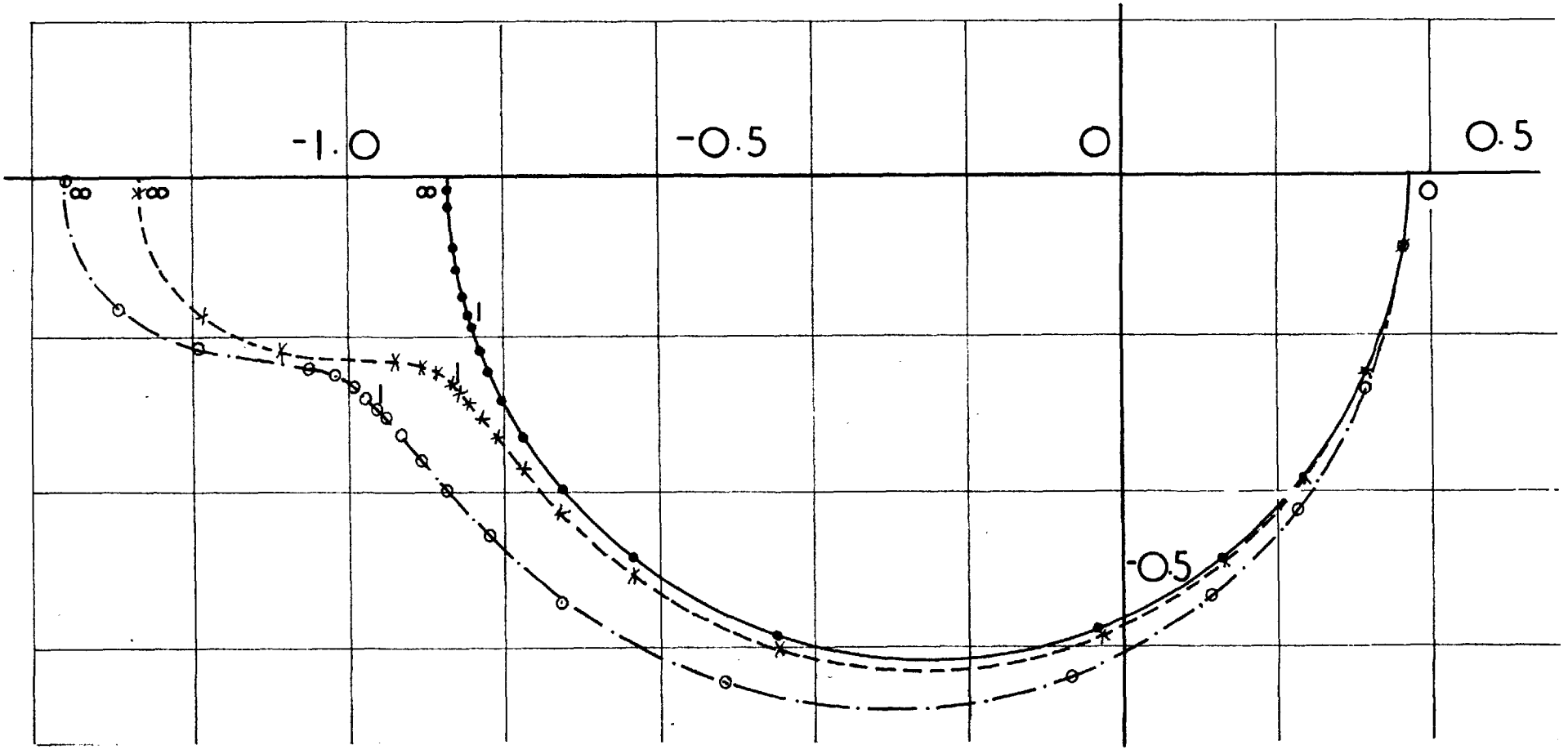

FIG.4.1b PLOTS OF A_{135} $\delta_g = 110°$

• ——— NO DAMPING

x - - - - - DAMPING $r_a = 0$

⊙ —·—·— DAMPING AND r_a

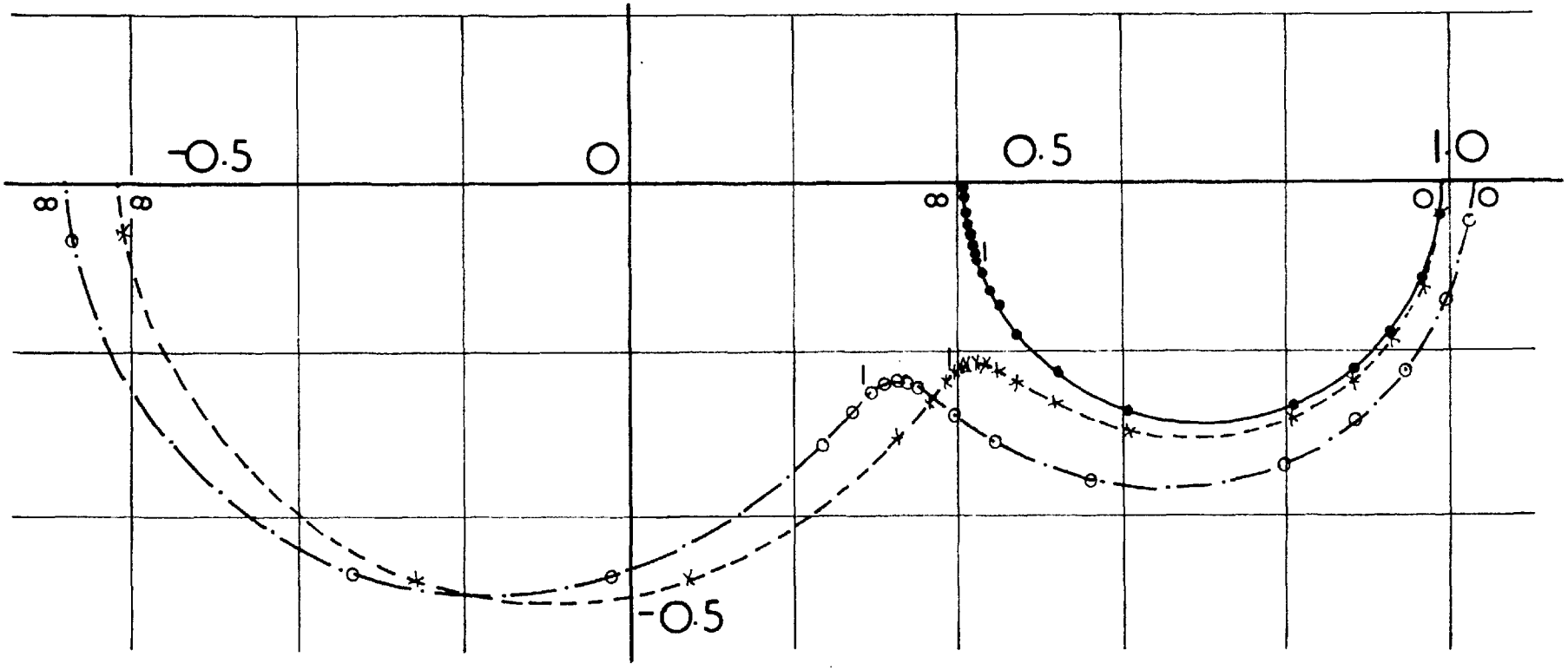

FIG. 4.1c PLOTS OF A_{135} $\delta_g = 140°$

• —— NO DAMPING

x - - - - DAMPING $r_a = 0$

⊙ —·—·— DAMPING AND $r_a =$

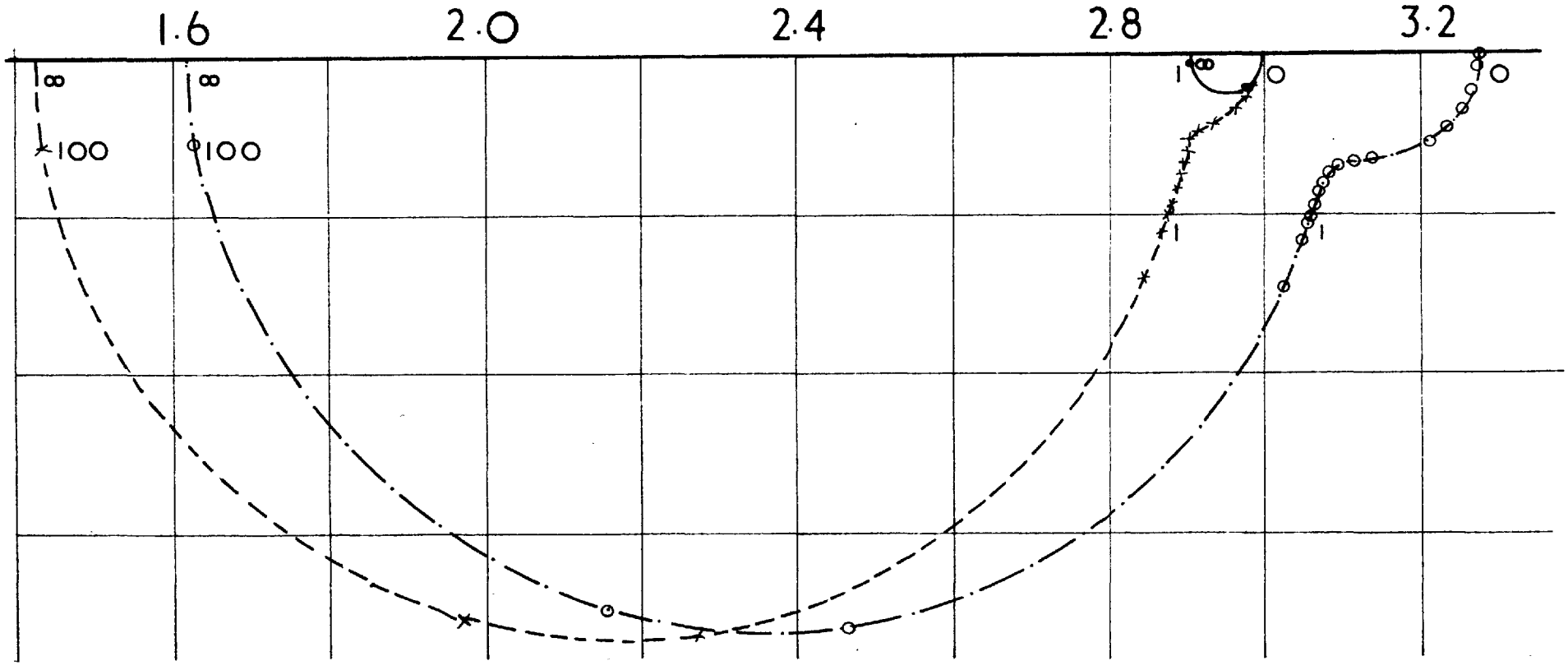

FIG. 4.1d PLOTS OF A_{135} $\delta_g = 165^\circ$

• —— NO DAMPING

x - - - - DAMPING $r_a = 0$

o —·—· DAMPING AND r_a

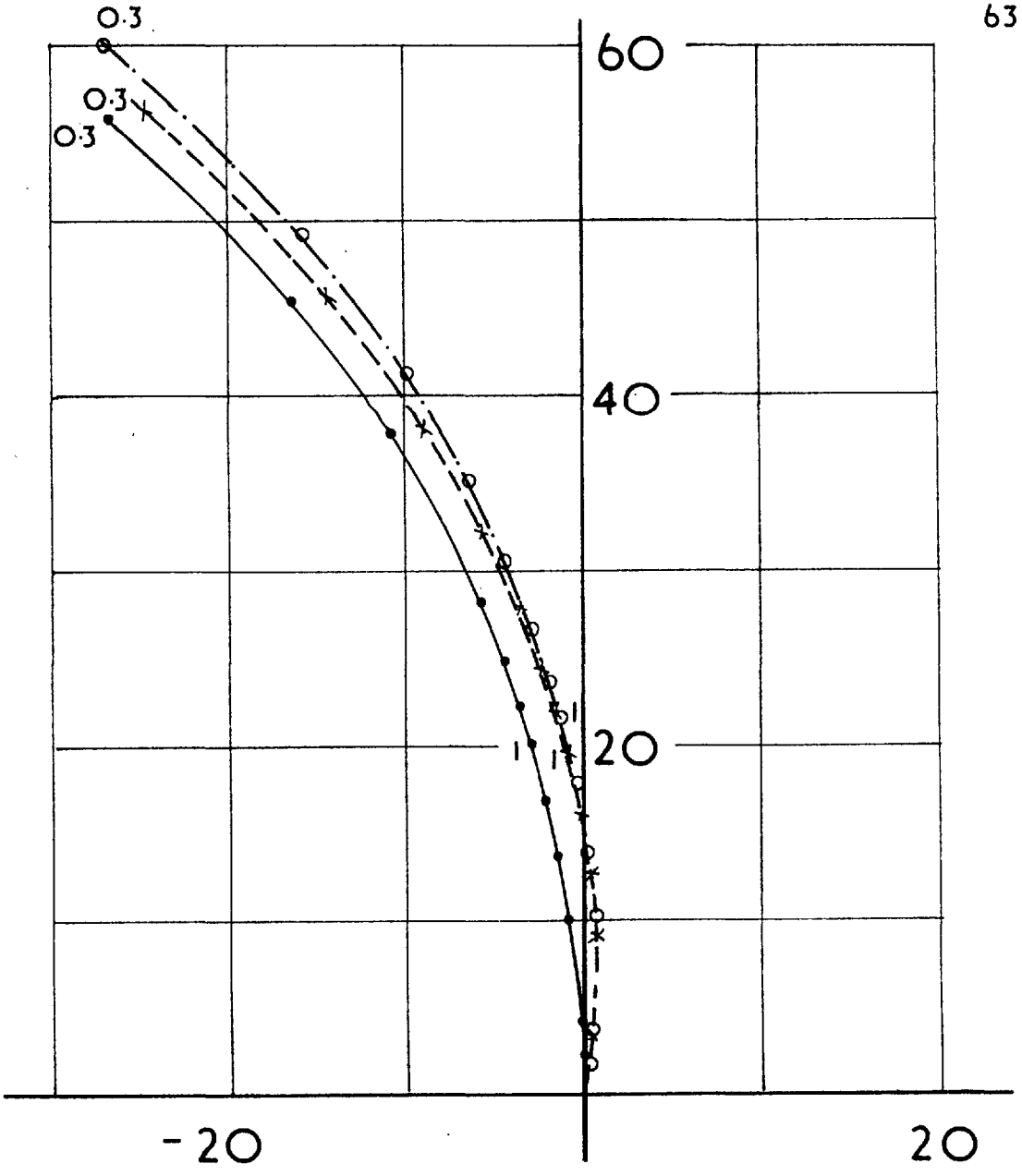

FIG. 4.2a PLOTS OF $-A_{235}$ $\delta_g = 80°$

• ——— NO DAMPING

x - - - - DAMPING $r_a = 0$

o —·—·— DAMPING AND r_a

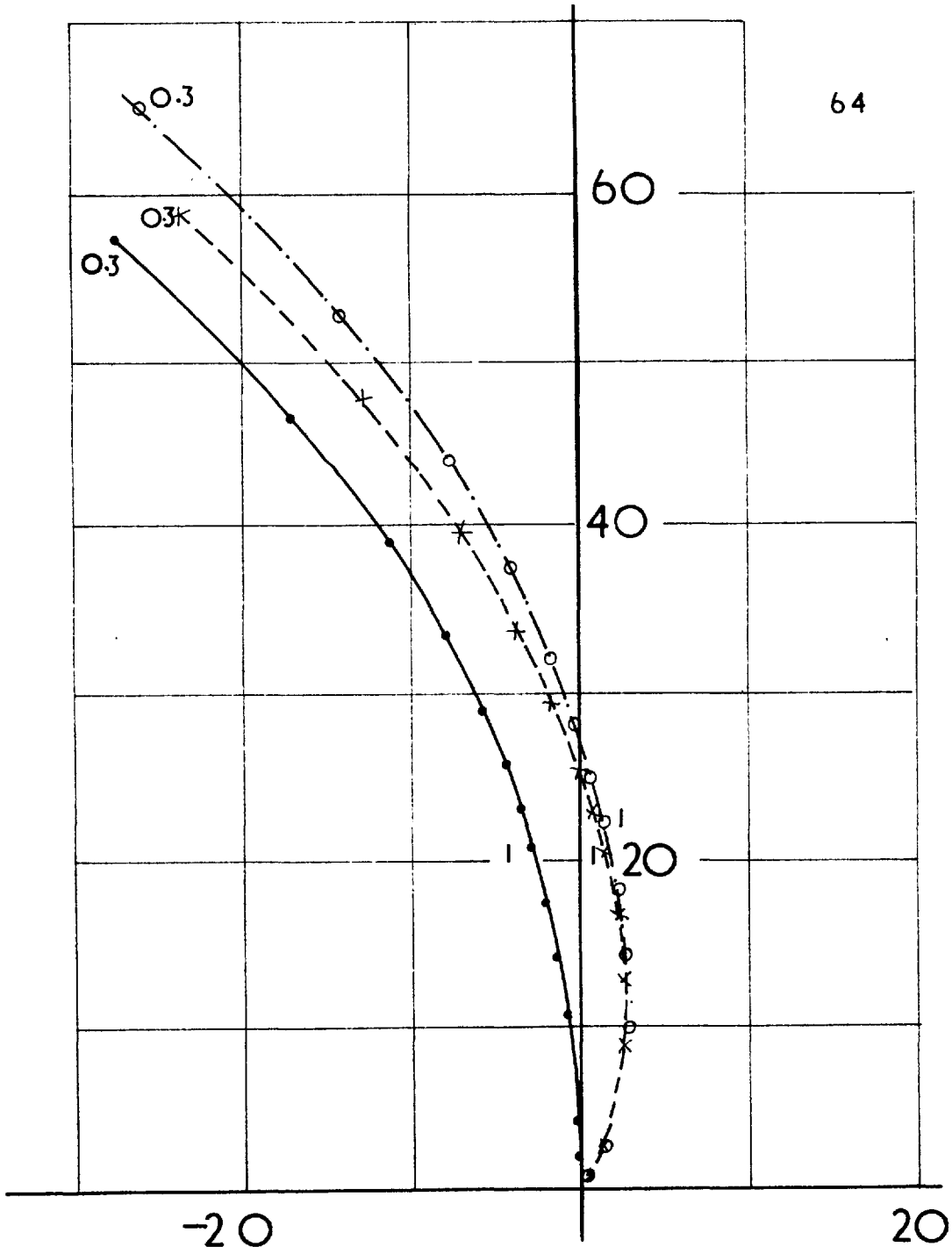

FIG.4.2b PLOTS OF $-A_{235}$ $\delta_g = 110°$

• ——— NO DAMPING

× - - - - DAMPING $r_a = 0$

⊙ —·—·— DAMPING AND r_a

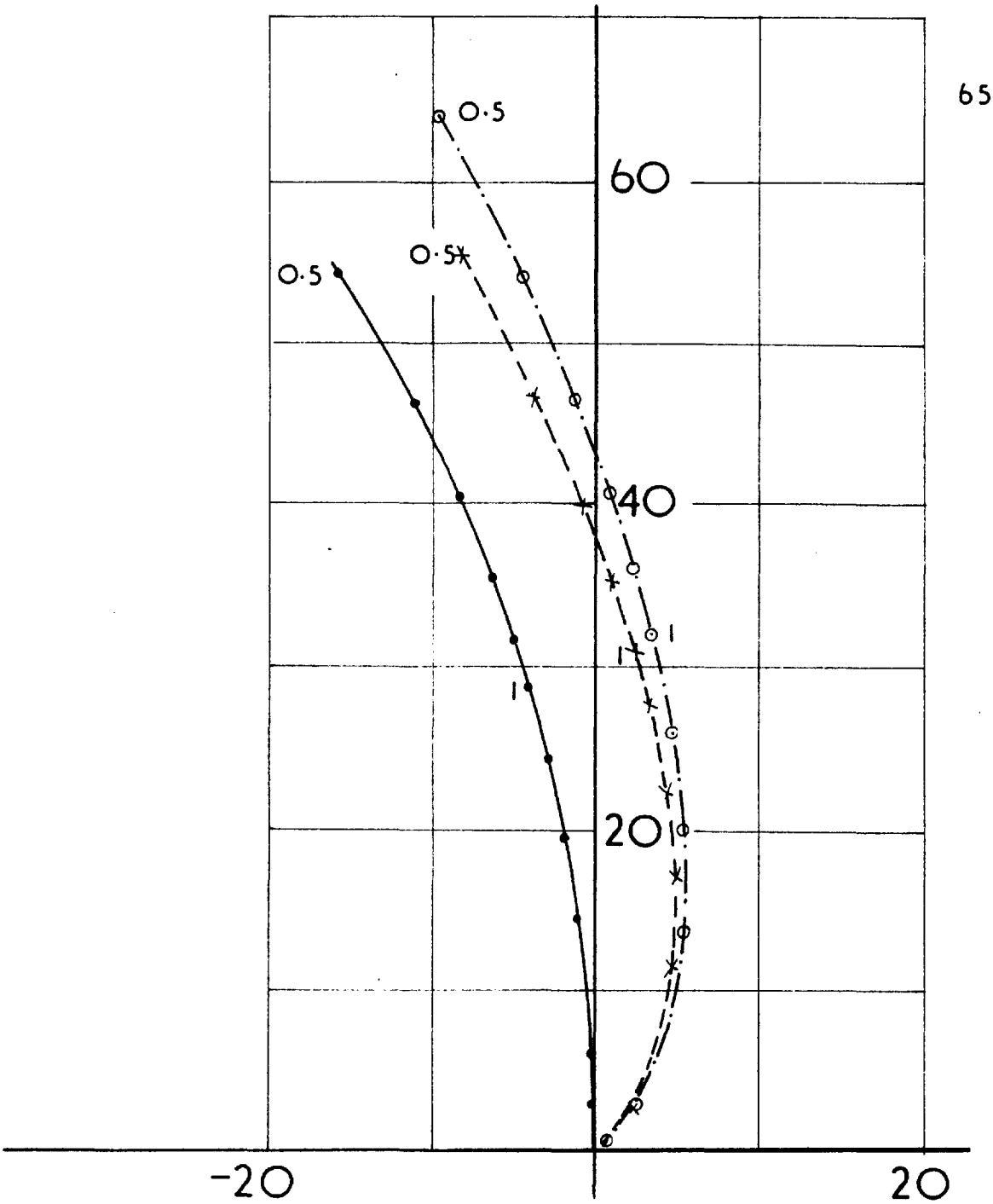

FIG.4.2c PLOTS OF $-A_{235}$ $\delta_g = 140°$

• ——— NO DAMPING

x - - - - DAMPING $r_a = 0$

⊙ —·—·— DAMPING AND r_a

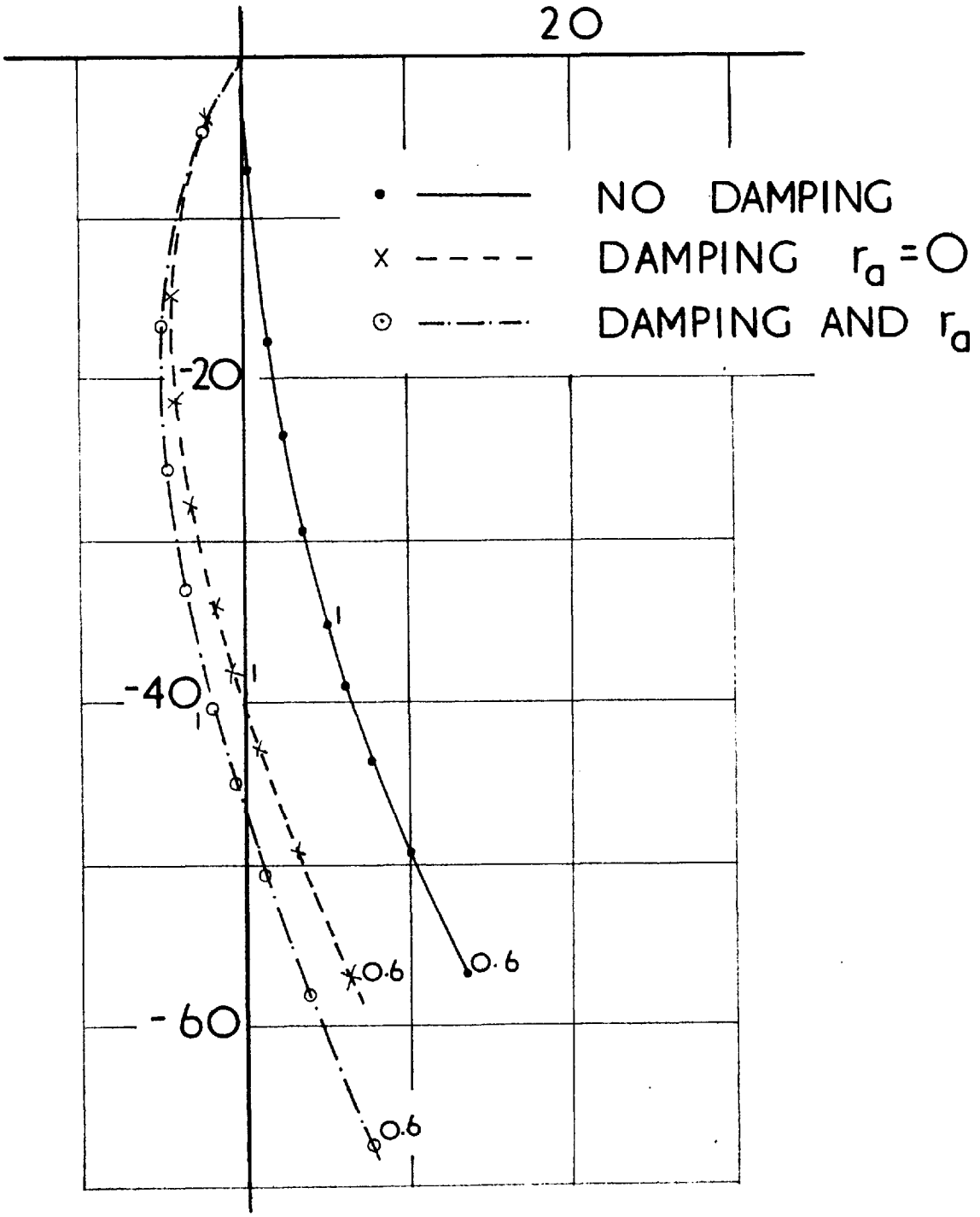

FIG 4.2d PLOTS OF $-A_{235}$ $\delta_g = 165°$

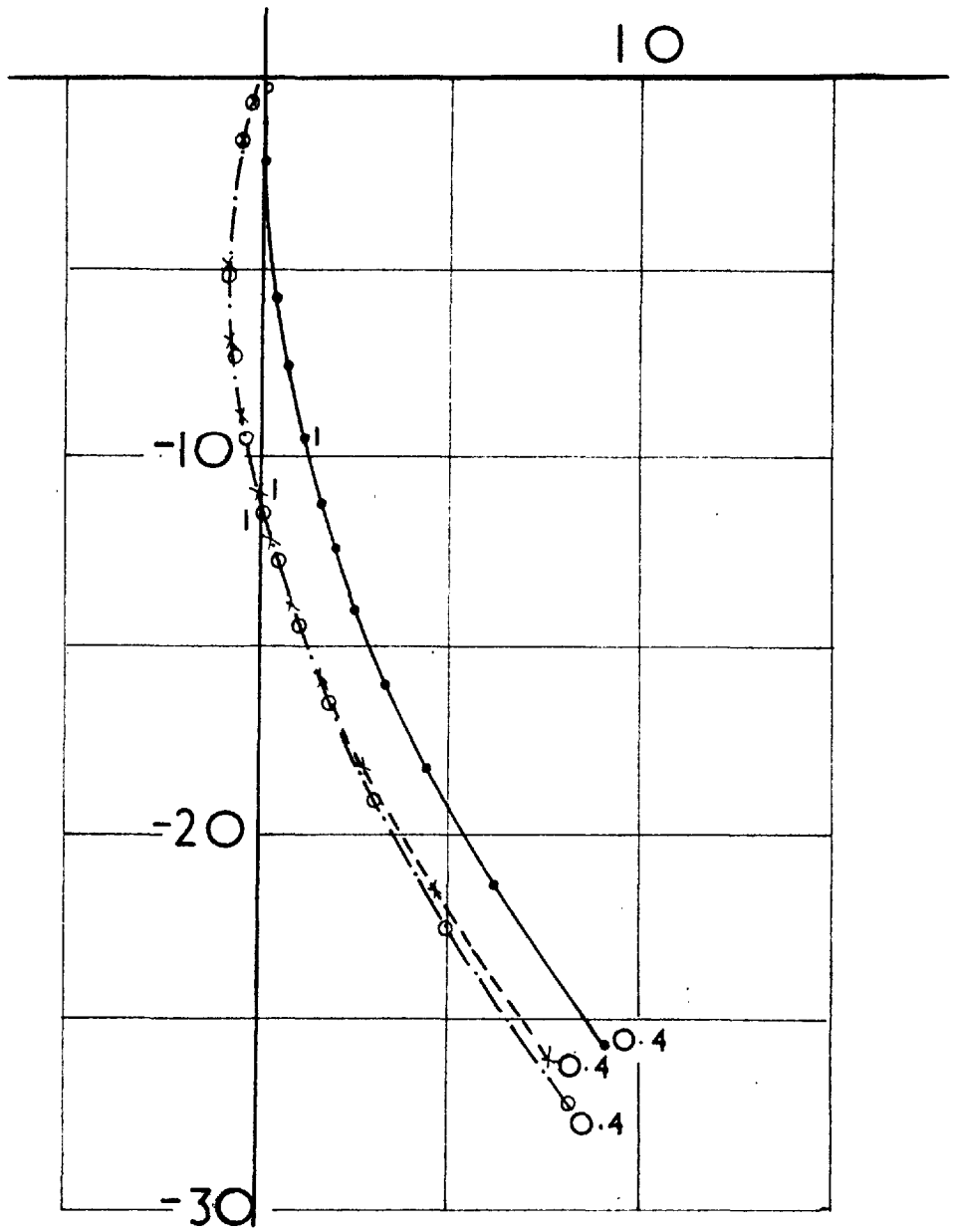

FIG. 4.3a PLOTS OF $-A_{245}$ $\delta_g = 80°$

• ——— NO DAMPING

x - - - - DAMPING $r_a = 0$

⊙ —·—·— DAMPING AND r_a

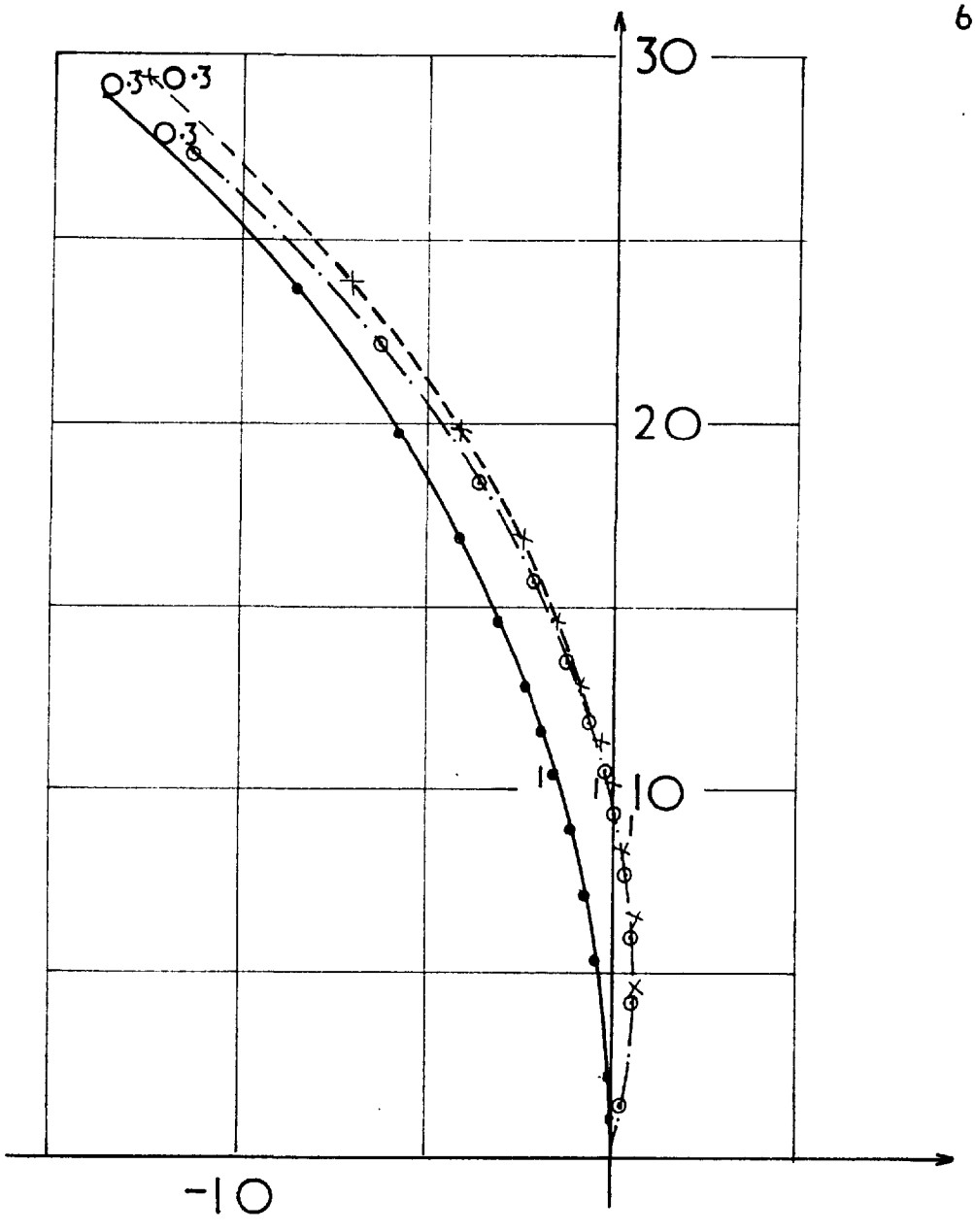

FIG. 4·3b PLOTS OF $-A_{245}$ $\delta_g = 140°$

• ——— NO DAMPING

× - - - - DAMPING $r_a = 0$

⊙ —·—·— DAMPING AND r_a

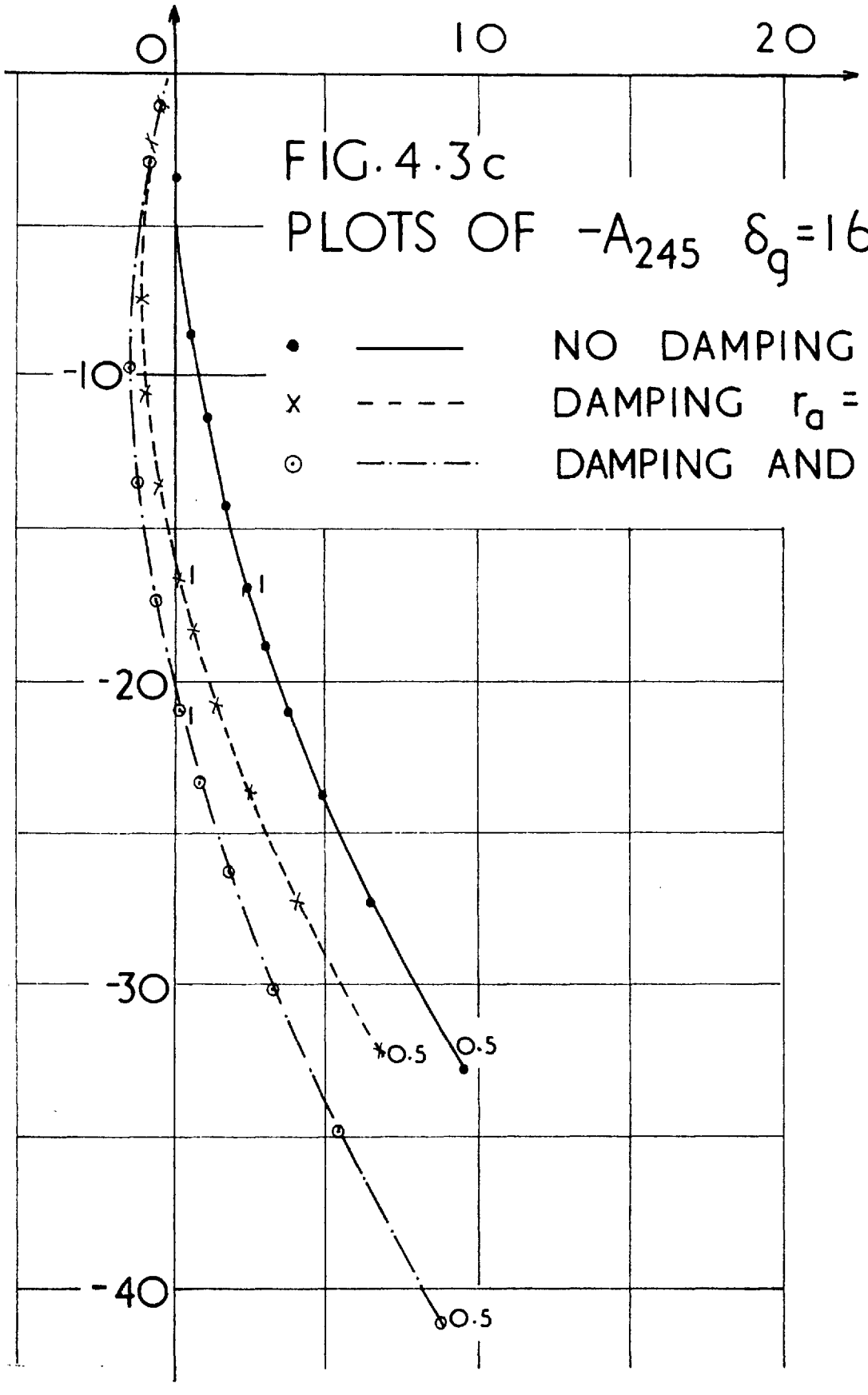

FIG. 4.3c
PLOTS OF $-A_{245}$ $\delta_g = 165°$

for the operational admittances in partial fraction form. For the derivation see Ref. 52-3.

$$Y_d(j\lambda) = Y_d + (Y'_d - Y_d)\frac{j\lambda T'_d}{1 + j\lambda T'_d} + (Y''_d - Y'_d)\frac{j\lambda T''_d}{1 + j\lambda T''_d} \tag{4.1}$$

$$Y_q(j\lambda) = Y_q + (Y''_q - Y_q)\frac{j\lambda T''_q}{1 + j\lambda T''_q} \tag{4.2}$$

Also

$$F(j\lambda) = \frac{G(j\lambda)}{X_d(j\lambda)} = \frac{X_{md}}{r_f X_d}\,\frac{(1 + j\lambda T_{kd})}{(1 + j\lambda T'_d)(1 + j\lambda T''_d)} \tag{4.3}$$

If damping is neglected the last term in each of Eqns. (4.1) and (4.2) is zero and $F(j\lambda)$ is simplified to

$$F(j\lambda) = \frac{X_{md}}{r_f X_d}\,\frac{1}{(1 + j\lambda T'_d)} \tag{4.4}$$

4.1 The Locus of A_{135}.

Substituting Eqns. (4.1) and (4.2) into Eqns. (2.14) neglecting damping, we have,

$$A_{135} = -\left(Q_o + V_{qo}^2 Y_q + V_{do}^2 Y_d + V_{do}^2(Y'_d - Y_d)\frac{j\lambda T'_d}{1 + j\lambda T'_d}\right) \tag{4.5}$$

Thus the locus is a semicircle with diameter $V_{do}^2(Y'_d - Y_d)$ and a time constant of T'_d, see Fig. 4.1 full line. Since $V_{do} = V \sin \delta_o$ the diameter of the locus is reduced as δ_g is increased beyond 90^o. Also Q_o, the reactive power, becomes more negative as δ_g is increased and, as shown in Fig. 4.4, $A_{135}(0)$ is rapidly increased at large values of δ_g

Define S_o and S'_o as follows:

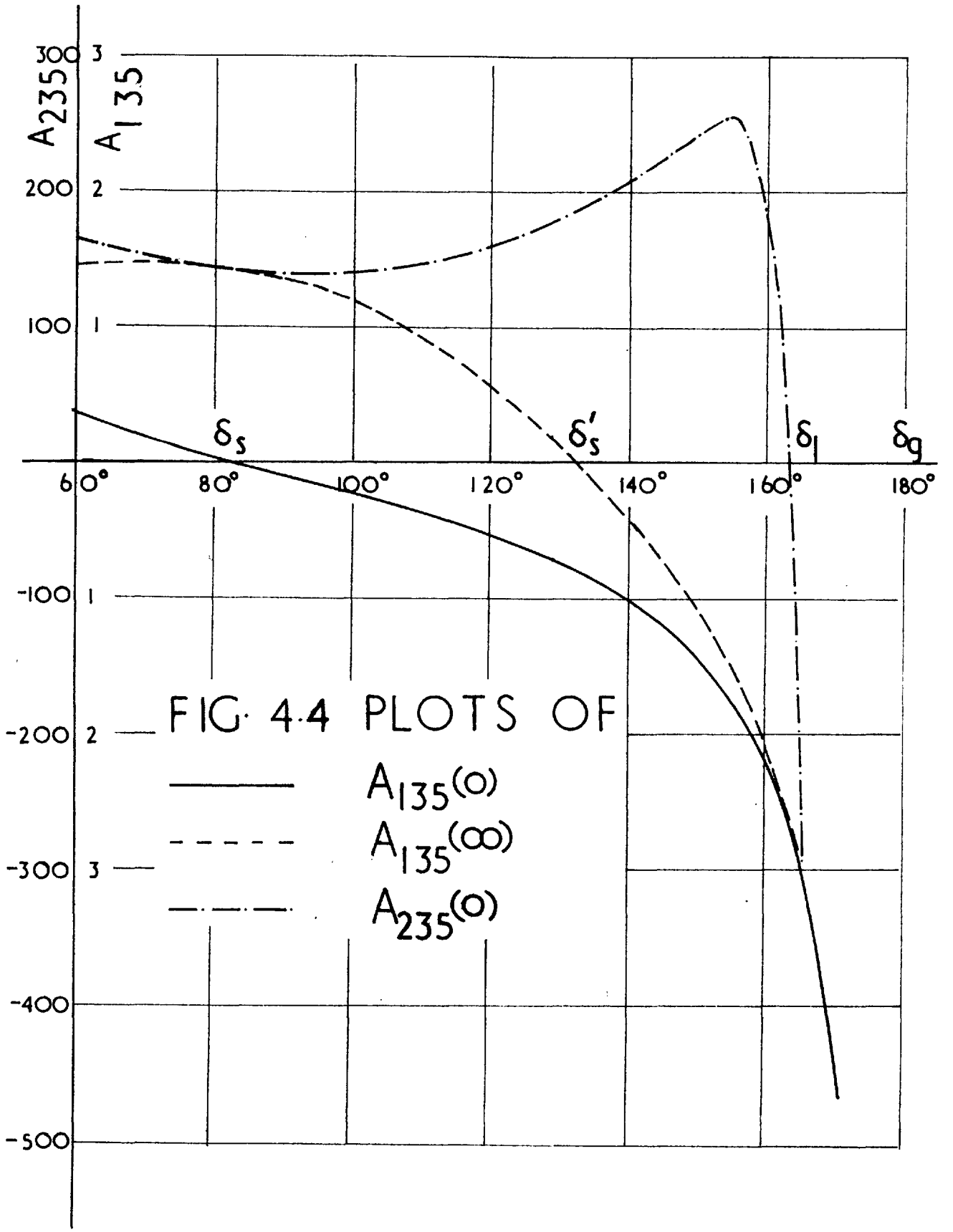

FIG. 4.4 PLOTS OF

$$S_o = Q_o + V_{qo}^2 Y_q + V_{do}^2 Y_d \qquad (4.6)$$

$$S'_o = Q_o + V_{qo}^2 Y_q + V_{do}^2 Y'_d \qquad (4.7)$$

It can easily be verified that,

$$A_{135} = - \frac{S_o + j\lambda T'_d S'_o}{1 + j\lambda T'_d} = \frac{a + j\lambda b}{1 + j\lambda T'_d} \quad \text{say} \qquad (4.8)$$

The functions S_o and S'_o are important quantities in synchronous machine theory. Substituting for Q_o, V_{qo} and V_{do} we have,

$$S_o = \frac{V_o V}{X_d} \cos \delta_o + V^2 \left(\frac{1}{X_q} - \frac{1}{X_d}\right) \cos 2\delta_o \qquad (4.9)$$

$$S'_o = \frac{V'_o V}{X'_d} \cos \delta_o + V^2 \left(\frac{1}{X_q} - \frac{1}{X'_d}\right) \cos 2\delta_o \qquad (4.10)$$

where V'_o is the q-axis component of the voltage behind the transient reactance. The right hand sides of Eqns. (4.9) and (4.10) are the well known expressions for the slopes of the power-angle curves for the steady state and the transient condition respectively, see Ref. 47-1. The peak of the steady power angle curve corresponds to the steady state stability limit in the conventional theory. Hence, when r_a is neglected δ_s is calculated from,

$$S_o = 0 \qquad (4.11)$$

The concept of a transient power-angle curve is used in approximate transient stability calculations where the rotor flux linkages are assumed constant. It is apparent that Eqn. (4.10) is obtained from Eqn. (4.9) if X_d is replaced by X'_d. Corresponding to Eqn. (4.11) let the value obtained from

$$S'_o = 0 \qquad (4.12)$$

be denoted by δ'_s . Fig. 4.4 shows the variation of S_o and S'_o with δ_g at P = 0.8 p.u. Both curves tend to (-) infinity as $\delta_g \longrightarrow 180^\circ$.

If the effect of damping is taken into account, with r_a still neglected, the complete expressions for $Y_d(j\lambda)$ and $Y_q(j\lambda)$ should be substituted in Eqn. (2.14) to give,

$$A_{135} = -\frac{S_o + j\lambda T'_d S'_o}{1 + j\lambda T'_d} + V_{do}^2 (Y''_d - Y'_d) \frac{j\lambda T''_d}{1 + j\lambda T''_d} + V_{qo}^2 (Y''_q - Y_q) \frac{j\lambda T''_q}{1 + j\lambda T''_q} \qquad (4.13)$$

Thus the original semicircular locus is modified by the addition of two semicircles of diameter $V_{do}^2 (Y''_d - Y'_d)$ and $V_{qo}^2 (Y''_q - Y_q)$ and with time constants T''_d and T''_q respectively. In practice T''_q and T''_d are of same order and the locus of A_{135} appears as the sum of two semicircles as shown in Fig. 4.1, dotted line.

Since $V_{qo} = V_m \cos \delta_o$ the effect of the q-axis damper is small at $\delta_g = 80^\circ$ or 110°. For both these angles then the locus of A_{135} is approximately a plot of $Y_d(j\lambda)$ to a different scale and to a different origin. At $\delta_g = 140^\circ$ however, V_{qo} is larger than V_{do} and since $(Y''_q - Y_q)$ is larger than $(Y'_d - Y_d)$ the effect of damping on the locus is very significant. As δ_g is further increased the transient semicircle is reduced and the effect of the q-axis damper predominates. Clearly, the effect of damping is a minimum when $\delta_g = 90^\circ$ and a maximum when $\delta_g = 180^\circ$ or 0 . One of the significant changes brought about by damping is the increase in the imaginary part of the locus at frequencies in the region of 1 c/s.

The contribution of the r_a terms on $A_{135}(o)$ is small and it is not obvious why it should change sign between $\delta_g = 110^\circ$ and 140° . The same applies to $A_{135}(\infty)$ where the change of sign of the effect of r_a occurs between 140° and 165° . For frequencies in the region of 1 c/s the imaginary part of A_{135} is consistently increased although by an amount

smaller than that of damping alone. The change on the real part of A_{135} at 1 c/s, except for $\delta_g = 165^\circ$ is comparable with the change produced by damping alone.

Fig. 4.1 shows that the locus of A_{135} is considerably affected by damping and r_a. It should be noted, however, that the critical frequencies of the system are low and that the errors involved by neglecting damping and r_a, although significant, are not as large as it may appear at first sight.

4.2 The Locus of A_{235}.

Neglecting damping and substituting Eqns. (4.1), (4.2) and (4.4) into Eqn. (2.15) we have,

$$A_{235} = \frac{X_{md}\, X_c}{r_f\, X_d} \cdot \frac{(Q_o X_c + V^2)\,(I_{do} + V_{qo} Y_q)}{V_{to}(1 + j\lambda T'_d)} = \frac{c}{1 + j\lambda T'_d} \qquad (4.14)$$

where c is defined here. The locus is a semicircle with "time constant" T'_d. Only part of the semicircle is shown in Fig. 4.2 for frequencies higher than 0.5 c/s to show the effect of damping and r_a (see below). The rest of the locus is a semicircle completely determined by $A_{235}(0)$, a graph for which is shown in Fig. 4.4.

$(I_{do} + V_{qo} Y_q)$ corresponds to OA in Fig. 2.1 and is therefore approximately proportional to V_o i.e. proportional to i_f. As δ_g is increased above 90° $(I_{do} + V_{qo} Y_q)$ increases tending to $+\infty$ as $\delta_g \longrightarrow 180^\circ$. $(Q_o X_c + V^2)$ is positive for small δ_g but is continuously reduced as δ_g is increased. Thus $A_{235}(0)$ does not change much until $(Q_o X_c + V^2)$ approaches zero, see Fig. 4.4. The value of δ_g when this happens is important. From the phasor diagram, Fig. 2.1

$$Q_o X_c + V^2 = V\, V_{to} \cos(\delta_o - \delta_t)$$

Thus A_{235} becomes zero when the angle between the infinite bus and the machine terminal voltage becomes 90°. Let the corresponding value of δ_g

be denoted by δ_1 . For the experimental machine $\delta = 163.2^\circ$, see Fig. 4.4.

When damping is taken into account the terms affected, see Eqn. (2.15) are $F(j\lambda)$ and $(I_{do} + V_{qo}Y_q(j\lambda))$. $F(j\lambda)$ is changed by the addition of two terms, see Eqn. (4.3) and for the frequencies in the region of 1 c/s the effect is mainly an increase of phase-shift with a small attenuation. The change of $F(j\lambda)$ affects all the loci for the four angles in the same way. The effect of damping on $(I_{do} + V_{qo}Y_q(j\lambda))$ depends on the operating condition and again for frequencies in the region of 1 c/s the change is mainly phase-shift with a small attenuation. For $\delta_g = 90^\circ$ the change is in the opposite direction from the change in $F(j\lambda)$. Thus for $\delta_g = 80^\circ$, see Fig. 4.2a the difference between the full line (no damping) and the dotted line (damping is not large). For $\delta_g > 90^\circ$ the sign of V_{qo} changes and its value is increased as δ_g increases. Hence the difference between the two cases, with and without damping is increased, see Figs. 4.2b and c. However I_{do} is also increasing with increasing δ_g and Fig. 4.2d shows that the effect of damping for $\delta_g = 165^\circ$ is of the same order as for $\delta_g = 140^\circ$.

For the four cases quoted in Fig. 4.2 the effect of resistance is to increase the phase-shift but to reduce the attenuation for a given frequency. It should be noted that, although the effect of r_a appears at first sight to be insignificant, the phasor difference is approximately the same as between damping and no damping.

4.3 The Loci of A_{245} and A_{145}.

Consider A_{245} first. Neglecting damping in Eqn. (2.16) we have

$$A_{245} = - \frac{X_{md} X_c (V_{qo} + X_c I_{do})}{r_f X_d V_{to}(1 + j\lambda T'_d)} = \frac{d}{(1 + j\lambda T'_d)} \qquad (4.15)$$

where d is defined here. The locus, like that for A_{235} , is a semi-circle with time constant T'_d and tends to zero as $\lambda \longrightarrow \infty$. Fig. 4.3 shows plots of A_{245} for the same load angles as before except that $\delta_g = 110^\circ$ is not included. It may be seen from Fig. 4.5, which shows a

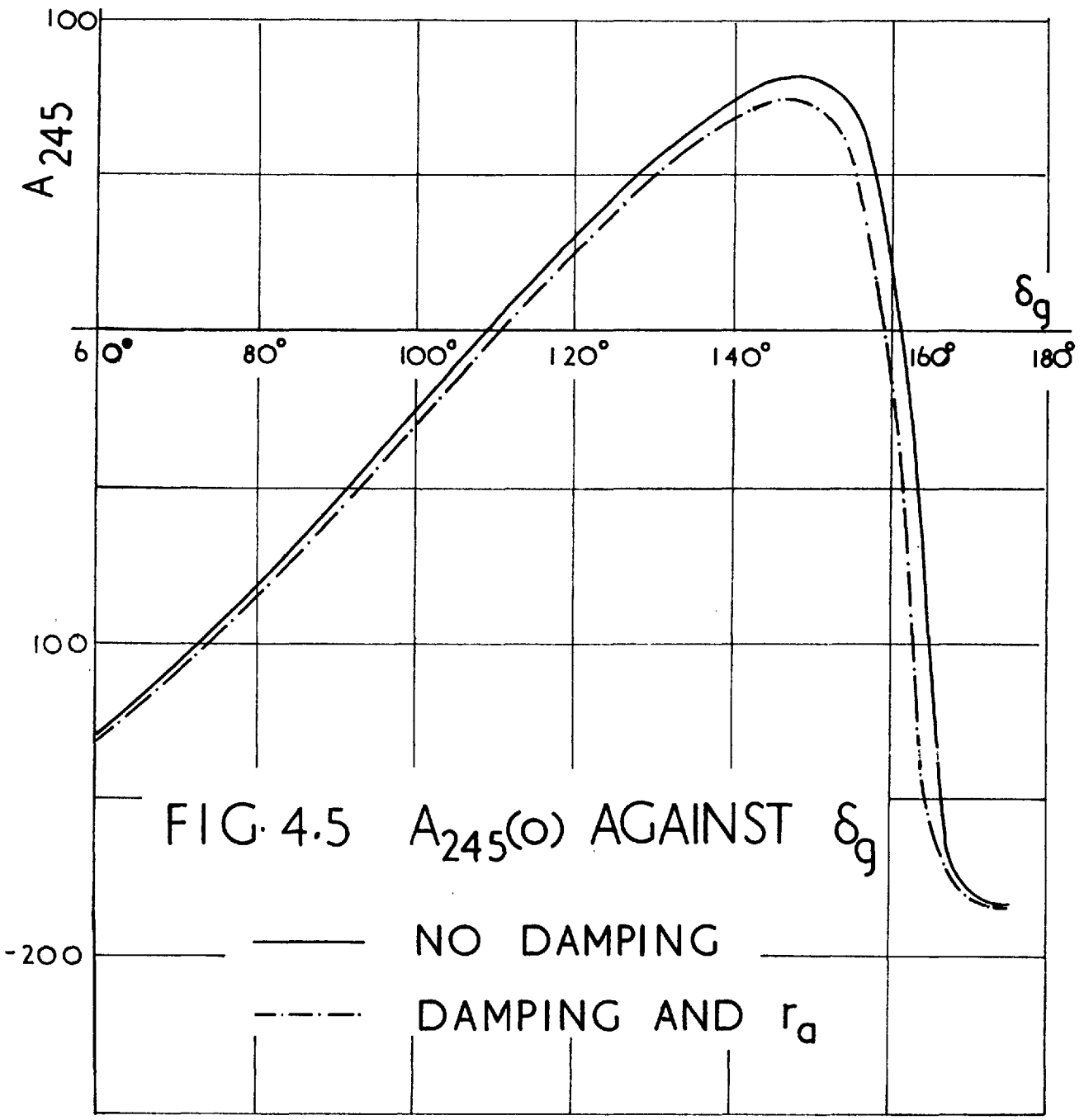

FIG. 4.5 $A_{245}(o)$ AGAINST δ_g

graph of A_{245} against δ_g, that at $\delta_g = 110^\circ$ $A_{245}(0)$ happens to be approximately zero. Again only frequencies from 0.5 c/s are considered.

It may be deduced from the phasor diagram, Fig. 2.1 that

$$\frac{V_{qo} + X_c I_{do}}{V_{to}} = \cos \delta_t \qquad (4.16)$$

Hence $A_{245}(0)$ is proportional to $\cos \delta_t$ and Fig. 4.5 shows, in effect, how $\cos \delta_t$ varies with δ_g. Apparently δ_t increases, numerically as δ_g is increased and has a maximum value when δ_g is about 150°. Then it is rapidly reduced and tends to zero as $\delta_g \longrightarrow 180^\circ$.

The only term affected by damping is $F(j\lambda)$. The dotted curves in Fig. 4.3 show an increased phase-shift with a small attenuation as before with the A_{235} locus (section 4.2). It should be noted that the locus of A_{245}, irrespective of the operating point, is the same as the locus of $F(j\lambda)$ to a different scale, i.e. the effect of damping is independent of δ_g.

Fig. 4.5 shows that $A_{245}(0)$ is reduced when the effect of r_a is included. The additional term containing the armature resistance includes $(V_{do} - X_c I_{qo})$, see Appendix II. Thus, from the phasor diagram, Fig. 2.1, the effect of the armature resistance is proportional to $\sin \delta_t$. Considering Figs. 4.3 a and b only it may be seen that the effect of r_a is approximately the same. Since $A_{245}(0)$ has a different sign in each case the effect of r_a on the magnitude of $A_{245}(j\lambda)$ is to increase it at $\delta_g = 80^\circ$ and to reduce it at $\delta_g = 140^\circ$, for λ in the region of 0.5 to 1c/s. The locus for $\delta_g = 165^\circ$ is considerably modified by r_a as shown in Fig. 4.3 c.

The locus of A_{145} is constant and equal to unity if r_a is neglected. Although Eqn. (II.4) shows that r_a has some effect, in practice unless r_a is very large it may be neglected. For the experimental machine the worst case involves a phasor of magnitude 0.006+j 0.002. Thus from now on A_{145} is assumed to be equal to unity.

5. ANALYSIS OF STABILITY BASED ON TORQUE FEEDBACK

The torque feedback method forms the link between the conventional approach to the stability of synchronous machines, using the synchronising and damping torques, and the method of small oscillations using the Nyquist test. The unregulated machine is a special case of the complete system with the regulator gain set to zero and can be analysed by both methods. Since this section is intended to link the two approaches the effects of rotor damping and of the armature resistance are neglected. Also only the simple regulator is considered.

Expressions for the synchronizing and damping torques for the regulated machine are developed. These should be useful when the operational characteristics of a synchronous machine with a voltage regulator are investigated.

5.1 General Considerations.

For the torque feedback method the system is represented by Fig. 1.5 and the open loop transfer function has been determined, see Eqn. (2.19). With the simple type of regulator that is considered in this section $K(j\lambda)$ is a constant,

$$K(j\lambda) = K \qquad (5.1)$$

Eqn. (2.19) becomes,

$$\frac{\Delta T_e}{\Delta T_i} = \frac{A_{135} + K K_o A_{235}}{J\lambda^2(1 + K K_o A_{245})} \qquad (5.2)$$

Fig. 1.5 has been drawn to agree with the equations and the forward and feedback branches are not physically separable. The action however, may be visualised as follows. The disturbance is introduced at ΔT_m and an error torque ΔT_i acts on the machine inertia to produce $\Delta\delta$ in the forward branch. $\Delta\delta$ in the alternator produces the

electromagnetic torque ΔT_e in the feedback branch. The difference between the electromagnetic and the turbine torques is ΔT_i.

The function $\phi(j\lambda)$, in Fig. 1.5 is given by

$$\phi(j\lambda) = \frac{\Delta T_e}{\Delta \delta} = \frac{A_{135} + K K_o A_{235}}{1 + K K_o A_{245}} \qquad (5.3)$$

It is found convenient to plot the Nyquist locus in two steps

(i) Plot $\phi(j\lambda)$.

(ii) Divide each point of the $\phi(j\lambda)$ plot by $J\lambda^2$ to obtain the Nyquist plot. It should be noted that this step introduces a double pole at the origin and by section AIII.3 the Nyquist locus describes a full clockwise circle, with "infinite radius" as λ goes through zero.

5.2 The System without a Regulator.

With $K = 0$ the open loop transfer function becomes,

$$\frac{\Delta T_e}{\Delta T_i} = \frac{\phi(j\lambda)}{J\lambda^2} = \frac{A_{135}}{J\lambda^2} \qquad (5.4)$$

It is shown in section 4.1 that, if the armature resistance and damping are neglected, the locus of A_{135} is a semicircle as shown by the full lines of Fig. 4.1. It is apparent from the expression for A_{135}, Eqn. 2.14 that A_{135} does not have any poles with positive real parts and thus for the application of the Nyquist test $P = 0$.

The locus of $\phi(j\lambda)$ for $\delta_g = 80^\circ$ is drawn, not to scale, in Fig. 5.1 a together with the corresponding Nyquist locus. The $(-1, 0)$ point is not encircled by the latter and therefore the system is stable for $\delta_g = 80^\circ$. Figs. 5.1 b and c show the $\phi(j\lambda)$ loci for $\delta_g = 110^\circ$ and 140° respectively, together with the corresponding Nyquist loci. In both cases there is one encirclement of the $(-1, 0)$ point and for

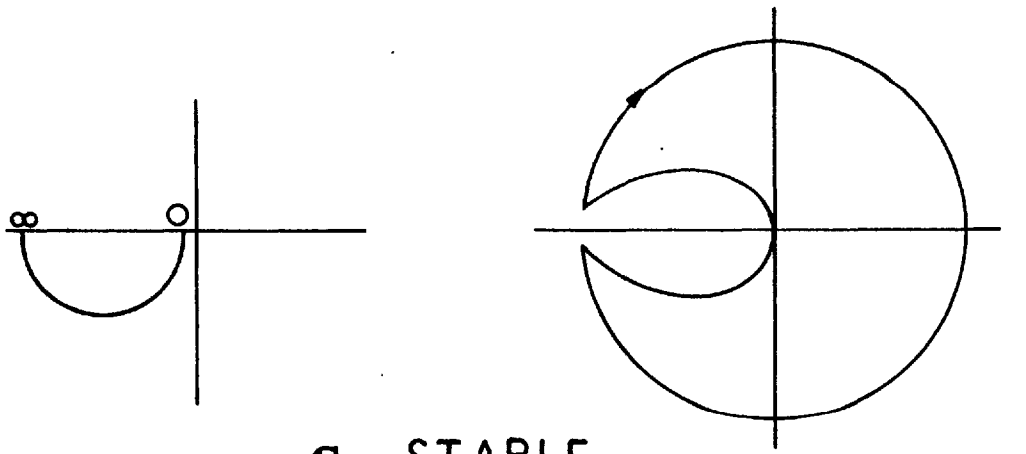

a STABLE

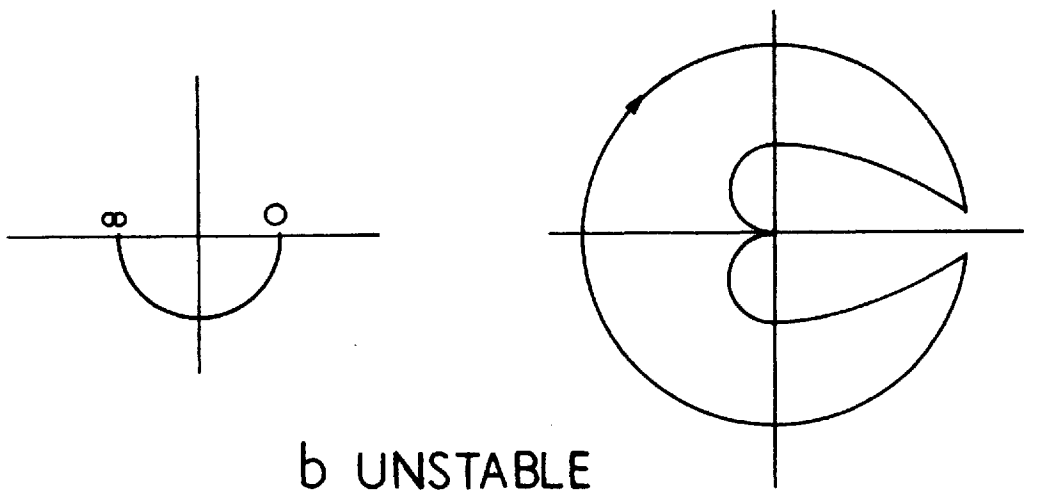

b UNSTABLE

$\phi(j\lambda)$ Loci Nyquist Loci

FIG. 5.1 TORQUE FEEDBACK DIAGRAMS

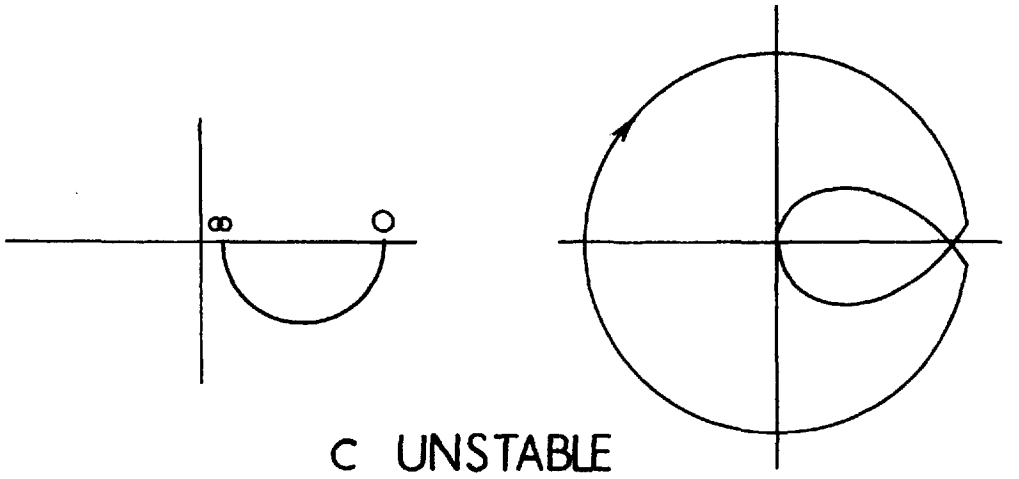

c UNSTABLE

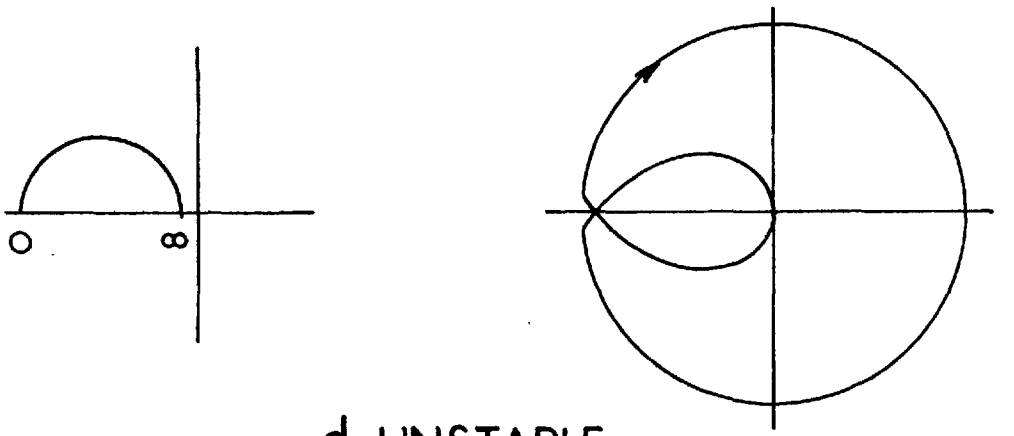

d UNSTABLE

$\emptyset(j\lambda)$ Loci Nyquist Loci

FIG. 5.1 TORQUE FEEDBACK DIAGRAMS

both these angles the system is unstable. It is not necessary to consider the case $\delta_g = 165^\circ$ separately since the Nyquist locus has the same shape as that for $\delta_g = 140^\circ$ and therefore denotes an unstable system.

The change in the Nyquist locus from that of a stable to that of an unstable system occurs when $A_{135}(0)$ becomes positive. Thus the condition of stability for the system without a voltage regulator is

$$A_{135}(0) < 0$$

viz:

$$Q_o + V_{qo}^2 Y_q + V_{do}^2 Y_d > 0$$

The stability limit thus occurs when

$$S_o = 0 \qquad (5.5)$$

Comparison with Eqn. (4.9) shows that Eqn. (5.5) expresses the well known result for the stability limit of an unregulated machine, see Eqn. 4.11. Thus the Nyquist method gives the familiar result. The critical portion of the A_{135} locus is at low frequencies. The presence of rotor damper circuits does not, therefore, affect the steady state stability limits of an unregulated machine, as is well known. Moreoever, if the armature resistance is also taken into account the expression for $\phi(j\lambda)$ becomes

$$\phi(j\lambda) = \frac{A_{135}}{A_{145}} \qquad (5.6)$$

and it may be shown that the real and imaginary parts of $\phi(j\lambda)$ correspond to the synchronising and damping torques as follows;

$$\phi(j\lambda) = -(K_s + j\lambda K_d) \qquad (5.7)$$

In fact Eqn. (5.6) may be obtained from the expression given by Adkins[57-6]

for K_s and K_d if the rate of change of flux terms are neglected. See also Ref. 52-3.

In the conventional theory for stability $K_s > 0$ and this is of course the same as $\phi(0) < 0$ which is the result obtained from the Nyquist method.

It may be noted here that K_s and K_d are used for studying hunting of synchronous machines. If both K_s and K_d satisfy certain conditions then hunting is not possible. It can be shown that the same results may be obtained by the Nyquist method as applied in this section. The term hunting is conventionally applied to loss of steady state stability when there is no excitation regulator and this usually occurs at light loads. In this sense hunting lies outside the scope of the present investigation.

5.3 The System with a Simple Regulator.

The function $\phi(j\lambda)$ is given in Eqn. (5.3). If we substitute for A_{ijk} from Eqns. (4.8), (4.14) and (4.15) we have,

$$\phi(j\lambda) = \frac{(a + K K_o c) + j\lambda b}{(1 + K K_o d) + j\lambda T'_d} \qquad (5.8)$$

Eqn. (5.8) has the same form as Eqn. (4.8) and the locus of $\phi(j\lambda)$ is a semicircle for $\lambda = 0 \longrightarrow \infty$. Also

$$\phi(j\infty) = \frac{b}{T'_d} = A_{135}(j\infty)$$

i.e. the infinite frequency point of $\phi(j\lambda)$ is not affected by the presence of a regulator.

Before applying the Nyquist test to the locus of $\phi(j\lambda)$ the possibility of poles with positive real parts must be investigated.

From Eqn. (5.8), if $K.K_o\ d < -1$ then there is one such pole, i.e. $P = 1$ (see Appendix III). With the parameters of the experimental machine however this occurs at very high values of K and for the following discussion it is assumed that $P = 0$.

Figs. 5.2 and 5.3 show plots of $\phi(j\lambda)$ for $\delta_g = 80^\circ$ and 110° respectively for various values of K. The effect of increasing the gain is to shift the zero frequency point of the locus to the left. Considering Fig. 5.3, as the gain is increased $\phi(0)$ is reduced until it becomes negative, e.g. at $K = 5$. The position of the $\phi(j\lambda)$ locus is then the same as Fig. 5.1a and therefore the Nyquist locus shows no encirclement of the $(-1, 0)$ point. Hence the system is stable for this value of K. If, however the gain is further increased there comes a time when,

$$\phi(0) < \phi(j\infty)$$

and the locus of $\phi(j\lambda)$ goes over to the second quadrant, e.g. for $K = 15$. Fig. 5.1d shows that the Nyquist locus corresponding to this case encircles the $(-1, 0)$ point twice and hence the system is unstable. Thus, for $\delta_g = 110^\circ$ the regulator stabilizes the system only for a definite range of values of K. Fig. 5.2 shows that for large values of gain instability occurs even for $\delta_g = 80^\circ$, e.g. for $K = 150$.

Although a more detailed study for various load angles is deferred until section 7, it is worth pointing out here that as δ_g is increased the infinite frequency point of $\phi(j\lambda)$ moves to the right and eventually becomes positive. When this happens it is no longer possible to stabilise the system using a simple regulator with constant gain. Clearly this occurs at $\delta_g = \delta_s'$.

The concepts of the synchronizing and damping torques may be extended to include the regulated machine. To avoid confusion with the unregulated machine the 2nd suffix r is used.

FIG. 5.2 LOCI OF $\emptyset(j\lambda)$ $\delta_g = 80^\circ$

DIFFERENT REGULATOR GAINS

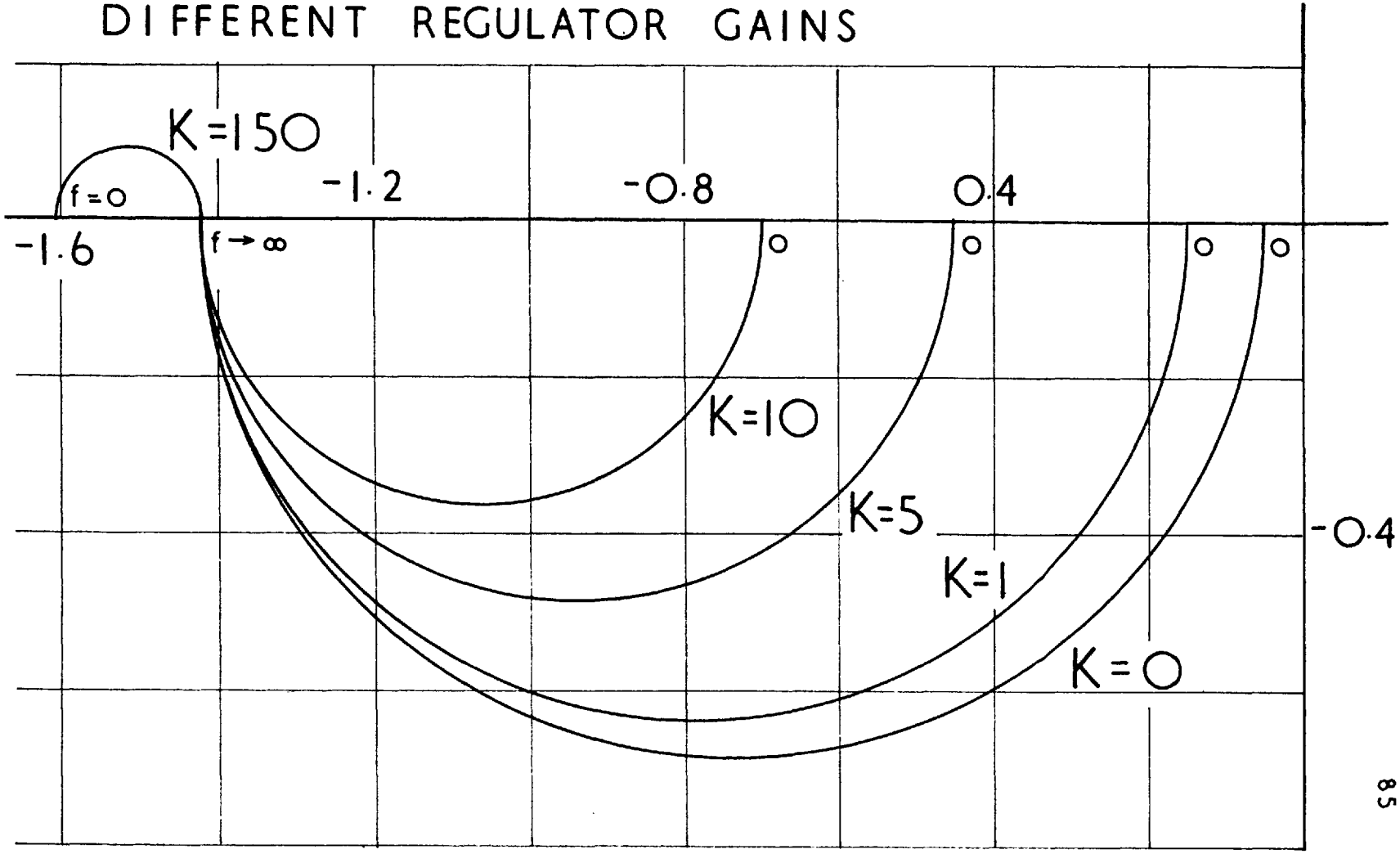

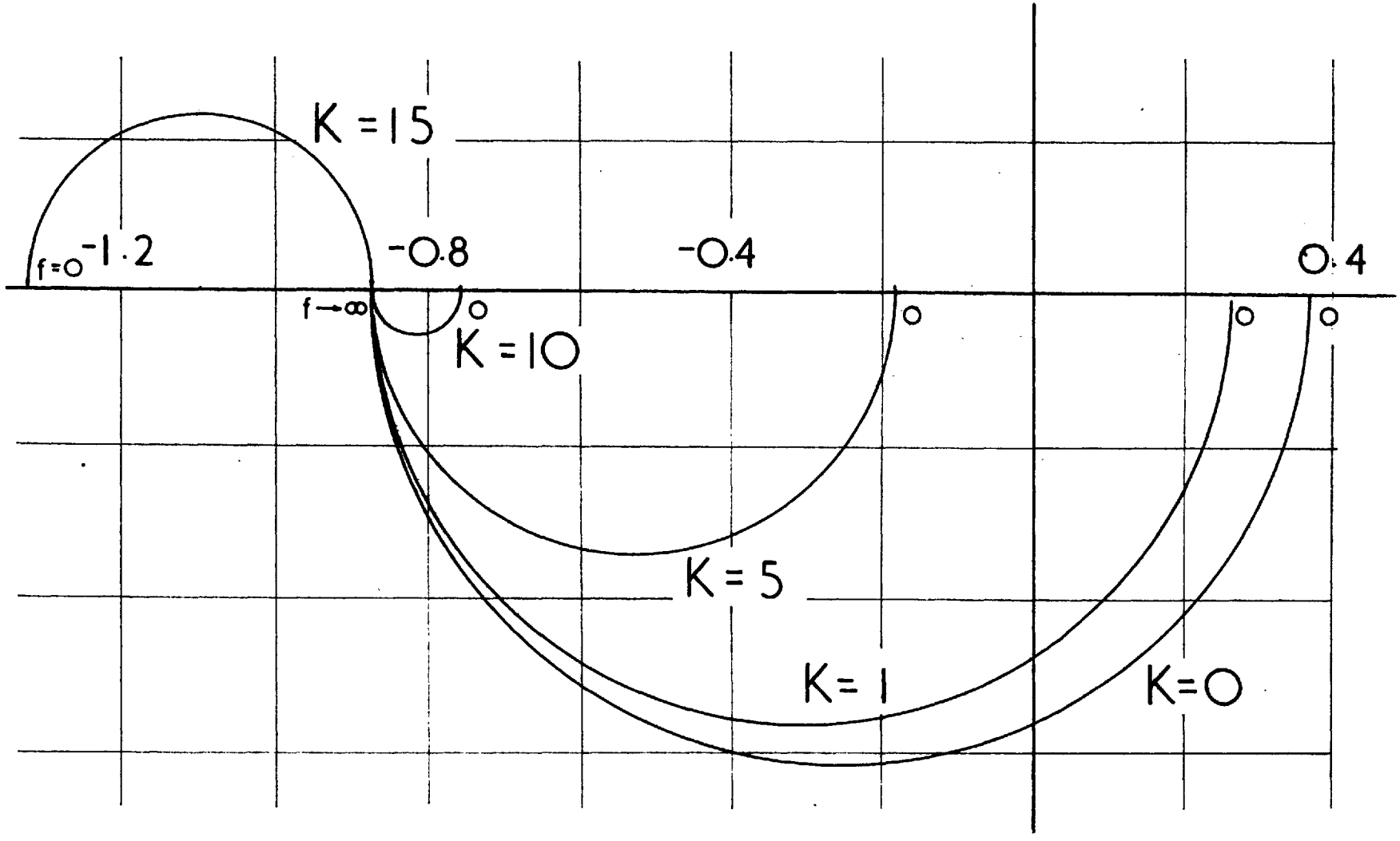

FIG. 5.3 LOCI OF $\emptyset(j\lambda)$ $\delta_g = 110^\circ$
DIFFERENT REGULATOR GAINS

$$K_{sr} + j\lambda K_{dr} = - \frac{A_{135} + K(j\lambda) K_o A_{235}}{1 + K(j\lambda) K_o A_{245}}$$

$$= - \phi(j\lambda) \qquad (5.9)$$

Thus Fig. 5.2 and 5.3 are plots of $-(K_{sr} + K_{dr})$. The action of the regulator may be considered simply as increasing the synchronizing torque while at the same time reducing the damping torque. For $\delta_g = 110^o$ and $K = 0$ there is a negative synchronizing torque and a large damping torque. As the gain is increased the synchronizing torque becomes less negative until eventually it becomes positive, and the system is then stable. Increasing the gain further, the synchronizing torque is increased, and at the same time the damping torque is reduced. Ultimately the damping torque becomes negative, $\phi(j\lambda)$ locus has a positive imaginary part and instability occurs. This argument may be thought of as a proof of the following statement by Doherty[28-1]. "The regulator affords increased synchronizing power, but does so at the expense of positive damping".

This process is illustrated very well by experiment, see section 9.1. If the gain is low the machine goes out of step soon after $\delta_g = \delta_s$, when the gain is increased the machine operates stably up to a maximum angle about δ_s', if the gain is further increased the system develops large oscillations of stable amplitude at an intermediate value of δ_g.

It should be noted that the only Nyquist locus implying a stable system is Fig. 5.1a and it corresponds to both K_{sr} and K_{dr} being positive. In general, however $K_{sr} > 0$ and $K_{dr} > 0$ is not a sufficient condition for stability and cannot be used to replace the Nyquist test.

The torque feedback method is an important link with the existing theory and an introduction to the more useful voltage feedback method. It suffers from one major disadvantage, that the effect of changing the regulator parameters is difficult to visualize. A change of gain requires a new calculation. Although this may not be so cumbersome

when damping is neglected, the task becomes more difficult if the effects of damping and armature resistance are taken into account, and still more when dealing with regulators, for which $K(p)$ is a complicated function.

Another difficulty with the torque diagram concerns the experimental verification of the theory. One could conceivably inject small oscillations in the torque of the prime mover and measure changes in load angle and electrical power output of the alternator. It is easier, however, to inject a voltage into the excitation system and to measure the voltage fed back by the regulator itself.

6. THE ALTERNATOR TRANSFER FUNCTION.

The present section is devoted to the shape and salient features of the transfer function of the alternator when the system is analysed by the Voltage Feedback Method. For reasons stated at the end of the last Chapter the Torque Feedback Method is abandoned and from now on the term alternator transfer function refers to that obtained by the Voltage Feedback Method.

The expression for the alternator transfer function is complicated and in order to determine the frequency response loci for the complete system including the armature resistance and damping recourse must be made to graphical and numerical work. All computations and numerical results quoted refer to the experimental machine, the parameters of which are given in Table II p.222. . It should be repeated here that the machine is assumed to operate at 0.8 p.u. power and that the infinite bus voltage is 1 p.u.

The expression for the frequency response locus is considerably simplified if the rotor damper circuits and the armature resistance are neglected. As before the procedure is first to examine the conditions algebraically with this simplification and then to consider the relation between the formulae and the shape of the locus. The rotor damper circuits and the armature resistance are then considered as modifying the simpler frequency response locus obtained when their effects are neglected. It is required to determine the nature of such modifications. In order to do this the functions A_{ijk} are combined together to form the loci for the numerator and for the denominator of the alternator transfer function. These loci are plotted for the three cases namely, a) without damping, $r_a = 0$, b) with damping but with $r_a = 0$ and c) with damping and including the effect of r_a.

It is convenient to define two new symbols. Let $L(j\lambda)$ be the

open loop transfer function of the system i.e.

$$L(j\lambda) = \frac{\Delta V_t}{\Delta V_{fe}} K_o K(j\lambda) \qquad (6.1)$$

and let

$$H(j\lambda) = \frac{\Delta V_t}{\Delta V_{fe}} K_o \qquad (6.2)$$

i.e. $H(j\lambda)$ is proportional to the alternator transfer function. Since K_o is introduced for convenience, see section 2.2, and affects only the units, $H(j\lambda)$ may be referred to as the alternator transfer function. Hence

$$H(j\lambda) = - \frac{r_f}{X_{md}} \cdot \frac{A_{235} + A_{245} J\lambda^2}{A_{135} + A_{145} J\lambda^2} \qquad (6.3)$$

6.1 The Locus of $H(j\lambda)$

Figs. 6.1 to 6.3 show several frequency response loci of $H(j\lambda)$. The computation would not have been possible except by means of a digital computer. Details of the programmes need not be considered here. It is sufficient to say that the first stage of the computation gave the functions A_{ijk} and $H(j\lambda)$ was obtained from them.

A complete family of $H(j\lambda)$ loci for load angles from 60° to 165° is shown in Fig. 6.1. Damping and armature resistance effects have been included. These are the main loci used in the subsequent calculation of the stability limit with different regulators. Since the algebraic analysis can only be made if both the rotor damping and the armature resistance are neglected Fig. 6.2 shows a comparison between the three cases for selected angles. The region round the origin is not clearly shown in either figure and so an enlarged plot is given in Fig. 6.3. The importance of this region lies in the fact that, for angles less than 70° the $H(j\lambda)$ does not cross the negative real axis.

FIG. 6.1 PLOTS OF $H(j\lambda)$

DAMPING AND r_a

FREQUENCY IN c/s

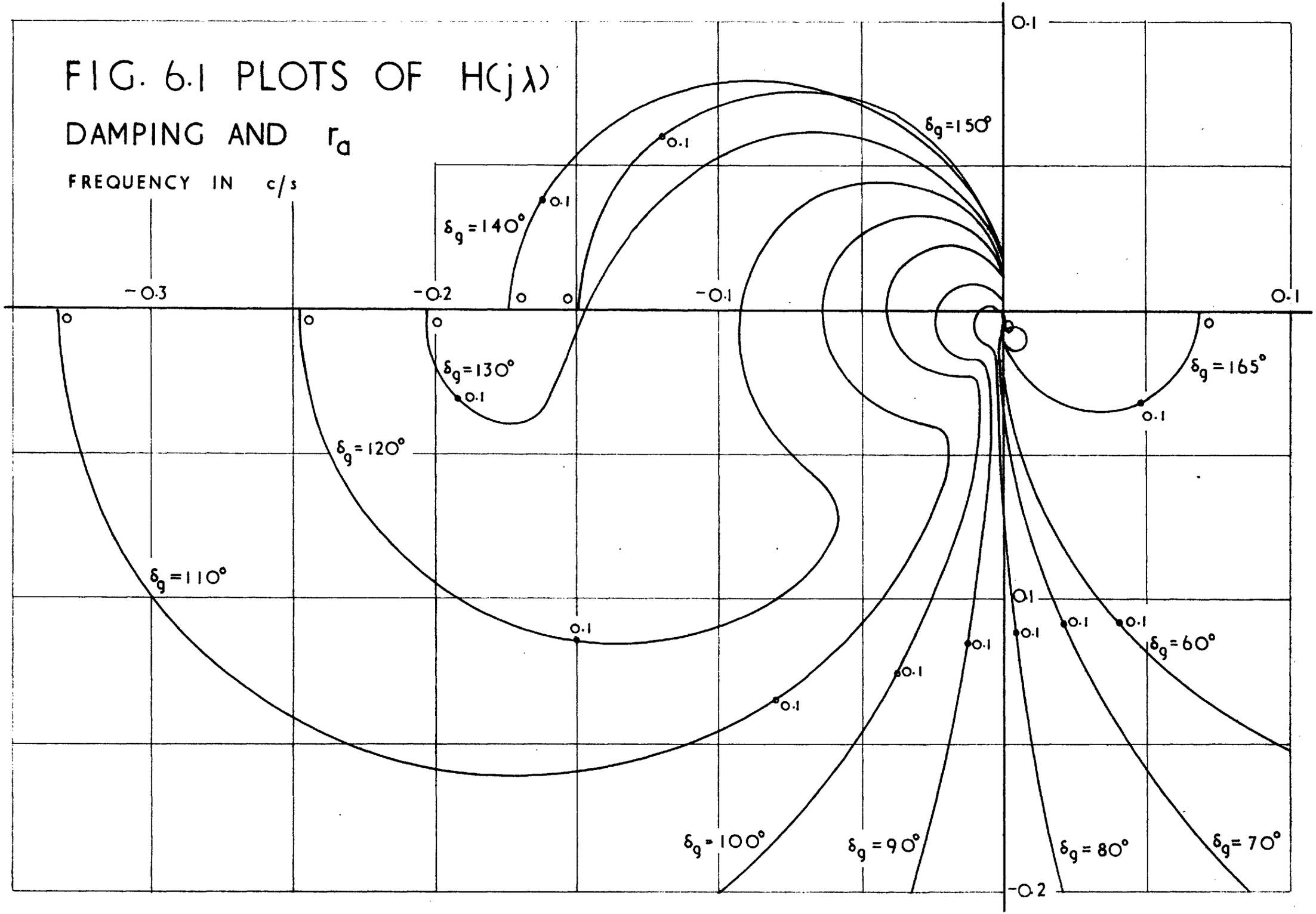

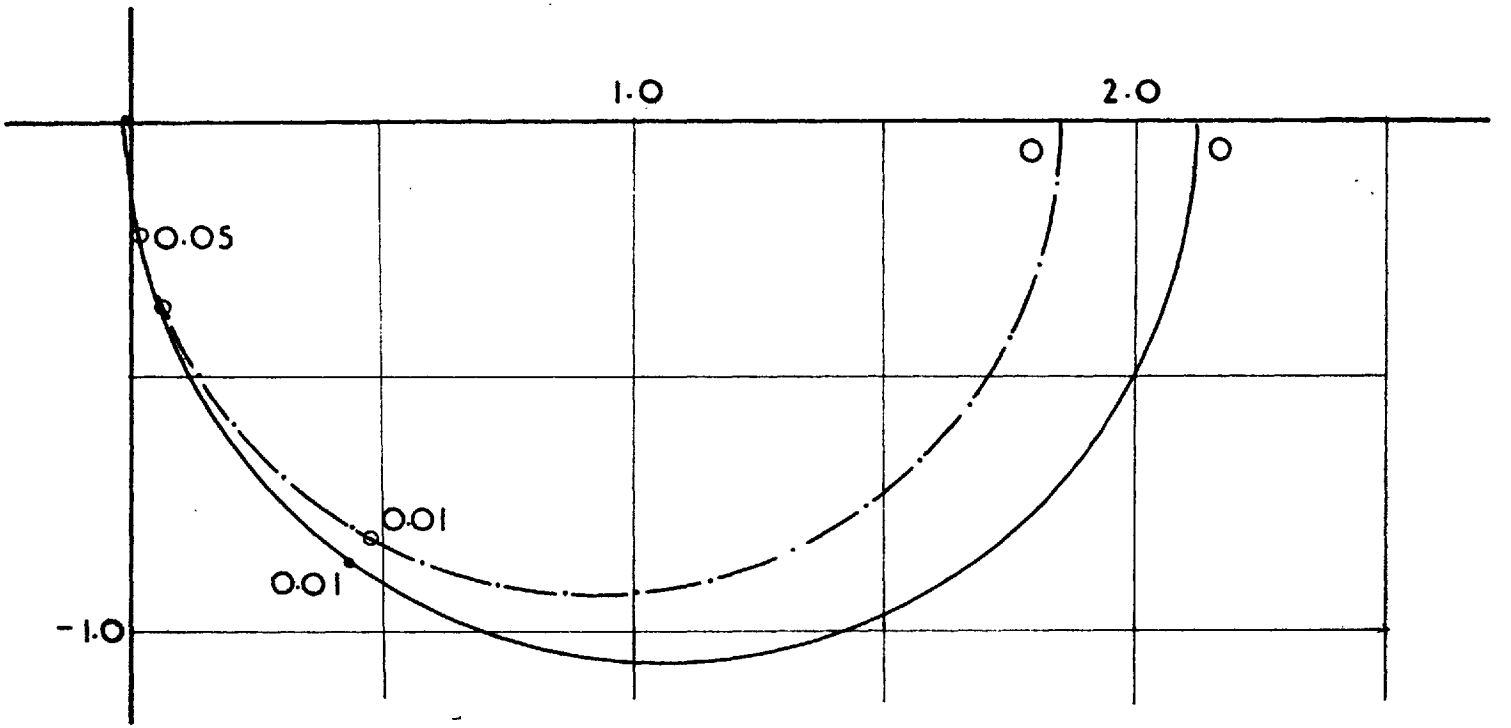

FIG. 6.2a PLOTS OF $H(j\lambda)$ $\delta_g = 80°$

• —— NO DAMPING

DAMPING $r_a = 0$ coincides with the no damping curve

⊙ —·—·— DAMPING AND r_a

FIG. 6.2b
PLOTS OF $H(j\lambda)$ $\delta_g = 110°$

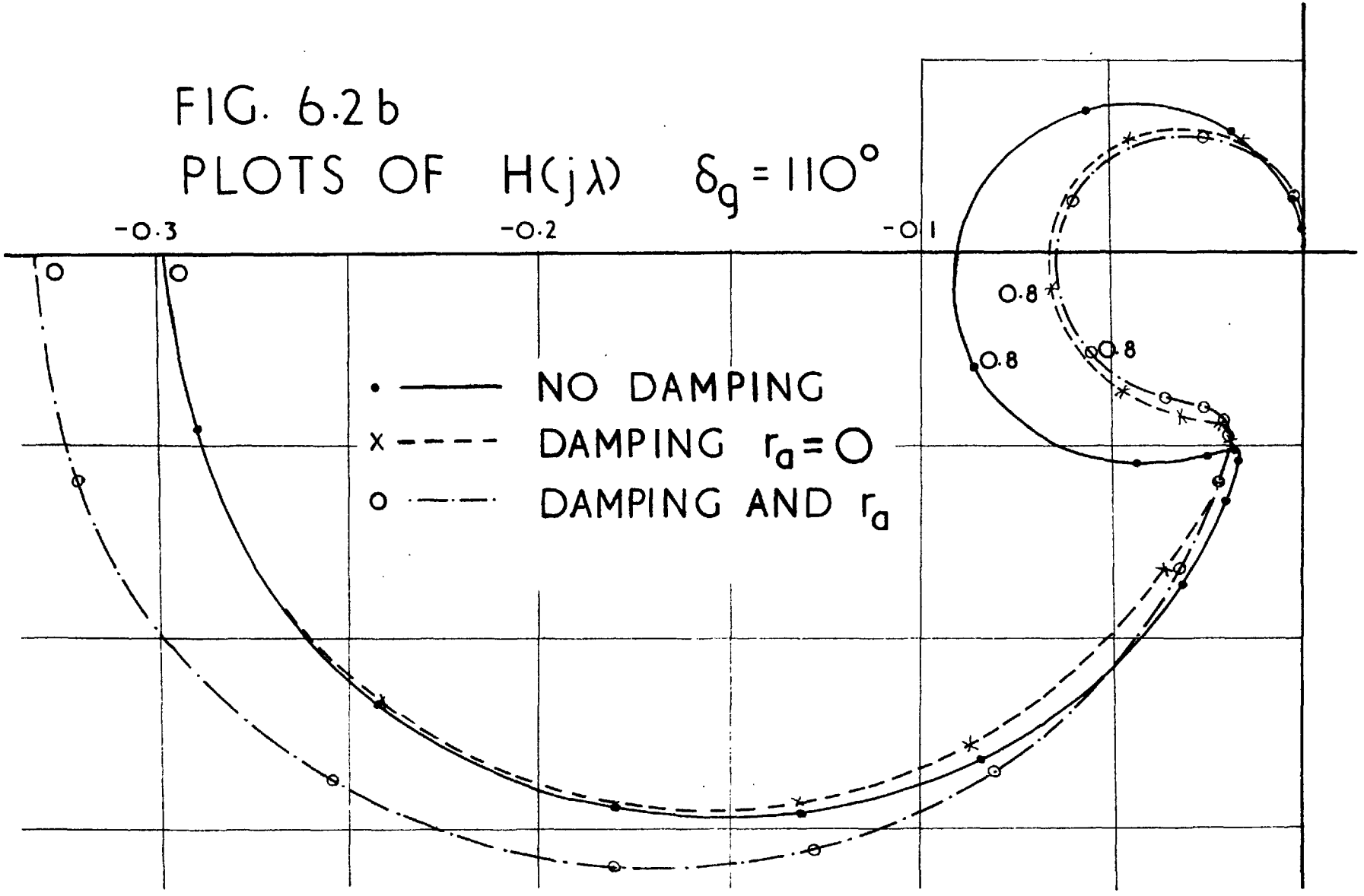

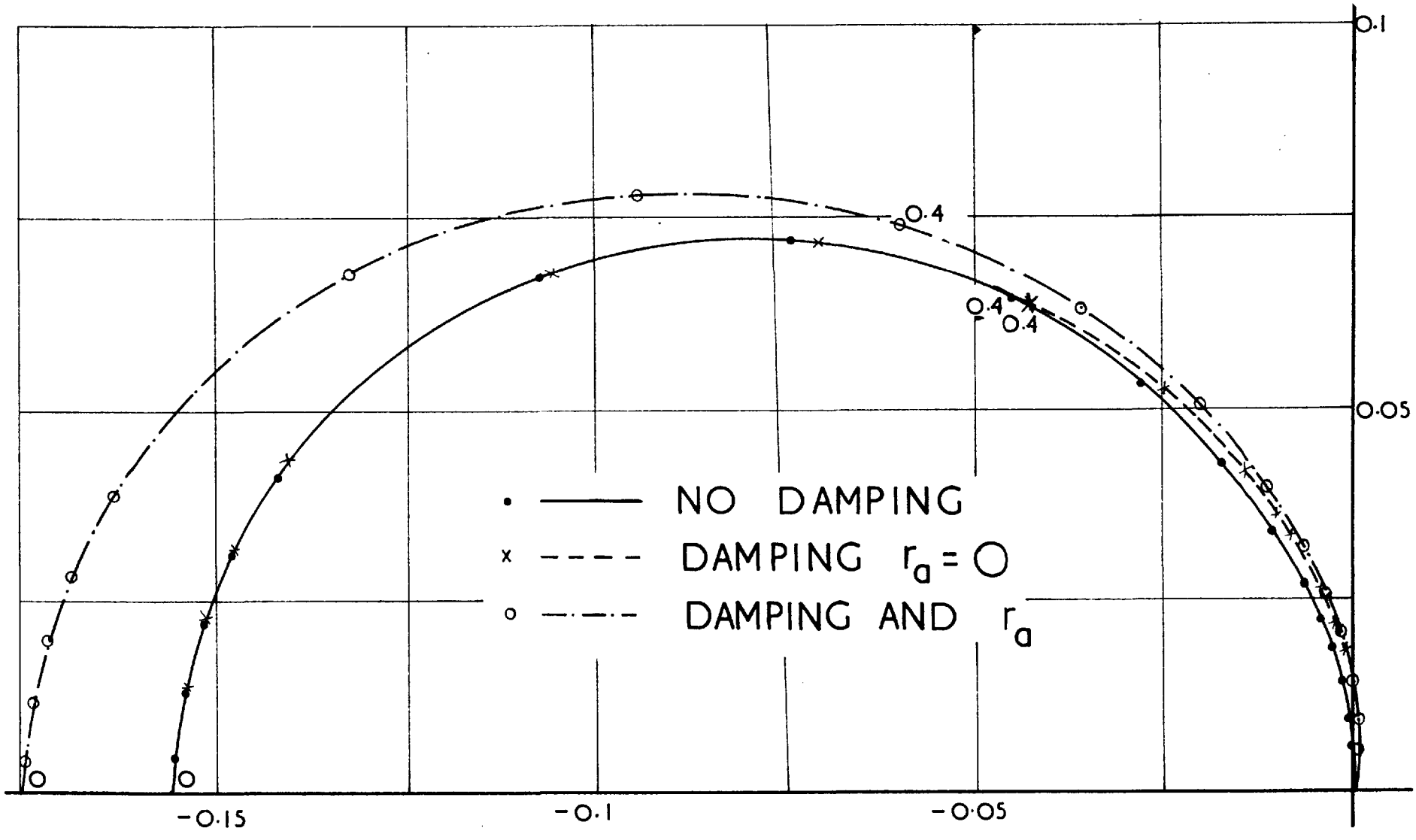

FIG. 6.2c PLOTS OF $H(j\lambda)$ $\delta_g = 140°$

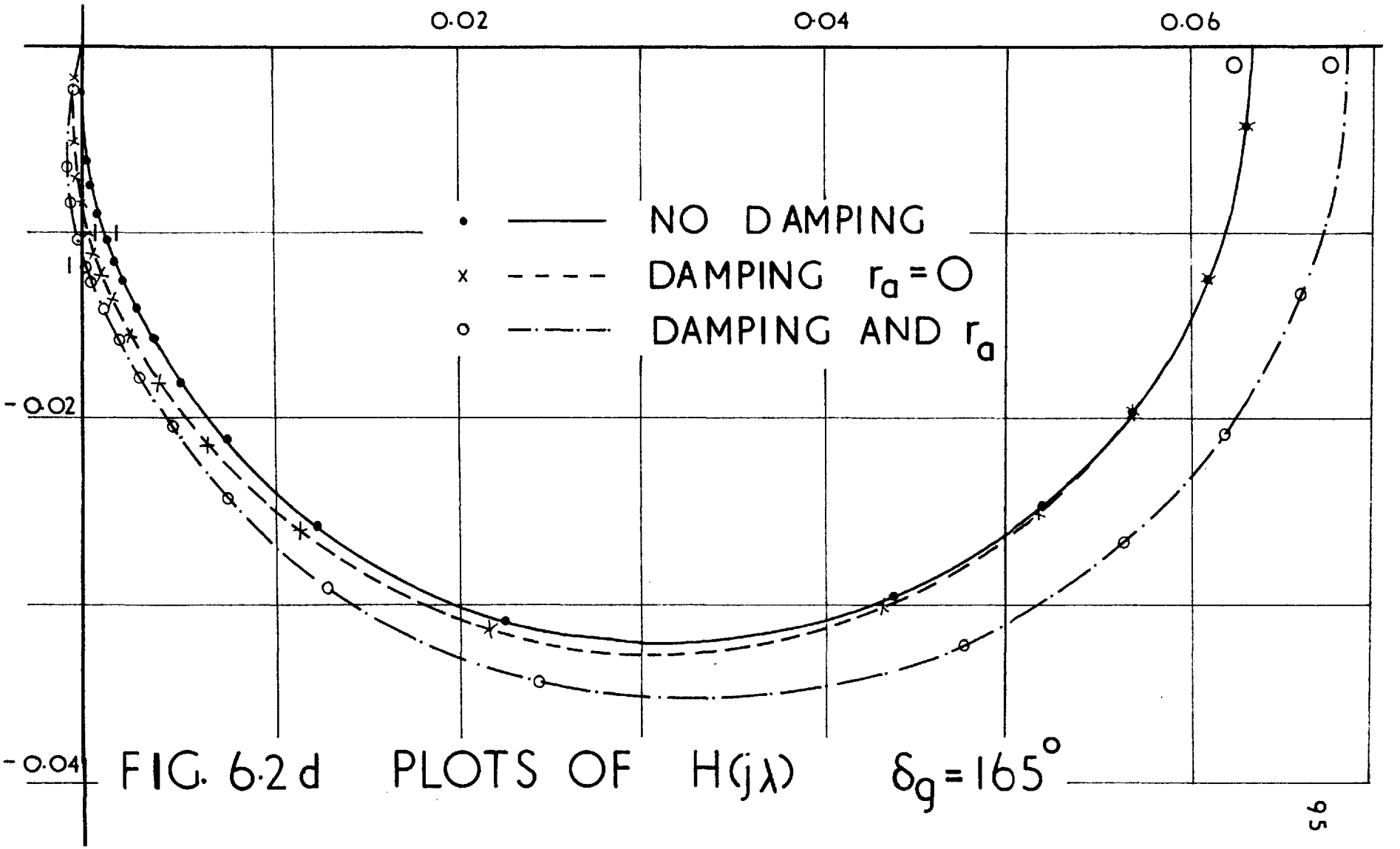

FIG. 6.2 d PLOTS OF $H(j\lambda)$ $\delta_g = 165^\circ$

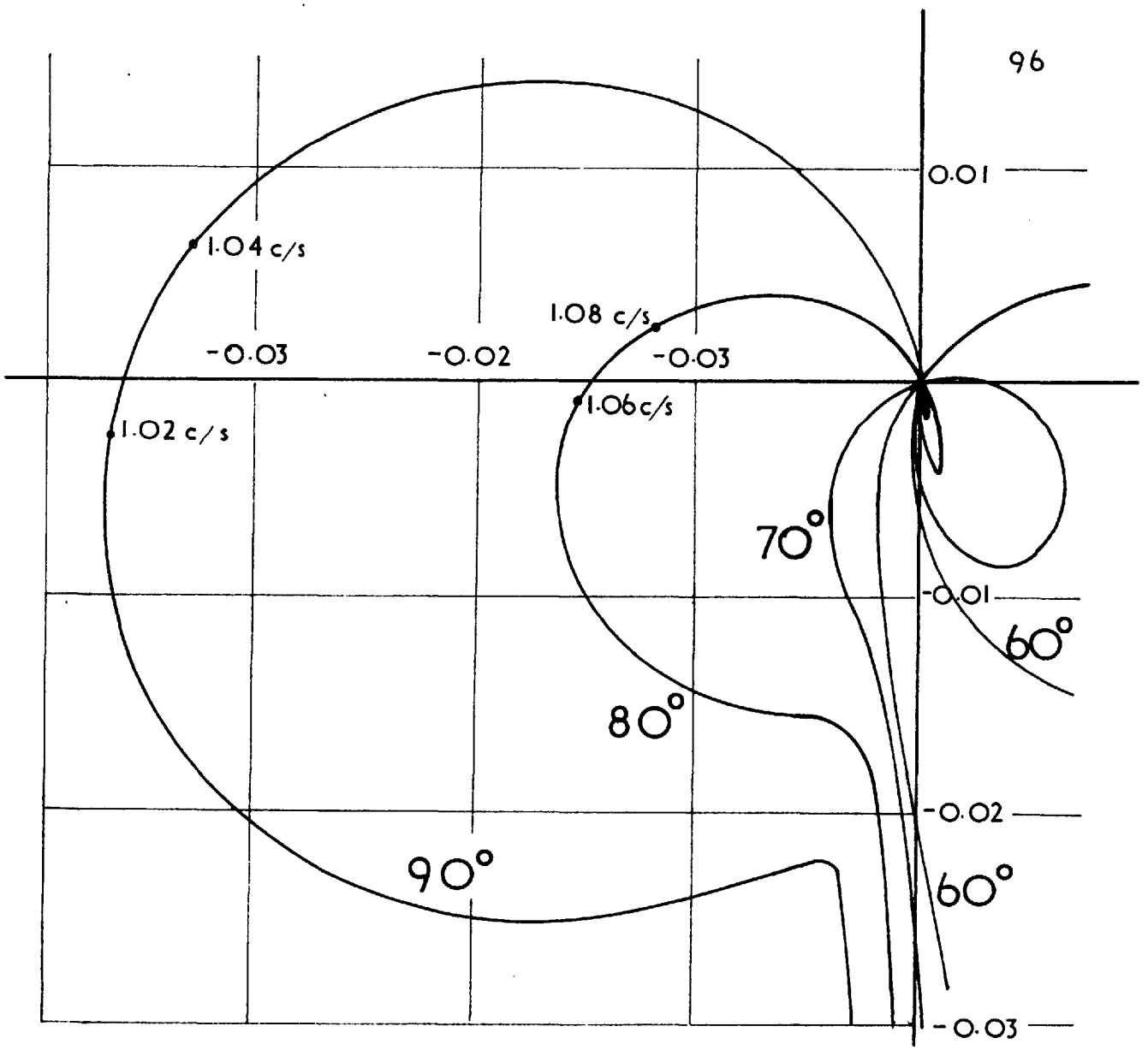

FIG. 6.3a
ENLARGED PLOT OF H(jλ)

NO DAMPING

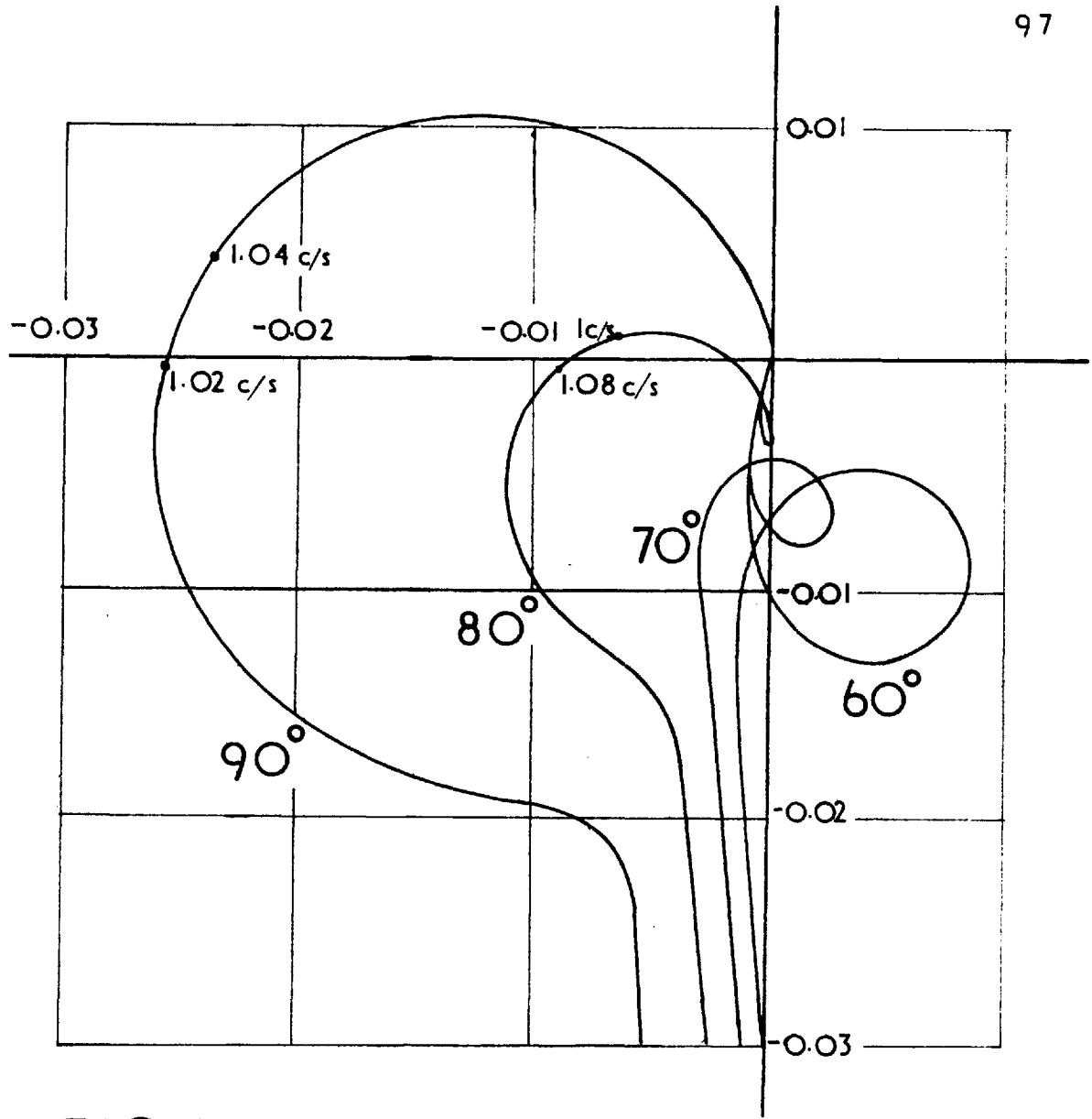

FIG. 6.3b

ENLARGED PLOT OF $H(j\lambda)$

DAMPING $r_a = 0$

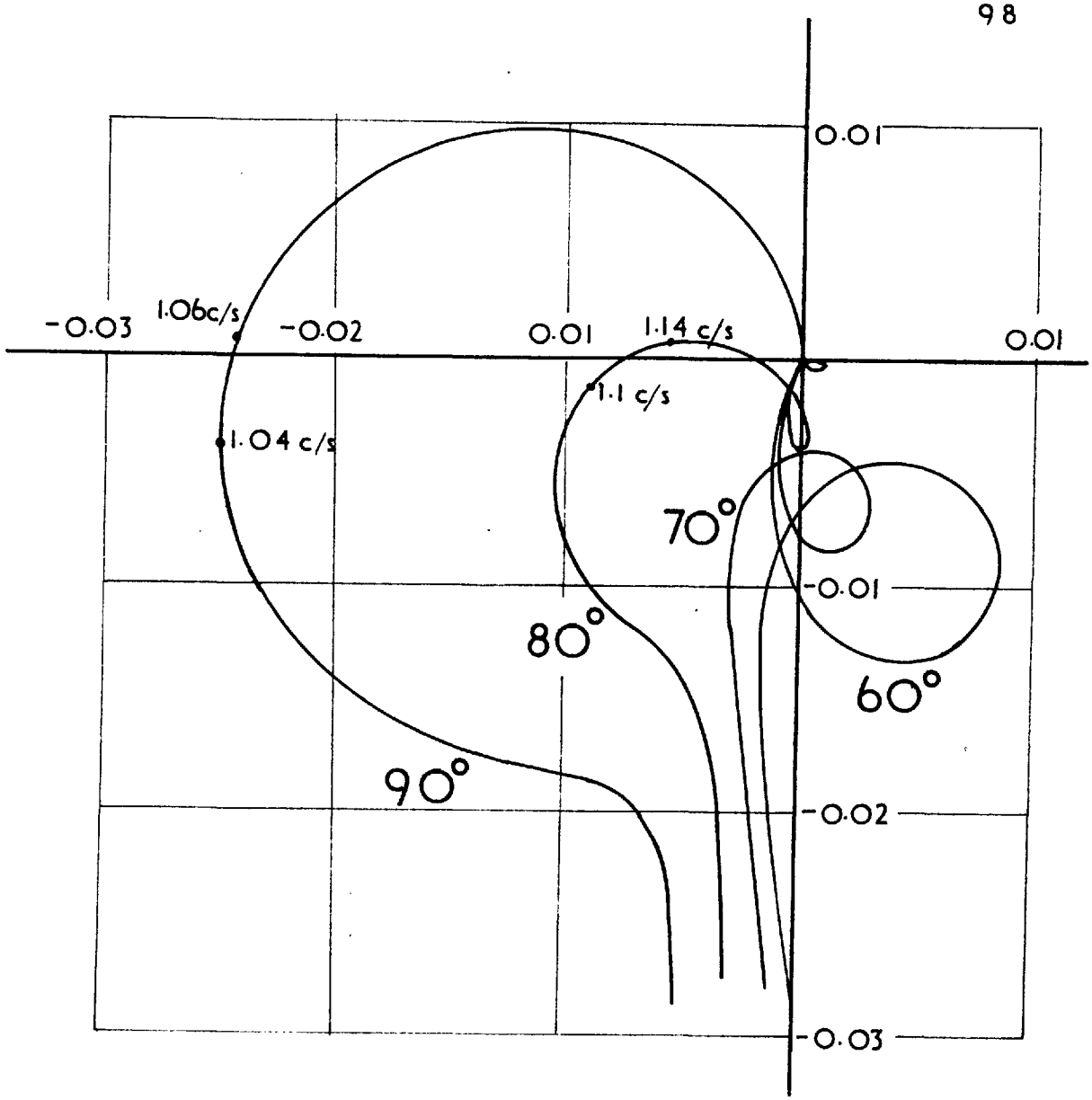

FIG. 6.3c

ENLARGED PLOT OF $H(j\lambda)$

DAMPING AND r_a

Let the $H(j\lambda)$ locus intersect the negative real axis when $\lambda = \lambda_1$. This is an important quantity and it will be shown later that it corresponds to the natural frequency of the system when $K(p)$ is constant.

It is apparent that the following changes take place as the load angle δ_g increases. The values of δ_g when some of the changes occur correspond to symbols already defined in section 4. These are given here, although the connection is not so apparent. Thus at a point between:

a) 70° and 80° the locus intersects the negative real axis. Define δ_k as the value of δ_g in this case.

b) 80° and 90° $H(0)$ becomes negative. The transition occurs when $\delta_g = \delta_s$.

c) 130° and 140° $H(j\lambda)$ does not intersect the negative real axis, except when $\lambda = 0$. This occurs when $\delta_g = \delta'_s$.

d) 160° and 165° $H(0)$ becomes positive once again. δ_g is then equal to δ_1.

The discussion of the significance of these changes on the stability of the system is deferred until section 7.

6.2. Algebraic Analysis.

Any analytical investigation must be confined to the case where damping and the effect of the armature resistance is neglected. When this is done substitution of the expressions for A_{ijk} from Eqns. (4.5), (4.14) and (4.15) into Eqn. (6.3) results in

$$H(j\lambda) = - \frac{X_c\left[(Q_o X_c + V^2)(X_q I_{do} + V_{qo}) - X_q(V_{qo} + X_c I_{do})\, J\lambda^2\right]}{V_{to} X_d X_q \left[J\lambda^2 - S_o - j\lambda T'_d(S'_o - J\lambda^2)\right]} \qquad (6.4)$$

From the phasor diagram Fig. 2.1 the following identities can be deduced:

$$V_{qo} + X_q I_{do} = \frac{X_q I \cos\varphi}{\sin \delta_o} = \frac{X_q P}{V \sin \delta_o} \qquad (6.5)$$

$$V_{qo} + X_c I_{do} = V_{to} \cos \delta_t \qquad (6.6)$$

$$Q_o X_c + V^2 = V V_{to} \cos (\delta_o - \delta_t) \qquad (6.7)$$

and when these are substituted in Eqn. (6.4)

$$H(j\lambda) = \frac{X_c \left(P \cos(\delta_o - \delta_t) - J \lambda^2 \sin \delta_o \cos \delta_t \right)}{\sin \delta_o X_d \left(S_o - J \lambda^2 + j\lambda T'_d (S'_o - J \lambda^2) \right)} \qquad (6.8)$$

The three most important features of Figs. 6.1 to 6.3 are

(i) The value of $H(j\lambda)$ at $\lambda = 0$, i.e. $H(0)$.

(ii) The value of $H(j\lambda)$ at the second intersection with the real axis i.e. $H(j\lambda_1)$.

(iii) The natural frequency λ_1.

Expressions for these may readily be obtained from Eqn. (6.8).

6.2.1 The Alternator Transfer Function at $\lambda = 0$.

Letting $\lambda = 0$ in Eqn. (6.8) we have,

$$H(0) = \frac{X_c P \cos (\delta_o - \delta_t)}{X_d S_o \sin \delta_o} \qquad (6.9)$$

$(\delta_o - \delta_t)$ is the angle between the infinite bus and the machine terminal voltage, For δ_g in the range 70° to 140°, $(\delta_o - \delta_t)$ varies from 15.5° to 26°. Thus $\cos(\delta_o - \delta_t)$ may be considered as constant in this region. It is apparent that $H(0)$ changes sign when $S_o = 0$ i.e. when $\delta_g = \delta_s$. Also as $\delta_g \longrightarrow \delta_s$, $H(0) \longrightarrow \infty$

If saliency is neglected,

$$S_o = \frac{V V_o}{X_d} \cos \delta_o = P \frac{\cos \delta_o}{\sin \delta_o} \qquad (6.10)$$

Hence, very approximately in the region 70^o to 140^o at $P = 0.8$ p.u.

$$H(0) \approx \frac{a_1}{\cos \delta_o} \qquad (6.11)$$

where a_1 is a positive constant dependent on the machine parameters and on $\cos(\delta_o - \delta_t)$.

As δ_g is increased the only term that changes sign is $\cos(\delta_o - \delta_t)$ i.e. $H(0)$ becomes positive again when

$$\cos(\delta_o - \delta_t) = 0 \qquad (6.12)$$

This implies that the angle between the terminal voltage and the infinite bus is 90^o and the corresponding value of δ_g is δ_1, see section 4.2. For the experimental machine $\delta_1 = 163.2^o$.

Since Eqns. (6.9) to (6.12) refer to $\lambda = 0$ they are valid for the case where damping is taken into account. They are approximately valid, however, when r_a is included.

6.2.2 The Natural Frequency λ_1.

The frequency at the second intersection with the real axis is obtained when the imaginary part of the denominator of $H(j\lambda)$ in Eqn. (6.8) is set to zero i.e.

$$J \lambda_1^2 = S'_o \qquad (6.13)$$

i.e.

$$\lambda_1 = \sqrt{\frac{S'_o}{J}}$$

Fig. 6.4 (simple regulator case) shows λ_1 as a function δ_g when damping and r_a are included. It is apparent that λ_1 does not change much for δ_g in the region 80° to 120°.

When $S' < 0$ the $H(j\lambda)$ locus does not cross the real axis, except when $\lambda = 0$. The value of δ_g when this occurs is given by

$$S'_o = Q_o + V_{qo}^2 Y_q + V_{do}^2 Y'_d = 0 \qquad (6.14)$$

and comparison with Eqn. (4.7) shows that $\delta_g = \delta'_s$, at the peak of the transient power angle curve.

It is interesting to note that Eqn. (6.13) occurs in investigations of synchronous machine hunting, see e.g. Adkins[57-6] or Laible[52-3].

6.2.3 The Alternator Transfer Function when $\lambda = \lambda_1$.

Substituting Eqn. (6.13) in Eqn. (6.8) we have,

$$H(j\lambda_1) = - \frac{X_c \left(P \cos(\delta_o - \delta_t) - S'_o \sin \delta_o \cos \delta_t \right)}{X_d V^2 (Y'_d - Y_d) \sin^3 \delta_o} \qquad (6.15)$$

$H(j\lambda_1)$ does not "exist" for $\delta_g > \delta'_s$. For the experimental machine in the region δ_g from 100° to δ'_s the second term in the numerator is less than 20% of the first term and so

$$H(j\lambda_1) \approx \frac{X_c P \cos(\delta_o - \delta_t)}{X_d V^2 (Y'_d - Y_d) \sin^3 \delta_o} \qquad (6.16)$$

since $\cos(\delta_o - \delta_t)$ is approximately constant, see section 6.2.1,

$$H(j\lambda_1) \approx \frac{a_2}{\sin^3 \delta_o} \qquad (6.17)$$

where a_2 is a positive constant. For the region 70° to 100° the second term in the numerator cannot be neglected. In fact when

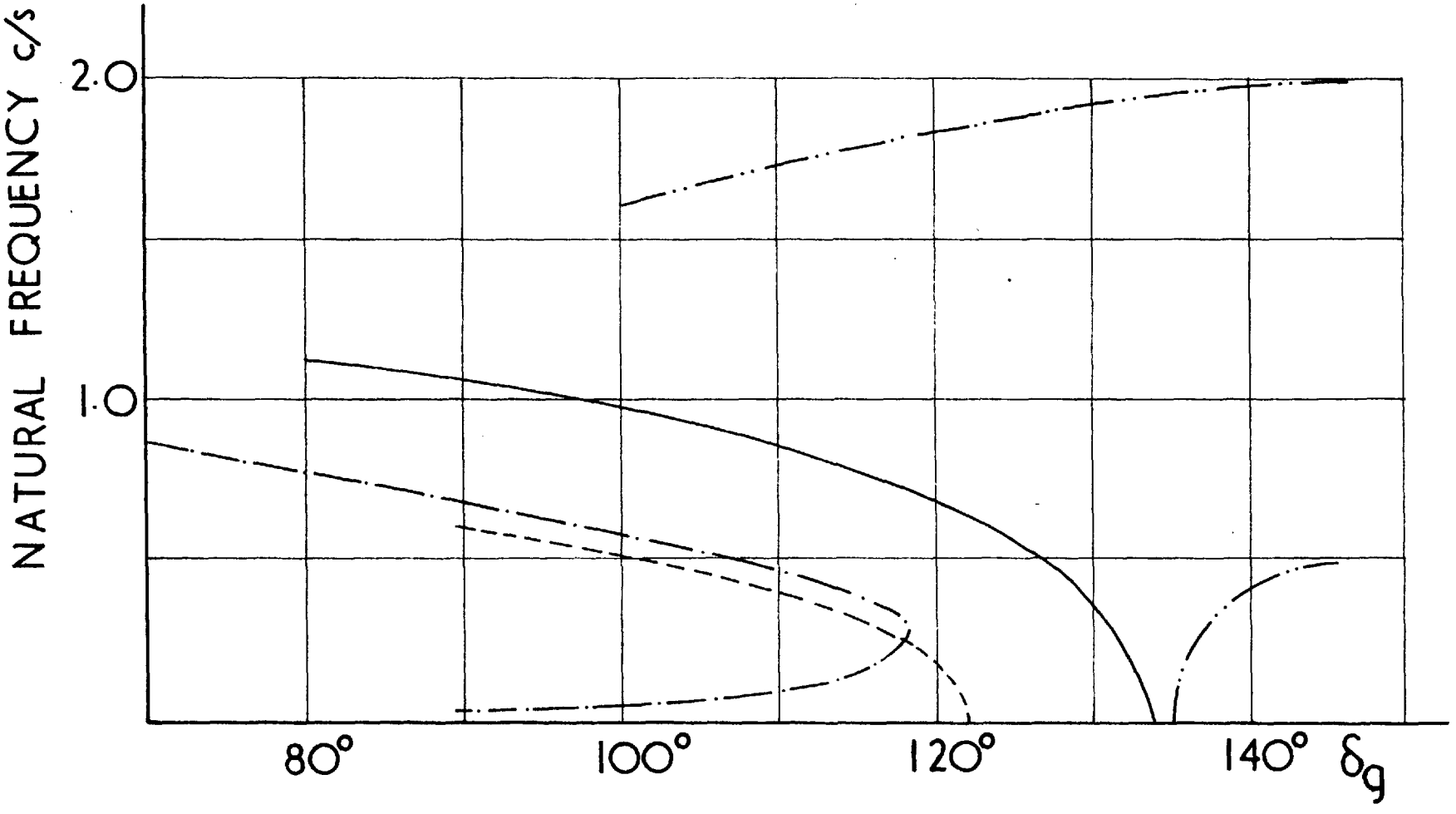

FIG. 6.4 THE NATURAL FREQUENCY

—— Simple - - - - Delay —·—·— Integrator —··—·— Derivative

$\delta_g < 71.5^\circ$ $H(j\lambda_1')$ becomes positive, see Fig. 6.3, because

$$A_{235} + A_{245} J \lambda_1^2 < 0$$

Combining Eqns. (6.9) and (6.16),

$$\frac{H(0)}{H(j\lambda_1')} \approx - \frac{V^2 (Y_d' - Y_d) \sin^2\delta_o}{S_o} \qquad (6.18)$$

From Eqn. (6.10)

$$\frac{H(0)}{H(j\lambda_1')} \approx - \frac{V^2 (Y_d' - Y_d) \sin^3\delta_o}{P \cos \delta_o} \qquad (6.19)$$

Hence, for P = constant, the ratio $H(0)/H(j\lambda_1')$ is rapidly reduced as δ_g increases beyond 90°. It should be noted that when this ratio becomes unity the $H(j\lambda)$ locus no longer crosses the real axis. From Eqn. (6.18) this occurs when

$$S_o + V^2 (Y_d' - Y_d) \sin^2\delta_o = 0$$

i.e. when

$$S_o' = 0$$

which is the same condition as Eqn. (6.14). No approximation is involved since the second term in the numerator of Eqn. (6.15) is zero.

6.3 Application of the Inverse Frequency Response Locus

The general shape of the $H(j\lambda)$ locus may be investigated using the inverse frequency response locus. If the $J\lambda^2$ term in the numerator of $H(j\lambda)$ in Eqn. (6.8) is neglected then,

$$1/H(j\lambda) = C \left(S_o - J\lambda^2 + j\lambda T_d' (S_o' - J\lambda^2) \right) \qquad (6.20)$$

where C is a positive constant. Fig. 6.5 shows a plot of $1/H(j\lambda)$ for $\delta_g = 110^\circ$ and the curve may be divided into three sections, AB, BC and CD. Comparison with Fig. 6.1 shows that they correspond to the following portions of the $H(j\lambda)$ locus.

AB is obtained for small values of λ when the λ^2 terms are small. It is approximately a straight line giving on inversion the large semicircle on the $H(j\lambda)$ locus. The "time constant" of the semicircle is $T'_d S'_o / S_o$.

CD is obtained for lage values of λ when the λ^2 terms predominate. It is approximately another straight line further away from the origin than AB and thus gives the small circle in the $H(j\lambda)$ locus. The centre of this circle lies on a line at an angle $-\gamma$ with the real axis.

BC is the transition between the two straight lines, i.e. the two circular parts of the $H(j\lambda)$ locus.

OA and OE are $1/H(0)$ and $1/H(j\lambda_1)$ respectively. It is apparent from Eqn. (6.20) that the $1/H(j\lambda)$ locus does not intersect the real axis when $S'_o < 0$. The inverse Nyquist test, as described in Appendix III can be applied and a new family of transfer functions calculated. The inverse plot, however, is not stationary as $\lambda \longrightarrow \infty$, and this results in certain complications making its application unprofitable as far as the determination of stability is concerned.

6.4 Geometrical Analysis of the $H(j\lambda)$ Loci.

When the effects of rotor damping and of the armature resistance are taken into account the expressions for $H(j\lambda)$ become very long and the algebraic analysis impossible. One way of proceeding would be to make several calculations, using the digital computer, of the frequency response locus of $H(j\lambda)$ changing the various parameters. It is considered however, that by deeper probing into the constituent parts of $H(j\lambda)$ it is possible to make more general deductions on the nature of the system.

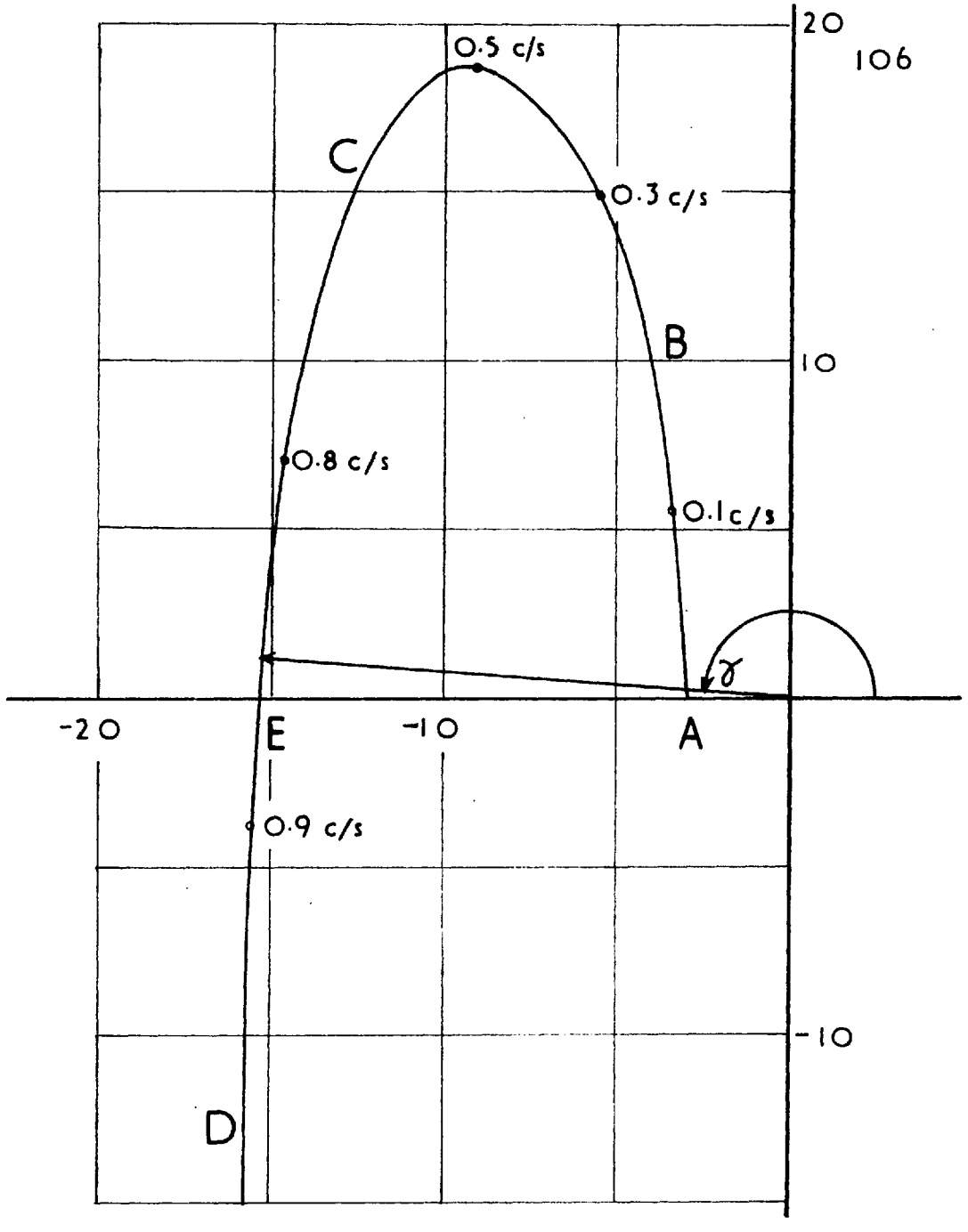

FIG. 6.5
INVERSE NYQUIST LOCUS
DAMPING AND r_a

The effect of damping and r_a on the loci of A_{ijk} functions has been considered in Chapter 4. These functions are now combined together to form the numerator and the denominator of $H(j\lambda)$.

6.4.1. Plots of the Numerator and of the Denominator of $H(j\lambda)$.

Fig. 6.6 shows the loci obtained with $\delta_g = 80^\circ$, 110° , 140° and 165° for the numerator and the denominator of $H(j\lambda)$. Again three cases are considered as indicated on the figures: a) without damping, b) with damping, $r_a = 0$, and c) with damping and r_a . Since the numerator of $H(j\lambda)$ is $(-)(A_{235} + J\lambda^2 A_{245})$ and the denominator $(A_{135} + J\lambda^2 A_{145})$ Fig. 6.6 is derived directly from Figs. 4.1 to 4.3. For the numerator plots only points for $\lambda/2\pi$ greater than 0.5 c/s are shown, c.f. Figs. 4.2 and 4.3. It should be noted that the scales for the numerator and the denominator are different as shown on each figure.

It is clear that the $H(j\lambda)$ loci may be obtained from Fig. 6.6. If two straight lines are drawn from the origin to the numerator and the denominator curves for a given λ then $|H(j\lambda)|$ is the ratio of the lengths of the two lines and Arg $H(j\lambda)$ is the difference of their argument.

A_{245} changes sign at about 110° and again at 160° , see Fig. 4.5. Comparison between Figs. 6.6 and 4.2 shows that the effect of the $A_{245} J\lambda^2$ is small for $\delta_g = 80^\circ$, 110° and 165° but significant for 140°. As $\lambda \longrightarrow \infty$

$$(-)(A_{235} + J\lambda^2 A_{245}) \longrightarrow -j\infty \quad \delta_g = 80^\circ$$

$$\longrightarrow +j\infty \quad \delta_g = 110^\circ, \ r_a \text{ neglected}$$

$$\longrightarrow -j\infty \quad \delta_g = 110^\circ, \ r_a \text{ included}$$

$$\longrightarrow +j\infty \quad \delta_g = 140^\circ$$

$$\longrightarrow -j\infty \quad \delta_g = 165^\circ$$

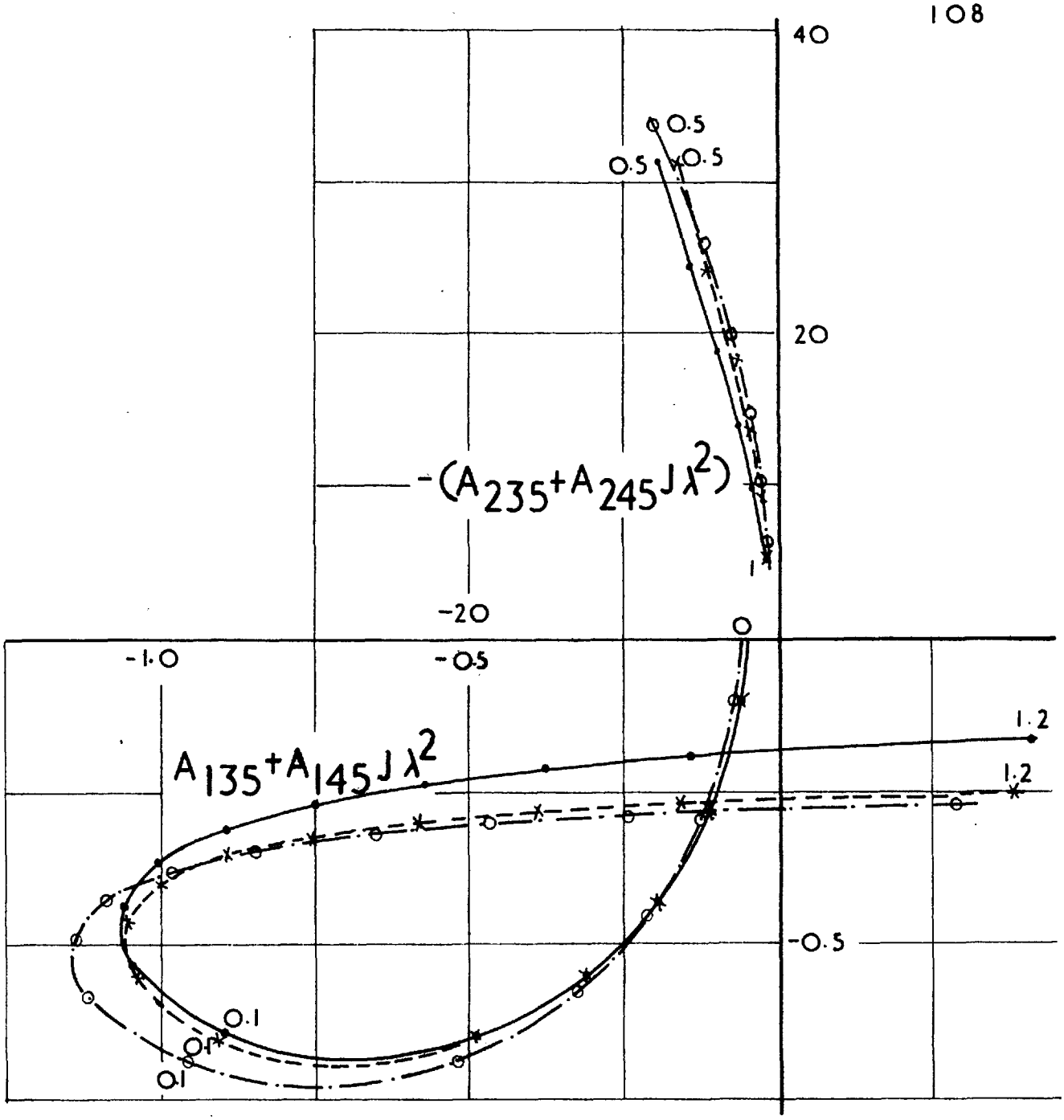

FIG. 6.6a PLOTS OF NUMERATOR AND DENOMINATOR OF $H(j\lambda)$

• ——— NO DAMPING

x ------ DAMPING $r_a = 0$

o —·—·— DAMPING AND r_a

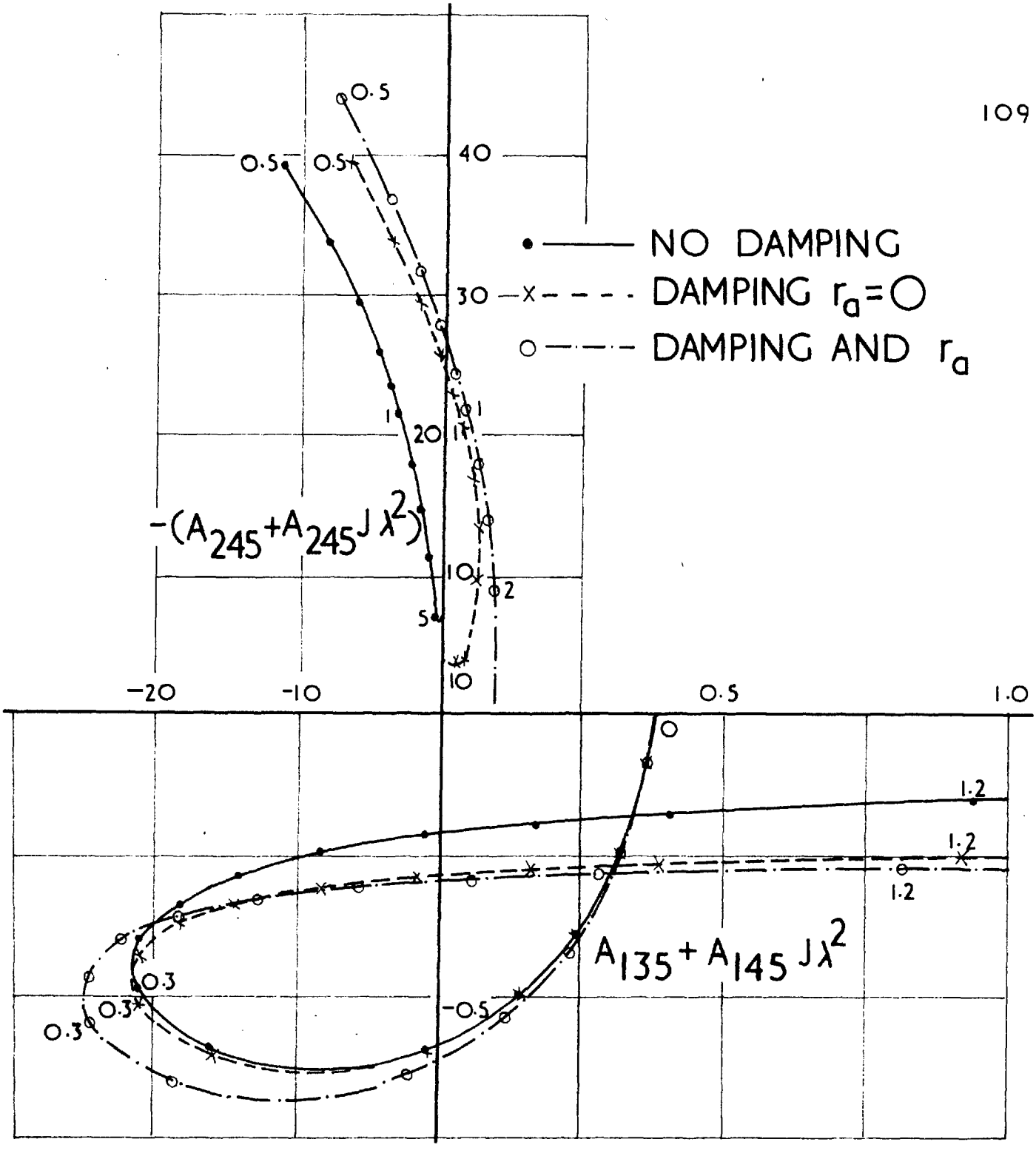

FIG. 6.6b PLOTS OF NUMERATOR AND DENOMINATOR OF $H(j\lambda)$

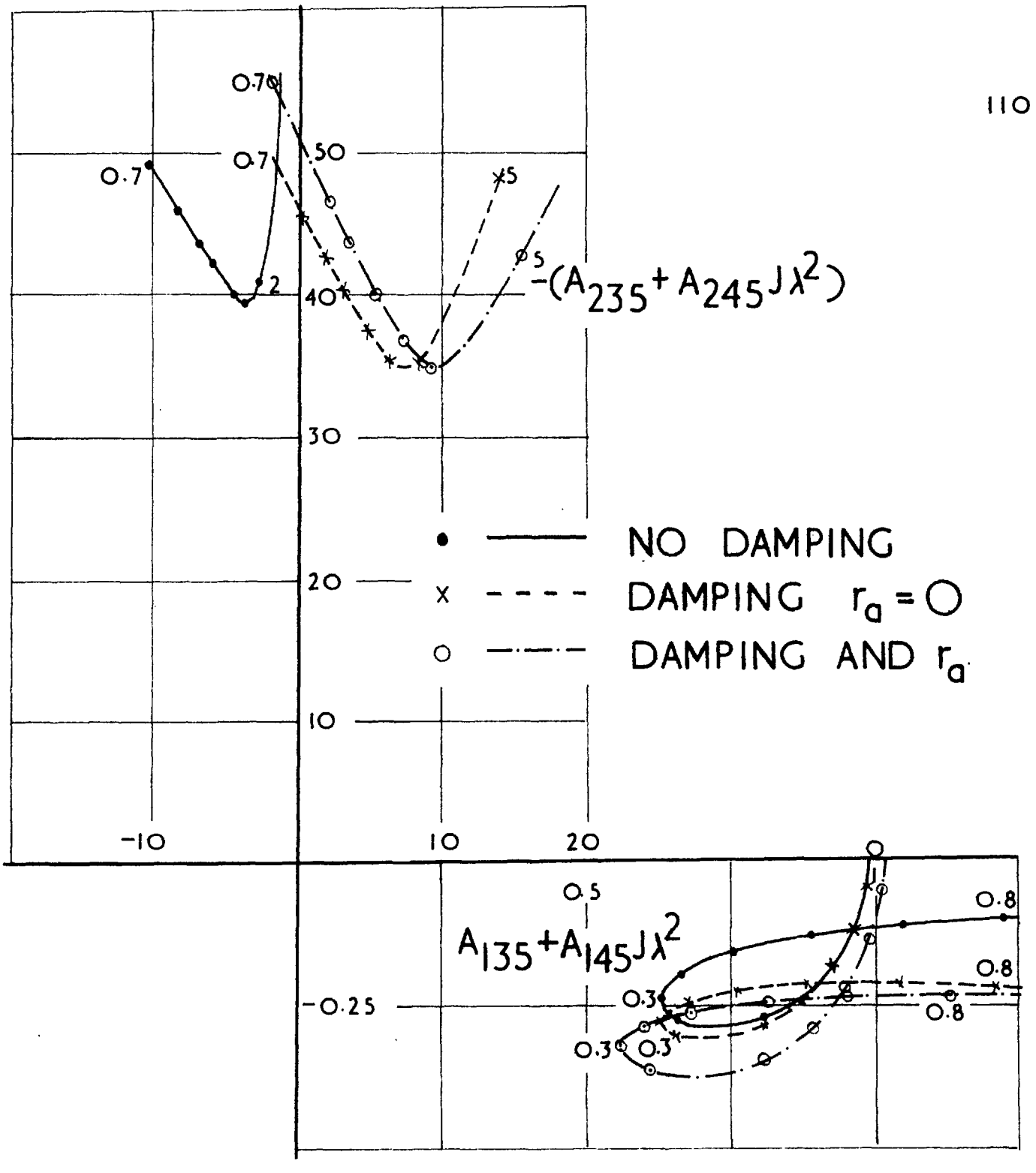

FIG. 6.6c PLOTS OF NUMERATOR AND DENOMINATOR OF $H(j\lambda)$

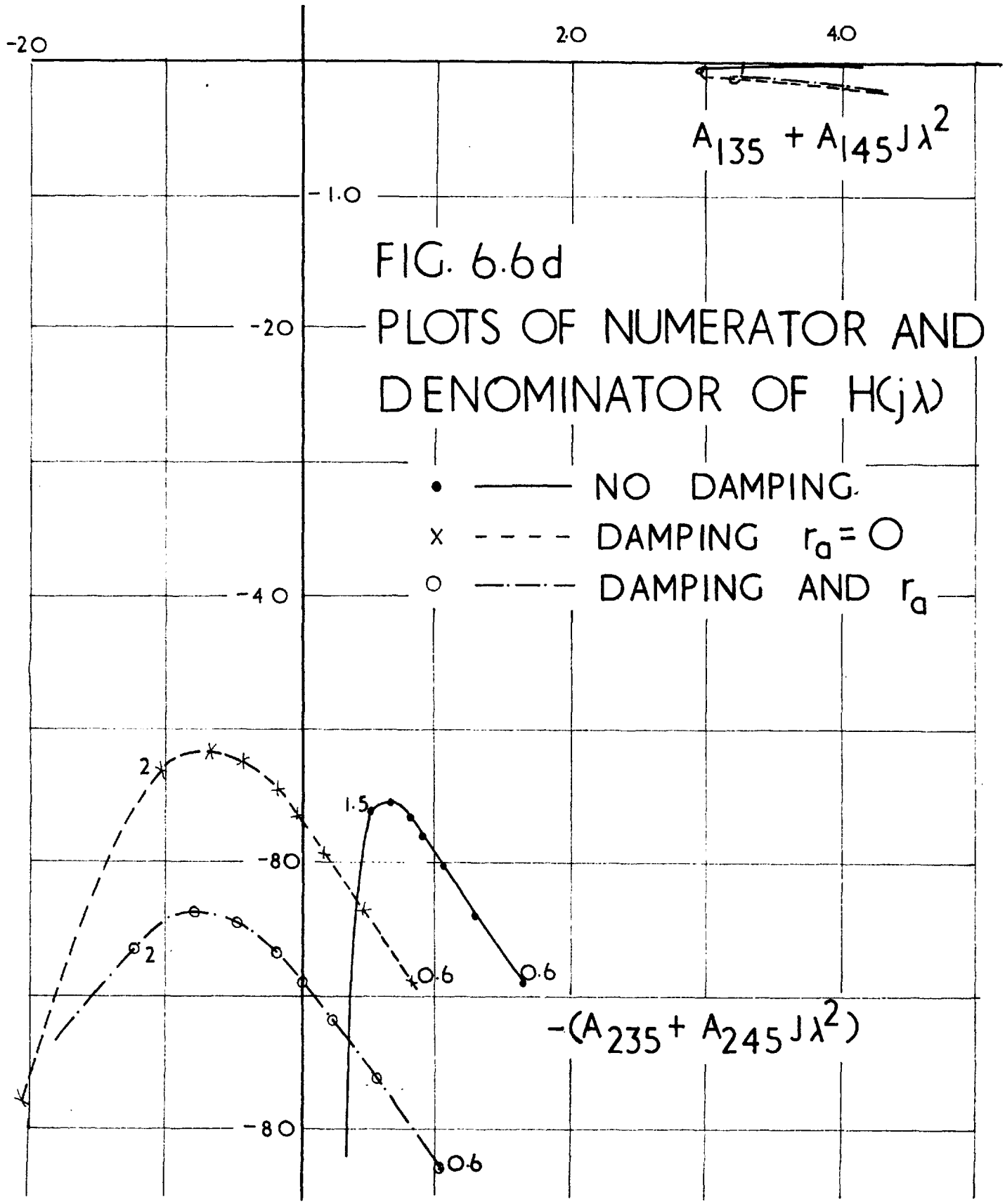

FIG. 6.6d
PLOTS OF NUMERATOR AND DENOMINATOR OF $H(j\lambda)$

The effect of damping on the numerator locus is to increase the phase-shift with respect to the zero frequency point and at the same time the amplitude is slightly reduced. When r_a is included both the phase shift and the amplitude are increased. It was stated in section 4.3 that A_{145} may be taken as unity. Hence the imaginary part of the denominator is the same as the imaginary part of A_{135}. Thus the effects of damping and r_a on the shape of the denominator locus are implied in the A_{135} locus, see section 4.1 and need not be considered here.

Since the denominator locus does not cross the negative imaginary axis the phase-shift and attenuation introduced by the denominator are progressively reduced as δ_g is increased. Thus for $\delta_g > \delta'_s$ the $H(j\lambda)$ locus becomes more and more similar to the numerator locus i.e. essentially a semicircle.

6.4.2 The Effect of Damping on $H(j\lambda_1)$ and λ_1.

Discussion here is necessarily limited to the angles for which the $H(j\lambda)$ locus intersects the negative real axis i.e. for $\delta_g < \delta'_s$. For both Figs. 6.6a and b the argument of $(-)(A_{235} + J\lambda^2)$ in the region of λ_1 is nearly equal to 90° and does not change much with frequency. Hence

$$H(j\lambda_1) \approx \frac{A_{235} + J\lambda_1^2 A_{245}}{\text{Imag. Part of } A_{135}(j\lambda_1)} \qquad (6.21)$$

It is shown in Figs. 6.6a and b that the magnitude of the numerator is not greatly affected by damping. Hence Eqns. (4.14) and (4.15) may be used and

$$A_{234}(j\lambda_1) + J\lambda_1^2 A_{245}(j\lambda_1) = \frac{c + d J \lambda_1^2}{1 + j\lambda_1 T'_d} \approx \frac{c + d J \lambda_1^2}{j\lambda_1 T'_d} \qquad (6.22)$$

where it was assumed that $(\lambda_1 T'_d)^2 \gg 1$. If, in addition, $(\lambda_1 T''_d)^2 \ll 1$ and $(\lambda_1 T''_q)^2 \ll 1$ then,

Imaginary Part of $A_{135}(j\lambda_1)$

$$= -\left(\frac{1}{\lambda_1 T'_d}(Y'_d - Y_d) + (Y''_d - Y'_d)\lambda_1 T''_d\right) V^2_{do} - (Y''_q - Y_q)\lambda_1 T''_q V^2_{qo} \qquad (6.23)$$

Both Figs. 6.6 a and b show the contribution of damping to the imaginary part when the denominator locus intersects the negative imaginary axis. Since the magnitude of the numerator does not change much with damping it is apparent from Eqn.(6.21) that when damping is included $H(j\lambda_1)$ is reduced. This is shown clearly in Figs. 6.2 a and b.

Eqn. (6.22) shows that part of the denominator is inversely proportional to T'_d and Figs. 6.6 a and b show that this part is about $\frac{1}{2}$ of the imaginary part of A_{135}. Small changes in T'_d therefore have little effect on $H(j\lambda_1)$. If T'_d could be made much larger than $H(j\lambda_1)$ would be reduced and thus $H(0)/H(j\lambda_1)$ would be increased. This important ratio (see section 7.1.1) will also be increased if, for the same δ_g, damping is made more effective i.e. T''_q, T''_d, Y''_d and Y''_q are increased or if λ_1 could be increased. One way of reducing λ_1 is by increasing J.

The effect of damping on the critical frequency λ_1 is not very significant. Since the argument of $(-)(A_{235} + J\lambda_1^2 A_{245})$ is approximately 90° we have from Figs. 6.6 a and b.

$$J\lambda_1^2 \approx \text{Real Part of } A_{135}(j\lambda_1)$$

c.f. Eqn. (6.13) for the case without damping. In the experimental machine λ_1 is low so that damping does not affect the real part of A_{135} to a great extent and,

$$\text{Real Part of } A_{135}(j\lambda_1) \approx S'_o$$

Thus the real part of $A_{135}(j\lambda_1)$ is dependent on Y'_d. Hence reduction of X'_d increases λ_1. Since X'_d, however, includes X_c, the line reactance, the machine transient reactance must be reduced considerably in order to have any effect. Small changes in T'_d do not affect λ_1, but if the rotor damping is made more effective then λ_1 will be increased.

6.4.3 The Effect of Damping and r_a on $H(0)$, $H(j\lambda_1)$ and λ_1.

$H(0)$ depends only on $A_{235}(0)$ and $A_{135}(0)$ and obviously is not affected by damping. As stated in section 4.1 the effect of r_a is to reduce $A_{135}(0)$ for $\delta_g = 80^\circ$ and 110° and to increase it for $\delta_g = 140^\circ$ and 165°. Also $A_{235}(0)$ is increased when r_a is included for $\delta_g < \delta_1$ and reduced for $\delta_g > \delta_1$, see section 4.2. The net result is that $H(0)$ is numerically increased when r_a is taken into account, the increase being maximum about $\delta_g = 120^\circ$.

The effect of r_a on $H(j\lambda_1)$ and λ_1 is shown in Figs. 6.6 a and b. Considering λ_1 first it is clear that it is increased because the real part of A_{135} is numerically increased. The imaginary part of the denominator is also increased by a small amount. Thus one would expect a reduction in $H(j\lambda_1)$ since the numerator is inversely proportional to λ_1, see Eqn. (6.22). The numerator, however, is also increased when r_a is included and thus $H(j\lambda_1)$ is increased only by a small amount, see Figs. 6.2 a and b.

It is not possible to make general comments on the effect of r_a and damping on the shape of the numerator and the denominator plots for $\delta_g = 140^\circ$ and 165°, since there is no frequency corresponding to λ_1. It should be noted, however, that the effects of both damping on its own and together with r_a are more pronounced, especially for $\delta_g = 140^\circ$, see Figs. 6.6 c and d.

It should be pointed out that some of the transition points considered in section 6.1 are affected by r_a, but only to a small extent. The only significant change is in the value of δ'_s which is

132° or 133.8° depending on whether r_a is neglected or included respectively.

6.4.4 Analysis of the Components of the Numerator and of the Denominator of $H(j\lambda)$ Using a Phasor Diagram.

Fig. 6.7 shows a phasor diagram of the constituent parts of the numerator and of the denominator of $H(j\lambda)$ for a) no damping b) damping, $r_a = 0$ and c) damping and r_a, at $\delta_g = 110^{\circ}$. The value of $\lambda/2\pi$ chosen, 0.9 c/s is near the critical frequency. Again as in Fig. 6.6 the scales above and below the real axis are different. It should be noted that, since the load angle is kept the same the reactive power is slightly changed when the armature resistance is included, but this change is not shown on the diagram.

Consider the numerator first. The increase of phase shift when damping is introduced and the increase of amplitude when the effect of r_a is included are both shown. The contribution of the $J\lambda^2 A_{245}$ term is negligible. As has already been pointed out, however, see Fig. 4.5 this is due to a coincidence.

Turning now to the denominator, phasors oa, ob and oc correspond to A_{135} for each of the three cases a, b and c respectively. When damping is neglected $V_{qo}^2 Y_q$ is real and the imaginary part of $V_{do}^2 Y_d(j\lambda)$ is smaller than when damping is included. The imaginary part of A_{135} is further increased when the effect of the armature resistance is included but only by a small amount. The effect on the real part is more significant, see phase cb.

Since the $H(j\lambda)$ locus intersects the negative real axis when the numerator and the denominator phasors are 180° apart, it is apparent that the effect of damping and r_a is to increase λ_1. Also the increase in the magnitude of the denominator, when damping and r_a are included, is greater than the corresponding increase in the numerator. Hence $|H(j\lambda_1)|$ is reduced.

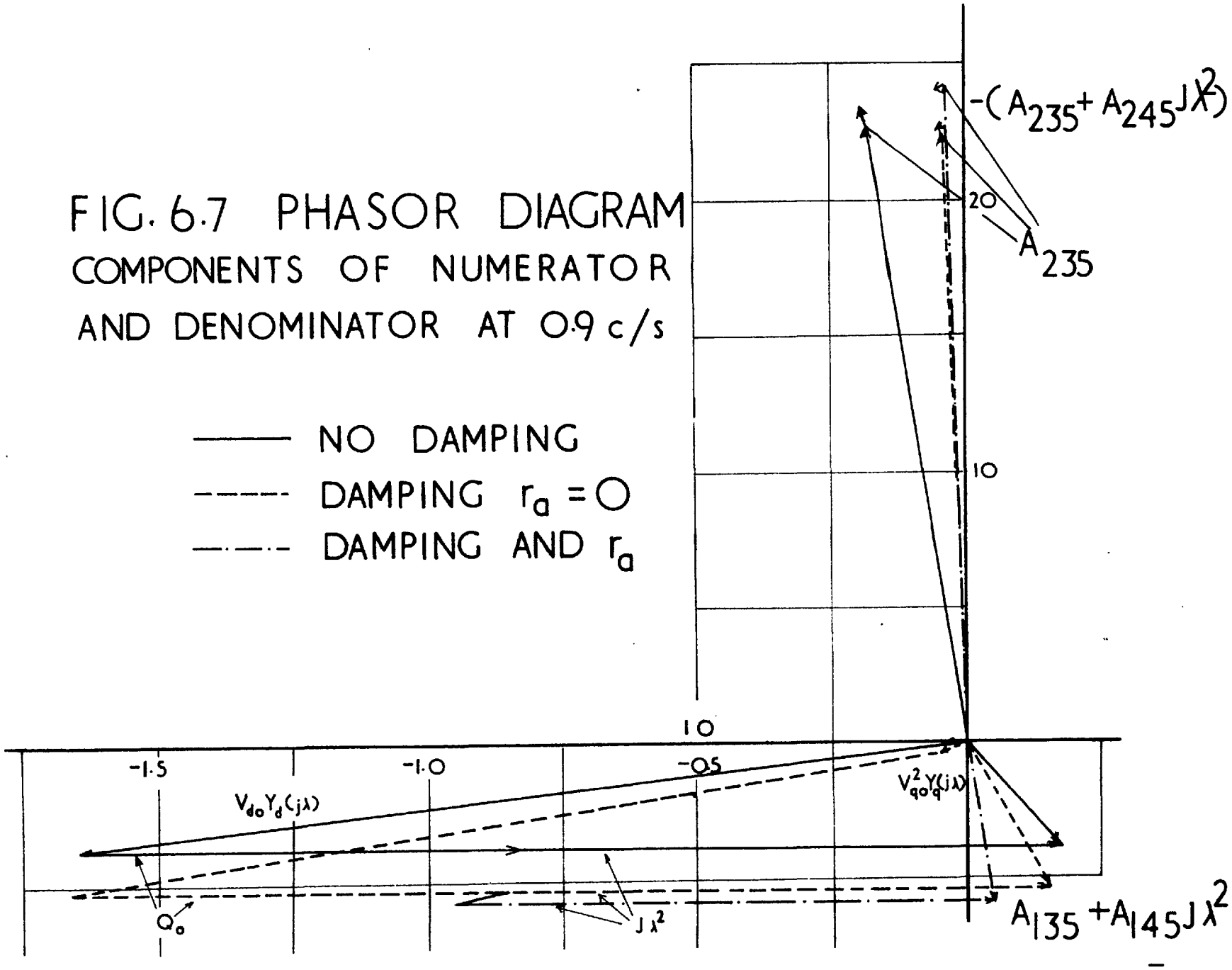

FIG. 6.7 PHASOR DIAGRAM
COMPONENTS OF NUMERATOR
AND DENOMINATOR AT 0.9 c/s

—— NO DAMPING
– – – – DAMPING $r_a = 0$
—·—·— DAMPING AND r_a

7. DETERMINATION OF THE SYSTEM STABILITY LIMIT.

In the present section $H(j\lambda)$ is combined with $K(j\lambda)$ and the stability of the system is investigated by means of the resultant open loop transfer function. It is considered advantageous to start with a regulator having a constant transfer function, i.e. with the simple regulator. The $H(j\lambda)$ plots may be used directly for determining stability and the discussion is considerably simplified.

The next step is the application of the method to regulators used in practice. It is difficult, however, to select typical regulators because of the enormous variety of different arrangements and secondly because of lack of information on the values of the parameters. Thus, before proceeding, it is necessary to consider an extensive review of practical regulators.

Strict classification according to the form of the transfer function is found impracticable because it leads to too many types having similar behaviour. Also as Fig. 6.1 suggests we are mainly interested in the phase-shift and attenuation of $K(j\lambda)$ for $\lambda/2\pi$ up to about 2 c/s . Hence regulators are classified according to the position of the $K(j\lambda)$ locus in the complex plane for this range of frequency.

A typical example from each class is then chosen for a detailed investigation on the stability of the system.

7.1 The Simple Regulator.

When $K(p) = K$ the locus of the open loop transfer function, $L(j\lambda)$ is the same as that of $H(j\lambda)$ to a different scale, determined by the value of K . The Nyquist criterion can be applied to the $H(j\lambda)$ locus if the $(-1, 0)$ point is thought of as moving on the negative real axis depending on K .

Before applying the Nyquist test, however, P , the number of poles with a positive real part of $L(j\lambda)$ must be known, see Appendix III.

The numerator, $K K_o (A_{235} + A_{245} J \lambda^2)$, has no such poles since it contains only terms of the form $(1 + j\lambda T)$ in its denominator. Hence P is the number of zeros with a positive real part of $(A_{135} + J \lambda^2)$. As described in Appendix III, a plot should be made of $A_{135}/J \lambda^2$ for $\lambda = -\infty \longrightarrow 0 \longrightarrow +\infty$. The number of encirclements of the $(-1, 0)$ point gives P. Such a plot, however is shown in Figs. 5.1 a, b and c and was used to investigate the stability of the unregulated machine by the torque feedback method, see section 5.2. The fact that damping was then neglected does not affect the conclusions since the deciding factor is $A_{135}(0)$. Also the effect of r_a is merely to change the value of $A_{135}(0)$, but otherwise the following conditions are valid.

$$P = 0 \qquad \text{for } \delta_g < \delta_s$$
$$P = 1 \qquad \text{for } \delta_g > \delta_s$$

The system is then stable if the $L(j\lambda)$ locus,

(i) does not encircle the $(-1, 0)$ point for $\delta_g < \delta_s$ and

(ii) encircles the $(-1, 0)$ point once in a counterclockwise direction for $\delta_g > \delta_s$.

It should be pointed out that this result merely states that the system is unstable on open loop, i.e. without a regulator, for $\delta_g > \delta_s$. It is necessary, however, to establish that there is only one unstable root so that the correct number of encirclements may be established. No proof of this important result could be found in the literature.

three four

The significance of the four of the five transition points of the $H(j\lambda)$ locus discussed in section 6.1 is now apparent. The meaning of the fifth point viz. δ_1 is discussed in section 7.3.3.

a) For $\delta_g < \delta_k$ P = 0 and $H(j\lambda)$ does not cross the negative real axis. Hence the $L(j\lambda)$ locus does not encircle the $(-1, 0)$ point regardless of the value of regulator gain and so the system is always

stable. This result is of no practical value since at high frequencies the regulator transfer function is bound to have some phase-shift and a sufficiently high gain will always cause instability at any value of δ_g.

b) For $\delta_k < \delta_g < \delta_s$ $P = 0$ and if the gain is high enough the $(-1, 0)$ point is encircled in a clockwise direction resulting in instability at load angles for which the unregulated machine is stable.

c) For $\delta_s < \delta_g < \delta_s'$ $P = 1$. The $L(j\lambda)$ locus encircles the $(-1, 0)$ point once in a counterclockwise direction if

$$\left| K_o H(0) \right| > 1/K > \left| K_o H(j\lambda_1) \right|$$

i.e. if the $(-1, 0)$ point lies between the first, at $\lambda = 0$, and the second, at $\lambda = \lambda_1$ intersections with the real axis. Thus the system may be stabilized with a suitable choice of gain.

d) and e) For $\delta_g > \delta_s'$ $P = 1$. Since the $H(j\lambda)$ locus does not cross the real axis it is not possible to encircle the $(-1, 0)$ point with any value of gain. The system is thus unstable for all K.

It is desirable to define K_{min} and K_{max} as the limiting values of gain and to extend the definition for any type of regulator. Thus for the simple regulator,

$$K_{min} = \frac{1}{K_o H(0)} \qquad (7.1)$$

$$K_{max} = \frac{1}{K_o H(j\lambda_1)} \qquad (7.2)$$

7.1.1 The Stability Limit Curve with a Simple Regulator.

Fig. 7.1 shows K_{min} and K_{max} as functions of δ_g obtained from Fig. 6.1. From the last section K_{min} is defined for $\delta_g > \delta_s$ and K_{max} for $\delta_s' > \delta_g > \delta_k$. It is clear, however, that K_{min} has no significance for $\delta_g > \delta_s'$. Nevertheless the two curves are

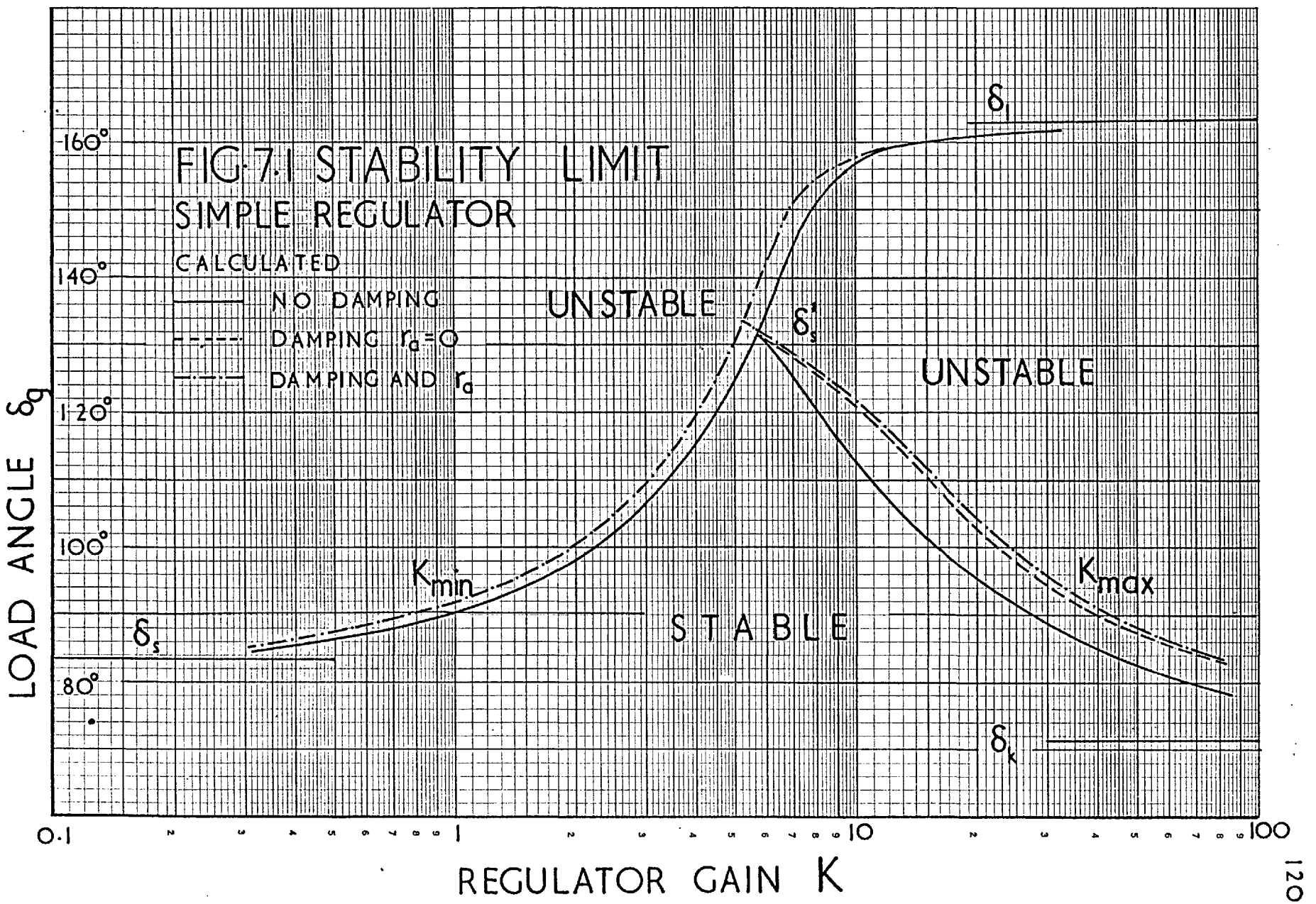
FIG 7.1 STABILITY LIMIT
SIMPLE REGULATOR
CALCULATED
NO DAMPING
DAMPING $r_d = 0$
DAMPING AND r_d
UNSTABLE
UNSTABLE
STABLE
δ_l
δ_s'
K_{min}
K_{max}
δ_s
δ_k
160°
140°
120°
100°
80°
LOAD ANGLE δ_g
0.1
1
10
100
REGULATOR GAIN K
120

distinct and there is a discontinuity at their intersection, which corresponds to δ_s' . K_{min} has two asymptotes at $\delta_g = \delta_s$ and δ_1 and K_{max} one asymptote at δ_k .

Ignoring the part of K_{min} for $\delta_g > \delta_s'$ the two curves give the stability limit against the regulator gain. Define K_{ss} as the gain resulting in the maximum extension of the steady state stability limit, again applicable to any type of regulator. Clearly for the simple regulator

$$K_{ss} = K_{min} = K_{max} = \left| \frac{1}{K_o H(0)} \right|_{\delta_g = \delta_s'}$$

From Eqns. (6.9), (6.11), (6.16) and (6.17) for constant power and V we have,

$$K_{min} = \frac{X_d S_o \sin \delta_o}{K_o X_c P \cos(\delta_o - \delta_t)} \qquad (7.3)$$

$$\propto \cos \delta_o$$

$$K_{max} \approx \frac{X_d V^2 (Y_d' - Y_d) \sin^3 \delta_o}{K_o X_c P \cos(\delta_o - \delta_t)} \qquad (7.4)$$

$$\propto \sin^3 \delta_o$$

i.e. in Fig. 7.1 K_{min} is a cosine curve and K_{max} approximately a sine cubed curve respectively.

Let G denote the ratio K_{max}/K_{min} . It is desirable to have a large G for two reasons: a) The regulator gain may be set between K_{min} and K_{max} and if G is large, K will be sufficiently removed from the stability limit. Alternatively, referring to Fig. 6.1 the further the Nyquist locus lies from the (-1, 0) point the more stable the system, see Thaler and Brown[60-11]. For this reason G is referred to as the stability ratio. b) As will be seen in section 8.2 good steady

state regulation requires a large value of K_{max}. From Eqn. (6.19), for the simple regulator

$$G \approx \frac{V^2 (Y'_d - Y_d) \sin^3\delta_o}{P \cos \delta_o}$$

i.e. the stability ratio is rapidly reduced as δ_g is increased beyond 90^o.

The effects of damping and r_a have been discussed in section 6. Fig. 7.1 shows that K_{max} is mainly affected by damping and K_{min} by r_a. Of the four angles shown in Fig. 7.1 only δ'_s is affected to any extent when r_a is included see section 6.4.3. None is affected by damping only. The same symbol is used when r_a is included although the values are slightly different. It should be pointed out that the value of G at $\delta_g = 110^o$ when damping and r_a are included is about 65% greater compared with the no damping case.

7.1.2 Kinds of Instability and the Natural Frequency of the System.

As has been stated, when K is less than K_{min} the Nyquist locus does not encircle the (-1, 0) point. Thus if Z and P are the zeros and poles with a positive real part, Z - P = 0 and since P = 1 for $\delta_g > \delta_s$ then Z = 1. Thus the system has one unstable root and this necessarily must be real. The loss of stability therefore is aperiodic corresponding to a term $e^{\alpha t}$ where α is a positive real quantity.

Similarly if K is greater than K_{max} the Nyquist locus encircles the (-1, 0) point once in a clockwise direction. Hence Z - P = 1 and again for $\delta_g > \delta_s$ P = -1 and thus Z = 2. The sudden appearance of two roots suggests that they are complex conjugates and therefore instability for high gain is associated with some form of oscillation corresponding to a term $e^{\beta t} \sin \gamma t$ with β, γ positive real quantities. In fact it may be shown that in this case the roots are complex, see Ref. 64-2. The two kinds of instability are illustrated by experiment see section 9.1.

When $K = K_{max}$, $\beta = 0$ and $\gamma = \lambda_1$, i.e. any oscillations set up are not damped out. Thus by comparison with a second order system λ_1 may be termed the natural frequency of the system for the simple regulator. The expression for λ_1 and the effects of damping and r_a on its value have been discussed in section 6.2.3, 6.4.2. and 6.4.3.

7.1.3 The Ultimate Stability Limit with a Simple Regulator.

The limiting value of δ_g for which the system may be stabilized with a simple regulator is given by Eqn. (6.14) and as has already been pointed out the value is at the peak of the transient power-angle curve δ'_s . Thus the following situation exists. An alternator without a voltage regulator becomes unstable when the slope of the steady power-angle curve is zero. If the alternator has a simple regulator with the optimum value of gain the stability limit is reached when the slope of the transient power-angle curve is zero. Thus the action of the regulator may be thought of as maintaining the voltage behind the transient reactance constant.

Although the present investigation is mainly concerned with operation at a fixed power, the locus of the ultimate stability limit is an important result and is shown on the Power Chart, Fig. 1.2. Substitution of Q_o , V_{do} and V_{qo} in Eqn. (6.14) yields,

$$P + \frac{V^2 \sin^3\delta_o}{\cos \delta_o} (Y'_d - Y_q) = 0 \qquad (7.5)$$

It should be pointed out that the value of K_{ss} required to achieve this stability limit depends on P . If saliency is neglected Eqn. (7.5) may be obtained from Eqn. (6.19) when $H(0)/H(j\lambda_1) = 1$. As may be seen from Eqn. (6.14) for a synchronous capacitor the load angle is zero and the stability limit becomes

$$Q_o = - V^2 Y_q$$

showing that no improvement is obtained at zero power (see Fig. 1.2).

7.2 Review and Classification of Regulators Used in Practice.

The literature contains a very large number of papers describing practical arrangements of voltage regulators. With only a few exceptions the regulators can be classified into four main types depending on the locus of $K(j\lambda)$ at low frequencies (0 to 2 c/s), as follows:

(i) Constant transfer function produced by rectifier excitation systems.

(ii) Delay or lagging regulators corresponding to a separately excited exciter.

(iii) Integrator or "buck-boost" regulators for which there are several connections, see Fig. 7.2.

(iv) Derivative or leading regulators combining 1st, and 2nd derivative as well as proportional signals.

Sections 7.2.1 to 7.2.4. deal respectively with the most important contributions for each type. Papers describing regulators not actually used on large machines are not considered. In order to avoid writing the transfer function each time the following general expressions is used

$$K(p) = K \frac{(1 + pT_\alpha)(1 + pT_\beta)(1 + k_\alpha p + k_\beta p^2)}{(1 + pT_1)(1 + pT_2)(k_o + k_1 p + k_2 p^2)} \qquad (7.6)$$

Only the parameters mentioned are present, the others being zero or negligible. For example quoting T_1 and T_2 implies a two delay regulator with no stabilization.

Details of components and the connections used are considered only in order to estimate the magnitude of the time constant involved. However, in many cases there is an element of doubt as full details of the transfer function are not often given.

There are several reviews of excitation systems dealing with several types but without introducing any variations. The most important

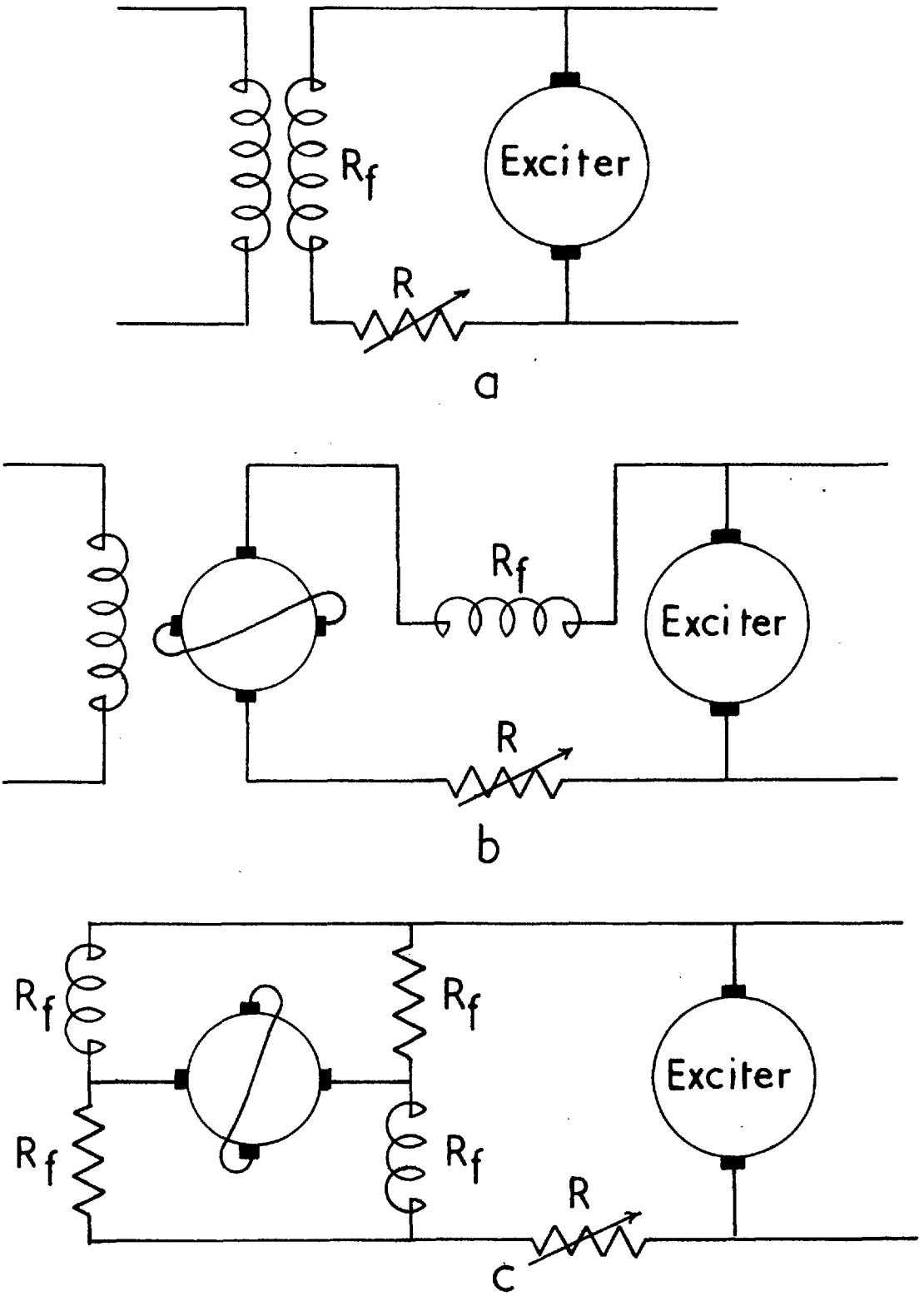

FIG. 7.2 INTEGRATOR CIRCUITS

of these are Gray and Fenwick[57-1]; Krochmann[60-6]; Achenbach[60-7] and Hefermann[62-7]. Practical aspects of design and construction are given in Zavalishin and Glebov[63-4] and Easton[64-4]. The last deals mainly with a.c. exciters having rotating or static rectifiers as well as with controlled rectifiers.

7.2.1 Practical Simple Regulators.

The simple regulator has already been defined as having a constant transfer function. For our purposes it is sufficient if, in the region of $\lambda/2\pi = 0$ to 5 c/s the maximum phase-shift and attenuation are 45° and 3 db respectively. Referring to Eqn. (7.6) if T_1 only is present it can be up to 30 msec.

The only way of achieving this is either by a controlled rectifier or a purely magnetic amplifier system. Feedback round a rotating amplifier is also a possibility but there is no indication in the literature that this degree of compensation is used in practice c.f. Bogoslovskii and Sovalov[63-5] p. 132. It should be mentioned that with a rectifier regulator the field current cannot reverse during transients. Rather than introduce a duplicate rectifier with complicated electrical changeover the solution adopted is to have a mechanical switch.

Roth[55-2] describes the only system approximating a simple regulator without controlled rectifiers. There is an inductor alternator on the main shaft giving a 420 c/s output which is rectified. The fields of the inductor alternator and the main alternator are connected in series and control of the voltage is as follows. The output voltage of the inductor alternator is very sensitive to the power factor of its load. Thus a magnetic amplifier is connected in parallel with the rectifier and is used as a variable impedance controlled by the error signal. Since the two fields carry the same current there is feedback proportional to i_f. It is not clear however, if this affects the transfer function to a large extent. A similar scheme is described by Zavalishin and Glebov[63-4] who state that it has been developed for large machines.

The last stage of the regulator considered by Ettinger, Gloukh and Chaly[58-6] consists of two rectifier bridges in parallel, both supplied from an auxiliary alternator, one at 460 V and the other at 1385 V. The 460 V bridge is used for normal operation and the 1385 V one for field forcing or quenching. The circuit diagram shows a change-over switch so that only one bridge is in operation at a time. No information is given on the transfer function of the rest of the regulator.

A straightforward rectifier regulator is described by Haamann[60-9]. A transistor regulator controls the firing angle and the rectifier power is supplied from the main alternator. A Bode plot is given of the frequency response of the open loop transfer function with the alternator on open circuit. It is stated that the rectifier has a deadband of 11 msec and this probably refers to the loss of control once a rectifier unit is turned on. Two innovations are introduced on a similar regulator described by Gruenberg[62-8]. Provision is made for varying the firing angle of the rectifier in response to digital signals from a distant control centre. Also an automatic mechanical changeover is used to reverse the alternator field current for rapid de-excitation. The ceiling voltage is 5 times the value required for normal voltage on open circuit. A similar arrangements for reversing the field current is described by Putz, Rieger and Rogowksy[63-3]. The mechanical changeover takes 220 msec compared to 80 msec of the Gruenberg regulator. This large dead band, however, does not appear to cause any anxiety.

Hefermann and Menstell[62-9] describe an interesting method for overcoming the difficulties associated with a rectifier taking its power from the main alternator. The field current is supplied from a rectifier which is controlled from a regulator having the conventional voltage feedback on which a compound signal depending on the alternator current has been added. The variation from the conventional set-up is that the voltage supplied to the rectifier is itself a combination of alternator voltage and current such that the rectifier voltage remains constant with changes of the alternator load. Various arrangements for supplying the rectifiers are discussed by Barral, Boulet and Carpentier[62-11]. One of

possibilities involves two rectifier units, one of which is supplied by a current transformer and the other by a voltage transformer. Thus the output of the excitation system is a function of both alternator current and terminal voltage.

7.2.2 Practical Delay Regulators.

This is a very common type and is the result of several amplifying stages in cascade, of which the final stage is usually a separately excited exciter. Very often there are feedbacks round each stage in order to reduce the effective delay. When there is a rotating exciter its time constant, being of the order of 0.3 to 2 sec completely swamps the time constants of any magnetic amplifiers (2 to 10 msec) or amplidynes (about 100 msec) that may be used. In such cases only the main exciter need be considered.

For the purposes of this study a regulator is considered to be of the delay type when the $K(j\lambda)$ locus lies in the 4th or in the 3rd and 4th quadrants for $\lambda/2\pi$ in the region 0 to 2 c/s excluding, of course, regulators with a $1/p$ term in the transfer function.

Doherty[28-1] described the first experimental operation in the artificial stability region in 1928. The regulator used was of the Tirrill type but since the frequency of operation of the contactsis about 10 c/s the action is effectively continuous. The contacts short-circuit a resistance in the shunt winding of a self-excited exciter. Hence ignoring the delay in the measuring element the transfer function is that of one delay equal to the exciter time constant. Tirrill regulators were fairly common in the 1930's but they were replaced because of their unreliability. Yttenberg[32-1] gives another example of a Tirrill regulator with the addition of a) a derivative feedback round the exciter using a transformer and b) compounding of the alternator voltage and current as the controlled variable.

Concordia[44-1] considers two values of T_1 namely 1.06 and 2.12

sec in a mainly theoretical investigation. Results similar to Fig. 7.1 are quoted and comparison is made with the simple regulator showing an improvement in the gain ratio G but reduction in the maximum stable angle, see section 7.3.1. This paper has already been discussed in section 1.1.3.

Barkle and Valentine[48-1] and Lynn and Valentine[48-2] use a rotating amplifier, the Rototrol, either as a main or as a pilot exciter. Although the Rototrol time constants are low it is unlikely that the transfer function of the simple regulator is achieved. One of the first minimum excitation limiters is described which comes into operation when the reactive power is a certain function of the active power preventing loss of steady state stability.

Kron[54-1] sets out various ways of stabilizing a delay regulator, one of which involves the use of a phase lead network in cascade with the amplifying stages. It is not clear, however, that the phase lead is sufficient to convert the regulator to the derivative type, since there are three delays in the denominator. It is likely that the purpose of the phase advance network is to reduce the phase lag of the delays. However the use of a cascade network specifically to change the transfer function is a major contribution although the result achieved, a term $(1 + pT_\alpha)$, is similar to that obtained with any derivative stabilizing feedback. A number of other signals is discussed for stabilizing the system, the most important of which is the use of a feedback proportional to the rate of change of field current. Aldred and Shackshaft[58-3] tried this with very good results both on transient and on steady state operation. As was stated in the Introduction, such a regulator can be analysed by the method used in the present investigation only if some of the equations of section 2 are modified. Another interesting possibility discussed by Kron is the control of the voltage anywhere in the system by simulating the system impedances.

In a regulator described by Achenbach[57-2] the terminal voltage is controlled by varying the loop gain rather than the reference. The

use of a loop gain dependent on the operating condition offers certain advantages, which however, are not discussed in the paper.

Two variations of the standard pattern of cascade amplifying stages are given by Frey and Noser[58-1]. In the first case feedback proportional to the field current is used as well as the normal exciter voltage feedback for stabilization. The second variation may be considered as the modern version of a Tirrill regulator. The field of the pilot exciter is supplied from a transistor regulator and the current is turned on and off. The output of the pilot exciter is proportional to the mark-space ratio. The use of a power transistor as a switch reduces the power dissipated considerably.

Pavesi and Simonetti[60-2] is one of the few papers giving a measured frequency response of the regulator transfer function. $T_a = 1$, $T_1 = 10$ and $T_2 = 0.02$ sec. An a.c. exciter, 400 c/s, with a rectifier follows three stages of magnetic amplifiers. Bode diagrams show the regulator response with and without stabilization. Operation in the artificial stability region is not considered and the aim is good voltage regulation and fast response.

In the regulator considered by Junior[60-5] the terminal voltage is compounded with the reactive current supplied by the alternator. The regulator itself is of the standard type with a magnetic amplifier, and amplidyne and a main exciter with derivative feedbacks. When fast de-excitation is required there is a negative feedback proportional to the field current.

In Happolt[60-8] several arrangements are discussed, including integrator types but there are no variations from the standard types. There is however an interesting application of a Schmidt trigger controlling a transistor amplifier which is followed by two exciters in series.

Easton, Fitzpatrick and Parton[60-10] considers a conventional delay

type regulator having an interesting angle limiter. The limiter may be set to operate at a low value of δ_g and then the regulator becomes effectively an angle regulator.

The regulator described by Ferguson, Herbst and Miller[60-13] and by Whitney, Hoover and Bobo[60-14] uses an a.c. exciter and rotating rectifiers. The field of the exciter is supplied by a magnetic amplifier. Since the alternator field voltage is not available for a stabilizing feedback the exciter transfer function is simulated by an RC network connected to the output of the magnetic amplifier. The output of the RC network is differentiated and fed to the first stage of the magnetic amplifier. The primary aim is good voltage regulation although operation in the underexcited region was studied by simulating the system on a differential analyzer; no results are given however.

The basic circuit of Harvey et al[61-1] is similar to that for an integrator regulator, Fig. 7.2b, but the field resistance is not adjusted to the critical value. Thus the effective time constant is increased and this partly offsets the advantage of fast response of an amplidyne as the main exciter. Since the power for the magnetic amplifiers exciting the amplidyne is obtained from the main alternator there is a duplicate regulator used during starting to control the amplidyne voltage. The main regulator takes over when the generator voltage is sufficient. It is stated that this regulator improves the steady state stability limit.

Venikov et al[63-1] describe a similar regulator with an artificially increased time constant applied to a synchronous condenser. The value of the effective time constant is not given but in Venikov[64-1] values of 10 - 20 sec are mentioned.

The transfer function of a typical delay type regulator in current use in Britain is as follows, Ref. 62-1.

$$\frac{354\ (1 + p)(1 + 2\ p)}{1 + 17.5\ p + 17.3\ p^2 + 0.81\ p^3 + 0.17\ p^4}$$

The voltage regulator used by Miles[62-2] has $T_\alpha = 2$, $k_o = 1$, $k_1 = 61.2$ and $k_2 = 4.5$.

Nielsen[62-6] quotes experiments made on micromachines in France. $T_1 = 0.3$ sec. is first considered and then there is another delay $T_\alpha = 20$ sec. added. Steady state stability was investigated experimentally by increasing the power slowly and a figure similar to Fig. 7.1 is quoted for a limited range of gains. A combination of voltage and angle regulator is also considered.

Shackshaft[63-2] gives full particulars of a regulator using an a.c. exciter. $T = 2$, $T = 0.1$, $k_o = 1$, $k_1 = 56.7$ and $k_2 = 6.53$. A frequency response of the regulator and alternator together is quoted. The alternator however was on open circuit and so no information on the steady state stability is obtained.

In Bogoslovskii and Sovalov[63-5] the exciter is separately excited by a controlled rectifier. The time constant, which is initially 0.87 sec. is reduced to 0.28 sec by splitting the field into 9 parallel branches. Then by using direct feedback the effective time constant is reduced to only 0.055 sec. It is interesting to note that the tests described in the paper were carried out to determine the steady state stability of the system with a "relatively large time constant".

7.2.3 Practical Integrator Regulators.

This type of regulator is also very popular because of its excellent steady state characteristics, see section 8.2. A regulator is defined to be of this type when there is a $1/p$ factor in the transfer function. An integrator on its own, however, does not enable the system to operate in the artificial stability region and often there is some kind of stabilization. Rather surprisingly, however, integrator type regulators with no stabilization are in use with large machines. Presumably the steady state stability limit is not approached. In practice the integrator transfer function is achieved either by electronic means or by

using one of the arrangements shown in Fig. 7.2.

Barkle and Valentine[48-1] and Lynn and Valentine[48-2] used the connection shown in Fig. 7.2a. It may be shown that, when R is adjusted so that the total field resistance has the critical value, an integrator transfer function results with a "built-in stabilizer" i.e. having a T_α term as well. The presence of this stabilizing term in the numerator does not appear to have been noted and there is no mention of operation in the artificial stability region.

The regulator described by Hedstrom[50-1] is a good example of the theory that the phase-shift introduced by each amplifying stage should be corrected by a corresponding feedback. There is a magnetic amplifier in cascade with two d.c. machines, the second of which is connected in the field of the main exciter, see Fig. 7.2b. Again it may be shown that when R is such that the total field resistance has the critical value for self-excitation the transfer function has a 1/p term. There are stabilizing transformers making three inner loops in addition to the main feedback from the alternator terminal voltage. The design objective is stated as the improvement of the speed of response. One unusual feature is the use of a variable feedback gain for controlling the terminal voltage. Similar regulators are described by Johansson[59-3] and Sohlstrom[59-4] but the feedback gain is constant. T_1 and T_2 are only 0.1 sec each. The three feedback circuits are adjusted to provide the "fastest possible restoration of generator voltage to its normal value after a disturbance". No details are given however, of the method used to determine the feedback transfer functions.

Two alternative methods of stabilization are considered in Concordia[50-2]. A voltage proportional either to dV_t/dt or to dV_{fe}/dt is added to the proportional feedback from the terminal voltage. Several combinations of parameters are investigated and it is found that for practical reasons the exciter voltage stabilizer should be preferred. An experimental verification of operation in the region of artificial stability on a large machine, 20.8 MVA , was made. The reference

voltage was reduced and it was observed that the field current showed a minimum. Instability occurred soon afterwards but the limiting angle is not given. See section 1.1.3 for the theoretical contents of this important paper.

An unstabilized integrator using the connection of Fig. 7.2 b is described by Hunter and Temoshok[52-2]. There is a VAr limiter similar in principle to that of Barkle and Valentine[48-1]. Although it is stated that the steady state stability is improved, in a figure quoted the VAr limiter is set at a load angle of only 63°. McClymont et al[56-5] referring to a similar unstabilized integrator claim operation just inside the artificial stability region. The VAr limiter in this case was set at 90° and it must be assumed that the combination of limiter and regulator produced some small stabilizing effect. Alternatively, it is possible that some form of stability feedback was used,which however is not mentioned in any of the three papers.

Cooper and Girling[60-4] found that it was necessary to use a direct feedback round their unstabilized integrator in order to improve the steady state stability. In doing so, however, the regulator becomes of the delay type with T_1 dependent on the amount of feedback.

Hosemann[60-1] is the first paper to describe an electronic stabilized integrator. The error signal is taken to a "black box" the output of which gives proportional, integral and derivative signals, in our notation k_α, k_β and k_1. These are used to control the firing angle of a rectifier supplying the alternator field. Thus no further delays are introduced. However, no details of the black box are given and moreover it is stated that the integral and derivative action is not important from the practical point of view.

Bloedt and Waldmann[62-4] approach the choice of suitable parameters in a very interesting manner. They consider an isolated machine on load and assume that the alternator transfer function may be taken as a single delay, neglecting damping, i.e. $V_s/(1 + T'_{dL}p)$. The exciter is another

delay T_e and so for optimum transient response a regulator with $T_\alpha = T'_{dL}$ and $T_\beta = T_e$ is required. Good steady state voltage regulation is achieved with an integrator and further conditions determine the gain. Having obtained the required transfer function they then proceed to use a unit described by Sichling and Rohloff[57-3] and Kessler[57-4], which consists of a high gain amplifier controlling a switching transistor. Depending on the type of negative feedback used various transfer functions may be obtained. It is appreciated that when the alternator is connected to a bus both V_s and T'_{dL} vary with the operating point. Two figures show that optimization for open circuit, gives a damped response on load. Unfortunately there is no mention of the steady state stability performance of this very interesting regulator.

Nielsen[62-6] in addition to the delay type regulator includes some results for an unstabilized integrator. It is argued by means of a Nyquist diagram that the maintenance of stability in the region of 90° is difficult.

The circuit shown in Fig. 7.2 c was used by Chambers, Rubenstein and Temoshok[62-10] to obtain an integrator transfer function. It appears that no stabilizing feedbacks are used and in figures quoted the VAr limiter is set to operate at angles considerably less than 90°. Ewart et al[65-2] used the same connection and with artificially high line reactance obtained an angle of 96°. It is not stated whether any stabilization was used and no stabilizing feedbacks are shown on the diagrams.

In the English Electric Regulator[64-7] the pilot exciter rather than the main exciter is connected as shown in Fig. 7.2a. There are two derivative feedbacks one from the exciter voltage and the other from the alternator terminal voltage. A rather elaborate limiter circuit is used which comes into operation when some function of the following quantities exceeds a preset value: a) i_f, b) i_{ac} c) d v_{fe}/dt d) dv_p/dt (pilot exciter voltage) and V_t. Other facilities include signals from other machines in the station for reactive power division and provision for regulating the voltage at some distant point in the system.

7.2.4 Practical Derivative Regulators.

A derivative regulator is one whose frequency response lies in the 1st or 1st and 2nd quadrants. This definition is, in a way, arbitrary since it excludes some regulators with T_α and T_β terms. In fact the majority of regulators on the other three types employ some kind of derivative feedback, which results in such terms. These terms, however are not sufficient to cancel the delays in the denominator and so the effect on stability is the same as that of a delay regulator. A possible exception to this is Kron[54-1], (see Section 7.2.3).

Both Venikov and Litkens[56-2] and Venikov[64-1] refer to a regulator with the following transfer function

$$K(p) = \left(1 + \frac{k_1 p}{1 + pT_1} + \frac{k_2 p^2}{1 + pT_2} \right) \frac{K}{1 + pT_3}$$

but no particulars are given of the circuits used except that the regulator is an electronic one. It is claimed that this type of regulator is used to extend the steady state stability limit beyond δ'_s. This this is certainly possible is proved below, see section 7.3.3., but no experimental results appear in the Russian literature available in English. The theoretical aspects of these two references are discussed in section 1.1.3 and a comparison with the Nyquist method is given in Appendix IV.

Details of a derivative regulator however are given in Venikov et al[63-1]. The derivatives are obtained by means of R.C sections followed by a single valve for amplification and impedance matching. No measures appear to have been taken to eliminate drift in spite of the simplicity of the circuit. No values of parameters are indicated.

7.4 The Effect of Regulators on the Steady State Stability.

The open loop transfer function of the system is the product of

$K(j\lambda)$ and $H(j\lambda)$ i.e.

$$\left|L(j\lambda)\right| = \left|H(j\lambda)\right| \cdot \left|K(j\lambda)\right| \qquad (7.7)$$

and $$\text{Arg } L(j\lambda) = \text{Arg } H(j\lambda) + \text{Arg } K(j\lambda) \qquad (7.8)$$

Having calculated $H(j\lambda)$ the determination of $L(j\lambda)$ is a simple matter for any type of regulator, however complicated. Eqns. (7.7) and (7.8) are easy enough for a hand calculation but since a large number of points is involved a digital computer was again used. One data tape contained the values of $H(j\lambda)$ for $\delta_g = 60^\circ$ to 165° and another, shorter, tape the sets of parameters of $K(j\lambda)$. In fact the effect of a particular regulator on stability may be seen, qualitatively at least, by inspection of the $K(j\lambda)$ and $H(j\lambda)$ plots.

The conditions that the $L(j\lambda)$ locus should satisfy for stability are the same as those for the simple regulator, see section 7.1, provided that $K(p)$ does not have unstable poles. Although there is no fundamental reason why the regulator itself should be stable on open loop, in practice this is invariably the case.

It is desirable to define a function μ as the value of λ at the second intersection of the $L(j\lambda)$ locus with the negative real axis. When there are two intersections as in the case of the integrator and derivative regulator for certain values of δ_g the suffixes 1 and 2 are used so that μ_1 refers to the lower and μ_2 to the higher value. It is apparent that μ depends on δ_g as well as on the regulator transfer function. Clearly μ is the natural frequency of the system and when $K(p)$ is constant $\mu = \lambda_1$.

7.3.1 The Effect of the Delay Regulator.

By the definition of this type of regulator Arg $K(j\lambda)$ is negative and therefore the $L(j\lambda)$ locus is obtained by rotating the $H(j\lambda)$ locus in a clockwise direction by an amount depending on λ. It is possible to make the following general deductions before considering a particular

example.

At some value of δ_g less than δ_s' the $L(j\lambda)$ locus no longer crosses the negative real axis. Hence the maximum value of δ_g for which the system may be stabilized by a suitable gain is reduced.

The natural frequency of the system, μ, is reduced.

$|K(j\lambda)|$ is reduced as λ is increased at a rate depending on the number and magnitude of the delays. By considering the shape of the $H(j\lambda)$ locus it may be deduced that, up to about $110^\circ - 120^\circ$, $L(j\mu) < H(j\lambda_1)$. Thus K_{max} is increased and since K_{min} remains the same the stability ratio is increased.

The majority of delay type regulators used in practice involve a separately excited exciter, the field time constant of which is the predominant term. Hence a typical transfer function is

$$K(p) = \frac{K}{1 + p\,T_1}$$

The regulator block diagram is simply made up of one delay as shown in Fig. 7.3 a. The frequency response of the regulator for $T_1 = 1$ sec and the corresponding $L(j\lambda)$ loci are shown in Figs. 7.4 and 7.5 respectively. The stability limit as a function of gain for $T_1 = 0.5$, 1 and 2 sec is shown in Fig. 7.6 together with the corresponding curve for the simple regulator.

The Nyquist locus for $\delta_g = 130^\circ$ in Fig. 7.7. does not cross the negative real axis and the system cannot be stablized beyond some value of δ_g between 120° and 130°. Fig. 7.6 shows that the maximum stability limit is reduced as T_1 is increased from 126.5° to 122° and to 117° for $T_1 = 0.5$, 1, 2 sec respectively. The value of K_{ss}, the optimum gain for steady state stability, is given by the intersection of the new curves for K_{max} and the simple regulator curve for K_{min}. Hence K_{ss} is reduced as T_1 is increased. The frequency at the second intersection

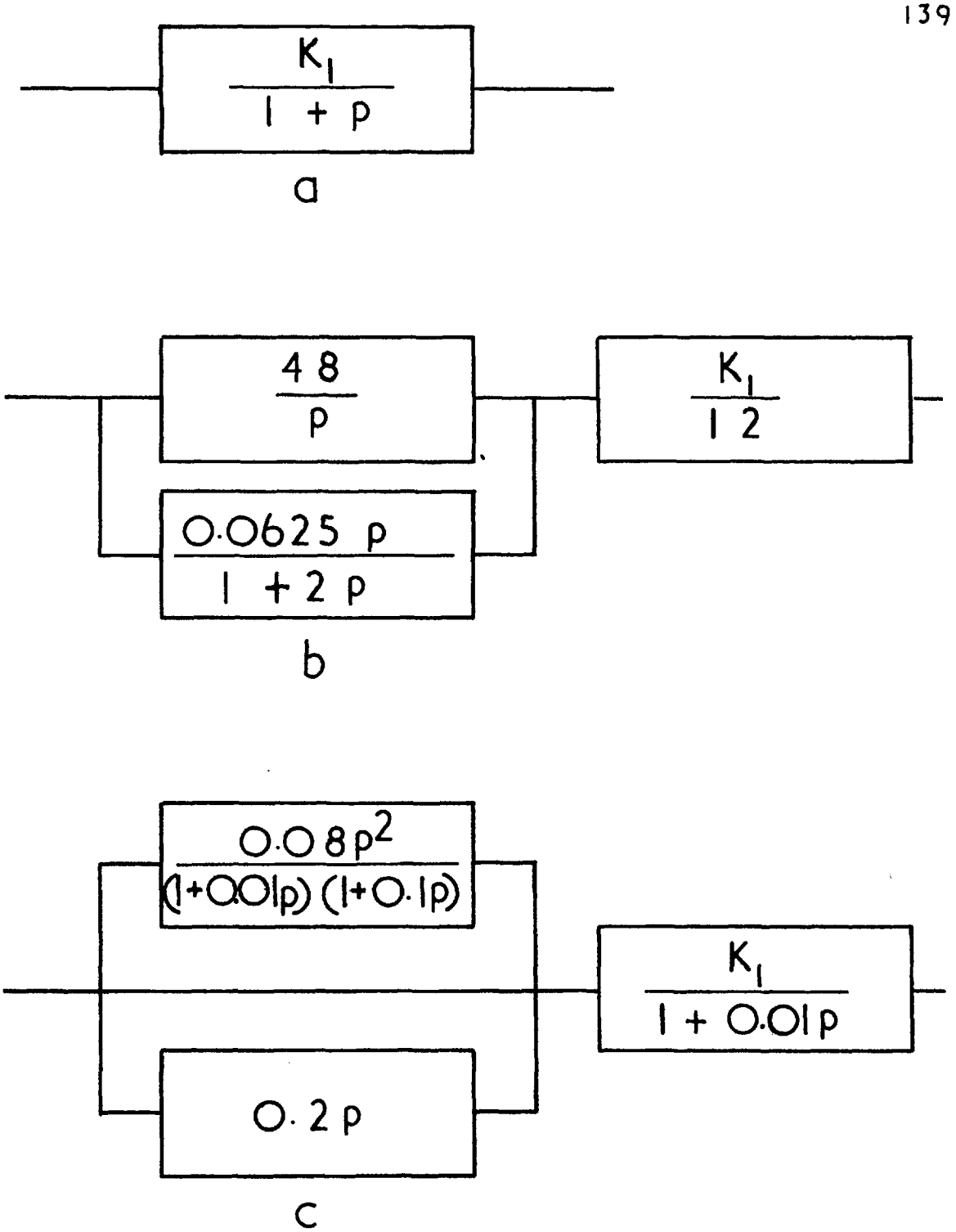

FIG.7.3 REGULATOR BLOCK DIAGRAMS

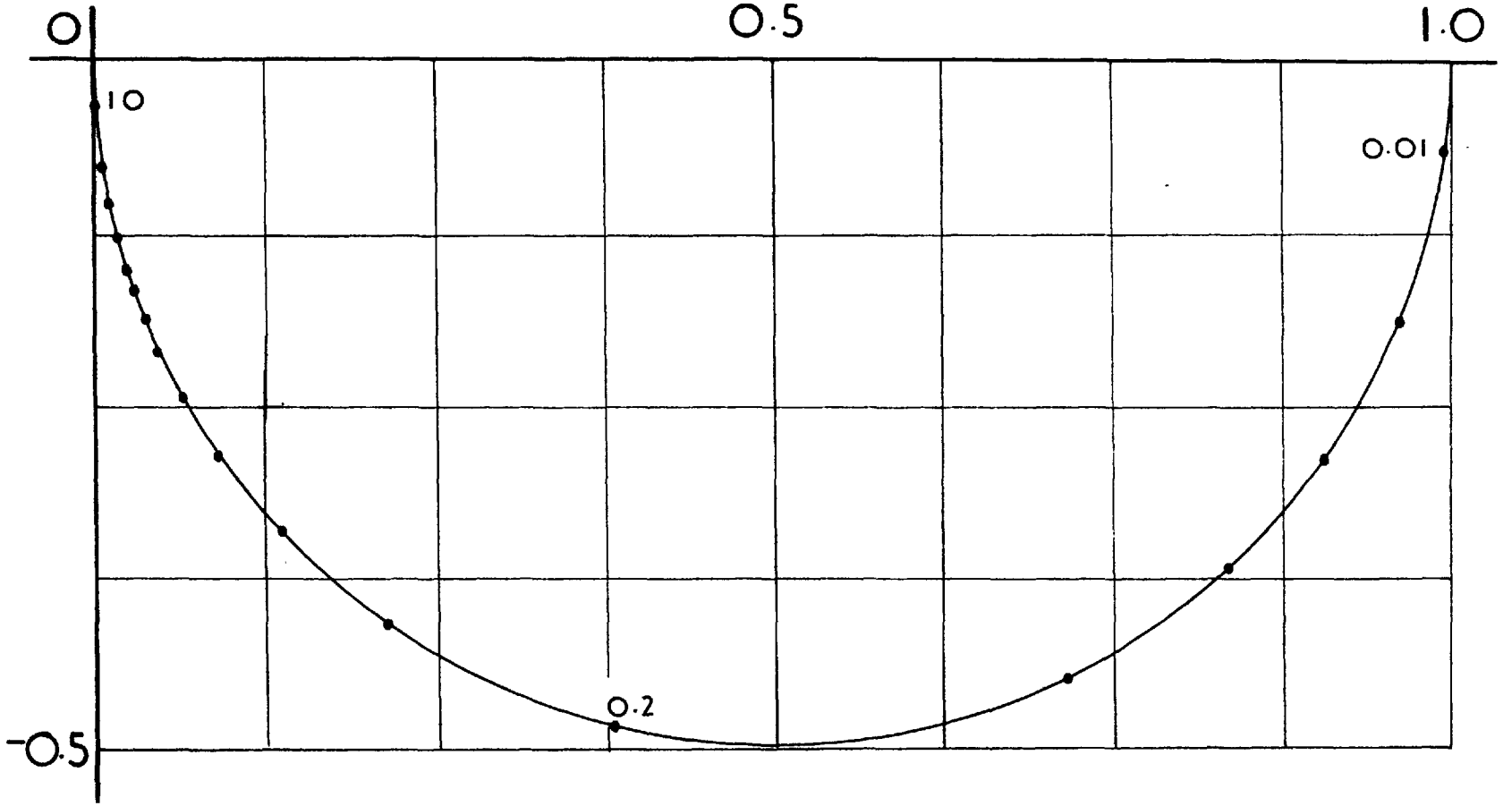

FIG. 7.4 REGULATOR TRANSFER FUNCTION

DELAY TYPE T_1 = 1 sec. Calculated

FIG 7.5 PLOTS OF L(jλ)

DELAY REGULATOR $T_1 = 1$ sec

DAMPING AND r_a

FREQUENCY IN c/s

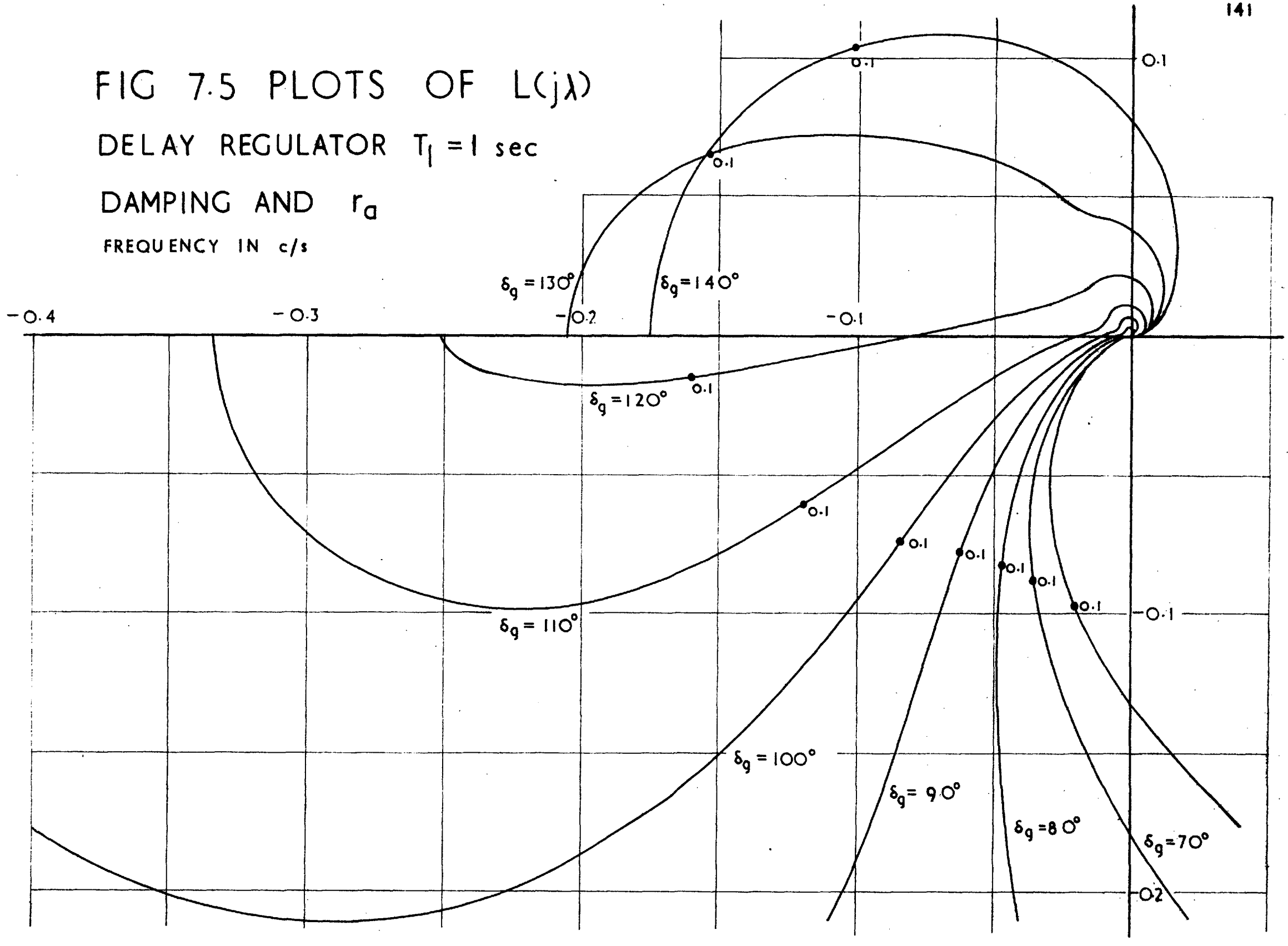

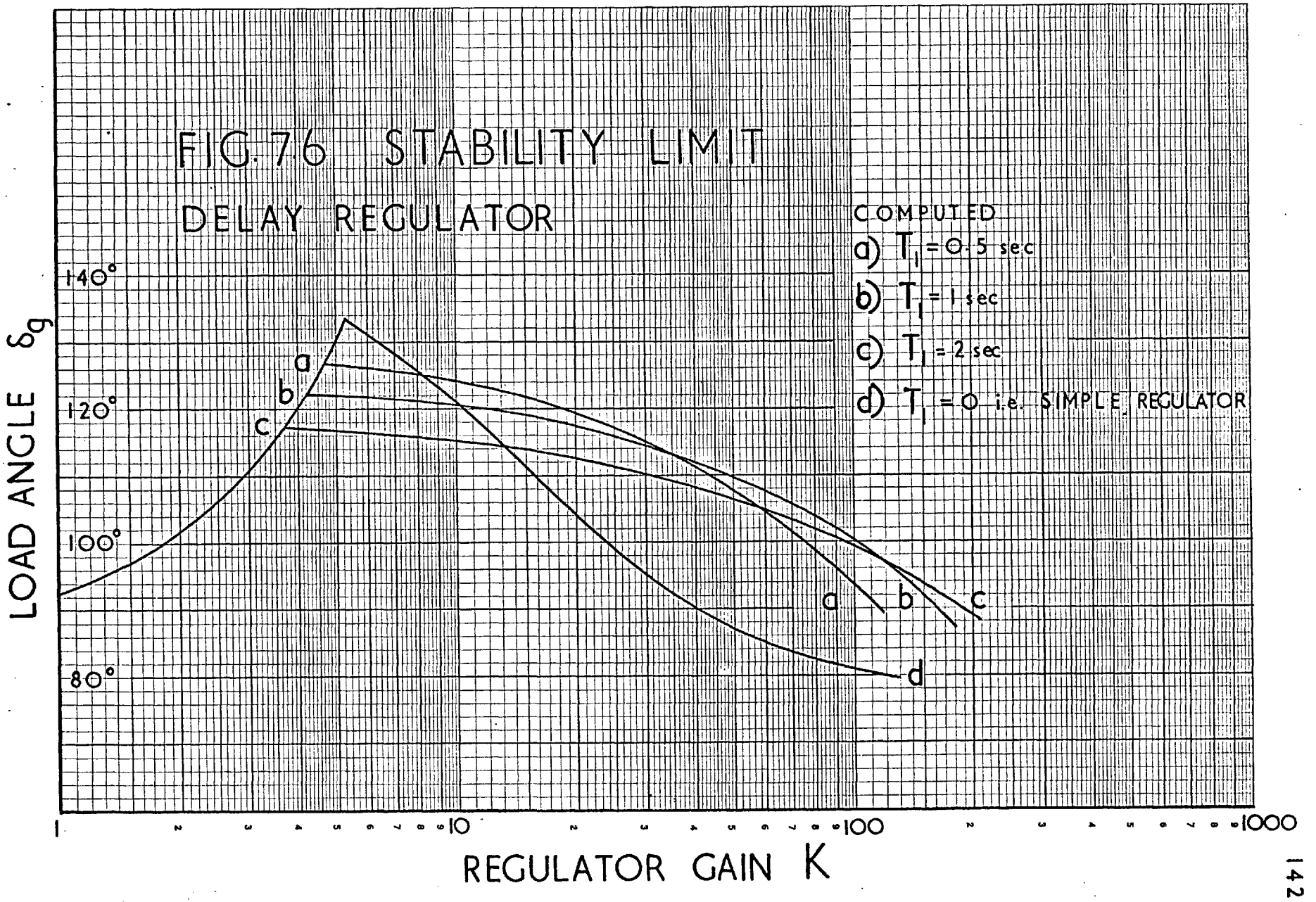
FIG. 7.6 STABILITY LIMIT
DELAY REGULATOR
COMPUTED
a) T_1 = 0·5 sec
b) T_1 = 1 sec
c) T_1 = 2 sec
d) T_1 = 0 i.e. SIMPLE REGULATOR
LOAD ANGLE δ_g
140°
120°
100°
80°
a
b
c
d
1
10
100
1000
REGULATOR GAIN K

μ is shown as a function of δ_g in Fig. 6.4 for $T_1 = 1$ sec. Thus at high values of gain there is oscillatory instability at a much lower frequency compared with the simple regulator. The reduction of μ implies that the effect of damping is less significant than for the simple regulator. Also the effect of r_a is produced mainly by the change in $H(0)$ and not by the frequency dependent terms.

The stability ratio G is increased as shown in Fig. 7.6. One cannot, however conclude that the system is, in general more stable with a delay regulator. From Control Systems Theory, see Ref. 60-11, the phase margin as well as the gain margin should be large. Fig. 7.4 shows clearly that, for 120°, although K can be chosen so that the gain margin is large the phase margin is reduced compared with the simple regulator. The use of artificially high values for T_1, 10 or 20 sec, has been tried by Nielsen[62-6] and was suggested by Venikov[64-1] as a means for increasing the regulator gain when operation for high values of δ_g is not required. It is apparent from Figs. 7.5 and 7.6 that such a regulator will hardly enable the system to operate in the artificial stability region.

Additional terms in Eqn. (7.9) should be considered only if they produce significant phase shift and attenuation for frequencies up to μ. Thus for $\delta_g = 110^\circ$ a delay of 100 msec produces 14° phase-shift at $\lambda = \mu$ and this does not affect the situation materially. The effect of a $(p T_\alpha + 1)$ term in the numerator and an additional delay $(pT_2 + 1)$ in the denominator of the transfer function may be approximated by

$$T_1 = T_1' + T_2 - T_\alpha$$

if T_1' is the main delay and T_2, T_α $<$ 100 msec.

7.3.2 The Effect of the Integrator Regulator.

The simplest form of an integrator regulator is

$$K(p) = \frac{K}{p} \qquad (7.10)$$

Since Arg $K(j\lambda) = 90^\circ$ and is independent of λ all points in the $H(j\lambda)$ locus are shifted, in a clockwise direction by 90°. It is apparent from Fig. 6.1 that for

$$\delta_g < \delta_s \qquad L(0) \longrightarrow -j\infty$$

$$\delta_g > \delta_s \qquad L(0) \longrightarrow +j\infty$$

In the second case the $H(j\lambda)$ locus does not enter the 4th quadrant and therefore the $L(j\lambda)$ locus never crosses the negative real axis. Hence a system with a simple integrator regulator as given by Eqn. 7.10. cannot operate in the artificial stability region and there seems little point in considering this case further. However many cases using integrator type regulators have some kind of stabilization, usually by derivative feedback e.g. as shown in Fig. 7.3 b. Hence the following may be considered as a typical transfer function

$$K(p) = \frac{K(p\,T_\alpha + 1)}{p(p\,T_1 + 1)} \qquad T_\alpha > T_1 \qquad (7.11)$$

Before proceeding to examine particular examples it is useful to consider some general deductions.

T_α and T_1 should be chosen so that the phase shift at the frequencies near the desired value of μ is small. Since however it is not possible to make Arg $K(j\lambda)$ positive in the transfer function of Eqn. (7.11) the maximum value of stable δ_g is less than δ_s'.

$L(0) \longrightarrow +j\infty$ for $\delta_g > \delta_s$ and therefore if the $L(j\lambda)$ locus intersects the negative real axis there are two intersections. This implies that when K is chosen so that the $(-1, 0)$ point does not lie between the two intersections, then there is a complex conjugate pair of roots with positive real parts. Hence instability should be expected to be oscillatory both for high and for low values of gain. Ewart et al[65-2]

observed low frequencies of oscillations with periods of oscillation 2-3 sec and 35 sec. See also section 9.1.

The numerical example chosen was obtained by simplifying the block diagram of a particular A.V.R. in current use in Britain, see Fig. 7.3 b. Referring to Eqn. (7.11) $T_a = 2$ and $T_1 = 0.5$ sec. Figs. 7.7 and 7.8 show the frequency response of $K(j\lambda)$ and the resultant $L(j\lambda)$ locus respectively. The corresponding stability limit curve is shown in Fig. 7.9 where it should be noted that K cannot be compared with the regulator gains for the other types of regulator since the gain of the integrator type at $\lambda = 0$ is infinite. The fact that the maximum δ_g occurs for values of K of the same order as before is merely due to the coincidence that $\mu \simeq 1$. Nevertheless there is still a value of gain corresponding to K_{ss} and upper and lower limits corresponding to K_{max} and K_{min}.

The maximum value of δ_g is now under 120° and Fig. 7.8 shows that the phase margin for 110° is small. The two values of μ are smaller than λ_1 and are shown on Fig. 6.4. Again the effect of damping and r_a is important in as far as it changes $H(j\lambda)$ for small λ.

If the feedback gain in Fig. 7.3b is increased so that $T_1 = 0.1$ sec then the stabilization is more effective and the minimum phase shift is reduced. Fig. 7.10 shows the stability limit curve for this case and the maximum value of δ_g is about 123°. Further improvement, however, is difficult without a 2nd derivative term in the numerator. Comparison between Figs. 7.9 and 7.10 shows that the stronger stabilization results in a reduction to the values of K_{min} and K_{max}. This affects the behaviour of the system to ramp functions but this problem lies outside the scope of the present investigation. See section 8.1 for the effect of the response to a step function.

7.3.3 The Effect of the Derivative Regulator.

Consider a regulator with first derivative and proportional signals

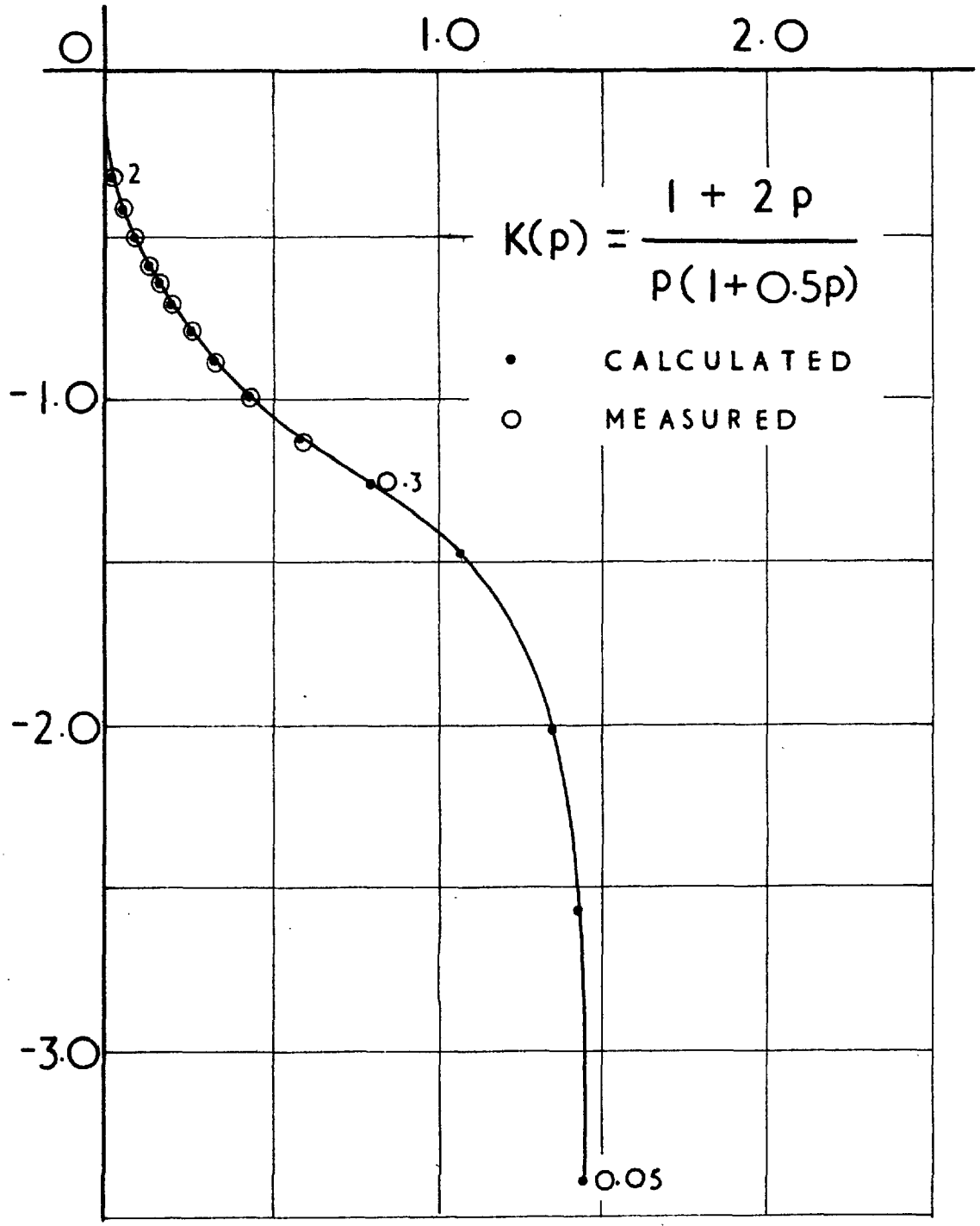

FIG. 7.7
REGULATOR TRANSFER FUNCTION
INTEGRATOR TYPE

FIG. 7.8 PLOTS OF $L(j\lambda)$

INTEGRATOR REGULATOR $T_I = 1$ $T_\alpha = 2$ sec

DAMPING AND r_a

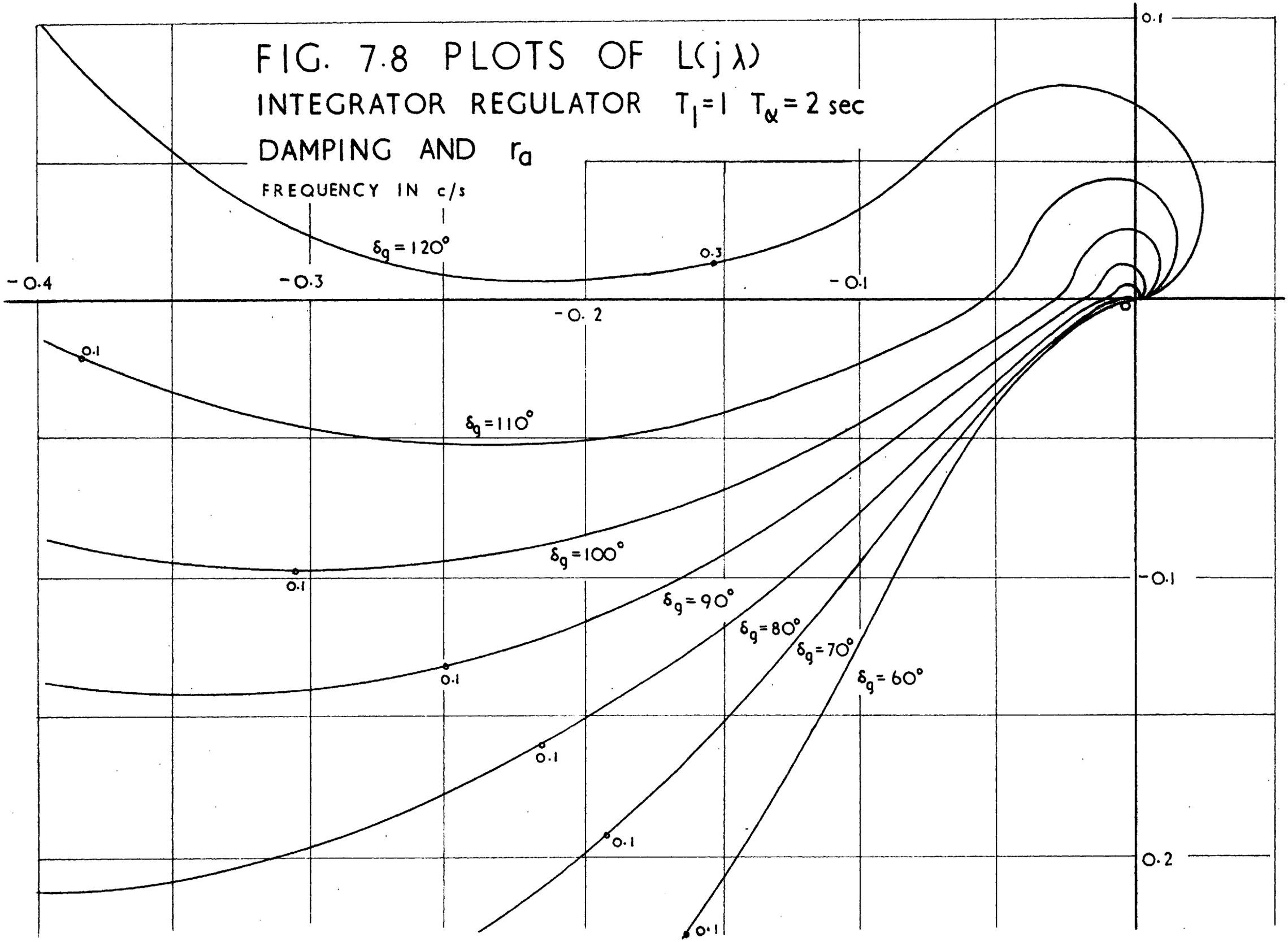

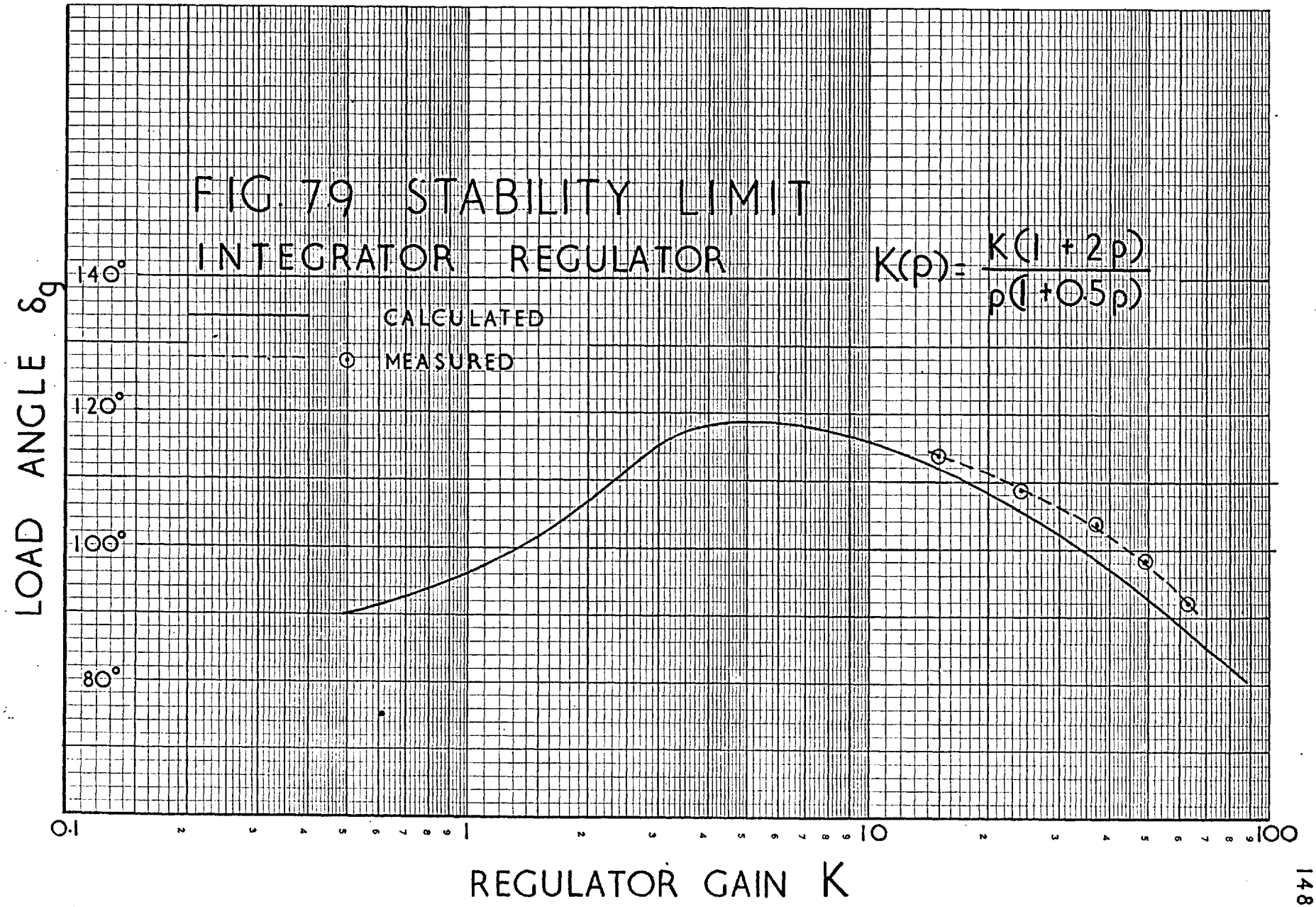
FIG. 79 STABILITY LIMIT
INTEGRATOR REGULATOR
$K(p) = \frac{K(1+2p)}{p(1+0.5p)}$
CALCULATED
MEASURED
LOAD ANGLE δ_g
140°
120°
100°
80°
0.1
1
10
100
REGULATOR GAIN K

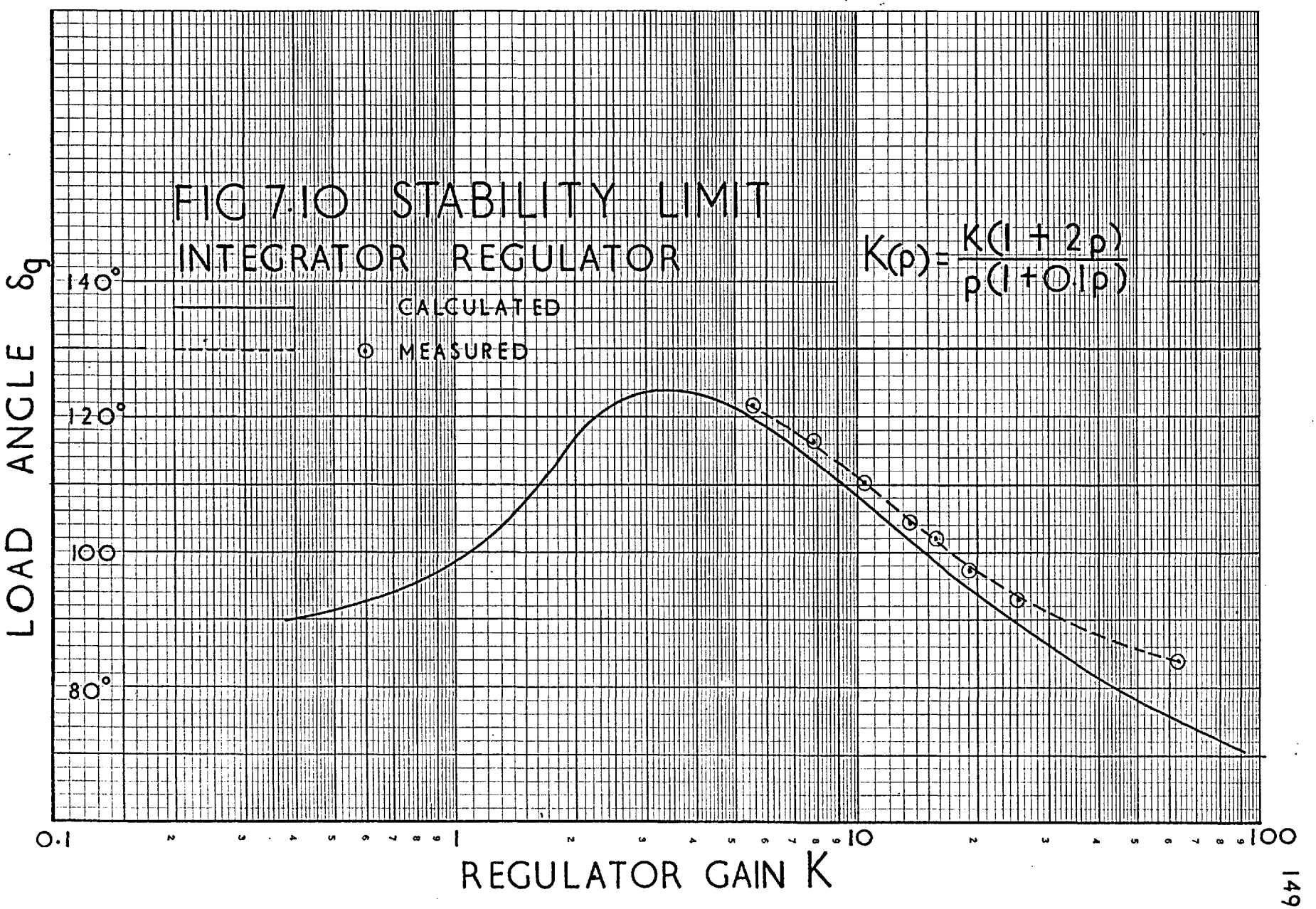
FIG 7.10 STABILITY LIMIT
INTEGRATOR REGULATOR
CALCULATED
MEASURED
$K(p)=\frac{K(1+2p)}{p(1+0.1p)}$
LOAD ANGLE δ_g
140°
120°
100
80°
0.1
1
10
100
REGULATOR GAIN K

only i.e.

$$K(p) = K(1 + K_\alpha p) \qquad (7.12)$$

Curve a in Fig. 7.11 gives the form of the frequency response locus for this case. The $H(j\lambda)$ locus for $\delta_g = 140^\circ$ is approximately a semicircle, with a time constant T_a say, as shown by curve b. Hence

$$L(p) = -\frac{H(0)\, K_o\, K\, (1 + k_\alpha p)}{1 + T_a p}$$

Thus the $L(j\lambda)$ locus is also a semicircle as shown by curve c, for $k_\alpha < T_a$ and curve d for $k_\alpha > T_a$. If K is adjusted so that the (-1, 0) point lies between the two intersections with the real axis for either case then both curves encircle the (-1, 0) point in a clockwise direction and hence the system is unstable for any value of k_α.

In practice a differentiator is not ideal as shown in Eqn. (7.12) and a delay is present i.e.

$$K(p) = K\, \frac{(1 + k_\alpha p)}{p\, T_1 + 1} \qquad (7.13)$$

and the form of this locus is shown by curve a'. For small T_1 the resultant $L(j\lambda)$ loci are as indicated by curves c' and d', corresponding to c and d. Again there can only be one clockwise encirclement of the (-1, 0) point and the system is unstable as before. It should be stated, however, that the $H(j\lambda)$ locus for $\delta_g = 140^\circ$ is only approximately semicircular. If T_a is small and if k_α is chosen to be within narrow limits it is theoretically possible to have a stable system. Nevertheless the stability ratio for $\delta_g > \delta_s'$ is nearly unity and the phase margin practically zero and hence it is valid to say that first derivative regulator cannot extend the stability limit beyond δ_s'.

In addition the stability ratio for $\delta_g < \delta_s'$ is reduced by a first

FIG. 7.11 PLOTS OF $L(j\lambda)$ WITH A 1st DERIVATIVE REGULATOR

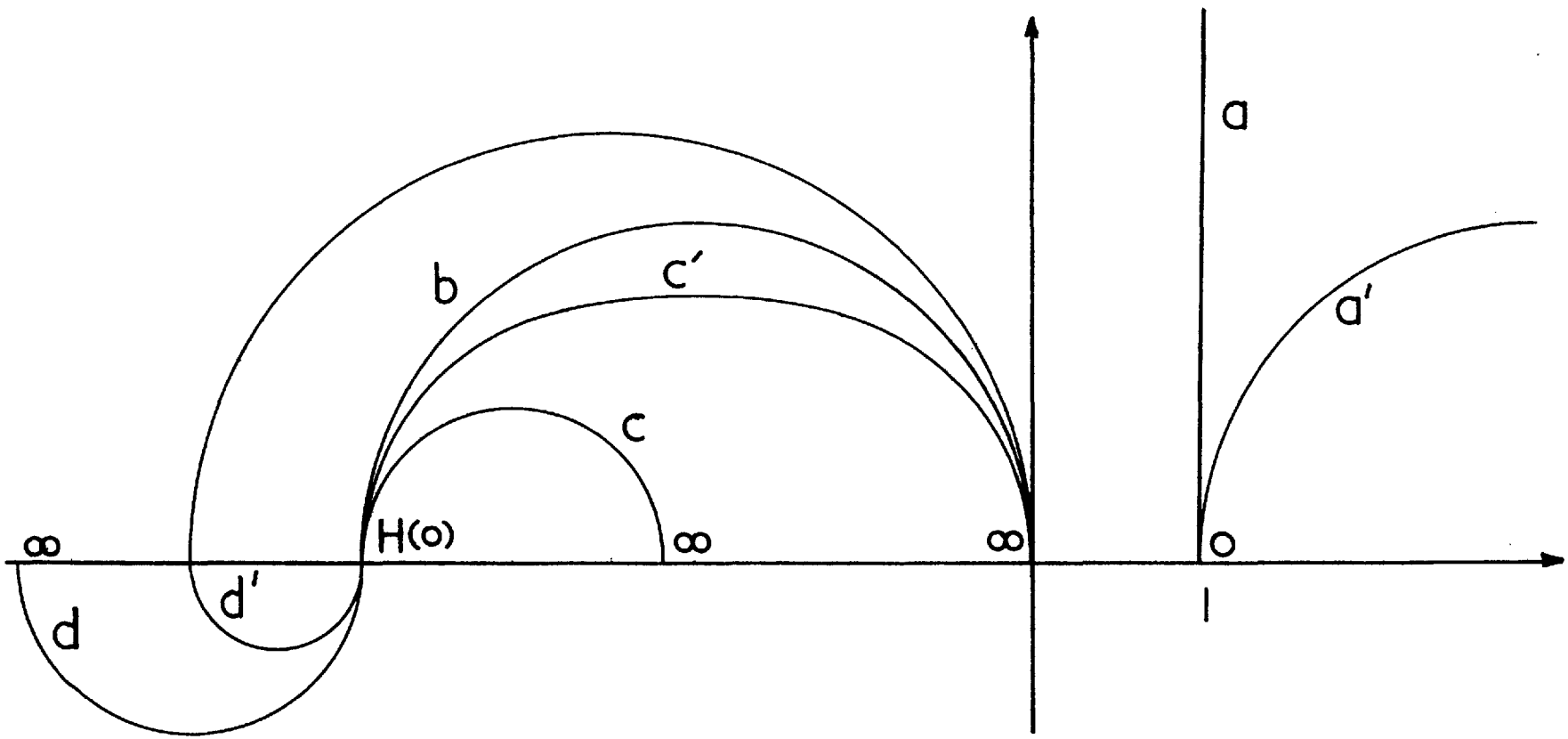

derivative regulator. Thus the performance of such a regulator from the stability point of view is not satisfactory.

It is now apparent that extension of the artificial stability region can only be achieved when part of the $K(j\lambda)$ locus lies to the left of curve a , Fig. 7.11 i.e. when there is a second derivative term as well as a first derivative one. As has already been mentioned practical differentiators have delays in their denominators. In the case of a synchronous machine regulator these delays are not a "nuisance" to be made as small as possible as implied by Venikov and Litkens[56-2] but play an important part in eliminating high frequency oscillations. In the example considered below there is an additional delay so that the gain at high frequencies is even further reduced. As shown in the block diagram Fig. 7.3 c there are three parallel branches giving proportional, 1st and 2nd derivative signals. These are added together and the extra delay is introduced.

$$K(p) = \frac{1}{1 + 0.01p}\left(1 + 0.2p + \frac{0.08\,p^2}{(1 + 0.1p)(1 + 0.01p)}\right) \qquad (7.14)$$

Fig. 7.12 shows the frequency response for this regulator. From the stability point of view only values of frequency up to about 2 c/s are of interest but the rest of the locus is shown as well to indicate the very high gain at approximately 17 c/s. The parameters in Eqn. (7.14) were chosen so that for frequencies up to 1 c/s Arg $K(j\lambda)$ is large and $K(j\lambda)$ small consistent with practical limitations on the experimental set-up, see section 9.1.

Fig. 7.13 shows the $L(j\lambda)$ loci obtained with this regulator. The curve for $\delta_g = 140^\circ$ crosses the negative real axis and it is possible to stabilise the system. Although the curve for $\delta_g = 150^\circ$ crosses the negative real axis the system cannot be stabilized since the (-1, 0) point can be encircled only in a clockwise direction. As Fig. 7.14 shows the maximum stable angle is 147° and K_{ss} is about 4

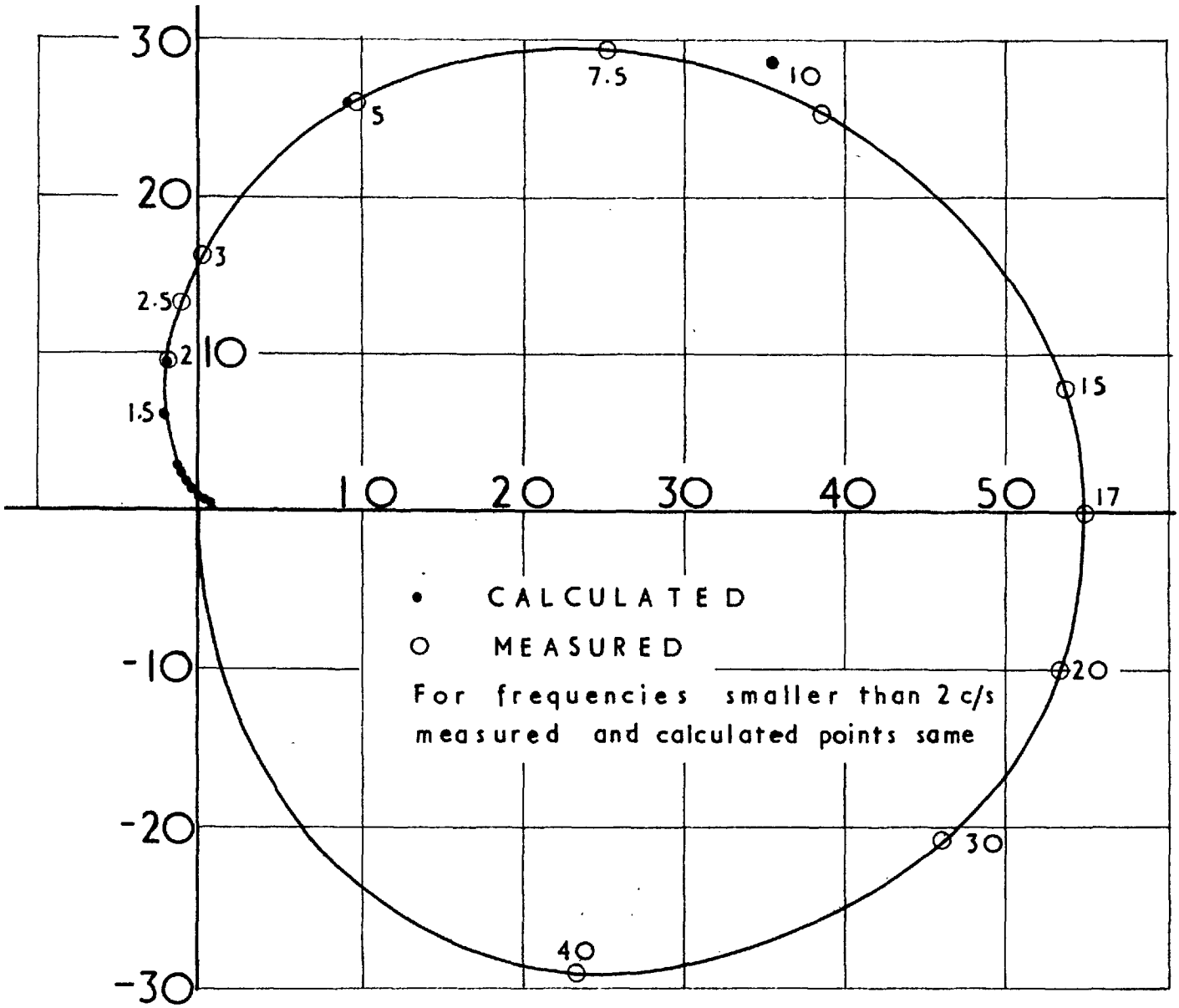

FIG. 7.12
REGULATOR TRANSFER FUNCTION
DERIVATIVE TYPE

FIG. 7.13 PLOTS OF $L(j\lambda)$

DERIVATIVE REGULATOR

DAMPING AND r_a

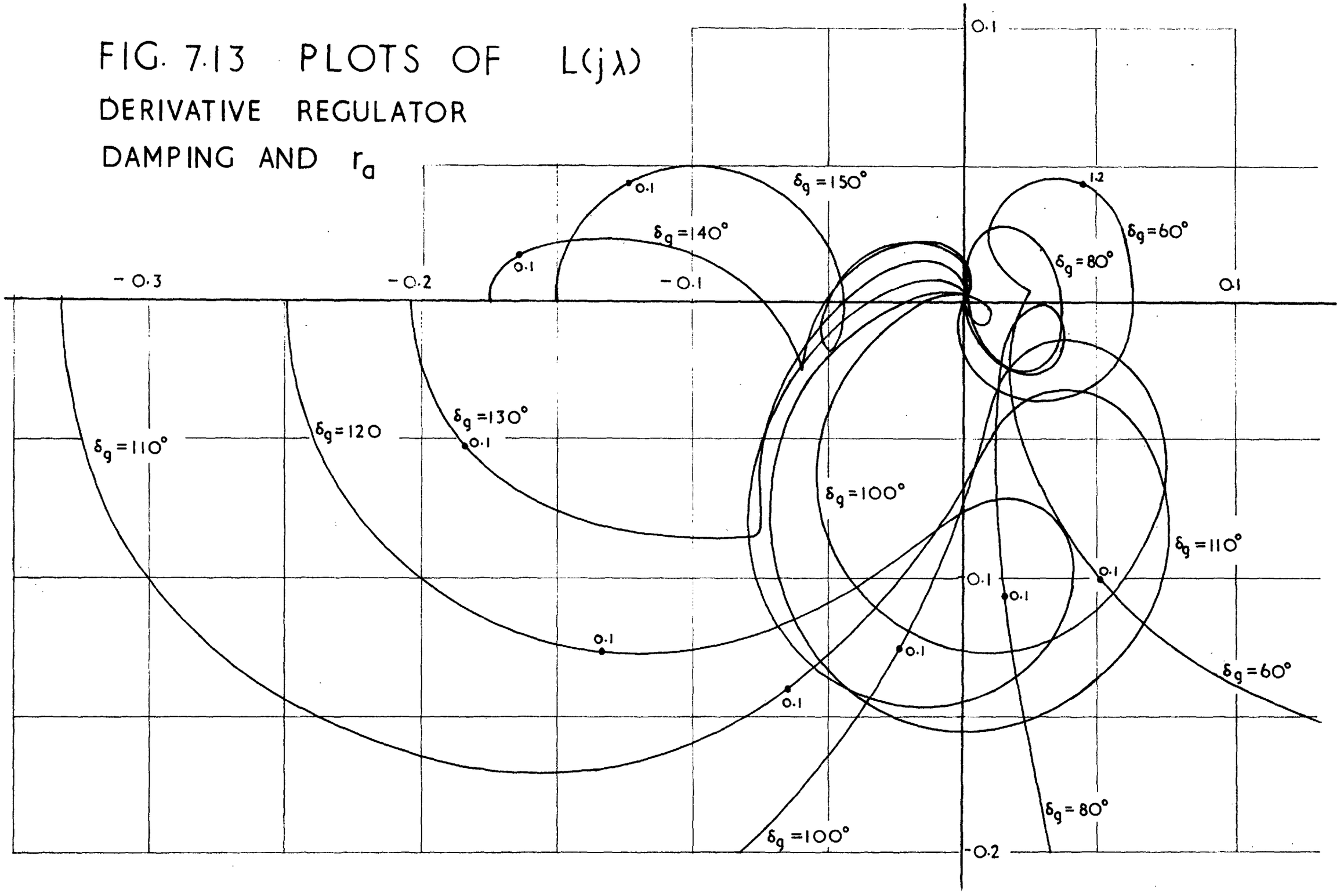

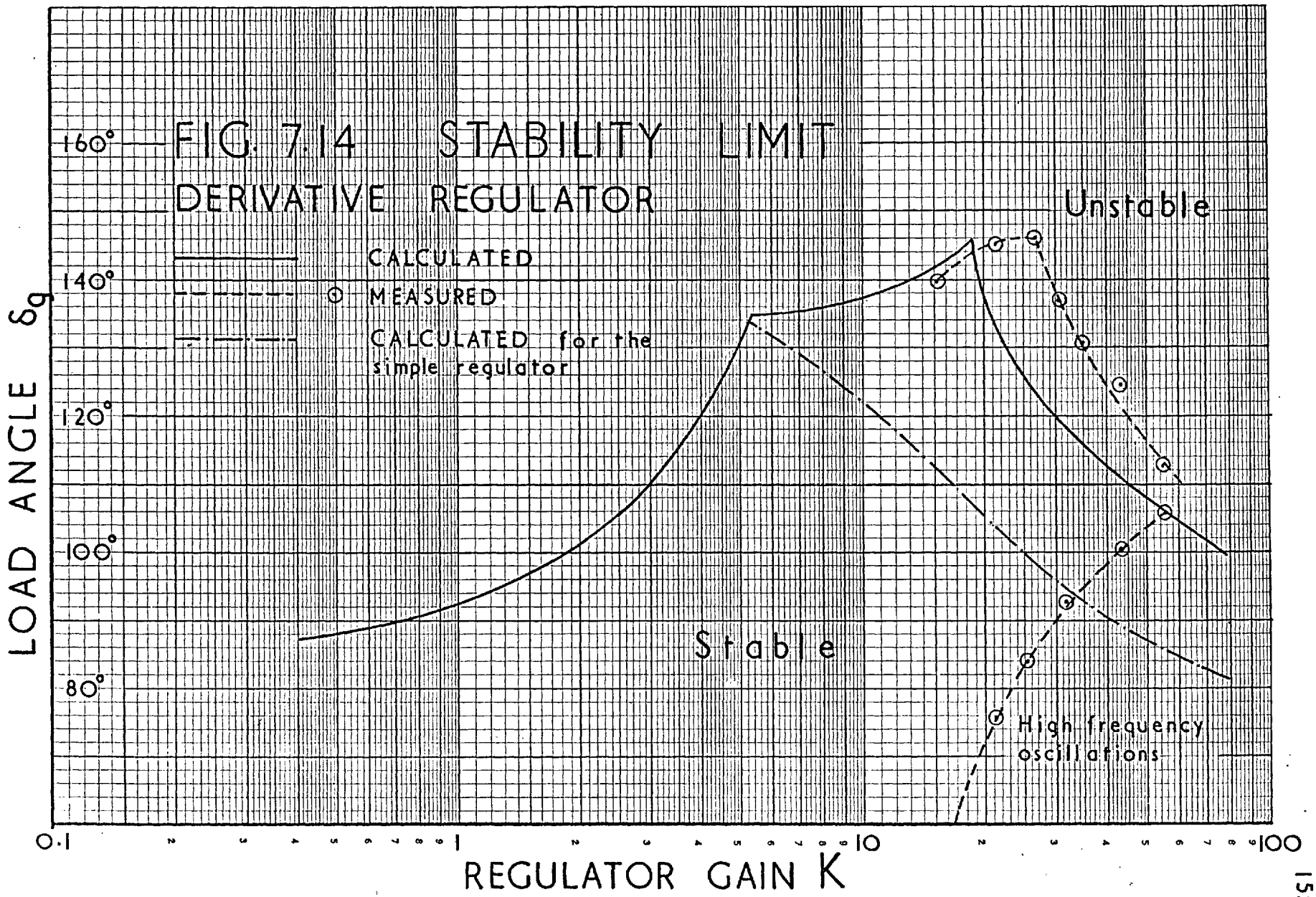
FIG. 7.14 STABILITY LIMIT
DERIVATIVE REGULATOR
CALCULATED
MEASURED
CALCULATED for the simple regulator
Unstable
Stable
High frequency oscillations
LOAD ANGLE δ_g
160°
140°
120°
100°
80°
0.1
1
10
100
REGULATOR GAIN K

times as large as with the simple regulator.

For $\delta_g > 135^\circ$ (approximately) the $L(j\lambda)$ locus starts in the 3rd quadrant and the same type of instability as with the simple regulator exists viz. aperiodic for low K and oscillatory for high, see section 7.1.2. For $147^\circ > \delta_g \gtrsim 140^\circ$ the $L(j\lambda)$ locus starts in the second quadrant and then crosses into the third. Hence we have for

$\lvert 1/L(0)\rvert$	$>$ K			Aperiodic instability
$\lvert 1/L(j\mu_1)\rvert$	$>$ K $>$	$\lvert 1/L(0)\rvert$		Oscillatory instability
$\lvert 1/L(j\mu_2)\rvert$	$>$ K $>$	$\lvert 1/L(j\mu_1)\rvert$		System is stable
	K $>$	$\lvert 1/L(j\mu_2)\rvert$		Oscillatory instability

Fig. 7.14 shows that the stability limit as a function of the regulator gain consists of 3 distinct curves, as opposed to two of the simple and the delay regulators.

a) The K_{min} curve which is the same as for the simple regulator but extending a little beyond δ_s'.

b) A curve corresponding to K_{max} but moved to the right so that K_{max} is now 3 - 4 times larger than the simple regulator values.

c) A transition curve joining a and b.

The natural frequency μ for $\delta_g > \delta_s'$ is considerably increased see Fig. 6.4 and thus the effects of damping and r_a are much more significant.

The significance of the angle δ_1, defined in section 6.1 now becomes apparent. As long as the $H(j\lambda)$ locus lies in the 2nd quadrant it is possible to stabilize the system using a derivative regulator. For $\delta_g > \delta_1$ however, as Fig. 6.1 shows, the $H(j\lambda)$ locus lies in the 4th quadrant and stabilization seems impossible. Stability at $\delta_g = \delta_1$ is an unobtainable limit since a very high gain is required. Stabilization at $\delta_g = 160^\circ$ seems feasible although it may be necessary to vary the

regulator gain in order to achieve stability at lower values of δ_g.

From Eqn. (6.9) H(0) becomes zero when

$$\cos(\delta_o - \delta_t) = 0$$

or by Eqn. (6.7) when

$$Q_o X_c + V^2 = 0$$

Hence the ultimate stability limit with a derivative regulator is obtained when the angle between the alternator terminal voltage and the infinite bus becomes 90°. This clearly corresponds to the condition that the alternator reactance is eliminated completely and in fact Eqn. (7.15) is the steady state stability limit of the transmission line.

It is stated in section 7.1.3 that the action of the simple regulator may be visualised as reducing the effective X_d to X'_d. Ideally the derivative regulator can eliminate X'_d completely, i.e. the system behaves as if V_t is absolutely constant. It is apparent however that the complete elimination of X'_d is a limiting case. Fig. 7.13 indicates that it may be possible to stabilize $\delta_g = 160^\circ$ but in practice the difficulties in combining the several parameters to form the required transfer function are considerable. With the regulator given in Eqn. (7.14) high frequency oscillations as well as large signals from 50 c/s pick-up were encountered. The practical problems of the derivative regulator are considered in section 9.1.4.

It is interesting to note here that the idea of a voltage regulator "cancelling" part of the synchronous reactance was first stated by Doherty[28-1]. It was then thought that the cancellation of part of the transient reactance would present special problems. See also Ref. 55-3.

8. SPEED OF RESPONSE AND ACCURACY OF REGULATION.

It is shown in the last section that, with the derivative regulator the region of artificial stability may be extended up to the stability limit of the transmission line. It is rarely, however, that alternators are required to operate at very large angles and hence there is a degree of freedom in choosing the regulator parameters. If the degree of stability is the only consideration then linear control system theory offers a simple solution. The parameters of $K(j\lambda)$ should be chosen so that the phase and gain margins of the $L(j\lambda)$ locus are a maximum at the required load angle. The method of domain separation offers an efficient method for optimizing the regulator in this case. Using this method Messerle[56-3] concluded that, for a single delay regulator with an exciter stabilizer, the regulator gain is approximately given by $K = K_{min} + \frac{1}{3}(K_{max} - K_{min})$.

Optimization of $K(p)$ however, should be given a broader meaning since, after all the first three functions of an excitation regulator, as given at the beginning of the Introduction, are often more important than operation in the artificial stability region. Hence a compromise may be necessary so that the regulator meets the requirements, which are different for different systems. It is necessary therefore, to be able to measure the performance of the system in its several aspects.

No analysis of the ability of an excitation regulator to maintain the terminal voltage constant or of the speed of response of the system on load could be found in the literature. The American I.E.E. Definitions[61-3] refer to accuracy "under specified conditions such as load changes, drift, temperature etc." In the literature, however, when figures are quoted these conditions are rarely given. Practical regulators are often supposed to have "fast response" but this seems to mean anything from highly oscillatory to overdamped voltage-time curves. The lack of accepted standards for the speed of response is shown in a paper by Harvey et al[61-1], where, in a step change test, a series resistance was inserted in the alternator field circuit,

reducing T'_d , and thus changing the system response completely.

In order to optimize the regulator transfer function it is necessary to digress from the main theme of steady state stability so that suitable performance indices for the speed of response and the accuracy of regulation may be defined. Corresponding to K_{ss} the symbol K_{sr} is used to denote the value of gain for optimum speed of response. Linear theory is used and the speed of response is defined for small step changes. It is realised that the effectiveness of a regulator depends on its ability to deal with large steps. It is reasonable to expect, however, that the response to a small step function bears a relation to the behaviour of the system under large transient conditions. Accuracy is improved as the gain is increased and hence there is no optimum value of gain in this case. It is still necessary however to be able to calculate the accuracy as a function of gain.

So far we have been dealing with the open loop transfer function of the system and hence it is immaterial whether $K(p)$ is in the feedback or in the forward part of the loop. When discussing stability it is desirable to separate the alternator and the regulator and thus $K(p)$ was assumed to be in the feedback part, c.f. Figs. 1.1 and 1.4. In practice, however, the transfer function from the terminal voltage to the comparator is constant and $K(p)$ follows the comparator. In the present section the closed loop response is required and hence the practical arrangement with unityfeedback is considered, see Fig. 8.1.

8.1. Speed of Response of the System.

As long as small step changes are considered the small oscillation theory, developed in section 2, may be used and the system may be analysed by linear control system theory. There are several performance indices for measuring the speed of response of a linear system, see Newton, Gould and Kaiser[57-7] e.g.

a) The Integral Square Error.

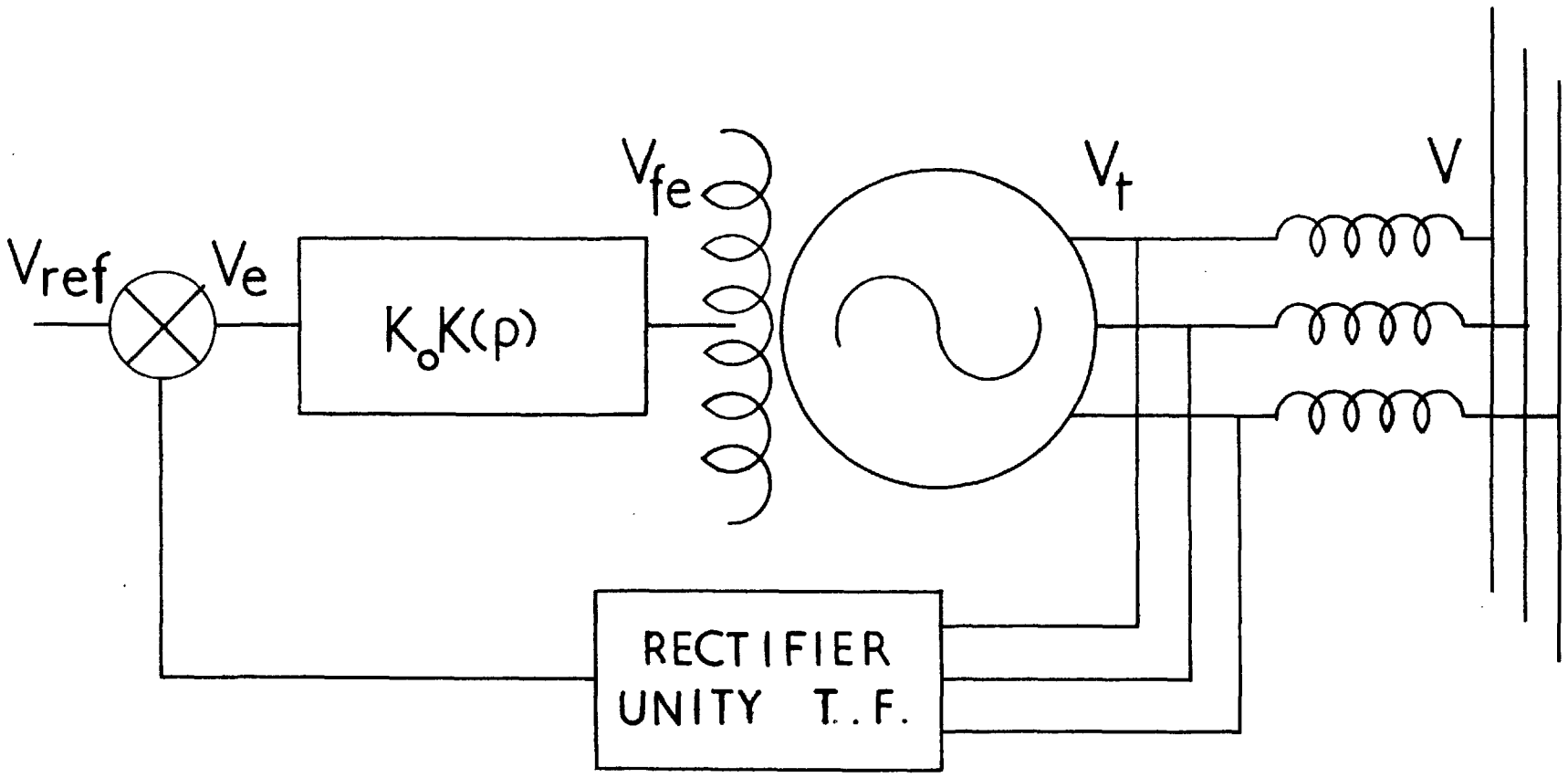

FIG. 8.1
THE SYSTEM WITH UNITY FEED BACK

b) The time that the error lies outside an allowable tolerance.

c) The maximum overshoot.

d) The integral of the modulus of the error etc.

Minimization of the integral square error ensures both small overshoot and adequate damping of oscillations. Since, in addition, there are analytical techniques for minimizing a which are not available for b or c the integral square error is the most popular method for measuring the speed of response and is adopted for the present investigation. The method of calculation described below can easily be modified to give b, c or d if these are required.

A simplified definition of the integral square error, ε , is as follows. Consider a linear control system and let its output following a unit step function input be $f(t)$. Also let $f(t) \longrightarrow f(\infty)$ as $t \longrightarrow \infty$.

$$\varepsilon = \int_0^\infty \left(1 - \frac{f(t)}{f(\infty)}\right)^2 dt \qquad (8.1)$$

Ref. 57-7 gives an elegant method for minimizing ε . Application of this method, however, involves, $T(p)$ the closed loop transfer function of the system, viz:

$$T(p) = \frac{H(p)\ K(p)}{1 + H(p)\ K(p)} \qquad (8.2)$$

expressed as a ratio of two polynomials. For the most complex case that we have to consider, i.e. with the derivative regulator, the numerator of $T(p)$ is of the 7th and the denominator of the 8th degree in p . The expressions resulting from this method are much too complicated, especially if the minimization is to be performed with respect to more than one parameter e.g. K and a time constant.

Alternatively $T(p)$ may be split into partial fractions and $f(t)$ determined using the Laplace transform. ε may then be plotted against the parameters with respect to which it should be minimized and the optimum values may then be chosen. In view of the degree of the denominator of $T(p)$ the splitting into partial fractions must be done with a digital computer. The formation of $T(p)$ for different regulators as well as the determination of $f(t)$ involves complicated programming.

The third alternative, which is adopted in the present investigation, appears at first sight to be very complicated. Indeed it is not possible to use this method without a digital computer. When a programme for the determination of $H(j\lambda)$ exists, however, the additional amount of programming is simple. The method is an application of the well known correspondence between the frequency and the transient response by means of the Fourier transform. Since $H(j\lambda)$ is known, see section 6, the determination of $T(j\lambda)$ from Eqn. (8.2) given the parameters of $K(j\lambda)$ is straightforward. $f(t)$ and ε may be calculated using the method described in the following section.

8.1.1. Method for the Determination of the Integral Square Error.

Consider a low frequency square wave with unity peak to peak value applied at V_{ref}, Fig. 8.1. Expressed as a Fourier Series the signal is,

$$\frac{2}{\pi}\left(\sin \xi t + \frac{1}{3}\sin 3\xi t + \ldots + \frac{1}{2n-1}\sin(2n-1)\xi t + \ldots\right) \qquad (8.3)$$

If the period, $2\pi/\xi$, is sufficiently long steady state conditions will be established before the end of the half cycle. In order to fulfil the usual condition of a step function that, at $t = 0-$, the disturbance is zero a "d.c." signal of magnitude $1/2$ is added. If

$$A_n = \left|T(jn\xi)\right| \quad \text{and} \quad \phi_n = \operatorname{Arg} T(jn\xi) \qquad (8.4)$$

then the output of the system to the nth harmonic of the input is

$$A_n \sin(n\xi t + \phi_n)$$

If, in addition, $A_o = T(0)$ then the output of the system to the displaced square wave is:

$$f(t) = \frac{1}{2} A_o + \frac{2}{\pi}\left(A_1 \sin(\xi t+\phi_1) + \frac{A_3}{3} \sin(3\xi t+\phi_3) \ldots. + \frac{A_{(2n-1)}}{2n-1} \sin(\overline{2n-1}\,\xi t + \phi_{(2n-1)}) \ldots. \right) \quad (8.5)$$

The integral square error can now be obtained from Eqn. (8.2) by numerical integration. The choice of ξ and n determines the accuracy, as well as the time taken on the computer. It was decided to make the positive part of the square wave last 50 sec, which was considered to be long enough for any transient to settle down. Hence $\xi/2\pi = 0.01$ c/s. The value of $f(t)$ for small t is mainly determined by the higher harmonics and, by inspection of Fig. 7.13 it was decided to extend the calculation to 1.5 c/s. However, even with the simple regulator, $f(0)$ had a finite value and eventually frequencies up to 2 c/s. were included. The choice of 2 c/s as the upper limit results in a large number of terms, $n = 99$, in the series but this is inevitable because of the large frequency range of $L(j\lambda)$. Yet, in spite of the number of terms, the maximum value of $f(0)/f(\infty)$ found was 0.05 for the derivative regulator with a high gain.

The result expressed by Eqn. (8.5) may be obtained formally, using the Fourier transform. The formula given by Lawden[59-1] for $f(t)$ includes an integral and if this is evaluated numerically Eqn. (8.5) results.

It is clear that it is impossible to obtain $f(t)$ from Eqn. (8.5) without a digital computer. Each point on the curve involves the

calculation of 99 terms and their summation. If any accuracy in the determination of ε is required then a large number of points must be computed. The digital computer programme to sum the series and to obtain ε is straightforward and we need not go into details. It was found convenient to have two data tapes. One containing the values of $H(j\lambda)$ for 0.01 c/s to 2 c/s which may be prepared by the computer itself as the output of the programme for $H(j\lambda)$. The other tape is shorter and contains the parameters for $K(j\lambda)$.

8.1.2. The Effect of the Regulator on the Response of the System to a Small Step.

Although the primary aim of the calculation described in the last section is the value of ε , the transient response, $f(t)$, is also available. An interesting set of curves is obtained illustrating the significance of the speed of response and showing the profound effect of the regulator on the transient behaviour of an alternator.

Figs. 8.2 to 8.5 show some typical results for the four regulators considered in section 7.3. They refer to $\delta_g = 110^\circ$, which was chosen as reference operating condition for all numerical results in this section. Excluding the integrator type the same three values of gain were used. Since higher gains may be used for the delay and the derivative types than for the simple regulator these curves cannot be used to compare the regulators. The capability of each type is determined from the minimum value of the integral square error, see section 8.1.3.

Increasing the gain results in a less damped response and when K approaches K_{max} the frequency of oscillations superimposed on the exponential approaches $\mu/2\pi$. When $K > K_{max}$ an interesting result is obtained. The curve goes to unity with no significant increase in the magnitude of the superimposed oscillations. If $f(t)$ is plotted to a large scale small oscillations of increasing amplitude begin to appear after several seconds of steady conditions at unity output. Thus

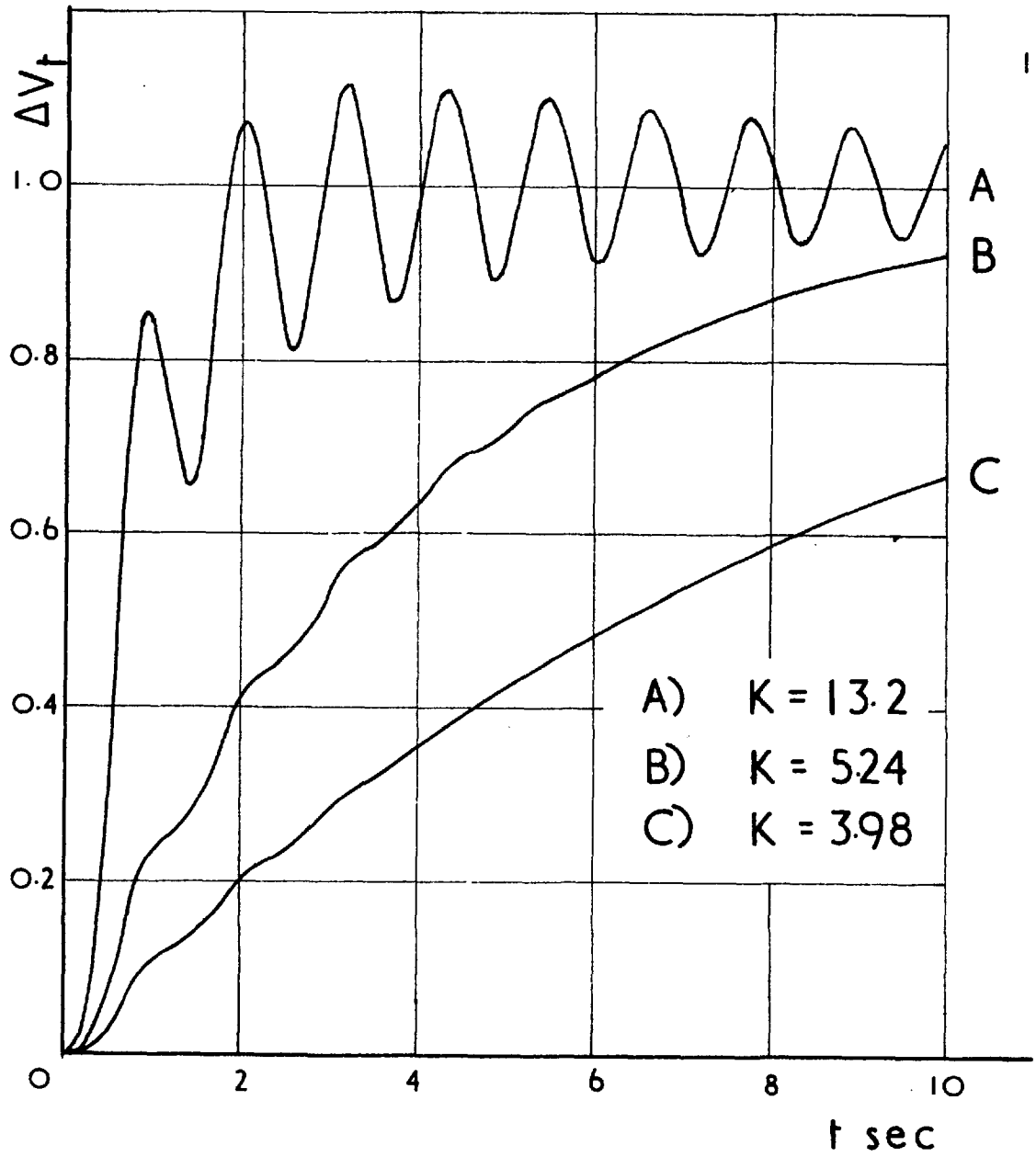

FIG. 8.2

RESPONSE TO STEP FUNCTION

SIMPLE REGULATOR Calculated

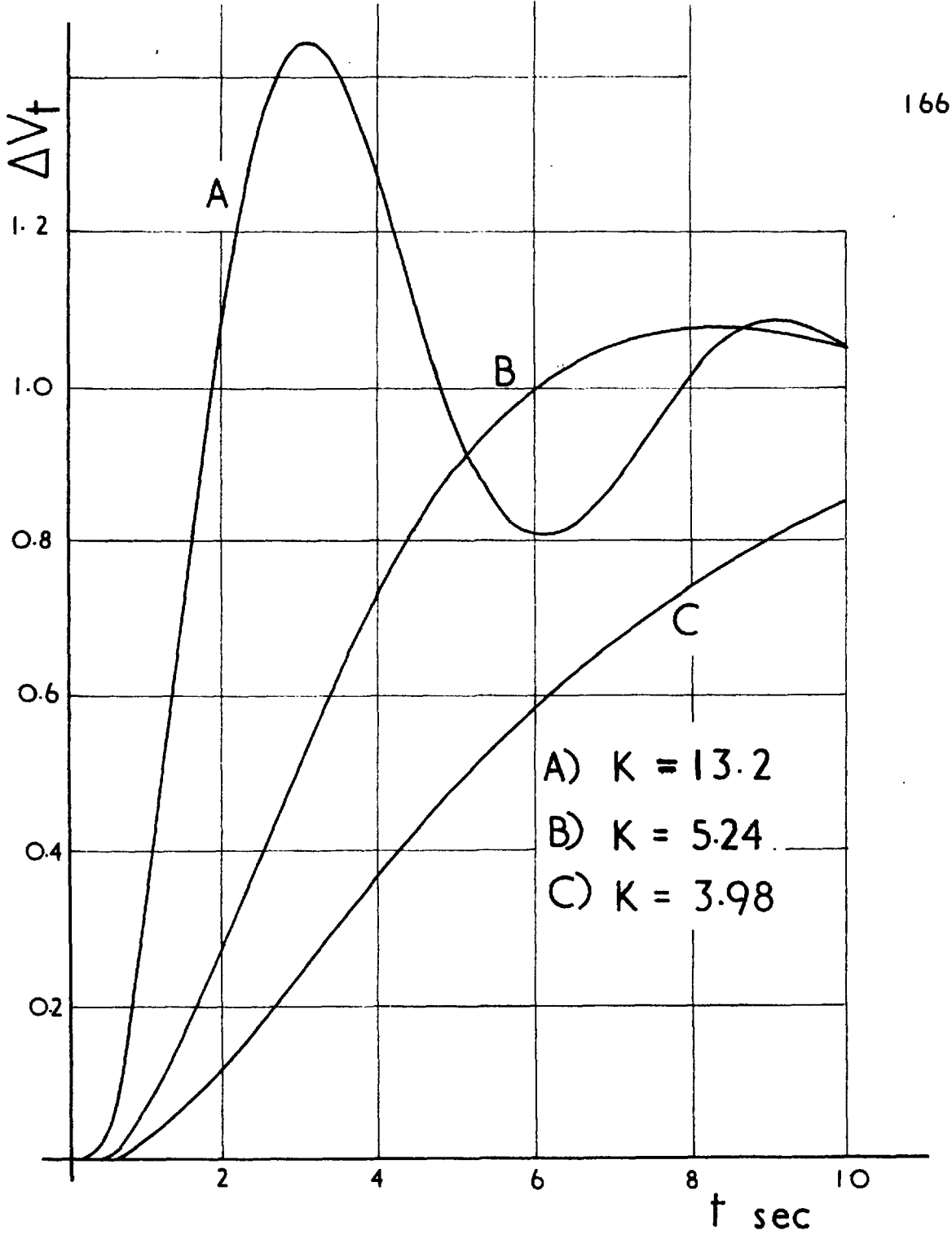

FIG. 8.3

RESPONSE TO STEP FUNCTION

DELAY REGULATOR T_1 = 1 sec Calculated

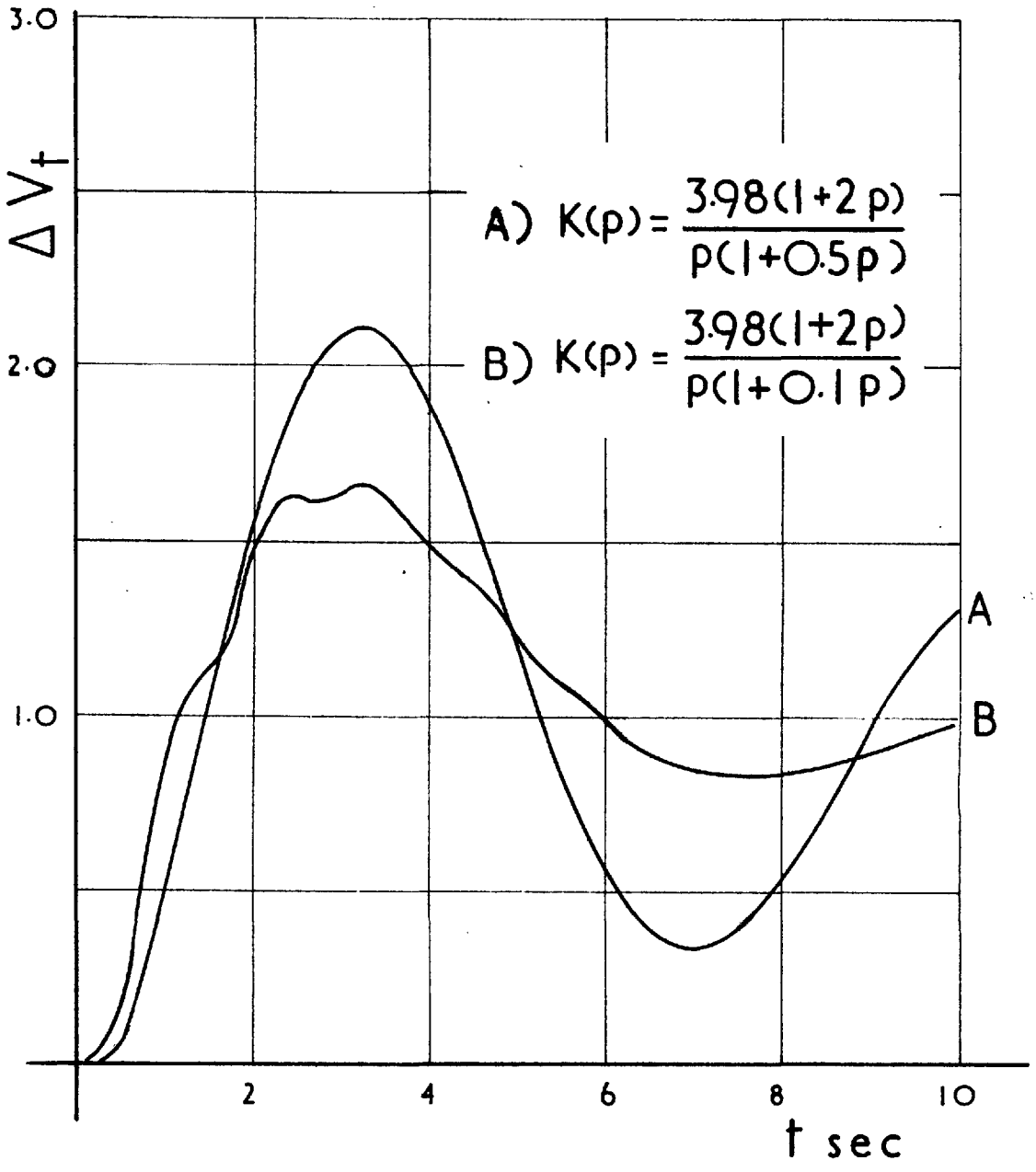

FIG. 8.4

RESPONSE TO STEP FUNCTION

INTEGRATOR REGULATOR Calculated

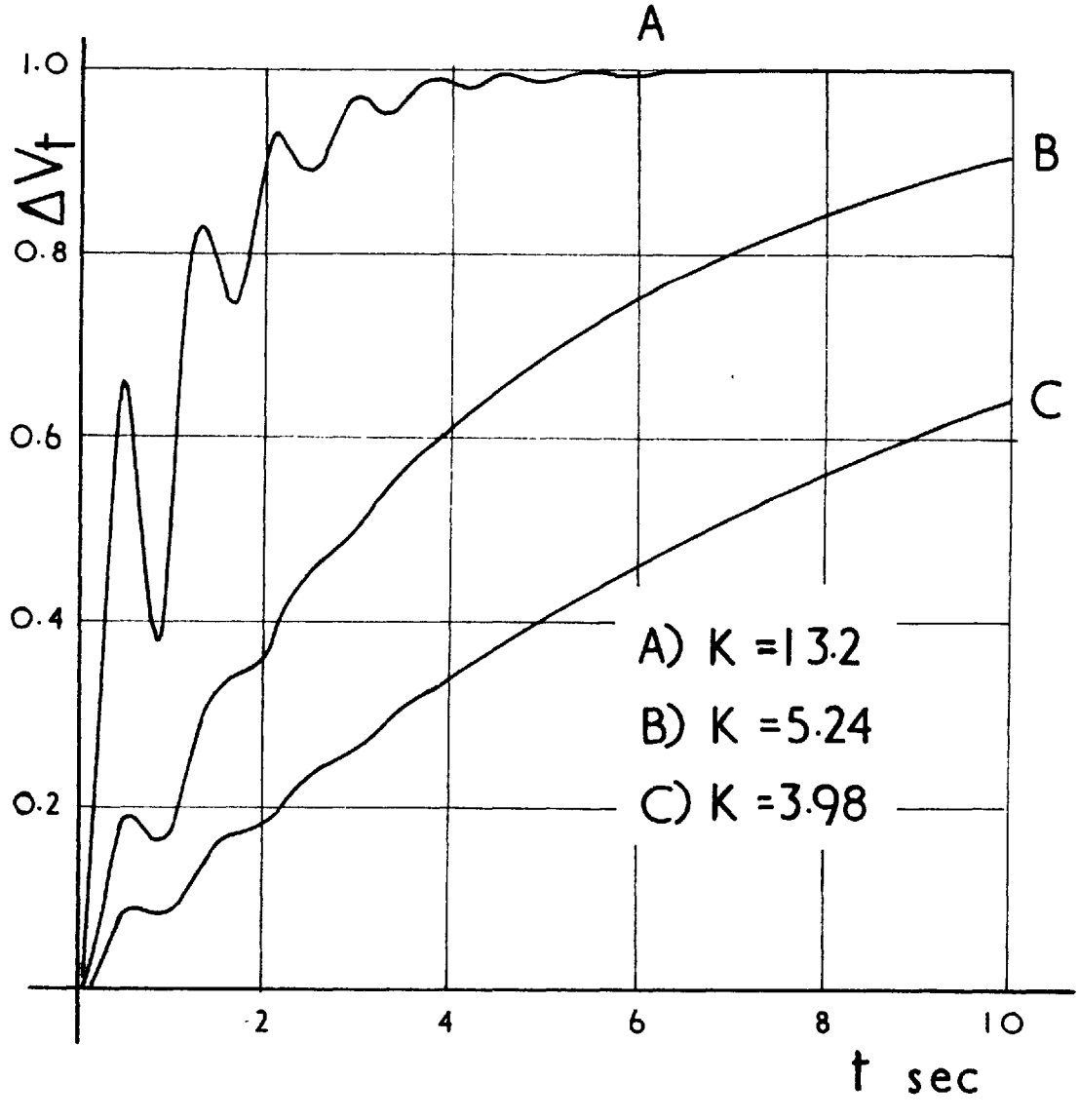

FIG. 8.5

RESPONSE TO STEP FUNCTION

DERIVATIVE REGULATOR Calculated

the solution consists of terms

$$e^{-\alpha t} + e^{\beta t} \sin \gamma t$$

where α , β and γ are positive and $\alpha \gg \beta$. When $K < K_{min}$ the transient is not completed at $t = 50$ sec and hence the method is not, strictly speaking, valid. The solution indicates the presence of a term $e^{\beta t}$ where β is positive and small. Hence, although it is not always obvious if the system is unstable close scrutiny of the result gives the correct answer. However, this is an inefficient method for determining stability and the regulator parameters should be such that the system is stable.

Referring to the $L(j\lambda)$ loci for $\delta_g = 90^\circ$ the value of K is chosen so that the $(-1,0)$ point lies between the two intersections with the negative real axis. From Eqn. (8.2) the denominator of $T(j\lambda)$ is equal, in magnitude and in phase, to the line drawn from the point $(-1,0)$ to $L(j\lambda)$. Hence if a second line is drawn from the origin to $L(j\lambda)$ representing the Numerator, $|T(j\lambda)|$ is the ratio of the lengths of the two lines and Arg $T(j\lambda)$ is the difference of their arguments.

If K is small the point $(-1,0)$ lies near $L(0)$ and $T(0)$ is large. With increasing frequency the denominator of $T(j\lambda)$ is rapidly increasing and as a result $A_n \ll A_o$ for large n and the higher terms in Eqn. (8.5) may be neglected. The transient response therefore at low gains does not have any high frequency terms superimposed. Also for small λ , $L(j\lambda)$ is approximately the same with either simple, delay or derivative regulator. Hence curves c are similar for the three cases, Figs. 8.2, 8.3 and 8.5. As K is increased the $(-1,0)$ point moves nearer $L(j\mu)$, $T(0)$ becomes smaller and $T(j\mu)$ increases. Thus the term in the series of Eqn. (8.5) for which $(2n-1)\xi \approx \mu$ is large and as $\underline{t}$ varies there is a superimposed oscillation of frequency approximately equal to $\mu/2\pi$.

The main rise time is determined by the rate of change of A_n with

n for small values of n . Consider the following simple example. If

$$T(p) = \frac{1}{1 + p\,T_1} \qquad (8.6)$$

then

$$A_n \approx 1 \quad \text{for} \quad n\xi < \frac{1}{T_1}$$

and

$$A_n \approx \frac{1}{T_1 n} \quad \text{for} \quad n\xi > \frac{1}{T_1}$$

Obviously for a small T_1 , $A_1 \approx 1$ for larger n and the rise time is shorter.

Thus although $T(j\lambda)$ is much more complicated than the simple delay it is apparent that the higher the gain the less rapidly A_n changes for small n and the shorter the rise time. This qualitative and imprecise argument points to the following important result. Since $L(j\lambda)$ is not affected by the type or regulator for small λ the initial "average rise time" is determined by K and not by the type of regulator. Average rise time in this case refers to the exponential curve drawn through the middle of any oscillations.

These remarks do not apply to the integrator type regulator which, as shown in Fig. 8.4 produces a highly oscillatory response. $K = 4$ is near the K_{max} for the regulator with $T_1 = 0.1$ sec and for this reason curve b shows a superimposed oscillation.

8.1.3. The Effect of the Regulator on the Integral Square Error.

Fig. 8.6 shows ε as a function of K at $\delta_g = 110^\circ$ for the regulators considered in section 7. K has values between K_{min} and K_{max} and hence each curve has different limits. All curves, except e,

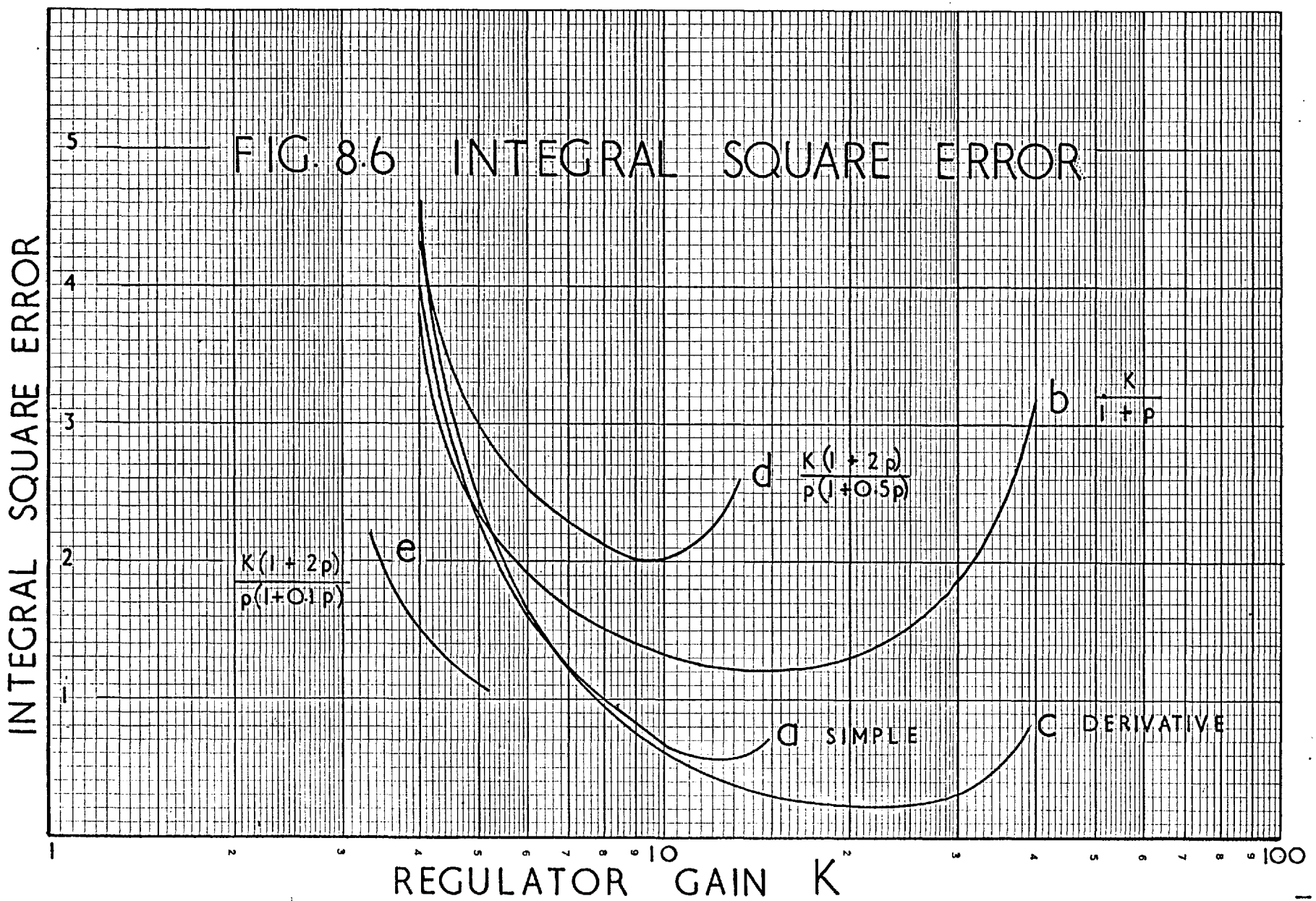
FIG. 8.6 INTEGRAL SQUARE ERROR
INTEGRAL SQUARE ERROR
REGULATOR GAIN K
a SIMPLE
b K/(1+p)
C DERIVATIVE
d K(1+2p)/p(1+0.5p)
e K(1+2p)/p(1+0.1p)

show a minimum indicating the value of K_{sr} in each case. The minimum value of ε is a direct measurement of the capability of each regulator to produce a fast response. Worst of those considered is the weakly stabilized integrator ($T_1 = 0.5$ sec) and best the derivative regulator. The integrator with strong stabilization ($T_1 = 0.1$ sec) appears to be quite reasonable.

The significance of the absolute value of ε may be illustrated by considering a step function applied to a simple control system having a single delay transfer function, as in Eqn. (8.6). Then

$$f(t) = 1 - e^{-t/T_1}$$

and it may be shown that

$$\varepsilon = T_1/2$$

Hence in terms of the integral square error: the integrator regulator gain can be adjusted to give as good a response as a 4 sec delay, and the derivative one as good as a 0.5 sec delay. For comparison the "time constant" of the large semicircle in the $H(j\lambda)$ plot for $\delta_g = 110^\circ$ is approximately 3 sec, see Fig. 6.1.

K_{sr} depends on the operating condition and in practice a compromise must be made so that an acceptable value over the region of operation of the alternator is used. Clearly, as Bloedt and Waldmann[62-4] have shown optimization on the transient response on open circuit is not satisfactory.

Although the minimization of ε involves a compromise between the requirements of several operating points it offers a systematic method for achieving optimum speed of response, at least as far as small steps are concerned. The question now arises whether a regulator designed for minimum ε gives optimum response with big changes of condition. However, the problem of correlating the results of the small

oscillation theory given here and the non-linear method for large changes lies outside the scope of the present investigation.

8.2. Accuracy of Regulation.

There are several ways of measuring the accuracy of regulation for our system.

a) It is possible to use the same concept of error as in a linear system applied to the linearized small oscillation equations. Referring to Fig. 8.1 the error is ΔV_e and it is small if $L(0)$ is large.

b) Alternatively, but also for the small oscillation equations, if V_{ref} changes by ΔV_{ref} it is desirable that $\Delta V_t = \Delta V_{ref}$, and that the equality is not affected by changes in the operating condition. Thus $T(0)$ must be equal to unity irrespective of the value of $H(0)$ and hence $K(0)$ must be large.

Both definitions are essentially the same and lead to the obvious conclusion that $K(0)$ should be large. If $K(0)$ is finite $T(0)$ varies from $+\infty$ to 1 as $K(0)$ varies from 0 to ∞. In such a case neither method gives a satisfactory measurement of the degree of accuracy.

c) The method finally adopted is simple to apply and the result has an important practical significance. The change of V_t is determined when the operating condition is altered with V_{ref} remaining constant. Two "basic" operating conditions are required and obvious choice for one is when the alternator is on open circuit. The other can be the normal operating condition at rated p.f. and power. However, since, throughout this investigation, operation in the artificial stability region is considered the point $\delta_g = 110^\circ$ with $P = 0.8$ p.u. was chosen for the numerical part.

8.2.1. Regulation as a Change of V_t.

Referring to Fig. 8.1 at any operating point

$$V_e = \frac{V_o r_f}{X_{md}} \cdot \frac{1}{K K_o} = \frac{V_o}{K} \qquad (8.7)$$

and $$V_{ref} = V_t + V_o/K \qquad (8.8)$$

Consider now operation on open circuit with V_{ref} the same and denote with a prime the quantities that are different.

$$V'_e = V_{ref} - V'_t$$

$$V'_t = K(V_{ref} - V'_t)$$

substituting from Eqn. (8.8)

$$V'_t = \frac{V_o + V_t K}{1 + K} \qquad (8.9)$$

and the regulation is defined as

$$\rho = \frac{V'_t - V_t}{V_t} = \frac{V_o/V_t - 1}{1 + K} \qquad (8.10)$$

when $K = 0$ the inherent regulation of the alternator is $(V_o/V_t - 1)$.

Fig. 8.7 shows a plot of the regulation against gain. It is apparent that, for large K, the curve is a hyperbola approaching zero with no minimum value for ρ. Hence it is not possible to define an optimum value of gain corresponding to K_{sr} and K_{ss}. Integrator regulators have $K(0) \rightarrow \infty$, and, as expected, the regulation is zero.

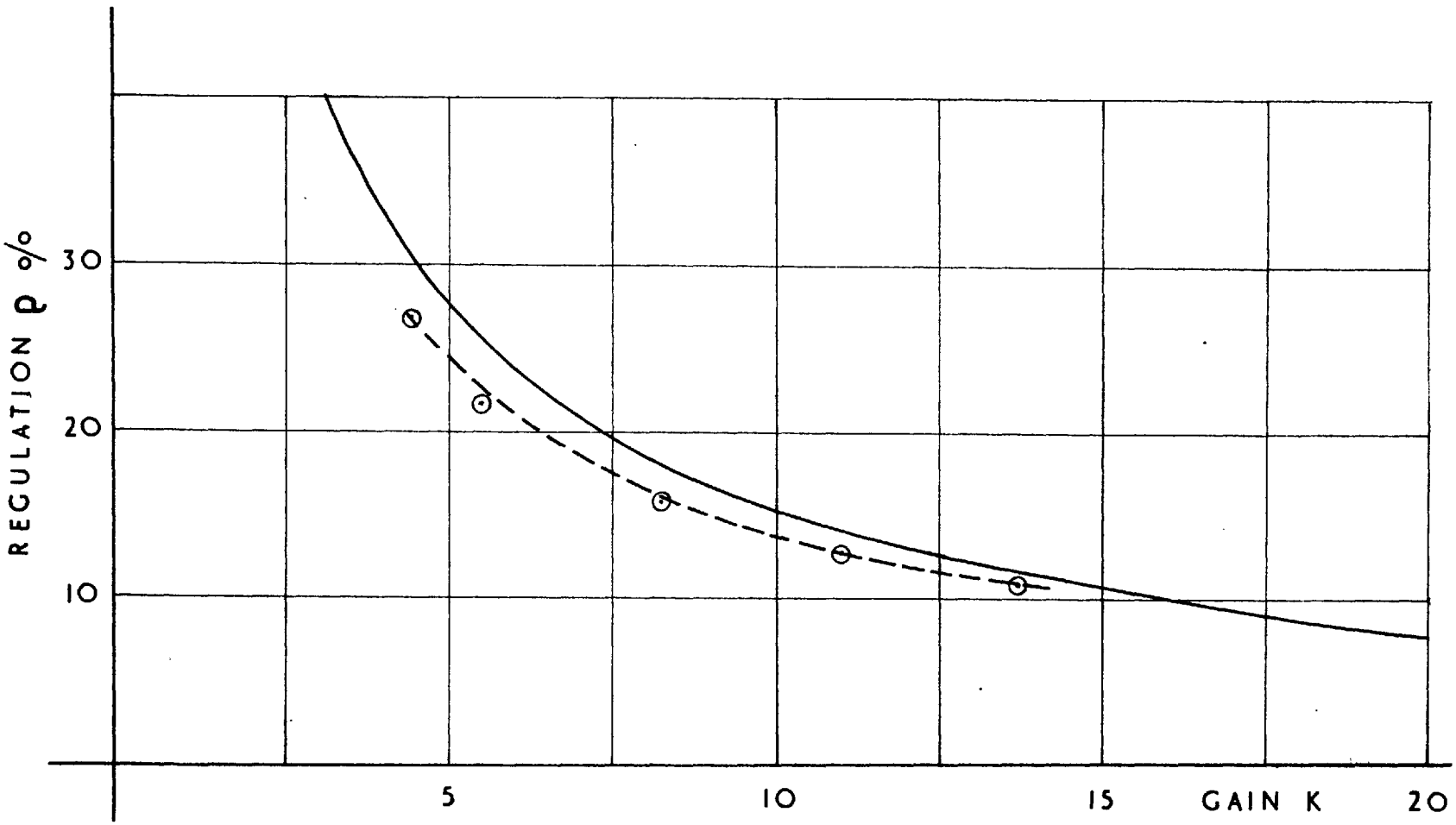

FIG. 8.7 REGULATION AGAINST GAIN

——— CALCULATED ⊙ ---- MEASURED

9. EXPERIMENTAL INVESTIGATION

An important part of the investigation is the experimental verification of the results obtained theoretically. It is possible to obtain a comparison for most of the calculated curves. Although some of the discrepancies cannot be fully explained the overall agreement justifies the theory developed. An inherent difficulty with the frequency response and the step function tests is the necessity for limiting the input signal to small values so that the validity of the small oscillation theory is not affected. Thus the measurement of the output produced is affected by drifts in the system and the supply voltages.

The experimental investigation revealed two important aspects of the operation of the system which were not predicted by the analysis. One is the sensitivity of the system to random signals producing variations in the operating point. This occurs with the integrator and the derivative regulators when the gain is low. The other result is the presence of high frequency oscillations with the derivative type regulator. Both aspects emphasise the importance of the experimental investigation.

The non-linearity of the system is illustrated by the step function tests where the response is different depending on whether the disturbance is applied or removed. However, the response is not materially changed with the larger steps and hence the theory developed in section 8 may be applied to finite changes as an approximation.

9.1 Steady State Stability Tests.

The aim is to determine the stability limit as a function of gain for the different types of regulator considered in sections 7.1 and 7.3. The procedure was the same in each case. The system was connected as shown in Fig. 3.1 with the alternator operating stably, at a certain value of regulator gain. The reference voltage V_{ref} was reduced slowly until instability occurred. The system was brought back

to stable operation and the process was repeated with a different value of K. The components of the analogue computer (see Fig. 3.1) were, in turn, connected to give the transfer functions of the different regulators. In practice this meant plugging-in a different patch-board. A block diagram for each regulator is shown in Fig. 7.3. The circuits used are indicated in principle in section 3.2.2 and need not be considered in detail.

Serious thought had to be given to the stability criterion used. It was observed that, depending on the value of gain and the type of regulator, there are four alternative phenomena associated with the beginning of instability.

1) Low values of gain (simple and delay type regulators). At the stability limit the load angle drifts slowly upwards until the alternator pulls out of step. In practice there are two difficulties. The bus voltage, V, and the d.c. voltage supplied to the driving motor change due to switching in the mains. Thus a finite sudden change is applied which may result in instability before the steady state stability limit is reached. Secondly the output of the time constant regulator tends to drift producing a general dither on the load angle at all times.

In order to achieve consistency the following procedure was adopted for low gains. The reference voltage was adjusted for a definite load angle. If the load angle did not change by more than $\pm 2^{\circ}$ in the following 1 min., the system was considered to be stable for that angle. The reference voltage was then reduced so as to increase δ_g by approximately 2° at a time and the process was repeated. If within the 1 min. δ_g was reduced by more than 2°, V_{ref} was adjusted to bring it back to the set value and the change was attributed to drift. If, on the other hand, δ_g increased by more than 2°, and continued to drift upwards, during the 1 min. at least twice, then the condition was considered unstable.

2) High values of gain. As V_{ref} is reduced the system enters

what is known in control systems analysis as a "limit cycle". That is, at the stability limit non-sinusoidal oscillations build-up to a finite amplitude although the alternator does not pull out of step. If the reference voltage is reduced further the amplitude of the limit cycle is increased until, eventually, synchronism is lost. Because of the dither in the load angle and the damped oscillations due to changes in the supply voltages already mentioned the start of the limit cycle is uncertain. However, since the frequency of the limit cycle can easily be determined by reducing V_{ref} further, it was decided that the stability limit is reached when definite oscillations of $\pm 1^{o}$ at the frequency of the limit cycle were observed.

The two kinds of instability observed for high and low values of gain correspond to the types of unstable roots discussed in section 7.1.2. The fact that for high gains the oscillations do not increase indefinitely is a consequence of the non-linear nature of the system. The linearised equations are valid only for small changes and during the limit cycle other factors come into operation.

3) Low values of gain (integrator and derivative type regulators). It is observed that the load angle drifts over a wide range long before the calculated limit is reached. When V_{ref} is further reduced the drifting remains approximately the same and near the computed limit the alternator, if left long enough, pulls out of step. The process seems to be random and it is possible that, because of the low gain the effect of the change in supply voltages is not completely corrected by the regulator. The error seems to have a cumulative effect since with the simple regulator, at the same values of gain, less than $\pm 1^{o}$ dither was observed. Since it is not possible to fix the stability limit the test for the two regulators was discontinued when these conditions were encountered.

4) High values of gain (derivative regulator) high frequency oscillations were observed, but since these are peculiar to the derivative regulator they are discussed below, see section 9.1.4.

The stability limit for the high values of gain is a compromise between the theoretical and practical requirements. A limit cycle of amplitude smaller than 1° could not be determined because of dither. It may be argued that small oscillations on the load angle are unimportant and that the system should be considered to be stable until synchronism is lost. Nielsen[62-6] used this criterion, but it is doubtful whether oscillations of up to $\pm 15^{\circ}$ would be acceptable in practice. It is interesting to note that B.S.S. 649, Ref. 35-1, specifies $2\frac{1}{2}^{\circ}$ as the maximum pulsation of δ_g when the alternator is driven by an internal combustion engine. The use of a stability criterion based on a $2\frac{1}{2}^{\circ}$ pulsation in the present case is not justified. From the linearised equations the system is unstable at the beginning of the limit cycle and any comparison with theory must be made with the minimum detectable oscillation. It is not possible to estimate the start of the limit cycle by extrapolation because the change in δ_g from a stable condition to large oscillations depends on the value of gain.

The existence of the limit cycle is not generally recognised in the literature. It is stated in Ref. 65-2 that the oscillation would build-up until synchronism is lost. One of the few exceptions is Ref. 65-4, which describes the process of loss of stability, for high gains, correctly . The transition from aperiodic to oscillatory instability at the optimum value of gain does not appear to have been noticed. There are very few references on the stability criterion used in experiments, see Table I p. 221 . It is thus considered desirable to describe in some detail the process of loss of stability. For this purpose three typical points are chosen and a summary of the conditions is given as the reference voltage is reduced. The process is described for a high and a low value of gain for the simple regulator and for $K = K_{ss}$ for the derivative regulator.

9.1.1 Stability with the Simple Regulator.

The analogue computer (see Fig. 3.1) was connected to give a constant gain and the test was carried out as described in the previous

section. The result is shown in Fig. 1.3. Taking the point with $K = 19.5$ as typical of the high gain points the oscillations developed as follows:

1) $\delta_g = 104^\circ$. Dither 1°.
2) $\delta_g = 106^\circ$. Dither greater than 1°.
3) $\delta_g = 108^\circ$. Dither greater than 1° but no definite oscillations.
4) $\delta_g = 110^\circ$. Oscillations of 1° amplitude superimposed on approximately 2° dither.
5) $\delta_g = 112^\circ$. Oscillations of $1\frac{1}{2}^\circ$ amplitude on a 3° dither.
6) $\delta_g = 114^\circ$. At first oscillations with 2° amplitude building up to non-linear oscillations between 102° and 122°.

It is apparent that the beginning of the limit cycle cannot be detected. Consistent with the criterion defined in the previous section the stability limit in this case was taken as 110°. Considering now a typical point with a low value of gain, say at $K = 2.5$ we have,

1) $\delta_g = 109^\circ$. Remains at $\pm 1^\circ$ for one minute.
2) $\delta_g = 112^\circ$. After 30 sec δ_g was approximately 110° and after 50 sec it was creeping past 114°.
3) $\delta_g = 112^\circ$. Drifted back to 109° and V_{ref} was adjusted to bring δ_g back to 112°.
4) $\delta_g = 112^\circ$. As 3.
5) $\delta_g = 112^\circ$. Remained within $\pm 1^\circ$ for 30 sec but at 60 sec load angle was 116° and was moving upwards.

The stability limit was taken as 109°.

Referring to Fig. 1.3 the measured stability limits are higher than the computed curve. This may have been expected for high values of gain since, at the stability limit the limit cycle has a finite amplitude. On the other hand the opposite was expected for low values of gain since any small change in the system would cause the machine to lose synchronism.

9.1.2 Stability with the Delay Regulator.

The regulator transfer function is given in Eqn. 7.9 and Figs. 9.1 and 9.2 show the stability limit as a function of K with $T_1 = 0.5$ and 1 sec respectively. As with the simple regulator the measured values are greater than the calculated limit. The natural frequency is reduced compared with the simple regulator and this makes the detection of the limit cycle slightly more difficult. The process of loss of synchronism is similar to that for the simple regulator and need not be described in detail.

9.1.3 Stability with the Integrator Regulator.

Before considering the stabilized integrator experiments, it is appropriate to mention a test performed with an unstabilized integrator regulator, Eqn. (7.10). Depending on the regulator gain a limit cycle was observed for δ_g in the range 60° to 80°. It is interesting to note that, when V_{ref} was further reduced the amplitude of the oscillation increased very slowly so that the alternator did not pull out of step for about 2 min. after the change in V_{ref} was made.

The transfer function of the stabilized integrator used is given in Eqn. (7.11) and Figs. 7.9 and 7.10 show a comparison between the calculated and the experimental results. $T_\alpha = 2$ and $T_1 = 0.5$ or 0.1 sec respectively. All measured points showed oscillatory instability. When the gain is reduced it becomes processively more difficult to determine the stability limit and for reasons discussed above the test was discontinued. Fig. 7.10 shows that with the stronger stabilization the maximum stable angle is approximately 7° larger than with the weaker stabilization, Fig. 7.9.

In practice it is important to determine the performance of the regulator when subject to drifts in the supply voltage etc. It appears that, with the integrator regulator the system is particularly sensitive to such drifts. The amount of drift in the terminal voltage of the alternator that can be tolerated in a practical system will have to be

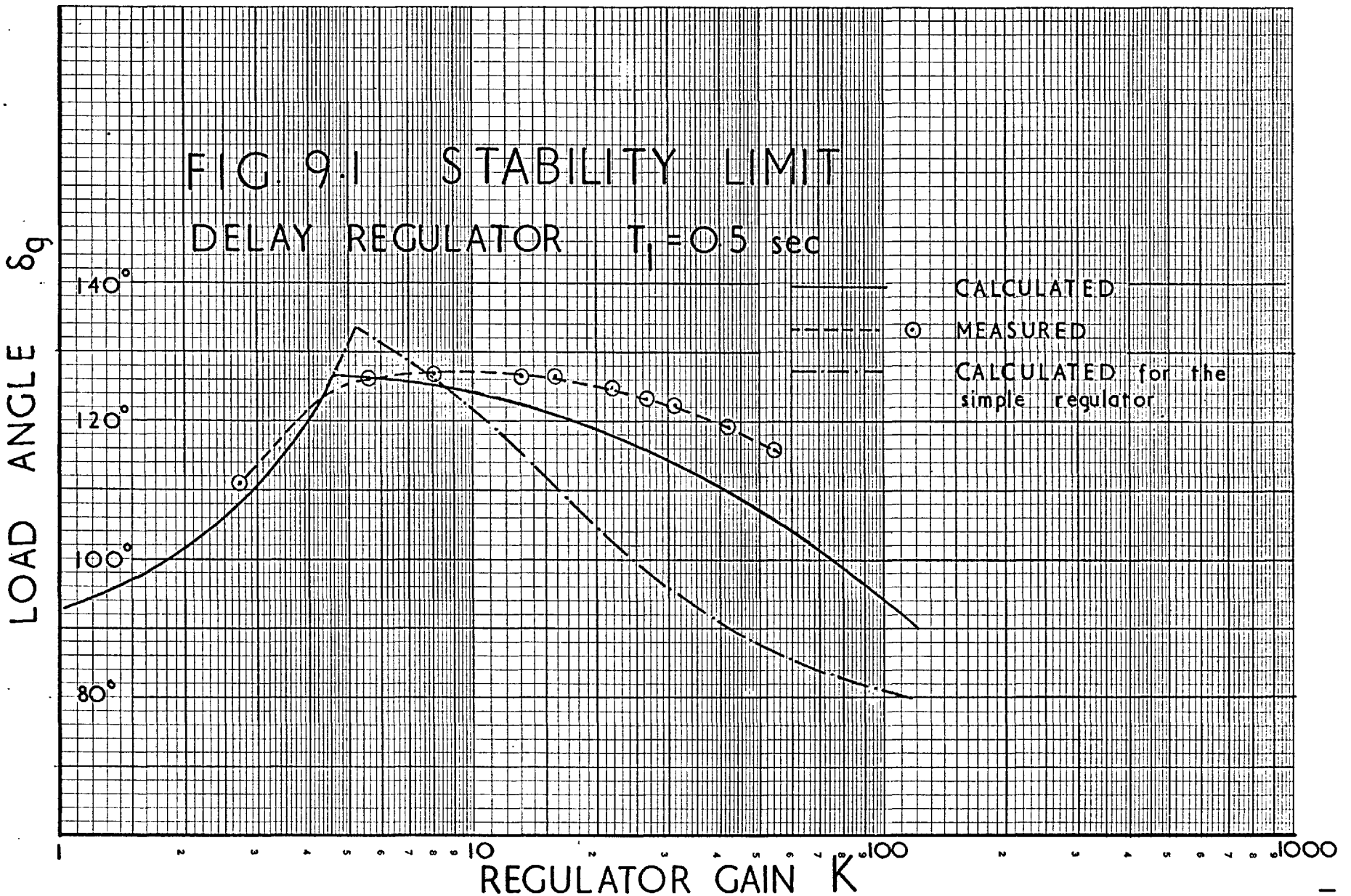
FIG. 9.1 STABILITY LIMIT
DELAY REGULATOR $T_1 = 0.5$ sec
LOAD ANGLE δ_g
140°
120°
100°
80°
CALCULATED
MEASURED
CALCULATED for the simple regulator
1
10
100
1000
REGULATOR GAIN K

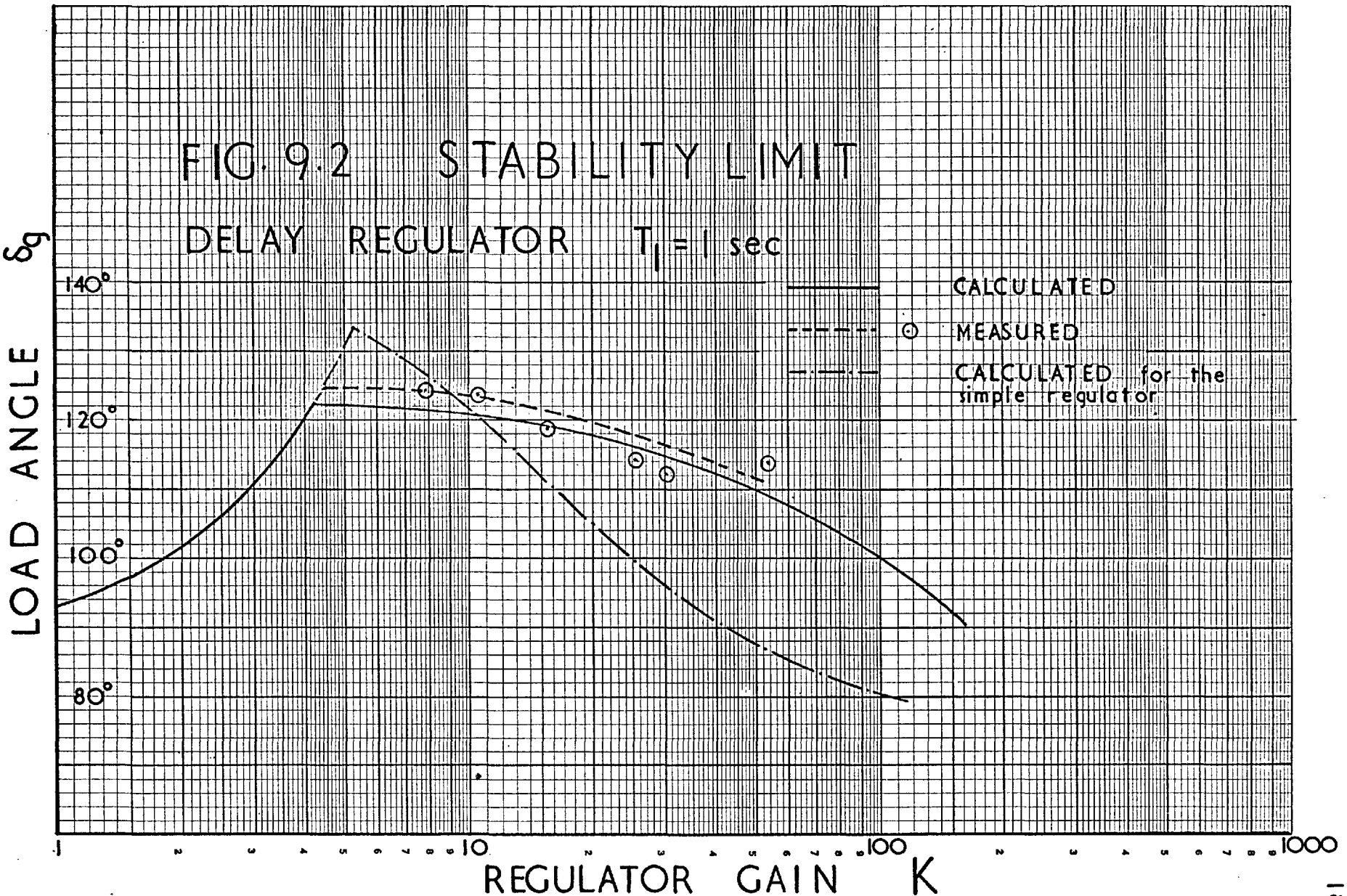
FIG. 9.2 STABILITY LIMIT
DELAY REGULATOR $T_1 = 1$ sec
LOAD ANGLE δ_g
140°
120°
100°
80°
CALCULATED
MEASURED
CALCULATED for the simple regulator
1
10
100
1000
REGULATOR GAIN K

decided and the gain may then be fixed to avoid such conditions.

9.1.4 Stability with the Derivative Regulator.

The regulator transfer function in this case is given by Eqn. (7.14) and Fig. 7.14 shows a comparison between the calculated and the experimental stability limits. The experimental points may be divided into 3 groups:

a) Corresponding to K_{max}. The usual limit cycle appears with a higher frequency than for the simple regulator. The measured points lie above the calculated curve and the discrepancy is not wholly due to the fact that the start of the limit cycle cannot be detected. At $K = 26.5$ the stability limit was established as follows. Because of the higher natural frequency the output voltage of the regulator is a sensitive detector of oscillations and for this test it was observed on a C.R.O. Nevertheless the same criterion, based on angle, was used as with the other regulators.

1) $\delta_g = 140^\circ$. There is a 2° dither on the load angle by no definite oscillation.

2) $\delta_g = 143^\circ$. The output of the voltage regulator on the C.R.O. wanders about with no definite oscillation. Dither on the load angle approximately 3°.

3) $\delta_g = 145^\circ$. There is a 3° dither on the load angle and it appears that there is an oscillation. However, output of the regulator does not show any oscillation.

4) $\delta_g = 147^\circ$. There is $3^\circ - 4^\circ$ dither on the load angle with 2 or 3 oscillation of initial amplitude 2°, which are quickly damped out.

5) $\delta_g = 149^\circ$. Again $3^\circ - 4^\circ$ dither for about 15 sec followed by few oscillations and the system then lost synchronism.

It was decided to take the stability limit at 146° since both 145° and 147° have reasonable claims to it.

b) Corresponding to K_{min}. The behaviour is similar to that with

the integrator regulator. There are no definite oscillations and the alternator does not lose synchronism. It appears that there is little damping os oscillations caused by disturbances and it is difficult to decide when the system becomes unstable. As with the integrator regulator the test was discontinued.

c) High frequency oscillations. As has been pointed out in section 7.3.3 the gain of the derivative regulator is high at approximately 17 c/s. Hence some instability may have been expected although the Nyquist locus, Fig. 7.13, does not approach the (-1, 0) point at high frequencies. It was found that a new kind of instability occurs at low values of δ_g as shown in Fig. 7.14. It is surprising that the frequency of the oscillations is 17 c/s and does not vary with δ_g. Since, by Eqn. (8.2) the frequency of the oscillations is given by

$$1 + H(j\lambda)\, K(j\lambda) = 0$$

and since $K(j\lambda)$ at 17 c/s is real $H(j\lambda)$ must also be real. However, inspection of the numerator and denominator plots of $H(j\lambda)$, Fig. 6.6 shows that at 17 c/s Arg $H(j\lambda) \longrightarrow \pm 90^{\circ}$. Hence it appears that the rate of change of flux terms in Eqn. (2.1) become significant and should not be neglected.

In fact the amplitude of these oscillations at the terminal voltage is less than 0.2 % and hence the operation of the alternator is not affected. Depending on the regulator gain, however, the oscillation is a larger part of V_e, (see Fig. 8.1). At the output of the regulator the oscillations are amplified about 55 times, see Fig. 7.11, and hence become large enough to saturate the limiter. Thus effective control of the excitation is lost.

Some difficulty was experienced with 50 c/s pick-up especially at high regulator gains, which was overcome by careful screening and positioning of equipment.

9.2 Measurement of $H(j\lambda)$.

A direct check of the theory can be made by measuring the frequency response of the alternator. It was decided to consider only one of the $H(j\lambda)$ loci shown in Fig. 6.1 and as for other experiments $\delta_g = 110^\circ$ was chosen. The simple regulator was used. Although such a test is usually straightforward for a linear system there are three complications in the present case.

a) For $\delta_g = 110^\circ$ the system is unstable without a regulator and therefore the open loop transfer function must be determined from a closed loop test.

b) Fig. 6.1 is determined for small oscillations but in order to improve the accuracy a large signal is desirable.

c) Because of the low frequencies involved an inaccurate test had to be used to measure $H(0)$.

9.2.1 Frequency Response Test.

Fig. 9.3 shows a block diagram of the system during this test. The oscillator of the transfer function analyser (T.F.A.) see section 3.0, was used to inject a small oscillation into the system as shown. As a result an oscillating component was superimposed on the voltages V_c and V_{fe} . These voltages were then, in turn, measured by the T.F.A. voltmeter, which is not shown in Fig. 9.3. Hence V_c and V_{fe} are known in magnitude and phase with respect to the output of the oscillator. Since the attenuation of the rectifier and the filter is 0.193, see section 3.2.3,

$$\Delta V_t = \Delta V_c / 0.193$$

and

$$H(j\lambda) = - \frac{\Delta V_c}{0.193 \ \Delta V_{fe}}$$

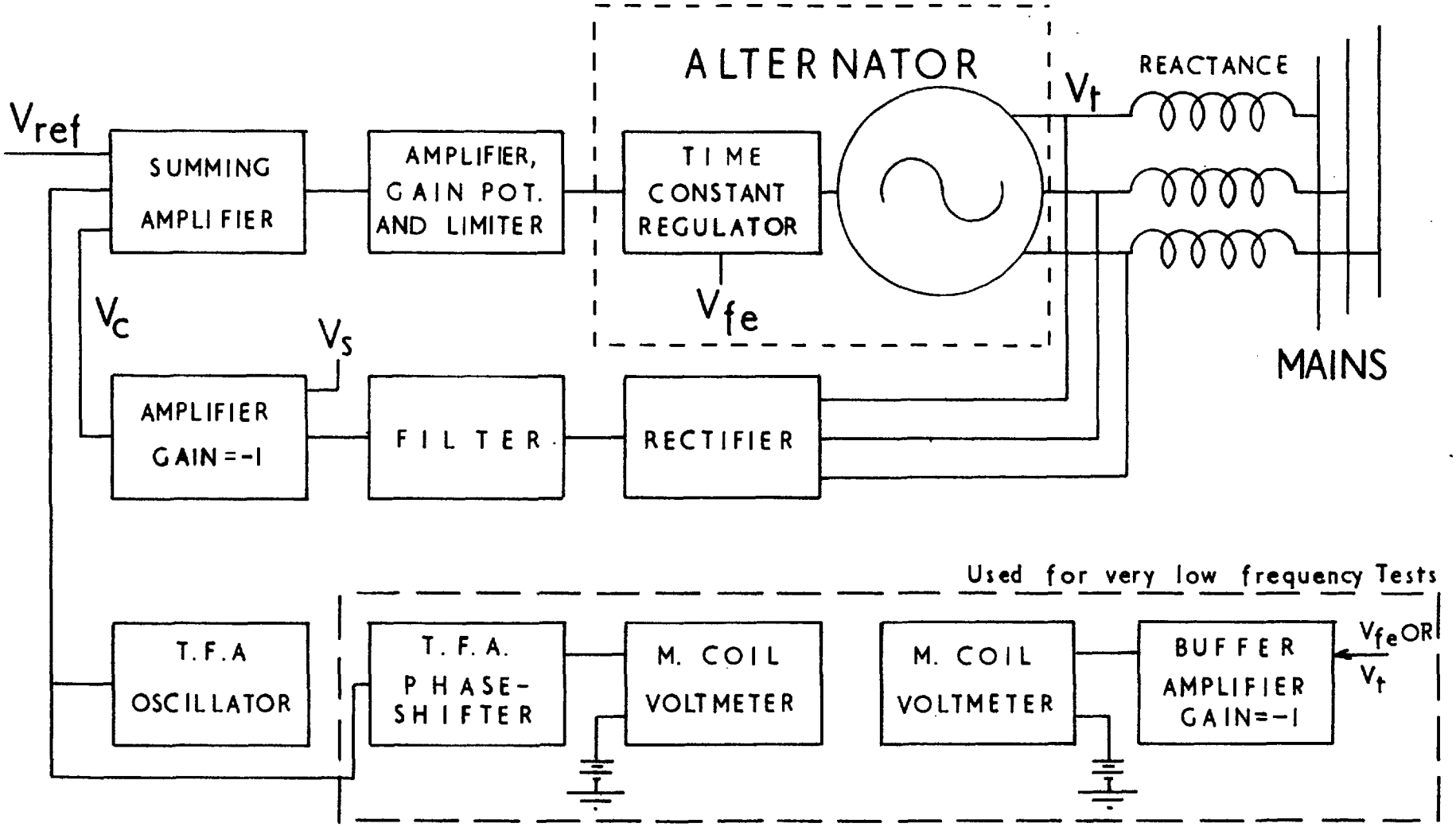

FIG. 9.3 EXPERIMENTAL BLOCK DIAGRAM

Below 0.7 c/s the pointers of the T.F.A. voltmeter oscillate about a mean position and below 0.4 c/s it was no longer possible to use the instrument.

For low frequencies the arrangement shown in the lower part of Fig. 9.3 was used. The output of the oscillator went through the phase-shifter to a moving coil voltmeter and the signal to be measured through a buffer amplifier to another moving coil voltmeter. The frequencies were low enough so that the oscillation could be observed on the instruments, which were biased from zero so that their reading was always positive. The magnitude of the signals was obtained by noting the maximum and the minimum readings. The phase-shifter was adjusted so that the pointers of the two moving coil instruments moved up and down together. The reading on the phase-shifter then gives the phase angle of ΔV_t and ΔV_{fe} with respect to the oscillator output.

The accuracy of the phase angle measurement is considerably reduced when using the two voltmeters as compared with the T.F.A. voltmeter, especially at the very low frequencies, where the error is possibly of the order of 10°. The measurement of the amplitude should be reasonably accurate. A source of error is that the peak-to-peak voltages were measured and it was assumed that the oscillator output as well as the signals measured were sine waves.

The magnitude of the a.c. signal injected into the system is a compromise between a large and a small value. The small value does not violate the conditions of the small oscillation theory but produces small signals at V_{fe} and V_c, which are difficult to measure. A large signal gives measurable voltages at V_{fe} and V_c but the results are affected by the non-linear nature of the system. As low frequencies the injected voltage was adjusted to give a swing in δ_g of 6°. At higher frequencies, however, a large signal is required for such a swing and it was decided to limit the injected voltage to approximately 8% of the reference voltage (a.c. Volts/d.c. Volts).

Another discrepancy from the assumed conditions is the variation of the torque of the d.c. shunt motor driving the alternator. The torque-speed characteristic of a d.c. shunt motor is such that a small change of speed produces a large change in torque. During the load angle swings therefore the mechanical torque does not remain constant. This torque oscillation was reduced by inserting a resistance in series with the armature of the motor.

The result of this test is shown in Fig. 1.6 together with the calculated curve. Two alternative methods were attempted for the very low frequency points and both were found unsatisfactory.

a) Using a C.R.O.

b) Subtracting a known fraction of the output voltage of the phase-shifter from the output voltage of the buffer amplifier (see Fig. 9.3) by means on another operational amplifier. If the two inputs to the second amplifier are arranged to be equal in magnitude and of opposite phase then its output would be zero.

9.2.2 Determination of H(0) .

The value of the alternator transfer function at zero frequency is given by the ratio of small steady changes in V_c and V_{fe} and it is measured by introducing a small change in the steady conditions, see Fig. 9.3. Normally the value of $H(0)$ would be obtained by reducing the frequency of the applied signal in the last test until the output is in phase with the input. The lowest frequency obtainable from the T.F.A. oscillator is 0.01 c/s and as it may be seen from Fig. 1.6 there is considerable phase-shift at this frequency.

The conditions are the same as for the frequency response test, section 9.2.1, with K adjusted to give stable operation up to $\delta_g = 120^\circ$. A step voltage V_s is introduced as shown in Fig. 9.3, the effect of which is the same as increasing the reference by V_s . After the transient dies away a new steady state condition is established corresponding to the increased reference voltage. If ΔV_t is the change

in V_t after the introduction of V_s then $\Delta V_t/V_s$ gives the closed loop response, from which the open loop response may be calculated.

Two series of tests were performed, in the first of which ΔV_t was determined by measuring V_t before and after the introduction on V_s. In the second series the change in V_t was calculated from the known bus voltage and power and the measured value of current in the line for the two steady conditions.

As in the frequency response test of the previous section the magnitude of the injected signal is a compromise between a small and a large value. Three values of V_s were used, 0.5, 1 and 1.5 V. It was hoped that the results obtained would change in one direction as V_s was increased, thus giving an indication as to where the value for small V_s would lie. There was considerable drift in the system probably due to changes in the a.c. and d.c. mains and the time constant regulator output, see section 9.1.1. The following method was adopted for the test in order to achieve some consistency.

The initial condition was established and the readings were taken starting with the load angle. If the angle had not changed in the meantime the step change V_s was applied. After about 30 sec the power was adjusted, if necessary, and the readings were once again taken. V_s was then removed and if δ_g returned to within $\pm 2^o$ of the original setting in approximately 30 sec the values were accepted and it was assumed that no serious drift had occurred. Otherwise the process was repeated.

The values of $H(0)$ obtained from this test are plotted against load angle in Fig. 9.4. It was assumed that a change from δ_a to δ_b corresponds to a small oscillation value at,

$$\delta_g = \frac{\delta_a + \delta_b}{2}$$

Because of the various drifts the scatter of results is large. However,

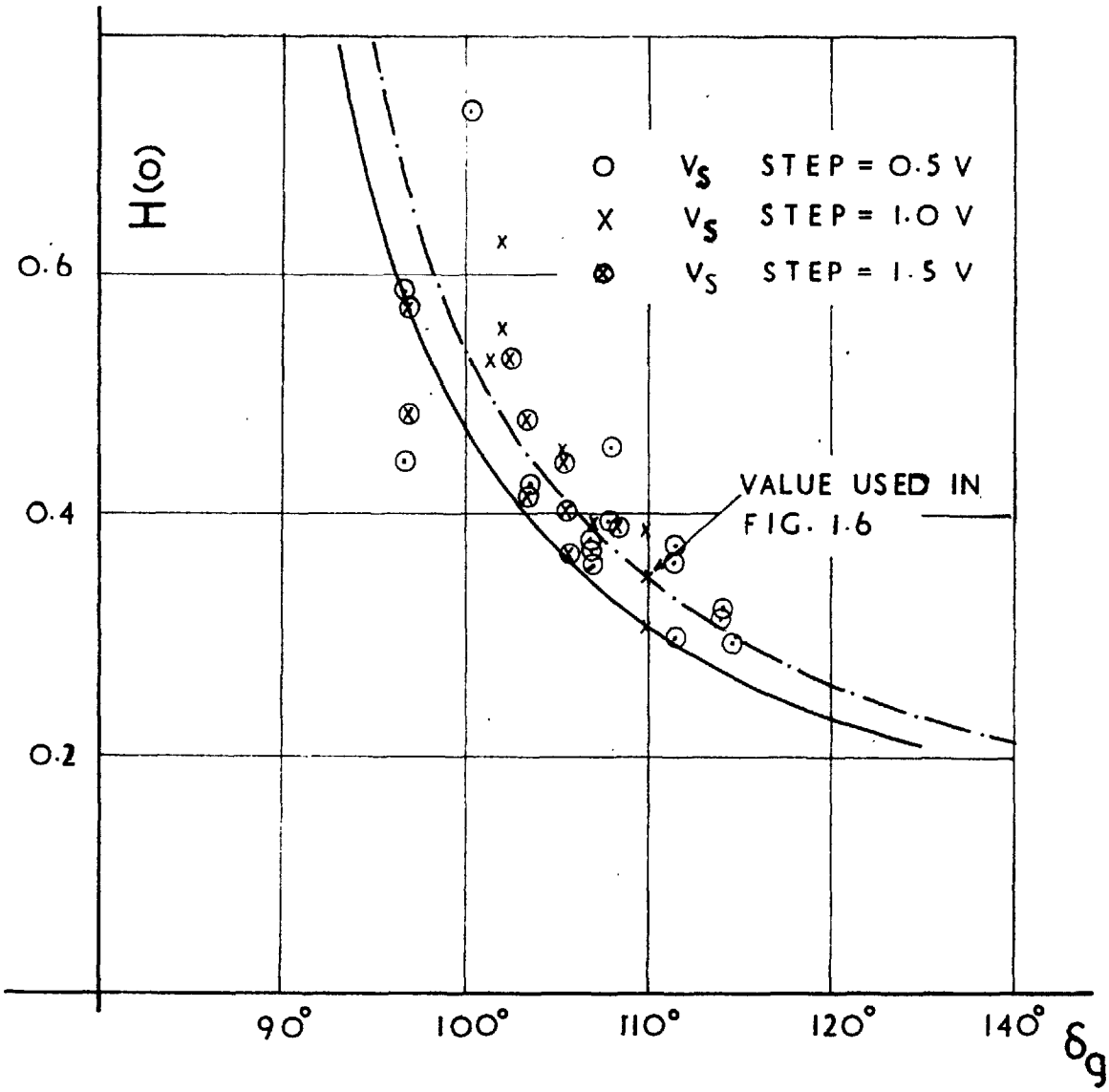

FIG. 9.4

H(o) FROM STEP CHANGE TESTS

——— Calculated $r_a = 0$

—·—·— Calculated r_a included

the calculated curve shows good agreement with the experimental points. The scatter does not diminish with increasing values of V_s. The value shown on Fig. 1.6 is the average result for $\delta_g = 110^o$.

9.3 Measurement of $K(j\lambda)$.

The frequency response of the regulator with the analogue computer set to unity gain has already been discussed, see section 3.2. The use of the analogue computer simplifies considerably the setting-up of any type of transfer function for the regulator. Although the actual transfer function can be written down by inspection of the patch-board it was decided to measure the frequency response for each regulator. Hence any mistakes in setting-up the computer could be detected. Figs. 7.7 and 7.12 shows the measured as well as the calculated points on the frequency response locus. The Transfer Function Analyser was used and hence there are no measurements below 0.4 c/s.

As stated in section 3.2.2 a precision decade potentiometer is used to vary the gain. It was found that, since the input resistance of the amplifier following the potentiometer is finite, a calibration is necessary in order to determine the gain in the computer at zero frequency with different positions of the potentiometer.

The Transfer Function Analyser was also used for adjusting the derivative regulator parameters so that the required frequency response was achieved. The oscillator was set to 0.6 c/s, which from Fig. 6.1 is a suitable frequency, and the computer coefficient potentiometers were adjusted so that the in-phase component of the output was zero.

9.4 Step Function Test.

The aim is to confirm the results of section 8.1 and the method is similar to that used for determining $H(0)$, see section 9.2.2. A step was injected as before but now the transient change in V_t was

recorded. The circuit used is shown in Fig. 9.3 with the Transfer Function Analyser disconnected. The analogue computer was adjusted, in turn to give the transfer functions of the regulators described in sections 7.1 and 7.3. It was found convenient to introduce the step function at the input of the summing amplifier (see Fig. 9.3) and to measure ΔV_t at V_c. Thus with V_c biased using a battery the scale of the recorder could be increased to show the small change.

The same difficulties as in section 9.2.2 were encountered and several measurements were made. A number of the recordings had to be discarded either because of an obvious disturbance during the test or because the initial steady state conditions were not established after the removal of the step, see section 9.2.2.

Typical results are shown in Figs. 9.5 to 9.8. The transient response is shown both when the step is applied and it is removed plotted with the same time origin and showing ΔV_t positive. The scale of the figures is arbitrary so that the change in V_t is equal to unity. The difference between the two curves illustrates the non-linearity of the system. For the simple and the delay regulators two values of step were used for each regulator gain producing a change from 120° to 100° and from 116°-117° to 104°-103°. As in section 9.2.2 it was hoped to establish some relationship between the size of the step and the departure from the calculated curve. One can only say, however, that the discrepancy between the curves obtained when the disturbance is applied and when it is removed, is increased with the larger step.

Since the system is unstable at $\delta_g = 120^\circ$ with the integrator regulator it is not possible to use the larger step in this case.

The result quoted for the derivative regulator is affected by the limiter and cannot be compared with the calculated curve. Clearly the output of a differentiator to a step function is large and as a

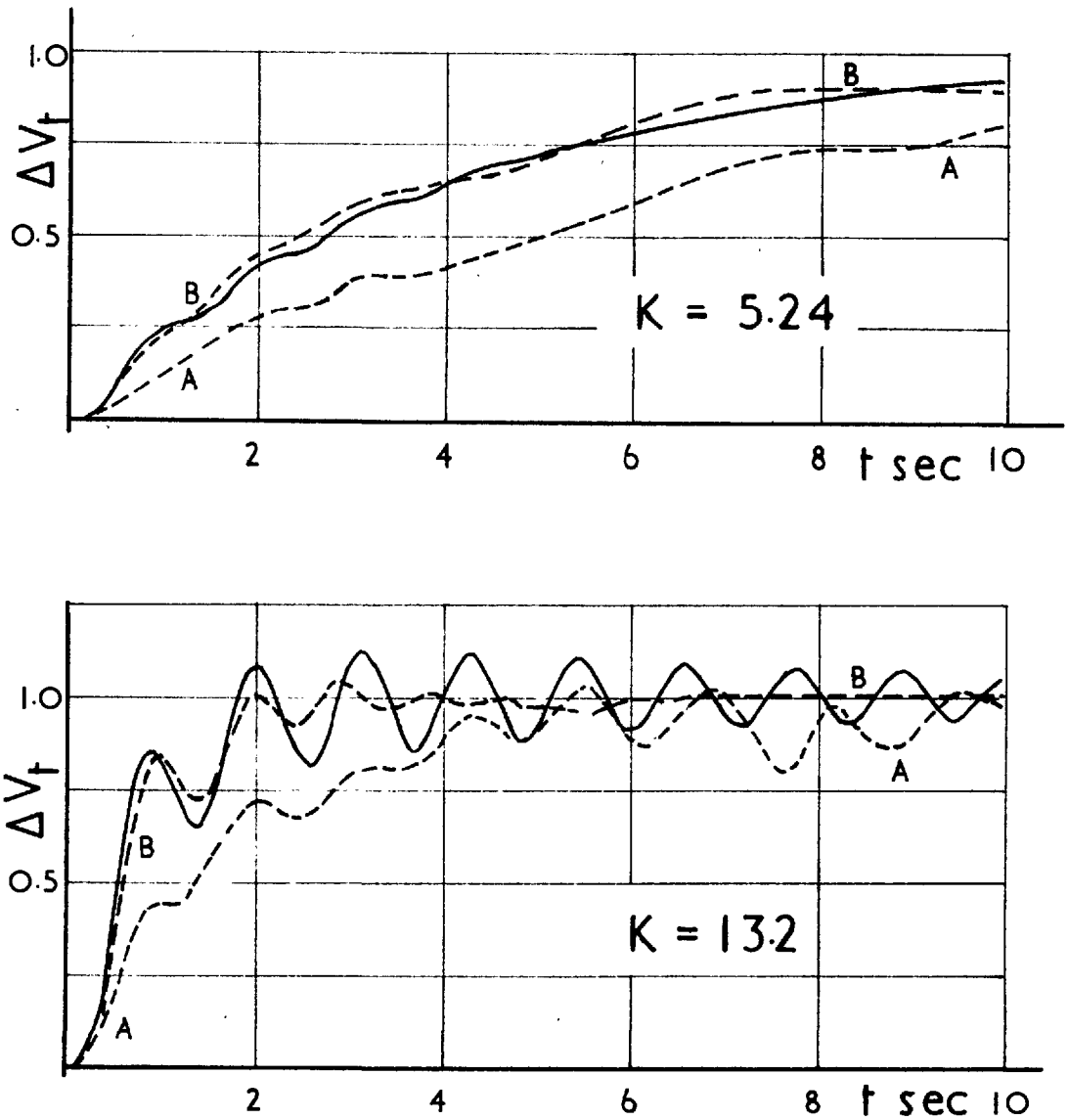

FIG. 9.5a

RESPONSE TO STEP FUNCTION

SIMPLE REGULATOR

——— CALCULATED ---- MEASURED FOR δ_g

A) FROM 100° TO 120°

B) FROM 120° TO 100°

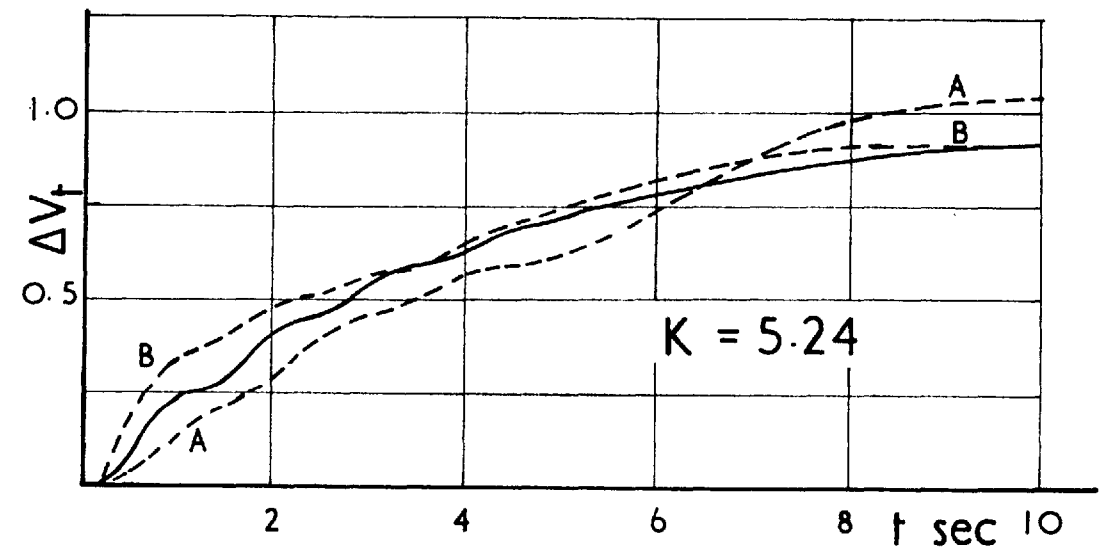

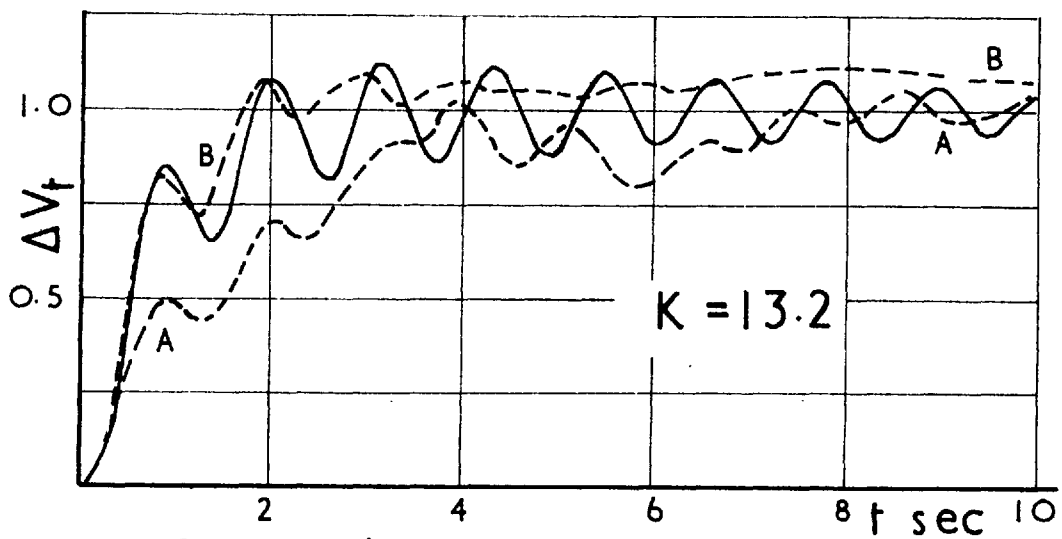

FIG. 9.5b

RESPONSE TO STEP FUNCTION

SIMPLE REGULATOR

——— CALCULATED ----- MEASURED FOR δ_g

A) FROM 104° TO 116°

B) FROM 116° TO 104°

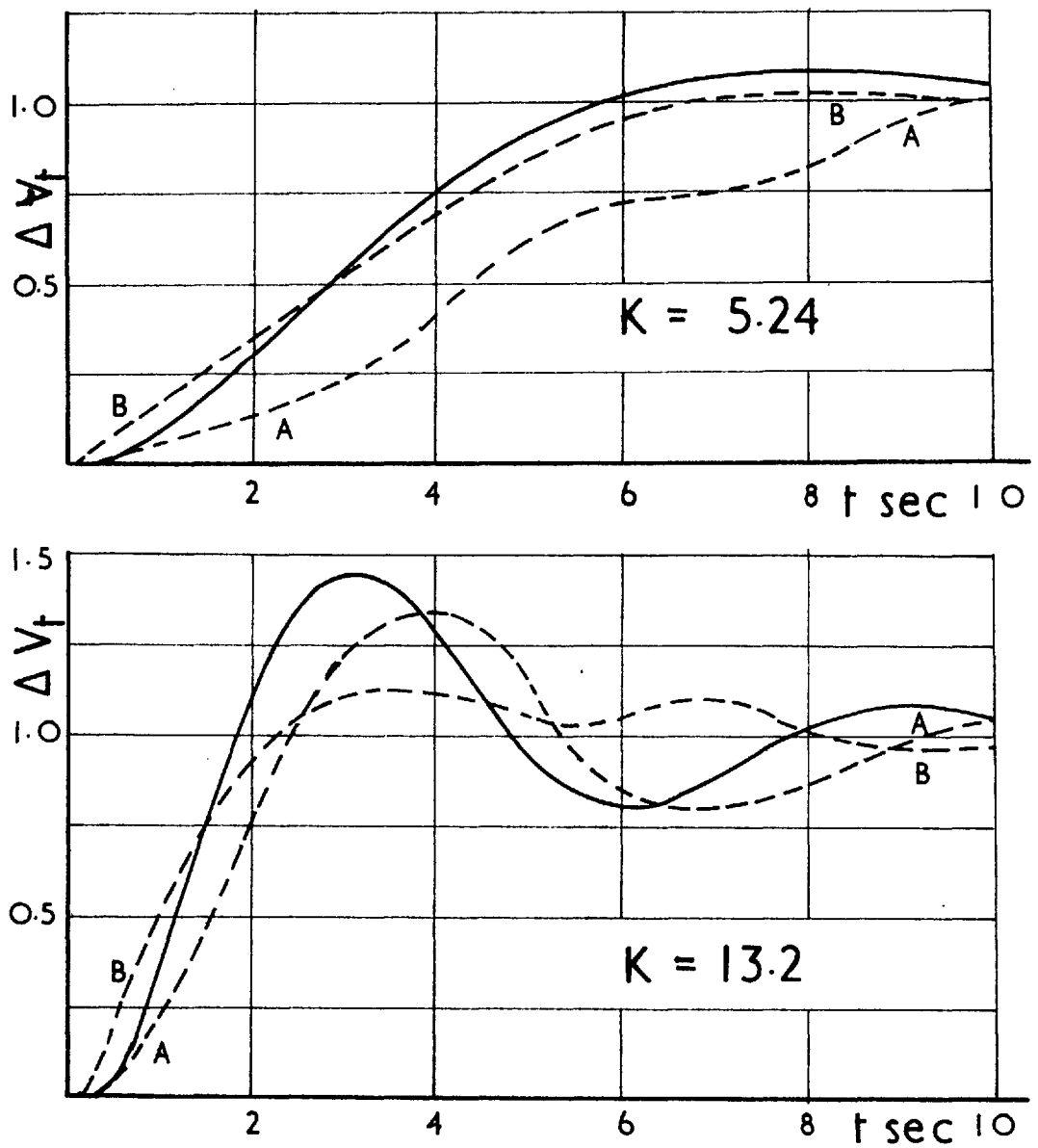

FIG. 9.6 a
RESPONSE TO STEP FUNCTION
DELAY REGULATOR $T_1 = 1$ sec

——— CALCULATED ---- MEASURED FOR δ_g
A) FROM 100° TO 120°
B) FROM 120° TO 100°

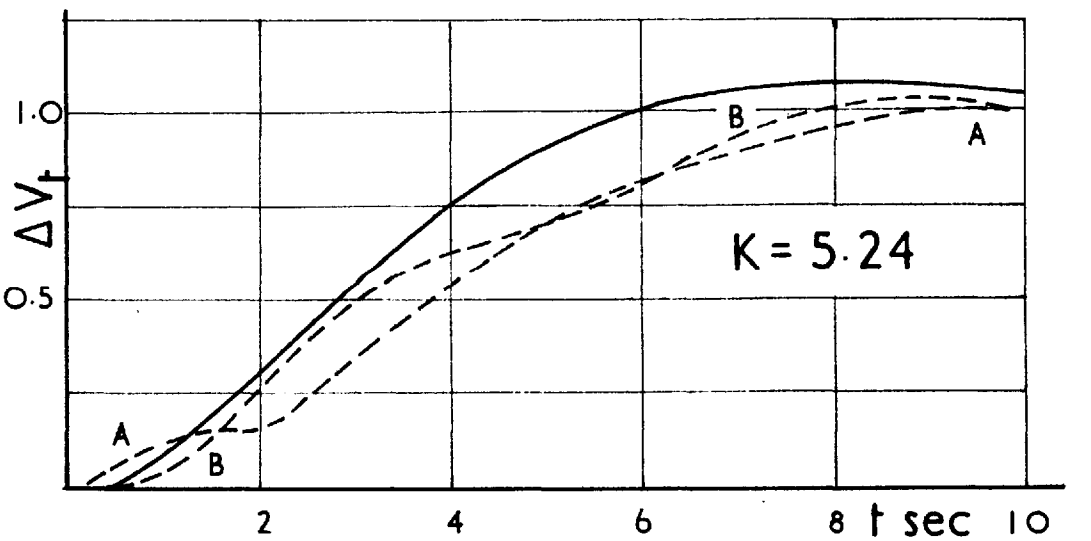

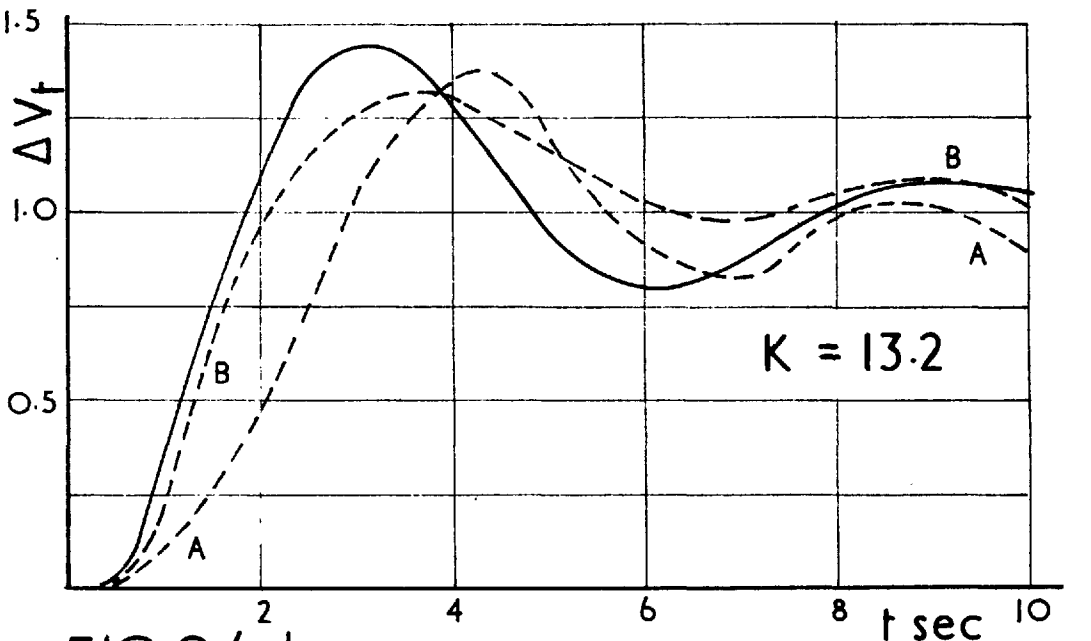

FIG. 9.6 b

RESPONSE TO STEP FUNCTION

DELAY REGULATOR $T_1 = 1$ sec

——— CALCULATED - - - -- MEASURED FOR δ_g

A) FROM 103° TO 117°

B) FROM 117° TO 103°

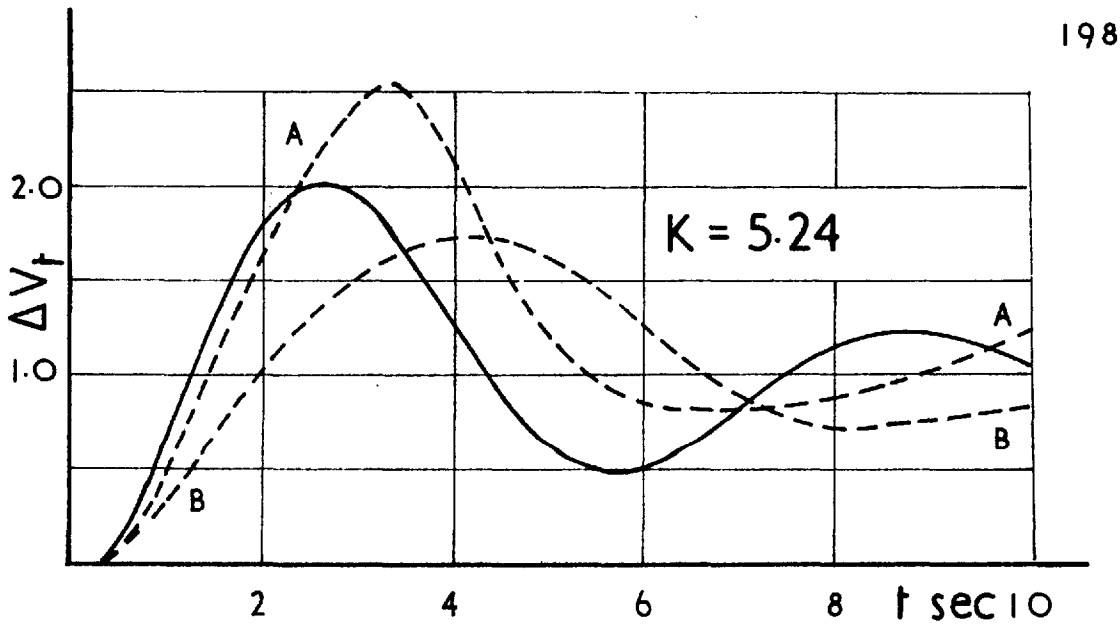

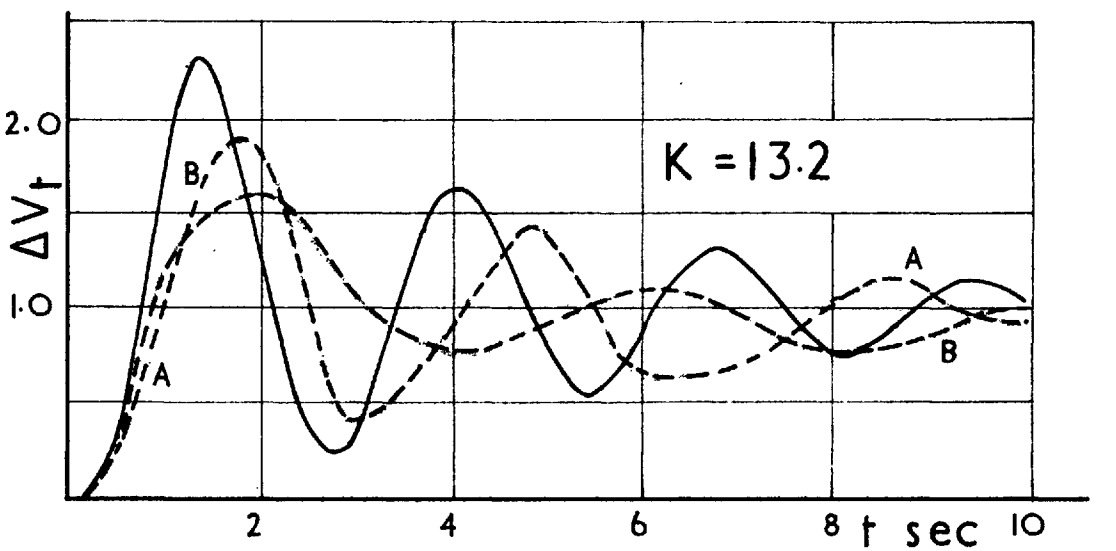

FIG. 9.7

RESPONSE TO STEP FUNCTION

INTEGRATOR REGULATOR $T_1 = 1$ $T_\alpha = 2$ sec

——— CALCULATED ---- MEASURED FOR δ_g

A) FROM 104° TO 116°

B) FROM 116° TO 104°

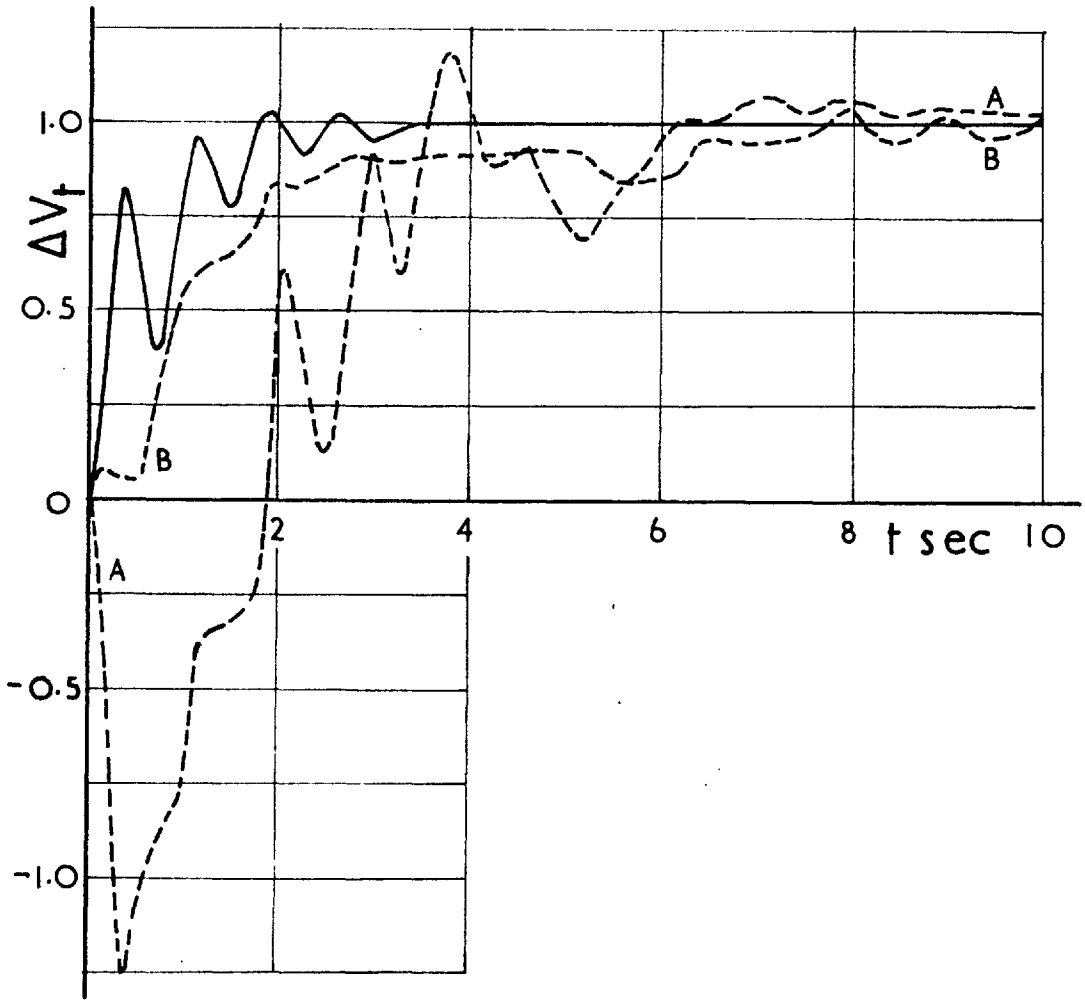

FIG. 9.8

RESPONSE TO STEP FUNCTION

DERIVATIVE REGULATOR K=18.5

——— CALCULATED - - - - - MEASURED FOR δ_g

A) FROM 100° TO 120°

B) FROM 120° TO 100°

result the limiter comes into operation. It is interesting to note that when the step is applied at $\delta_g = 100^\circ$ the alternator swings in the opposite direction and δ_g is less than 100° for approximately 2 sec. On the other hand when the step is removed at $\delta_g = 120^\circ$ the load angle goes directly to 100°.

9.5 Regulation Test.

The result of this simple test is shown in Fig. 8.6. The method used is as follows: The value of V_{ref} (Fig. 9.3) was noted when $\delta_g = 110^\circ$ and $P = 0.8$ p.u. for different regulator gains. The alternator was removed from the infinite bus and the speed adjusted to its normal value. The open circuit voltage was then measured when the gain was varied and V_{ref} adjusted to the corresponding values as before. The value of ρ is obtained from the first part of Eqn. (8.10).

Since the regulation is a function of $K(0)$ and does not depend on the type of regulator this test was carried out only for the simple and the integrator regulators. In the latter case it was confirmed that $\rho = 0$ for any value of K.

10. CONCLUSIONS.

Many of the conclusions derived in the present investigation are a direct result of deeper application of a well known method. The first important contribution to the solution of the problem using the small oscillation theory was made by Concordia[44-1] and the first use of the Nyquist criterion by Messerle and Bruck[55-1]. The system matrix is derived so that either the voltage or the torque feedback methods may be used. It is considered that the voltage method is more suitable for analyzing the effect of the excitation regulator. The torque method, however, links the conventional approach to steady stability with that of the small oscillation theory when there is no regulator. In addition the torque method may be used for studying the effects of governor on stability especially when the excitation regulator must also be taken into account.

When damping and the armature resistance are neglected formulae are derived for the salient features of $H(j\lambda)$. Many of these results are already known. However, by plotting the constituent parts of the $H(j\lambda)$ and by comparing the loci with those obtained when damping and r_a are included the effects of individual parameters are determined. It is shown that both damping on its own and r_a have a significant stabilizing effect. The contribution of rotor damping is particularly important since a higher value of gain may be used and as a result the accuracy of regulation is improved.

The following results are obtained for typical regulators used in practice. The simple regulator extends the region of artificial stability up to the peak of the transient power-angle curve, δ'_s. The maximum value of gain, K_{max}, that may be used for $\delta_s < \delta_g < \delta'_s$ is small so that the accuracy of regulation is poor. With the delay regulator the maximum stable value of δ_g is less than δ'_s and K_{max} is increased as the delay T_1 is increased. Thus if a large load angle is not required it is possible to use an artificially high T_1 to improve the accuracy

of regulation. When T_1 is large the regulator approaches the integrator type. This does not enable the system to operate in the artificial stability region without a stabilizer, but if suitable stabilization is provided, considerable extension of the stability region may be achieved. When a 2nd derivative regulator is used the stability region is extended beyond δ'_s and K_{max} is increased compared with the simple regulator. It is proved that the ultimate stability limit with a derivative regulator occurs when the angle between the infinite bus and the alternator terminal voltage is 90°. Although this result is stated in Venikov[64-1] it has not been possible to find a proof in the literature.

The majority of the theoretical papers use the Routh test. For the following reasons, however, it is considered that the Nyquist test is the most useful method:

1) The alternator and the regulator transfer functions are calculated separately and the number of the stability conditions is not affected by the degree of either $H(p)$ or $K(p)$. Hence an accurate representation of the alternator and consideration of complicated regulators are possible. The effects of rotor damping and of the armature resistance are included both of which appear to have been neglected in the literature, see section 1.1.3. Also it was possible to consider the 2nd derivative regulator, for which no analysis could be found in the literature. The amount of computation involved is considerable, but this is taken care of by using a digital computer. The computation is repetitive and can easily be programmed.

2) It is possible to verify intermediate results experimentally by measuring the frequency response of the system to small signals. The alternator transfer function, $H(j\lambda)$, need be measured only once since combination with the measured regulator transfer function gives the frequency response of the system for any regulator.

3) The effect of the regulator gain is apparent since only the scale of the frequency response locus is changed.

4) The overall effect of the various types of regulator may be obtained without computation, since multiplication of the $H(j\lambda)$ and the $K(j\lambda)$ loci may be visualized easily. It is apparent from Fig. 6.1 for example, that an unstabilized integrator regulator does not enable the alternator to operate in the artificial stability region. It is also obvious that only a regulator with a second derivative signal can extend the stability limit beyond the peak of the transient power-angle curve. A proof of either of these results could not be found in the literature.

5) Information about the degree of stability is obtained by using the phase and gain margins for each locus.

6) The most important advantage, however, of the Nyquist criterion is the possibility of synthesizing a regulator. In a particular case the $H(j\lambda)$ locus may be drawn from knowledge of the alternator and the system parameters. A suitable regulator transfer function may then be determined so that the system may operate up to the required stability limit. Finally the regulator components may be chosen so that the required transfer function is obtained.

The experiments described in section 9 approximately confirm the theoretical results. The ability of the derivative regulator to stabilize the system for $\delta_g > \delta'_s$ is established. The stability limit achieved, $\delta_g = 146^\circ$, is larger than the maximum value reported in the literature with a comparable system, see Table I p. 221. The system seems to be particularly susceptible to drift when the integrator or the derivative regulators are used at low gains. This, however, does not appear to be important in a practical system, where normally high gains should be used. Nevertheless, an additional performance index to measure drift may have to be defined. The American I.E.E. Definitions, Ref. 61-3, give drift as "a sepcified change for a specified period of time, for specified conditions". The calculation of a "drift index" and its measurement except on an actual system appear to be very difficult. A further investigation should be made into the high frequency oscillations

with the derivative regulator and the rate of change of flux terms should be included. It is probable that by careful choice of the delays in the regulator the high gains at high frequencies may be reduced without affecting the low frequency response and so this form of instability may be eliminated.

In determining the optimum transfer function of the regulator other factors may be considered in addition to the steady state stability. It is not often that a system is required to operate at extreme angles and hence it becomes necessary to determine suitable values of gain between K_{min} and K_{max}. Also several regulators may meet the stability requirements and the choice of the most suitable type should depend on other factors. It was decided to use two additional performance indices, namely, speed of response and accuracy of regulation. It appears that there are no accepted methods for determining either quantity and two methods of measurement and calculation are suggested in section 8.

The speed of response is defined for small changes but experiments show that for changes in load angle from 120° to 100° the linear theory is approximately valid and may be used as a guide. However, further investigation is necessary to establish the relation between the responses to large and to small changes. The importance of choosing the right value of gain to obtain a satisfactory response is demonstrated. The derivative regulator is shown to have the minimum integral square error and the integrator regulator to have a highly oscillatory response. The response with the derivative regulator, however, is affected by the limiter and it appears that high exciter ceiling voltages are necessary.

The accuracy of regulation is defined in terms of the change in V_t for two steady operating conditions. As expected the accuracy improves with increased gain and the regulation with an integrator regulator is zero.

A variable parameter regulator appears to offer the best compromise between the three performance indices. The regulator gain may be made a function of the operating condition so that, e.g. the integral square error is a minimum in the artificial stability region. For $\delta_g > \delta_s$ some compromise between the accuracy and speed of response may be used to determine K. Alternatively an integrator regulator may be used for small δ_g and a derivative regulator for $\delta_g > \delta_s$ with a change-over at $\delta_g = \delta_s$. Other parameters may be varied in a fully automated system. Further improvements may be achieved by using combinations of different controlled variables and their derivatives. However, there is a limit to the complexity of the regulator and the reliability of the excitation system is of paramount importance.

It was shown in the thesis that the performance of the alternator is greatly influenced by the excitation regulator. The extension of the steady state stability region that can be achieved appears to be greater than that required for practical systems. Thus the regulator transfer function should be chosen so that the system performance is optimum for a) steady state stability, b) speed of response, and c) accuracy of voltage regulation.

APPENDIX I

Expression of v_d, v_q in Terms of the Bus Voltage and the Load Angle.

Let the infinite bus voltage be

$$\left[V_{abc}\right] = V_m \begin{bmatrix} \sin \omega t \\ \sin(\omega t - \frac{2\pi}{3}) \\ \sin(\omega t - \frac{4\pi}{3}) \end{bmatrix}$$

$\left[V_{abc}\right]$ referred to the d- and the q- axes of the alternator is

$$\left[V_{dqo}\right] = \left[P\right] \left[V_{abc}\right]$$

where $\left[P\right]$ is the Park transformation matrix, see Ref. 57-6

$$\left[P\right] = \frac{2}{3} \begin{bmatrix} \cos\theta & \cos(\theta - \frac{2\pi}{3}) & \cos(\theta - \frac{4\pi}{3}) \\ \sin\theta & \sin(\theta - \frac{2\pi}{3}) & \sin(\theta - \frac{4\pi}{3}) \\ \frac{1}{2} & \frac{1}{2} & \frac{1}{2} \end{bmatrix}$$

where $\theta = \omega t - \delta$

Hence $$\left[V_{dqo}\right] = \begin{bmatrix} v_d \\ v_q \\ v_o \end{bmatrix} = V_m \begin{bmatrix} \sin\delta \\ \cos\delta \\ 0 \end{bmatrix}$$

APPENDIX II

Evaluation of A_{ijk} Including r_a.

$$B_{135} = \begin{vmatrix} -X_d(p) & v_{do} & r_a \\ -\frac{1}{2}v_{do} + r_a i_{do} & -Q'_o & -\frac{1}{2}v_{qo} + r_a i_{qo} \\ -r_a & v_{qo} & -X_q(p) \end{vmatrix}$$

Hence

$$A_{135} = -\Big(Q'_o + V_{qo}^2 Y_q(p) + V_{do}^2 Y_d(p) - 2r_a\big(V_{qo}I_{qo}Y_q(p) + V_{do}I_{do}Y_d(p)\big) - r^2(V_{qo}I_{do} - V_{do}I_{qo})Y_d(p)Y_q(p)\Big) \quad ..(II.1)$$

$$B_{235} = \begin{vmatrix} K_o K(p) G(p) A_1 & K_o K(p) G(p) A_2 & K_o K(p) G(p) A_3 \\ -\frac{1}{2}v_{do} + r_a i_{do} & -Q'_o & -\frac{1}{2}v_{qo} + r_a i_{qo} \\ -r_a & v_{qo} & -X_q(p) \end{vmatrix}$$

Hence

$$A_{235} = \frac{X_c(I_{do} + V_{qo}Y_q(p) - r_a Y_q(p) I_{qo}) \cdot (V^2 - 2r_a P' + X_c Q'_o)F(p)}{V_{to}} \quad (II.2)$$

where

$$P' = V_{do} I_{do} + V_{qo} I_{qo}$$

$$B_{245} = \begin{vmatrix} K_o\, K(p)\, G(p)\, A_1 & K_o\, K(p)\, G(p)\, A_2 & K_o\, K(p)\, G(p)\, A_3 \\ & -Jp^2 & \\ -r_a & v_{qo} & -X_d(p) \end{vmatrix}$$

. Hence

$$A_{245} = -\frac{X_c}{V_{to}}\left[(V_{qo} + X_c\, I_{do}) - r_a\, Y_q(p)\, (V_{do} - X_c\, I_{qo})\right] \quad \text{(II.3)}$$

$$B_{145} = \begin{vmatrix} -X_d(p) & v_{do} & r_a \\ & -Jp^2 & \\ -r_a & v_{qo} & -X_q(p) \end{vmatrix}$$

Hence

$$A_{145} = 1 + r_a^2\, Y_d(p)\, Y_q(p) \quad \text{(II.4)}$$

APPENDIX III

The Nyquist and Routh Stability Criteria

The block diagram of a single loop feedback system is shown in Fig. III.1. Each of the four functions C , D , E and F is a polynomial in **p**. From it the following equations may be written down:

$$\begin{aligned} \theta_e &= \theta_i - \theta'_o \\ \theta_o &= \frac{C(p)}{D(p)}\ \theta_e \\ \theta'_o &= \frac{E(p)}{F(p)}\ \theta_o \end{aligned} \qquad \text{(III.1)}$$

Eliminating θ'_o and θ_e from Eqns. (III.1) the differential equation of the system on closed loop is obtained,

$$\Big(D(p)\,F(p) + C(p)\,E(p) \Big)\ \theta_o = F(p)\,C(p)\ \theta_i \qquad \text{(III.2)}$$

and the Characteristic Equation is:

$$D(p)\,F(p) + C(p)\,E(p) = 0 \qquad \text{(III.3)}$$

The system is stable if all the roots of this equation have negative real parts. There are several methods available for determining the position of the roots of an equation without solving it. In this investigation the Nyquist criterion is used and is described in some detail in this Appendix. For many operating conditions the forward loop of the system is inherently unstable and this requires special considerations. The Routh criterion is an alternative method and because it is used in Appendix IV it is necessary to give a brief statement of it.

III.1 The Nyquist Test Applied to a Feedback Control System.

The Nyquist test is based on the Open Loop Transfer Function

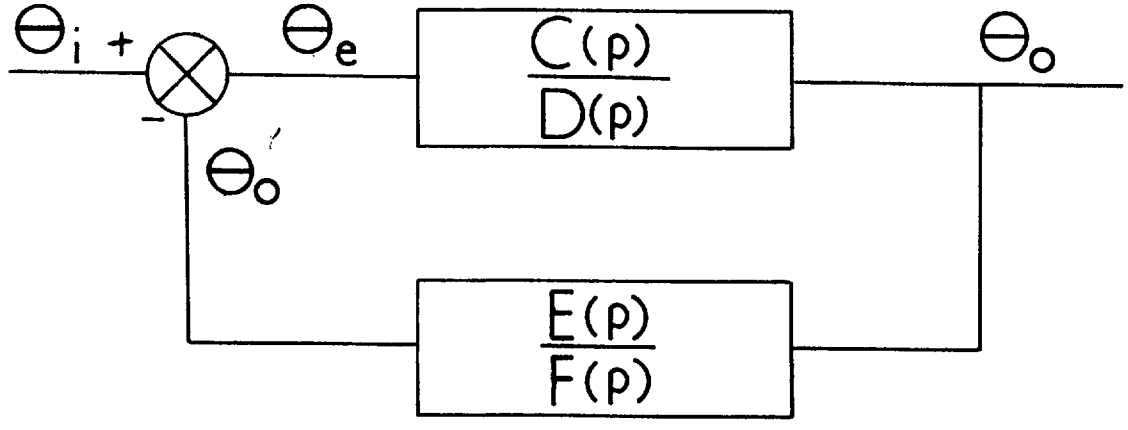

FIG III.1 GENERAL CLOSED LOOP SYSTEM

defined as follows; see Fig. III.1.

$$H(p) = \frac{\theta'_o}{\theta_e} = \frac{C(p)\,E(p)}{D(p)\,F(p)} = \frac{A(p)}{B(p)}$$

where $A(p)$ and $B(p)$ are polynomials in p. In a physical system the degree of $B(p)$ is higher than the degree of $A(p)$ and the open loop transfer function tends to zero as $p \longrightarrow \infty$. Eqn. (III.3) may be written as

$$A(p) + B(p) = 0 \qquad \text{(III.4)}$$

In order to introduce the open loop transfer function divide both terms by $B(p)$

$$\frac{A(p)}{B(p)} + 1 = 0 \qquad \text{(III.5)}$$

Eqn. (III.5) has the same roots, with positive real parts, as Eqn. (III.4) provided that $A(p)$ and $B(p)$ do not have a common zero which has a positive real part. This is most unlikely to happen in practice.

Consider the transformation from the p- to a w'-plane in two steps as follows:

$$w = \frac{A(p)}{B(p)} \qquad \text{(III.6)}$$

and

$$w' = w + 1 \qquad \text{(III.7)}$$

Let

$$w' = W\,\frac{(p - p_1)(p - p_2)\ \ldots\ldots}{(p - p_\alpha)(p - p_\beta)\ \ldots\ldots} \qquad \text{(III.8)}$$

The zeros of w' are p_1, p_2 etc., and the poles are p_α, p_β etc., but their values are not known. It should be noted that the zeros of w' are the same as the zeros of the characteristic equation and that the poles of w' are the same as the zeros of $B(p)$.

Fig. III.2 shows some typical poles and zeros on the p-plane. For stability p_1, p_2, ... should all lie to the left of the imaginary axis. Any closed contour C followed by a point Q in the p-plane is transformed by Eqns. (III.6) and (III.7) into a closed contour C' followed by a point Q' in the w'-plane. Let Q pass round the contour C in a clockwise direction. If C encloses a zero at p_1, Q' encircles the origin in a clockwise direction, and if C encloses a pole p_α, Q' encircles the origin once in a counterclockwise direction. Hence if C encloses P poles and Z zeros, Q' encircles the origin clockwise (Z - P) times. Curves (i), (ii) and (iii) of Fig. III.2 are obtained for Z - P = 1 (one excess zero), Z - P = -1 (one excess pole) and Z - P = 0 respectively.

Now choose for the contour C the path shown in Fig. III.3 consisting of the imaginary axis, a semicircle at infinity to the right-hand side and another semicircle of infinitesimal radius excluding the origin from C. If there are Z zeros and P poles of w' enclosed in this contour the origin of the w'-plane is encircled Z - P times in a clockwise direction. The transformation from the w- to the w'-plane is a simple change of origin. Hence when Z zeros and P poles of Eqn. (III.5) are enclosed in the contour of Fig. III.3 the w-plane contour encircles the (-1, 0) point Z - P times in a clockwise direction.

Thus the Nyquist test consists of plotting the open loop transfer function $w = A(p)/B(p)$ for values of p from $-j\infty$ to $+j\infty$ and along the semicircular parts of the p-plane contour and counting the number of clockwise encirclements of the (-1, 0) point. Since however, the requirement for stability is that Z shall be zero it is necessary to know the value of P. This is considered in the following section.

It should be noted that since w is the ratio of two polynomials the parts of C' corresponding to the positive and negative halves of the contour C are symmetrical about the real axis in the w-plane. Thus

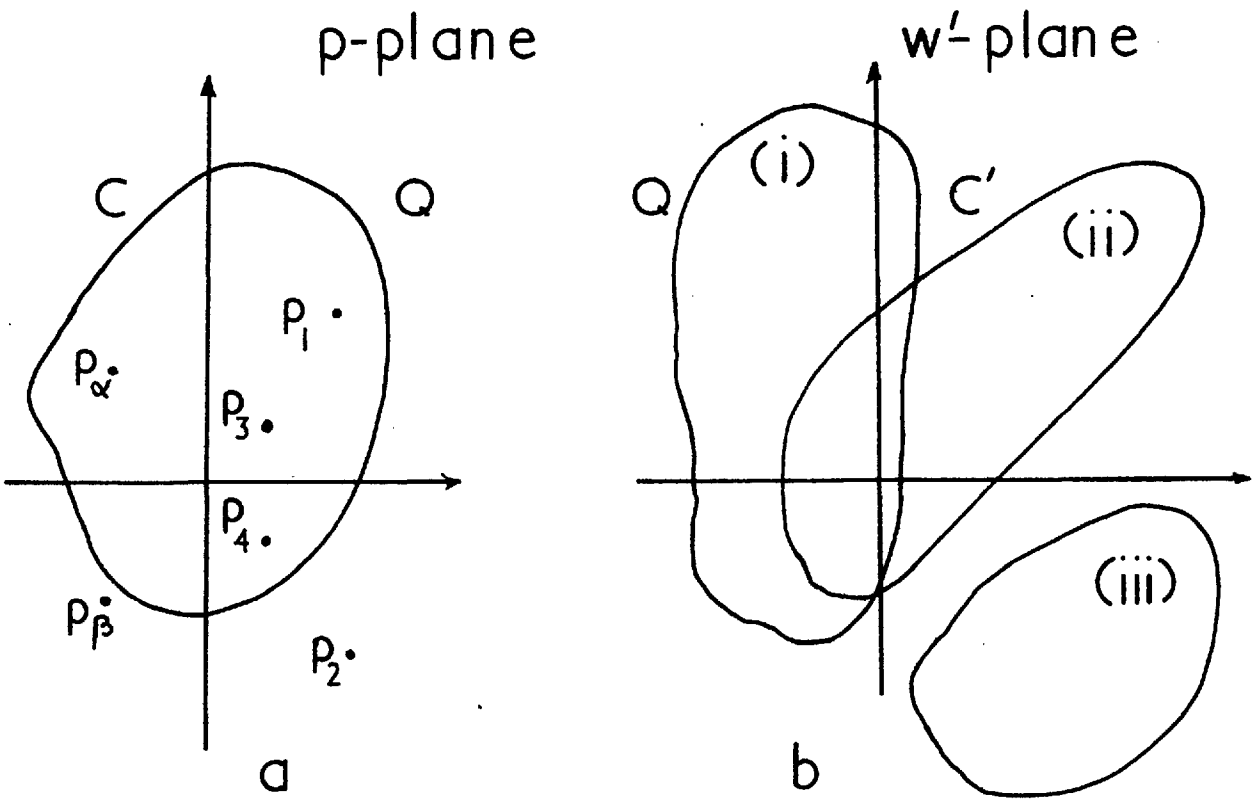

FIG. III.2 CONTOURS C & C'

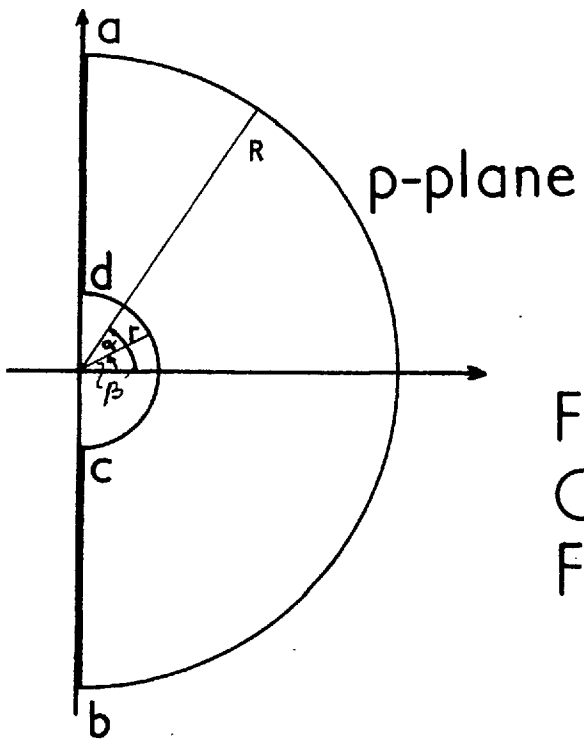

FIG III.3
CONTOUR C
FOR NYQUIST TEST

only the positive half of the imaginary axis need be considered when determining the w-plane contour.

III.2 Determination of P .

P is the number of poles of the open loop transfer function with positive real parts, and is equal to the number of zeros with positive real parts of B(p) . If the open loop system is stable P = 0, and the condition of stability as derived above is that the Nyquist locus shall not encircle the (-1, 0) point. However the alternator with its voltage regulator loop open is unstable for load angles greater than δ_s . In order to use the Nyquist test it is essential to determine P .

The same method as in section III.1 may be used. The transformation from the p-plane to the w'-plane is now,

$$w' = B(p) \qquad \text{(III.9)}$$

B(p) is a polynomial and has no poles. The number of zeros with positive real part is P and therefore the number of clockwise encirclements of the origin in the w'-plane when p describes the contour C of Fig. III.3 is equal to P . If B(p) is an nth order polynomial in p the w'-plane contour corresponding to the infinite semicircle of Fig. III.3 is given by Eqn. (III.9) describes n clockwise semicircles. If n is large this is cumbersome, and so an alternative method is used.

Let B(p) be expressed as:

$$B(p) = B_1(p) + B_2(p)$$

where $B_2(p)$ contains the highest power of p . A plot is made of

$$w = \frac{B_1(p)}{B_2(p)}$$

and the encirclements of the (-1, 0) point counted. It can be arranged that the zeros of $B_2(p)$ are easily determined.

III.3 Poles at the Origin.

When $H(p)$ is the open loop transfer function of a physical system $H(p) \longrightarrow 0$ as $p \longrightarrow \infty$. The semicircle at infinity of contour C Fig. III.3 is transformed into a point in the w-plane and there is no need to consider poles at infinity. It was shown in section III.2 however that the need arises to obtain Nyquist plots of functions which are not open loop transfer functions of a system. For this section only $H(p)$ is considered to be a ratio of two general polynomials.

Assume first that $H(p)$ has an nth order pole at infinity, i.e. the degree of the numerator $A(p)$ exceeds that of the denominator $B(p)$ by n. When $p = R\, e^{j\alpha}$ it can be shown that, for $R \longrightarrow \infty$:

$$H(p) = D_1 R^n e^{jn\alpha}$$

where D_1 is a constant. As point Q describes a b in a clockwise direction α changes from $\pi/2$ to $-\pi/2$. In Fig. III.3 the magnitude of $H(p)$ remains constant and its argument changes through n clockwise semicircles. Since $H(p)$ is an analytic function of p (ratio of two polynomials) angles are preserved in the transformation from the p- to the w-plane. Thus at both points a and b the argument of Q' on C' changes by $-\pi/2$, i.e. the locus turns to the right.

If $H(p)$ has an mth order pole at the origin the situation is very similar. Again for $p = r\, e^{j\beta}$ where $r \longrightarrow 0$

$$H(p) = \frac{D_2}{r^m} e^{-jm\beta}$$

where D_2 is another constant. Point Q describes c d in a

counterclockwise direction and hence point Q' describes m clockwise semicircles. Contour C' turns through 90^{o} to the right at both points corresponding to c and d.

III.4 The Inverse Nyquist Locus.

In the analysis of the alternator-regulator system it is found that the denominator of the open loop transfer function is the quantity that requires close examination. The effect of the various parameters is visualised better if the inverse Nyquist locus is used. The reciprocal of H(p) is plotted and corresponding to Eqn. (III.5) we have,

$$1 \Big/ \frac{A(p)}{B(p)} + 1 = 0 \qquad \text{(III.10)}$$

The roots of Eqn. (III.10) are the same as those of Eqn. (III.5). Hence if a plot is made of B(p)/A(p) the number of clockwise encirclements of the (-1, 0) point gives (Z - P'). P' is the number of zeros with positive real parts of A(p) .

III.5 The Routh Criterion.

The most direct method for determining whether the roots of a polynomial lie in the right half-plane is furnished by the Routh test. Let the characteristic equation, Eqn. (III.3), be arranged as:

$$a_o p^n + a_1 p^{n-1} + a_2 p^{n-2} + \ldots\ldots + a_n = 0 \qquad \text{(III.11)}$$

where a_o is positive.

Write down the coefficients as follows in two rows and then cross-multiply to form further rows

a_o a_2 a_4 etc

a_1 a_3 a_5 etc

$(a_1a_2-a_oa_3)$ $(a_1a_4-a_oa_5)$ $(a_1a_6-a_oa_7)$ etc

$= b_1$ $= b_2$ $= b_3$

$(b_1a_3-a_1b_2)$ $(b_1a_5-a_1b_3)$ $(b_1a_7-a_1b_4)$ etc

$= c_1$ $= c_2$ $= c_3$

etc

The number of columns is reduced by one each time and the process is repeated until only the first column is left. The Routh criterion states that there are as many roots of the characteristic equation with positive real parts as the number of changes of sign in the first column. It should be noted that there are $n+1$ terms in the first column and hence n conditions must be satisfied for stability. See Ref. 60-11 for details and further references.

APPENDIX IV

The Stability of the System Using the Routh Criterion

In this Appendix the stability of the system is analyzed using the Routh criterion and a comparison is made with the results given in Ref. 64-3. Armature resistance and damping are neglected and saliency is assumed to be zero.

From Eqn. (2.21) the characteristic equation of the system is

$$X_d(p)\, X_q(p) \left(A_{135} - J\, p^2 + K_o\, K(p)\, (A_{235} - J\, p^2\, A_{245}) \right) = 0 \qquad \text{..(IV.1)}$$

From Eqns. (4.8), (4.15) and (4.16)

$$A_{135} = -\frac{S_o + p\, T'_d\, S'_o}{1 + p\, T'_d} \qquad \text{(IV.2)}$$

$$A_{245} = \frac{X_c\, X_{md} \cos \delta_t}{r_f\, X_d (1 + p\, T'_d)} \qquad \text{(IV.3)}$$

and it may be shown from Eqn. (4.14) that

$$A_{235} = \frac{X_c\, X_{md}\, V\, V_o \cos(\delta_o - \delta_t)}{r_f\, X_d\, (1 + p\, T'_d)} \qquad \text{(IV.4)}$$

Thus with the simple regulator the characteristic equation may be written as,

$$a_o\, p^3 + (a_1 + \beta_1)\, p^2 + a_2 p + (a_3 + \beta_3) = 0 \qquad \text{(IV.5)}$$

where

$$a_o = J\, T'_d \;,\quad a_1 = J \;,\quad a_2 = S'_o\, T'_d \;,\quad a_3 = S_o$$

$$\beta_1 = -\frac{K J X_c}{X_d} \cos \delta_t \quad , \quad \beta_3 = -\frac{K X_c}{X_d^2} V V_o \cos(\delta_o - \delta_t)$$

It may be shown that Eqn. (IV.5) agrees with the characteristic equation as given in Ref. 64-3 but not with that of Ref. 64-1. As it has already been pointed out in section 1.1.3 an unjustified assumption is made in the latter case.

Since $a_o > 0$ the Routh conditions for stability are, see section III.5.

a) $a_1 + \beta_1 > 0$. This corresponds to $(1 + K K_o d) > 0$. in Eqn. (5.8) and is always satisfied for the parameters of the experimental system.

b) $(a_1 + \beta_1) a_2 - a_o(a_3 + \beta_3) > 0$. It may be shown that this leads to

$$K < \left| \frac{1}{K_o H(j\lambda_1)} \right| < K_{max}$$

with damping and the armature resistance neglected.

c) $a_3 + \beta_3 > 0$. Again it may be shown that this condition leads to

$$K > \left| \frac{1}{K_o H(0)} \right| > K_{min}$$

with the armature resistance neglected.

Hence the significant conditions for stability are the same as those derived in section 7. The two curves making up the stability limit in Fig. 1.3 correspond to conditions b and c. Condition a results in another curve which lies well above the stable region.

It is apparent from Eqn. (IV.1) that the conditions of stability are different for every type of regulator. Also with more complex regulators the degree of the characteristic equation is increased and the number of quantities that must be positive is increased, see

Section III.5. Moreover, the expressions become long and complicated and little useful information may be derived from them. The single delay regulator discussed in Ref. 64-1 illustrates this point. One is then reduced to numerical calculation and the chief advantage of Routh over the Nyquist Test is lost.

TABLE I

Operation in the Artificial Stability Region

Ref	Machine rating MVA	X_c p.u.	Power at Stab. Limit	Max. angle	δ'_s	Condition at Stab. Limit	Remarks
59-6	75 MVA	0.125	0.8	131°	142°	Beginning of the limit cycle.	
62-6	-	0.425	0.8	127°	126°	Loss of synchronism.	Model system, simple regulator.
63-5	690 MW	-	-	111°	-	-	Delay type T_1 = 0.055 sec. with current compounding.
64-6	39 MVA	0.2	0.25	100°	138°	Stable operation limited by 120% overcurrent	Voltage regulator. No details.
65-2	640 MVA	1.85	0.83?	96°	-	Low frequency oscillations	Integrator type.
57-5	30 kVA	-	-	110°	-	-	Model of 1480 MVA system, angle regulator.
60-10	75 MVA	-	0.8	109.5°	-	Settled to 109.5° after 0.5 p.u. step in MVAr.	Effectively angle regulator.

Note δ'_s is calculated from Eqn. (7.5) where the parameters are given.

TABLE II

Machine and System Parameters

Machine rating	2	kVA
Unit voltamperes	1825	VA
Unit voltage	186	V
Unit current	5.66	A.

Parameter	Per Unit Value	Test
X_d	2.321	Steady state operation at 0.8 p.u. power and δ_g from 70° to 120°. Includes line reactance X_c.
X_q	1.91	"
T'_{do}	4.75 sec	Sudden short-circuit of "field winding", alternator on open-circuit, measure decay time constant.
X'_d	0.544	Variable frequency static impedance test.
X''_d	0.482	"
X''_q	0.572	"
T''_{do}	0.06 sec	"
T''_{qo}	0.0816 sec	"
T'_d	1.11 sec	Calculated from T'_{do}, X_d and X'_d
T''_d	0.0533 sec	Calculated from T''_{do}, X'_d and X''_d.
T''_q	0.0244 sec	Calculated from T''_{qo}, X_q and X''_q.
X_a	0.431	Design value, includes line reactance X_c
r_a	0.0384	D.C. measurement, includes line resistance
r_f	0.001425	D.C. measurement
J	0.0318	Deceleration test.
X_c	0.321	A.C. measurement.

TABLE III

Frequencies Used for the Nyquist Loci Calculations (c/s)

0
0.01
0.03
0.05
0.07
0.1
0.2
0.3
0.4
0.5
0.6
0.7
0.8
0.9
1.0
1.2
1.5
2.0
5.0
10.0
100.0

REFERENCES

11-1 DREYFUS, L. Einfuehrung in die Theorie der selbserregten Schwingungen synchroner Machinen. Elektrotechnik und Maschinenbau. Heft 16 , 323-29 (1911) Heft 17 , 345-54 (1911).

28-1 DOHERTY, R.E. Excitation systems. Their influence on short circuits and maximum power. Trans. A.I.E.E. 47 , pt. 3, 944-56 (July 1928).

30-1 WAGNER, C.F. Effect of armature resistance upon hunting of synchronous machines. Trans. A.I.E.E. 49 , No. 3 , 1011-24 (July 1930).

32-1 YTTERBERG, A. The Asea high-speed voltage regulator for alternating-current generators. A.S.E.A. Journal 9 , 174-189 (1932).

35-1 British Standard Specification. Internal combustion engines. No. 649 (1935).

44-1 CONCORDIA, C. Steady-state stability of synchronous machines as affected by voltage regulator characteristics. Trans. A.I.E.E. 63 , 215-220 (1944).

45-1 A.I.E.E. Test code for synchronous machines. A.I.E.E. publication No. 503 (June 1945).

46-1 FREY, W. The stabilization of synchronous generators by high-speed regulation of the excitation in connection with power transmission over long distances. Brown Boveri Rev. 33 , No. 11 , 335-47 (1946).

46-2 LAVANCY, C. Experiments in stabilizing synchronous generators by high speed control of the excitation in connection with power transmission over long distances. Brown Boveri Rev. 33 , No. 11 , 348-54 (1946).

47-1	CRARY, S.B.	Power system stability. Vol. II Transient stability. Wiley (1947).
48-1	BARKLE, J.E. & VALENTINE, C.E.	Rototrol excitation systems. Trans. A.I.E.E. 67 , pt. I , 529-34 (1948).
48-2	LYNN, C. & VALENTINE, C.E.	Main exciter rototrol excitation for turbine generators. Trans. A.I.E.E., 67 , pt. I , 535-39 (1948).
48-3	CONCORDIA, C.	Steady-state stability of synchronous machines as affected by angle-regulator characteristics. Trans. A.I.E.E. 67 , 687-690 (1948).
50-1	HEDSTROM, S.E.	The use of transductor regulators with booster exciters. A.S.E.A. Journal 23 , No. 2 , 23-31 (1950).
50-2	CONCORDIA, C.	Effect of buck-boost voltage regulator on steady-state power limit. Trans. A.I.E.E. 69 , 380-385 (1950).
50-3	HEDSTROM, S.E. & JOHANSSON, K.E.	Exciter series winding in conjunction with high speed regulator. A.S.E.A. Journal. 23 , 157-8 (1950).
52-1	HEFFRON, W.G. & PHILLIPS, R.A.	Effect of a modern amplidyne voltage regulator on underexcited operation of large turbine generators. Trans. A.I.E.E. 71 , pt. III, 692-7 (1952) = Power Apparatus Syst. No. 1 (August 1952).
52-2	HUNTER, W.A. & TEMOSHOK, M.	Development of a modern amplidyne voltage regulator for large turbine generators. Trans. A.I.E.E. 71 , pt. III, 894-901 (1952) = Power Apparatus Syst. No. 2 (October 1952).
52-3	LAIBLE, Th.	Die Theorie der Synchronmaschine im nicht stationaeren Betrieb. Berlin, Springer Verlag (1952).

54-1 KRON, G. Regulating system for dynamoelectric machines. U.S. Patent Office. Patent 2, 692, 967 (October 26 1954).

54-2 HEFFRON, W.G. Jr. A simplified approach to steady state stability limits. Trans. A.I.E.E. 73 , pt. IIIA , 39 (1954) = Power Apparatus Syst. No. 10 (February 1954).

54-3 RUBENSTEIN, A.S. & TEMOSHOK, M. Underexcited reactive ampere limit for modern amplidyne voltage regulator. Trans. A.I.E.E. 73 , pt. III, 1433-8 (1954) = Power Apparatus Syst. No. 15 (December 1954).

55-1 MESSERLE, H.K. & BRUCK, R.W. Steady state stability of synchronous generators as affected by regulator and governors. Proc. I.E.E. 103 , pt. C, 24-34 (1956) (Monograph 134 S June 1955).

55-2 ROTH, H.H. Selecting excitation systems for hydro-generators. Allis-Chalmers Elect. Rev. 4th quarter 4-8 (1955) 2nd quarter 10-15 (1956).

55-3 KRON, G. A super-regulator cancelling the transient reactance of synchronous machines. The Matrix and Tensor Quarterly, 5 ; No. 3, 71-75 (1955).

56-1 FREY, W. Die Stabilitaetsprobleme des Parallelbetriebes. Dissert. No 2477, Eidgenoessischen Technischen Hochschule, Zurich, 181 pp (1956).

56-2 VENIKOV, V.A. & LITKENS, I.V. Experimental and analytical investigation of power system stability with automatically regulated generator excitation. C.I.G.R.E. No. 324, 26 pp (1956).

56-3 MESSERLE, H.K. The relative dynamic stability of large synchronous generators. Proc. I.E.E. 103 , pt. C, 234-42 (1956) (Monograph 159 S 1956).

56-4	PHILLIPS, R.A. & RUBENSTEIN, A.S.	Operation of large synchronous generators in the dynamic stability region with a modern amplidyne voltage regulator. Part I Recommendations for setting the underexcited reactive-ampere limit. Trans. A.I.E.E. 75 , pt. III, 762-6 (1956) = Power Apparatus Syst. No. 25 (August 1956).
56-5	McCLYMONT, K.R. et al.	Operation of large synchronous generators in the dynamic stability region with a modern amplidyne voltage regulator. Part II Operating tests and analytical studies. Trans. A.I.E.E. 75 , pt. III, 766-71 (1956) = Power Apparatus Syst. No. 25 (August 1956).
56-6	SEN, S.K. & ADKINS, B.	The application of the frequency response method to electrical machines. Proc. I.E.E. 103 , pt. C, 378-91 (1956) (Monograph 178 S 1956).
57-1	GRAY, A.H. & FENWICK, D.R.	Modern methods of excitation for large generators. Metropolitan-Vickers Gazette (August 1957) Reprinted as Publ. 2353 - 2 A.E.I. Instrumentation Division.
57-2	ACHENBACH, H.	Voltage regulator for large generators. Siemens Review 24 , No. 5/6 , 179-87 (1957)
57-3	SICHLING, G & ROHLOFF, E.	The switching transistor. Siemens Review 24 , No. 5/6 , 162-6 (1957).
57-4	KESSLER, C.	A transistor two-step controller. Siemens Review 24 , No. 5/6 , 169-73 (1957).
57-5	KOSTENKO, M.P.	Investigation of the automatic control of power systems using electrodynamic models. Izdat. Akad. Nauk. S.S.S.R., 60-91 Moscow (1957). C.E.G.B. Translation C.E. 1691 .
57-6	ADKINS, B.	The general theory of electrical machines. London, Chapman & Hall (1957).

57-7	NEWTON, G.C., GOULD, L.A. & KAISER, J.F.	Analytical design of linear feedback controls. New York, Wiley (1957).
58-1	FREY, W. & NOSER, R.	Recent developments in the excitation and control of synchronous machines. C.I.G.R.E. paper 127 , 23 pp (1958).
58-2	MESSERLE, H.K.	Dynamic stability of alternators as affected by machine reactances and transmission links. C.I.G.R.E. paper 315 , 23 pp (1958).
58-3	ALDRED, A.S. & SHACKSHAFT, G.	The effect of the voltage regulator on the steady state and transient stability of a synchronous generator. Proc. I.E.E. 105 , pt. A, 420-427 (1958) (Paper No. 2662 S 1958).
58-4	ETTINGER, E.L., GLOUKH, E.M. & CHALY, G.V.	Electronic exciters for hydrogenerators of the Kuibyshev hydroelectric power plant. C.I.G.R.E. (1958) Paper submitted after the beginning of the Conference and not included in the bound volumes.
58-5	MATIUKHIN, V.M.	The influence of the law of the excitation control on the damping of oscillation of a synchronous machine. Elektrichestvo No. 5, 27-31 (1958). Translation in Electric Technology U.S.S.R., 230 (1959).
59-1	LAWDEN, D.F.	Mathematics of engineering systems. London, Methuen 2nd Ed. (1959).
59-2	TSUKERNIK, L.V.	Lyapunov's general theory of stability and questions of power stability. Elektrichestvo No. 1 , 13-17 (January 1959) A.E.I. Translation No. 2882 .
59-3	JOHANSSON, K.E.	The voltage regulation of synchronous machines. A.S.E.A. Journal 32 , No. 9, 124-132 (1959).

59-4 SOHLSTROM, A. Regulators and regulating systems for synchronous machines. A.S.E.A. Journal 32 , No. 9 , 133-140 (1959).

59-5 KINITSKY, V.A. Automatic control of internal angle of synchronous machines. Trans. A.I.E.E. 78 , pt. IIIA, 225-31 (1959) = Power Apparatus Syst. No. 42 (June 1959).

59-6 MASON, T.H., AYLETT, P.D. & BIRCH, F.H. Turbogenerator performance under exceptional operating conditions. Proc. I.E.E. 106 , pt. A, 357-380 (1959) (Paper No. 2846 S 1959).

60-1 HOSEMANN, G. Large synchronous machine with rectifier excitation for sudden load changes at minimum dynamic voltage drops. C.I.G.R.E. paper 124 , 17 pp (1960).

60-2 PAVESI, P. & SIMONETTI, S. Excitation with semiconductor rectifiers and voltage regulation in a 28 MVA set for auxiliary services of a large thermal power plant station. C.I.G.R.E. pt. II, paper 128, 28 pp (1960).

60-3 ALDRED, A.S. & SHACKSHAFT, G. A frequency response method for the predetermination of synchronous machine stability. Proc. I.E.E. 107 , pt. C, 2-10 (1960) (Monograph 340 S).

60-4 COOPER, C.B. & GIRLING, L.R. Excitation control systems for large A.C. generators. A.E.I. Engng. Rev. 1 , No. 2, 75-82 (1960). Reprinted as Publ. 2353 - 3 A.E.I. Instrumentation Division.

60-5 JUNIOR, H. The voltage regulation of large synchronous generators with amplidyne rotary amplifiers and transductor regulators. A.E.G. Progress No. 1, 39-49 (1960).

60-6 KROCHMANN, E. Grundlegende Fragen der Spannungs - und Blindleistungsregelung. Elektrotechnische Zeitschrift - A, 81 , No. 7, 221-7 (1960).

60-7 ACHENBACH, H. Regelung grosser Wasserkraftgeneratoren. Elektrotechnische Zeitschrift - A, 81 , No. 7, 227-40 (1960).

60-8 HAPPOLDT, H. Regelung grosser Turbogeneratoren. Elektrotechnische Zeitschrift - A, 81 , No. 7, 240-46 (1960).

60-9 HAAMANN, K.P. Erregung und Regelung grosser Synchronmaschinen mit Stromrichter. Elektrotechnische Zeitschrift - A, 81 , No. 9, 317-23 (1960).

60-10 EASTON, V., FITZPATRICK, J.A.& PARTON, K.C. The performance of continuously acting voltage regulators with additional rotor angle control. C.I.G.R.E. Paper 309 pp (1960).

60-11 THALER, G.J. & BROWN, R.G. Analysis and design of feedback control systems. 2nd edition McGraw-Hill (1960).

60-12 GRUZDEV, I.A. & LEVINSHTEIN, M.L. The use of analogue computers for studying transients in electrical systems. Elektrichestvo No. 3, 1-13 (1960). A.E.I. Translation No. 2897.

60-13 FERGUSON, R.W., HERBST, R., & MILLER, R.W. Analytical studies of the brushless excitation system. Trans. A.I.E.E. 78 , pt. III, 1815-21 (1960) = Power Apparatus Syst. No. 46 (February 1960).

60-14 WHITNEY, E.C., HOOVER, D.B., & BOBO, P.O. An electric utility brushless excitation system. Trans. A.I.E.E. 78 , pt. III, 1821-8 (1960) = Power Apparatus Syst. No. 46 (February 1960).

61-1	HARVEY, L.M. et al.	Amplidyne main exciter excitation system. Trans. A.I.E.E. 80 , pt. III, 17-23 (1961) = Power Apparatus Syst. No. 53 (April 1961).
61-2	ALDRED, A.S. & SHACKSHAFT, G.	Frequency response analysis of the stabilizing effect of a synchronous machine damper. Proc. I.E.E. 108 , pt. C, 58-63 (1961) Monograph 393 S (July 1960).
61-3		Proposed excitation system definitions for synchronous machines. A.I.E.E. Committee Report. Trans. A.I.E.E. 80 , pt. III, 173-8 (1961) = Power Apparatus Syst. No. 54 (June 1961).
62-1		Equations used for analogue computer study of turbo-alternator stability. Analogue Computation Centre. C.E.G.B. (1962).
62-2	MILES, J.G.	Analysis of overall stability of multi-machine power systems. Proc. I.E.E. 109 , pt. A, 203-11 (1962)(Paper No. 3715 S.).
62-3	GLAVITSCH, J.	Theoretical investigations into the steady-state stability of synchronous machines. Brown Boveri Rev. 49 , No. 3-4, 95-104 (1962).
62-4	BLOEDT, K., & WALDMANN, H.	Spannungsregelung mit Transistor-Zweipunktregler und Transduktorstufe fuer Synchrongeneratoren. Siemens Zeitschrift 36 , No. 3, 148-53 (1962).
62-5	HAMDI-SEPEN, C.	Process for increasing the transient stability power limits on A.C. transmission systems. C.I.G.R.E. Paper 305, 10 pp (1962).
62-6	NIELSEN, B.	Contribution a l'etude de la stabilite statique des turboalternateurs. Rev. Gen. Elect. (France). 71, No. 5, 239-48 (May 1962).

62-7 HEFERMANN, F. Spannungsregelung von Synchrongeneratoren. B.B.C. - Nachrichten 44 , No. 8/9, 320-323 (1962).

62-8 GRUENBERG, D. Stromrichter zur Feldspeisung grosser Gleich- und Drehstrommaschinen. B.B.C. - Nachrichten 44 , No. 8/9, 324-34 (1962).

62-9 HEFERMANN, F. & MENSTELL, L. Kompounderregung fuer Synchrongeneratoren. B.B.C. - Nachrichten 44 , No. 8/9, 334-9 (1962).

62-10 CHAMBERS, G.S., RUBENSTEIN, A.S. & TEMOSHOK, M. Recent developments in amplidyne regulator excitation systems for large generators. Trans. A.I.E.E. 80 , pt. III, 1066-72 (1962) = Power Apparatus Syst. No. 58 (February 1962).

62-11 BARRAL, A., BOULET, R., & CARPENTIER, L. Recent progress and new possibilities for the excitation and the regulation of large synchronous machines. C.I.G.R.E. Paper No. 157, 33 pp (1962).

63-1 VENIKOV, V.A. et al. Forced regulation of alternator excitation. Gosenergoizdat, Moscow - Leningrad (1963) In Russian.

63-2 SHACKSHAFT, G. A general-purpose turbo-alternator model. Proc. I.E.E. 110 , 703-13 (1963).

63-3 PUTZ, W., RIEGER, E., & ROGOWSKY, Y. Excitation and voltage regulation of A.E.G. turbogenerators. A.E.G. Progress, 196-204 (1963).

63-4 ZAVALISHIN, D.A. & GLEBOV, I.A. Excitation systems for high-power synchronous machines. Izv. Akad. Nauk S.S.S.R., Otd. Tekh. Nauk, Energ. i Transport No. 2, 165-75 (1963) In Russian. A.E.I. Translation No. 3417.

63-5 BOGOSLOVSKII, A.V. & SOVALOV, S.A. Stability test on the "V. I. LENIN" Volga hydroelectric power station to Urals transmission. Elektrichstvo No. 8, 1-9 (1962) In Russian. Translation in Electric Technology U.S.S.R., p. 397 (1962).

63-6 ALFORD, R.J. The micromachine exciter system and time constant regulator. Power Systems Report No. 49. Imperial College of Science and Technology (1963).

63-7 BHARALI, P. Damping effects in a synchronous machine with a solid iron rotor. Ph.D. thesis, University of London (1963).

64-1 VENIKOV, V.A. Transient phenomena in electrical power systems. Trans. by B. Adkins and D. Rutenberg. Pergamon Press (1964).

64-2 STAPLETON, C.A. Root-locus study of synchronous-machine regulation. Proc. I.E.E. 111 , 761-68 (1964).

64-3 VENIKOV, V.A. Transient phenomena in electrical power systems. 2nd Edition, Moscow Gosenergoizdat (1964). In Russian.

64-4 EASTON, V. Excitation of large turbogenerators. Proc. I.E.E. 111 , 1040-48 (1964).

64-5 HAMDI-SEPEN, C. Process for increasing the transient stability power limits on A.C. transmission systems (Part II). C.I.G.R.E. Paper 304 , 14 pp (1964).

64-6 HANO, I. et al. Underexcitation tests of hydraulic-turbine generators connected to 275 kV transmission systems. C.I.G.R.E. Paper 307, 20 pp (1964).

64-7		Automatic voltage regulator, type ZVX (for steam turbo-alternator). English Electric Leo Computers Limited, Kidsgrove, (February 1964).
65-1	STEEDE, J.H., CROFT, P.J. & ELLIS, H.M.	Peace river E.H.V. transmission system. Trans. I.E.E.E., Paper No. 31, CP 65-55 (1965).
65-2	EWART, D.N. et al.	Stability studies and tests on a 532 MW cross-compound turbine-generator set. Trans. I.E.E.E., Paper No. 31, TP 65-186 (1965).
65-3	BATTISSON, M.J. & MULLINEUX, N.	Stability criteria for linear control systems. Proc. I.E.E., 112 , 549-56 (1965).
65-4	GOVE, R.M.	Geometric construction of the stability limits of synchronous machines. Proc. I.E.E. 112 , 977-85 (1965).